JPL Publication 97-3

Presentations of the Ninth Advanced Communications Technology Satellite Propagation Studies Workshop (APSW IX)

Held in Herndon, Virginia November 19–20, 1996

Nasser Golshan
Editor

January 15, 1997

National Aeronautics and
Space Administration

Jet Propulsion Laboratory
California Institute of Technology
Pasadena, California

JPL Publication 97-3

Presentations of the Ninth Advanced Communications Technology Satellite Propagation Studies Workshop (APSW IX)

Held in Herndon, Virginia November 19–20, 1996

Nasser Golshan
Editor

January 15, 1997

National Aeronautics and
Space Administration

Jet Propulsion Laboratory
California Institute of Technology
Pasadena, California

This publication was prepared by the Jet Propulsion Laboratory, California Institute of Technology, under a contract with the National Aeronautics and Space Administration.

ABSTRACT

The Advanced Communications Technology Satellite Propagation Studies Workshop (APSW) is convened each year to present the results of the ACTS Propagation Campaign. Representatives from the satellite communications (satcom) industry, academia and government are invited to APSW for discussions and exchange of information. The ACTS Propagation campaign is completing three years of Ka-Band data collection at seven sites in North America. Through this effort, NASA is making a major contribution to growth of satcom services by providing timely propagation data and models for predicting the performance of Ka-Band satellite communications systems.

PREFACE

The Advanced Communications Technology Satellite (ACTS) propagation campaign is completing three years of Ka-band data collection at seven sites. With the exponential increase of satcom industry interest in Ka-band, NASA is funding continued data collection and processing at least through September 1997. Through this effort NASA is making a major contribution to the growth of satcom services by providing timely data and models for performance prediction of Ka-band satcom systems. The Ninth ACTS Propagation Studies Workshop was held in Herndon, Virginia, at the Washington Dulles Marriott Suites, November 19 and 20, 1996. This meeting location was selected to provide for a visit to the ACTS Propagation Terminal at Stanford Telecommunications, Inc. (STEL) in Reston, VA.

This year the ACTS workshop focused on three areas:

1) Latest results and findings from ACTS propagation experimenters.

2) Theoretical and empirical considerations for a global model to predict the first-order and second-order temporal and spatial statistics on attenuation, scintillation, coherence bandwidth, and depolarization due to weather (precipitation and atmospheric interactions with the antenna) for satellite systems at the Ka-band.

3) Steps needed to assure the quality and continuity of ACTS propagation data collection and processing.

Session 1, chaired by R. Bauer of LeRc, provided an overview of ACTS spacecraft and program status as well as a summary of anomalies on the ACTS propagation beacon. ACTS propagation experimenter status reports from seven Ka-band sites, one combined Ka/Ku band site, as well as the ACTS Propagation Data Center were presented in Session 2, chaired by L. Ippolito of Stanford Telecom.

Session 3, chaired by W. Vogel of the University of Texas at Austin, covered three papers on rain effects propagation modeling for link performance prediction of Ka-band satcom system design, an overview on the status of the *Propagation Effects Handbook for Satellite Systems Design*, and a discussion of Ka-band depolarization effects due to propagation impairments. In Session 4, F. Davarian, guest editor for the IEEE special issue on ACTS propagation experiments, reported that high quality papers have been received and the special issue will be published in the near future after completion of the review process. Session 5, Plenary, was chaired by R. Crane and D. Rogers.

The success of the meeting owes a lot to the speakers, the session chairs, and the active participation of all attendees. I would like to express my thanks to Ms. Julie Feil of Stanford Telecom for arranging a visit to see the ACTS Propagation Terminal at the STEL facility. Last, but not least, I would like to thank Mardy Wilkins of JPL for meticulously caring for the many administrative details related to the meetings and to Roger Carlson of the JPL Technical Information Section for coordinating the publication of this document.

The next ACTS NAPEX meeting will take place on June 11-13, 1997, in Los Angeles, CA.

Page intentionally left blank

CONTENTS

omit 10
p. 1a

APSW IX

SESSION 1

SPACECRAFT AND PROGRAM UPDATES

R. Bauer ***(LeRC)***

Page intentionally left blank

ACTS PROJECT & PROPAGATION PROGRAM UPDATE

Robert Bauer
NASA Lewis Research Center
ACTS Propagation Studies Workshop IX
Herndon, VA
November 19, 1996

ACTS OPERATIONS UPDATE

- ACTS continues to operate nominally.
- Hydrazine depletion estimate remains July 1998.
- Decision to continue operations in an inclined orbit are TBD.
- Ka-band license extension requested with IRAC. Currently expires 12/31/96.

OPERATIONS UPDATE, cont.

- Triple eclipse experienced on 9/12/96.
  - Normal fall eclipse + 2 lunar obscurations within 12 hours
  - Spacecraft temp. dropped to lowest level ever (~ -8 C., lower limit is -5)
  - Heaters incapable of sufficient warming between shut-downs
  - No damage done

3

EXPERIMENTS PROGRAM

- Total proposals received (11/05/96) 150
- Number of approved experiments: 85
  - Experiments started: 68
  - Experiments completed: 40
  - Experiments yet to start: 17

4

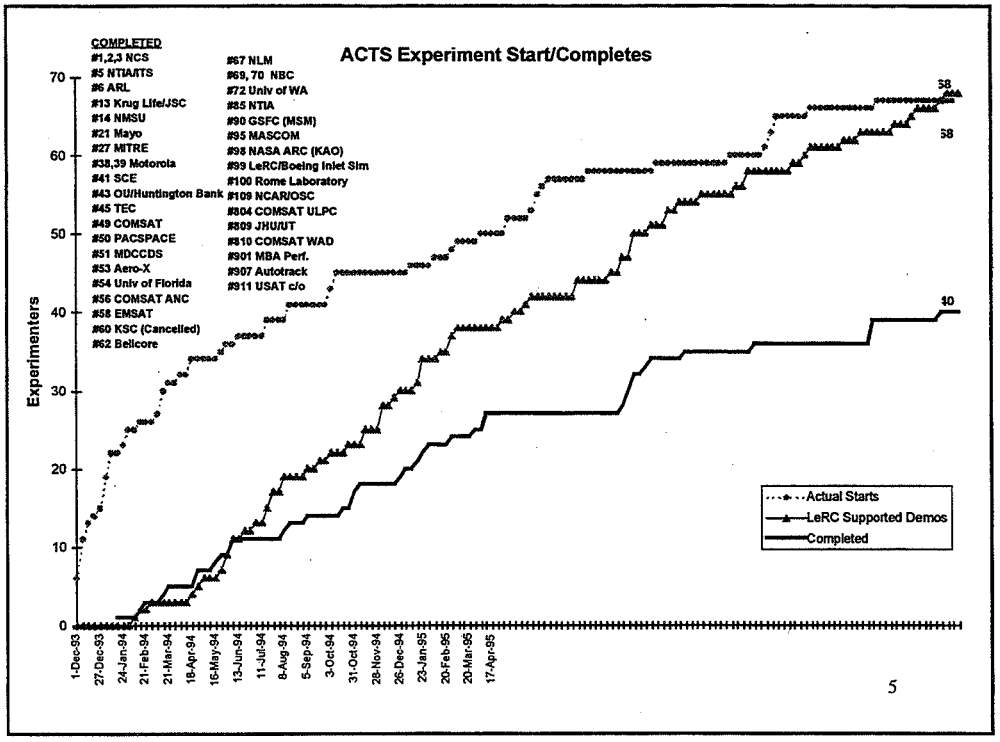
ACTS Experiment Start/Completes
COMPLETED
#1,2,3 NCS
#5 NTIA/ITS
#6 ARL
#13 Krug Life/JSC
#14 NMSU
#21 Mayo
#27 MITRE
#38,39 Motorola
#41 SCE
#43 OU/Huntington Bank
#45 TEC
#49 COMSAT
#50 PACSPACE
#51 MDCCDS
#53 Aero-X
#54 Univ of Florida
#56 COMSAT ANC
#58 EMSAT
#60 KSC (Cancelled)
#62 Bellcore
#67 NLM
#69, 70 NBC
#72 Univ of WA
#85 NTIA
#90 GSFC (MSM)
#95 MASCOM
#98 NASA ARC (KAO)
#99 LeRC/Boeing Inlet Sim
#100 Rome Laboratory
#109 NCAR/OSC
#804 COMSAT ULPC
#809 JHU/UT
#810 COMSAT WAD
#901 MBA Perf.
#907 Autotrack
#911 USAT c/o
Experimenters
Actual Starts
LeRC Supported Demos
Completed
58
58
40
1-Dec-93
27-Dec-93
24-Jan-94
21-Feb-94
21-Mar-94
18-Apr-94
16-May-94
13-Jun-94
11-Jul-94
8-Aug-94
5-Sep-94
3-Oct-94
31-Oct-94
28-Nov-94
26-Dec-94
23-Jan-95
20-Feb-95
20-Mar-95
17-Apr-95

5

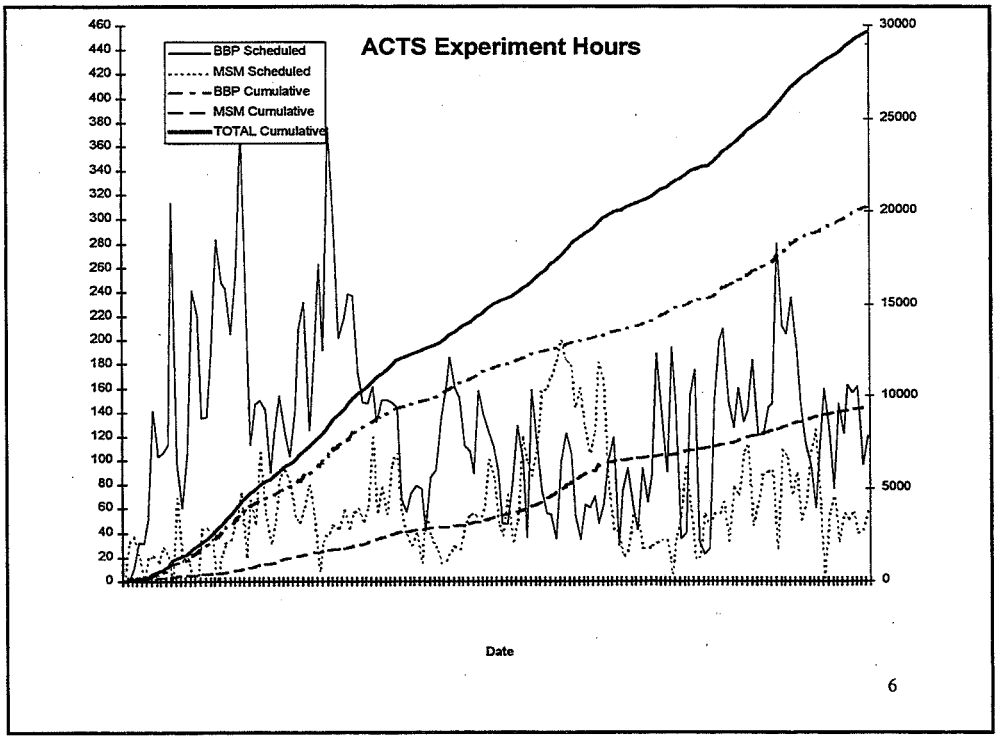
ACTS Experiment Hours
BBP Scheduled
MSM Scheduled
BBP Cumulative
MSM Cumulative
TOTAL Cumulative
Date

6

MAJOR ON-GOING/RECENT EXPERIMENTS

- Natl. Library of Medicine
  - High data rate (T1) transfer of medical archives
  - Communication protocol compatibility with high latency satellite link
- South America Distance Education
  - Regular classes between Georgetown Univ. and So. America began this fall
  - 5 classes/4 days a week

7

ON-GOING EXPTS., cont.

- HPCC - High Data Rate (OC-3, OC-12)
  - Keck Observatory, Hawaii and JPL
  - Global Climate Modelling, GSFC and JPL
- Army
  - Operations shift from USARSPACE, Colorado Springs, CO to 4th Infantry Division, Ft.Hood, TX completed
  - 2 major exercises in 1997 planned (Mar, Nov)

8

NEW EXPERIMENTERS

- ATDNet/MAGIC - High data rate (OC-3, OC-12) interoperability of fiber/satellite links.
- Naval Research & Development (NRaD) - Ship-to-shore communications including video, voice, data, and internet protocol eval. at T1 (1.544 Mbps).

9

NEW EXPERIMENTERS, cont.

- US Coast Guard - "Internet-to-the-Sea," database access, video teleconferencing, shipboard command & control, Ka-maritime channel fading characteristics.
- Globalstar - Encryption and error correction using random time smearing in mobile and personal satcomm.

10

MAJOR DEMOS

- Olympics (July16-Aug 5)
  - ACTS Mobile Terminal (JPL) support of US Marshalls and FBI requested before games
  - On-site within hours after Centennial Park bomb on July 26; provided phone, fax

11

MAJOR DEMOS, cont.

- Montana Telemedicine (July 17-18)
  - T1 rates through USAT between a Billings hospital, Exxon Clinic, and Crow Reservation
  - Remote patient diagonsis using special JSC Transportable Instrumentation Package (TIP) developed for space station

12

MAJOR DEMOS, cont.

- Suitcase Terminal (July 27-Aug7)
  - Rome Labs/Canadian Research Centre 0.5 m terminal
  - Data, voice, video from 512-1544 kbps
- Presidential Train (Aug 26-28)
  - AMT mounted on "21st Century Express"
  - Midwest route (WV, OH, MI, IN)

13

MAJOR DEMOS, cont.

- Hurricane Fran (Sept 10-15)
  - T1VSAT deployed from Lewis to Raleigh, NC
  - Damage not as bad as anticipated; terminal not used
- Lewis Business Industry Summit (Sept 19)
  - Northeast Ohio industry "open-house" at Lewis to increase govt/industry tech utilization

14

MAJOR DEMOS, cont.

- TECH 2006/Telecon XVI (Oct 29-31)
  - Full ACTS capabilities demonstrated with HDR, USAT, T1VSAT
  - Telemedicine and MPEG2 demos

15

UPCOMING ACTIVITIES

- "Live from Antarctica" - Interactive PBS broadcast; 3 live dates in Jan & Feb/97.
- Pacific Telecomm Conf. (PTC, Jan 19-23) - HDR and Lockheed Martin AstroLink product development demo with USAT.

16

ACTS Ka-FILER ACTIVITY

- Following firms now working directly with the ACTS Project to resolve issues related to their systems (e.g., technical experiments, product development & demos):
  - Hughes Spaceway (& GBS)
  - AT&T VoiceSpan
  - Lockheed Martin Astrolink
  - KaStar
  - Loral CyberStar

17

PROPAGATION PROGRAM

- Recommendation to continue program for 5 years (data collection through 11/98).
- Contract extensions needed.
- Funding through 9/97 in place.
  - FY 98 TBD

18

Propagation Program Timeline

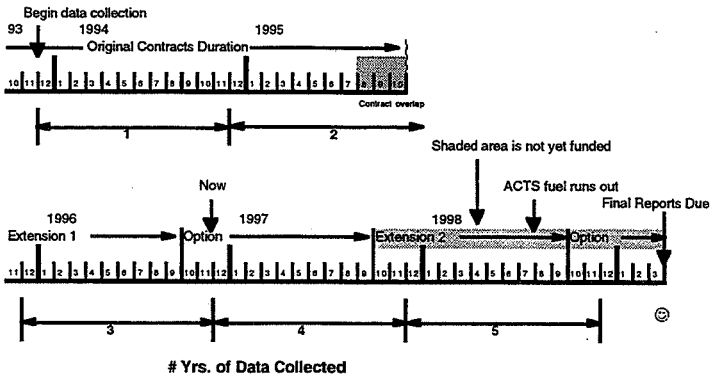

19

ACTS 20 & 30 GHz Fade Beacon System On-Orbit Performance

Dr. Roberto Acosta

NASA Lewis Research Center
Cleveland Ohio, 44145

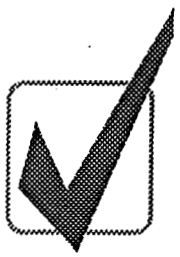

OUTLINE OF PRESENTATION

- S/C Sensor Location Diagram
- Typical Temperature Distribution Profiles
- Ground Station Calibration
- Typical Amplitude and Frequency Distribution
- 10 Days Data - Amplitude and Frequency
- Summary of Beacon Performance - 2 Years Data
- Beacon Anomalies Reported

Sensor Location on K-Band Antenna

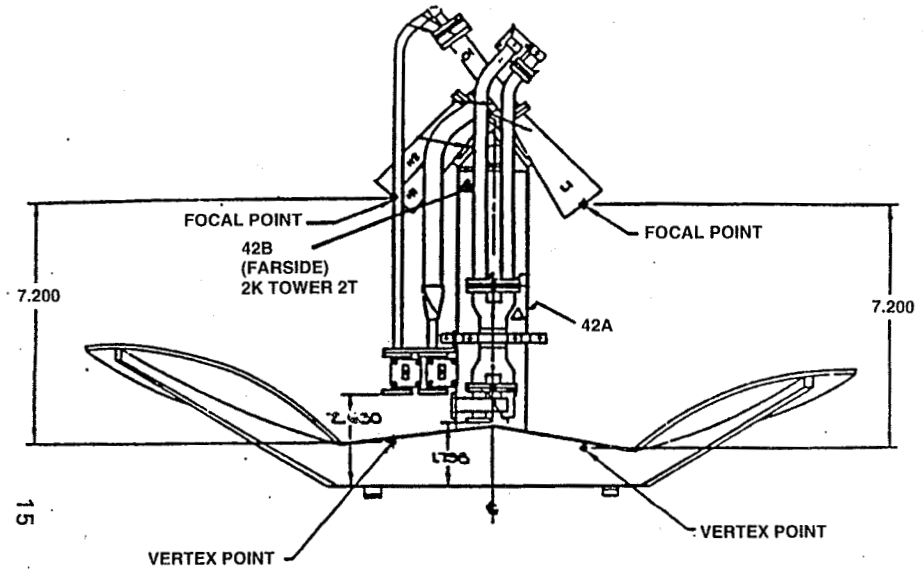

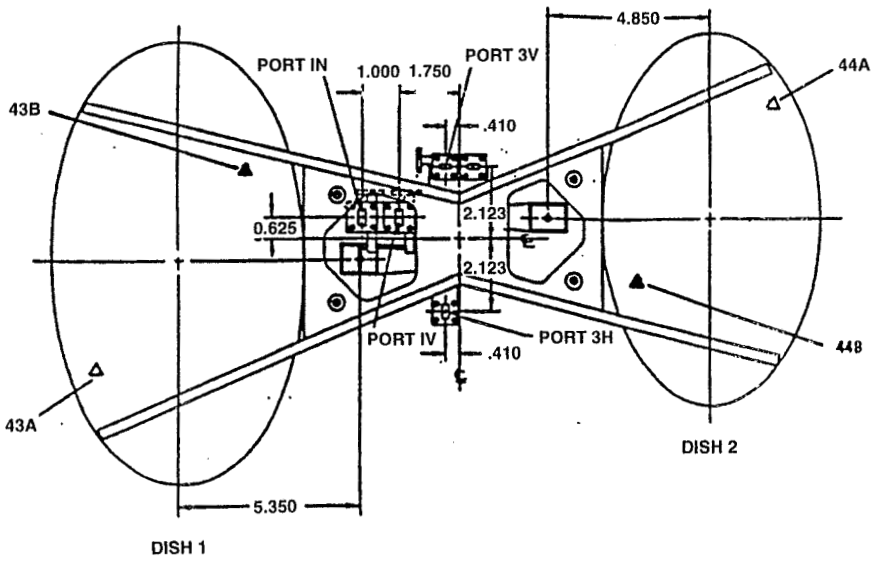

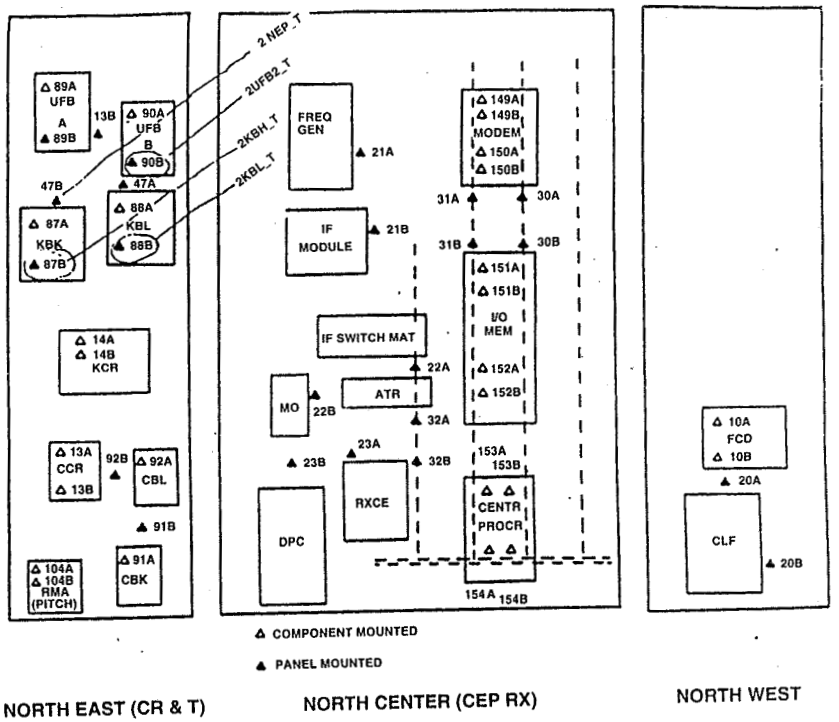

On-Orbit Temperature Distribution Fade Beacon System

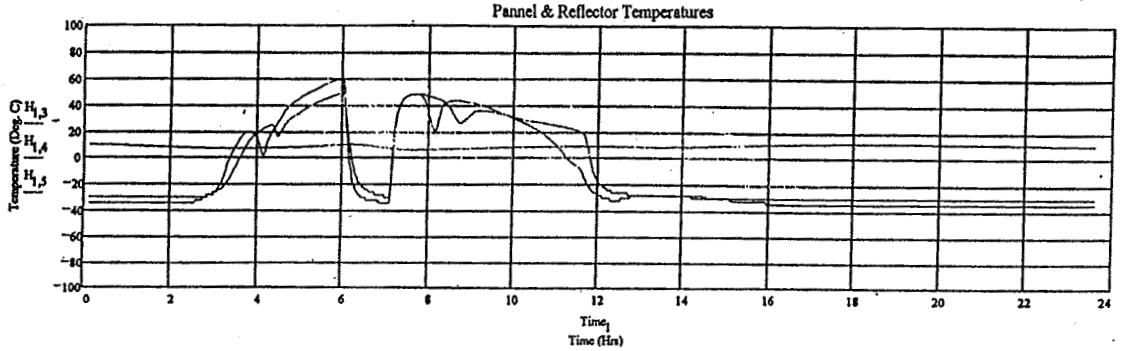

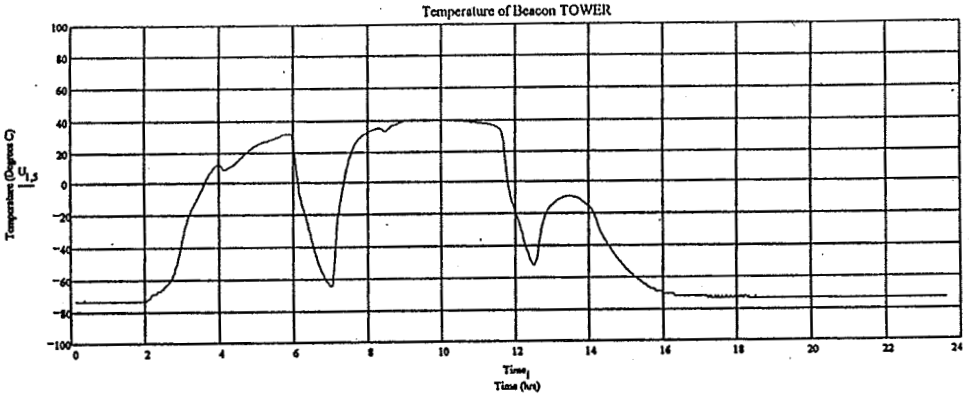

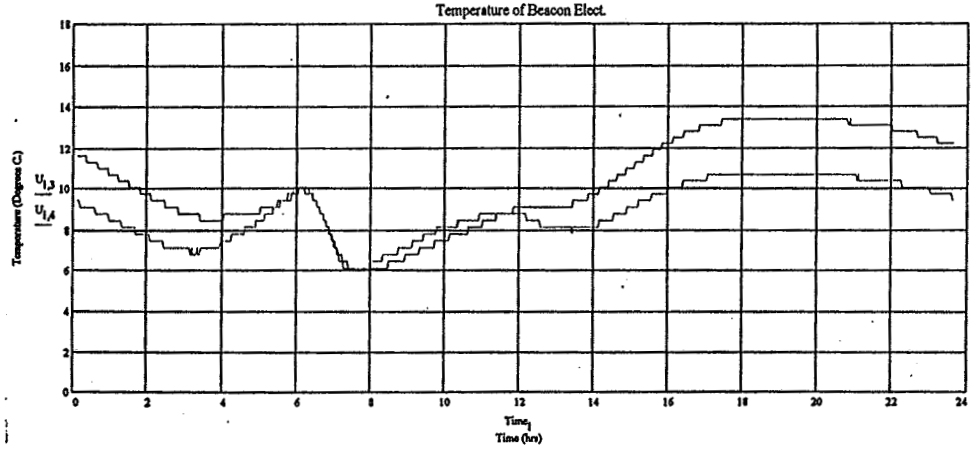

Ground Station Calibration

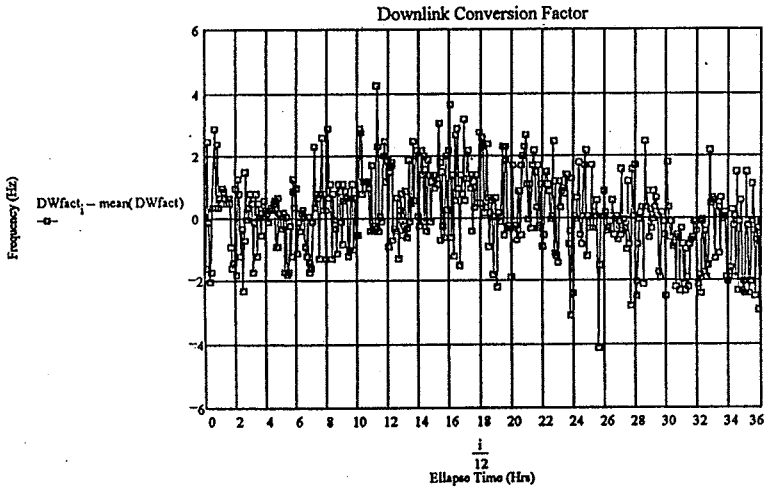

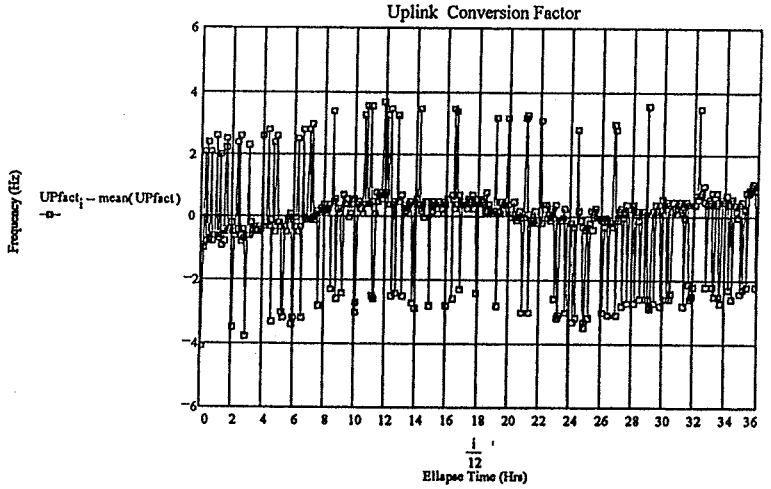

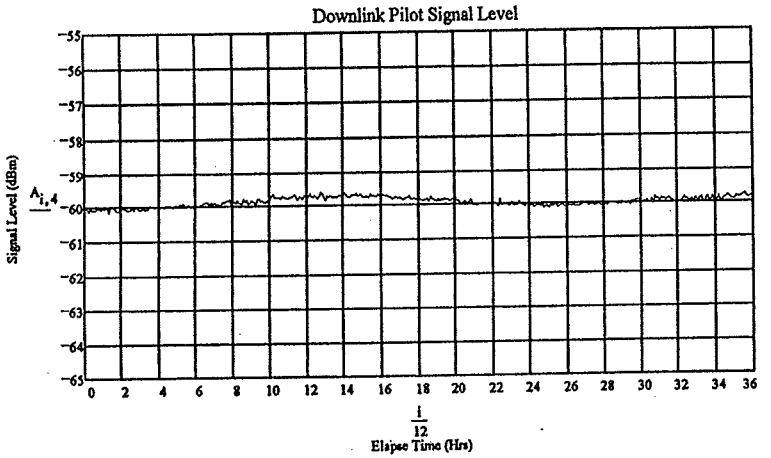

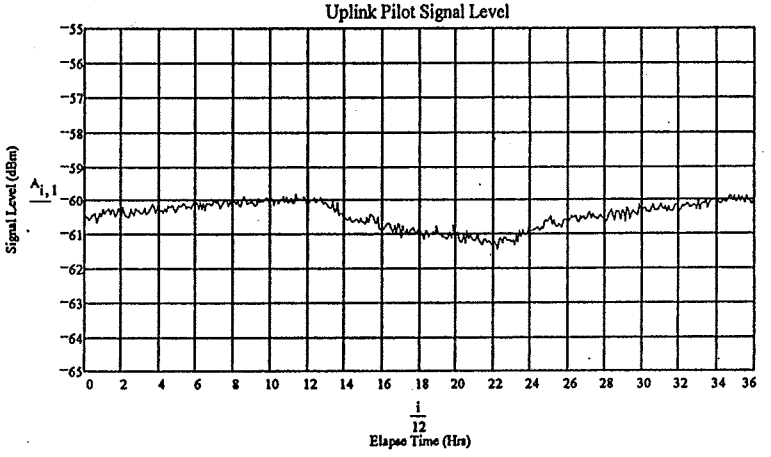

Amplitude and Frequency Distribution Fade Beacon System

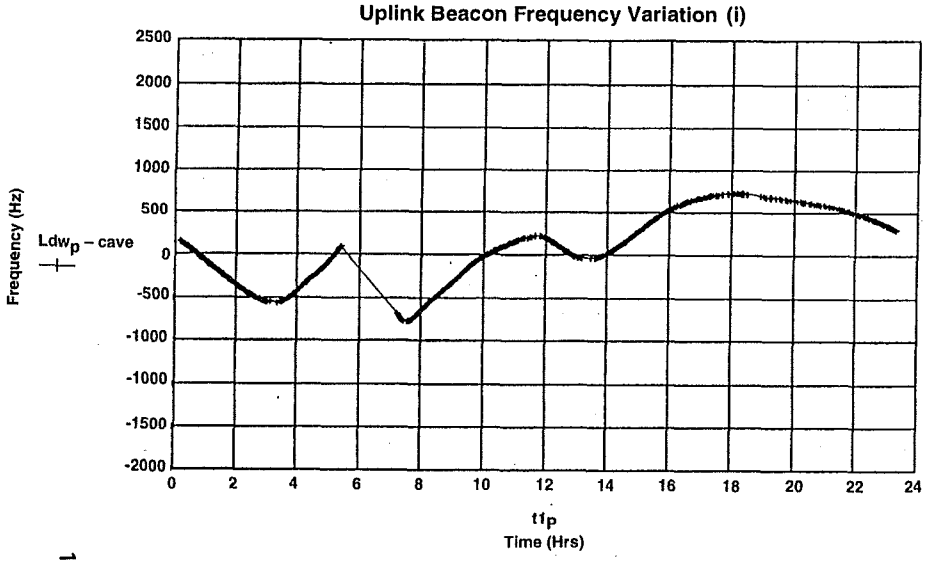

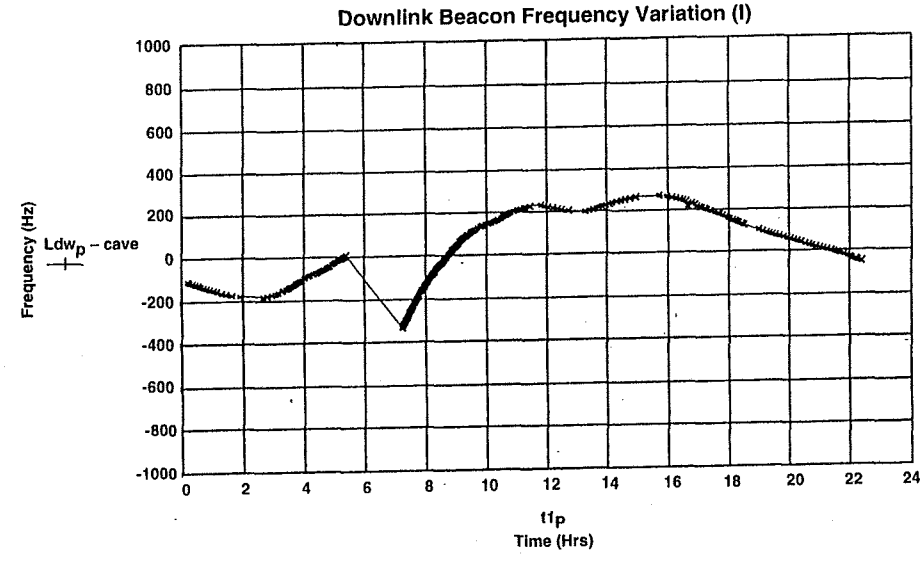

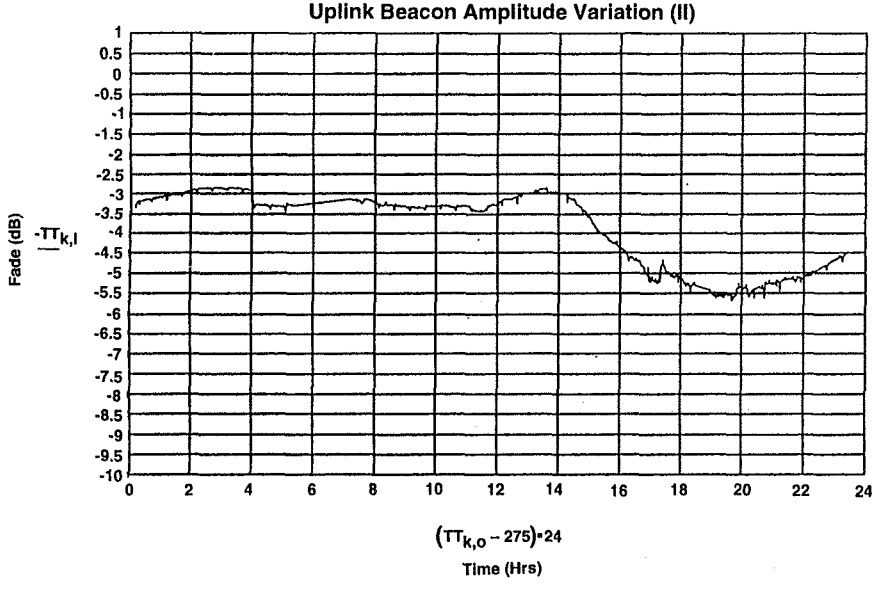

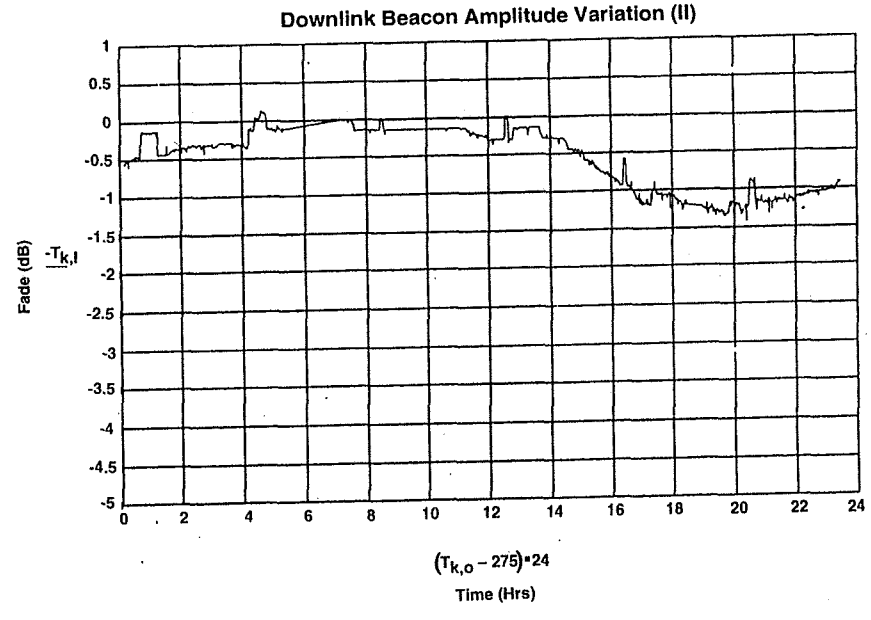

Amplitude and Frequency Distribution - 10 Days Data

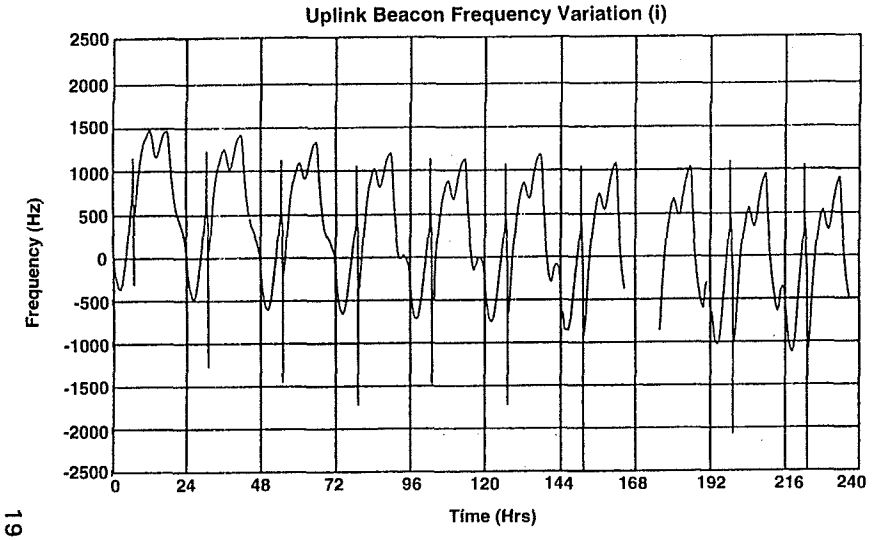

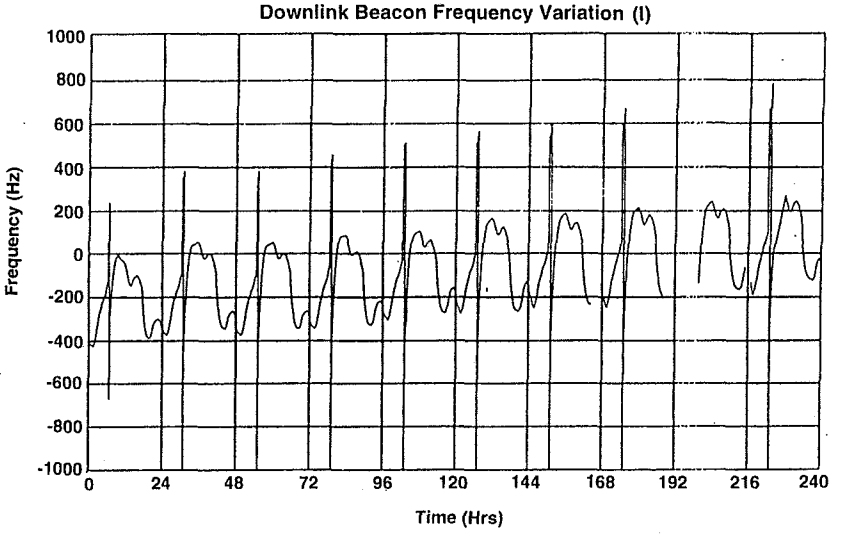

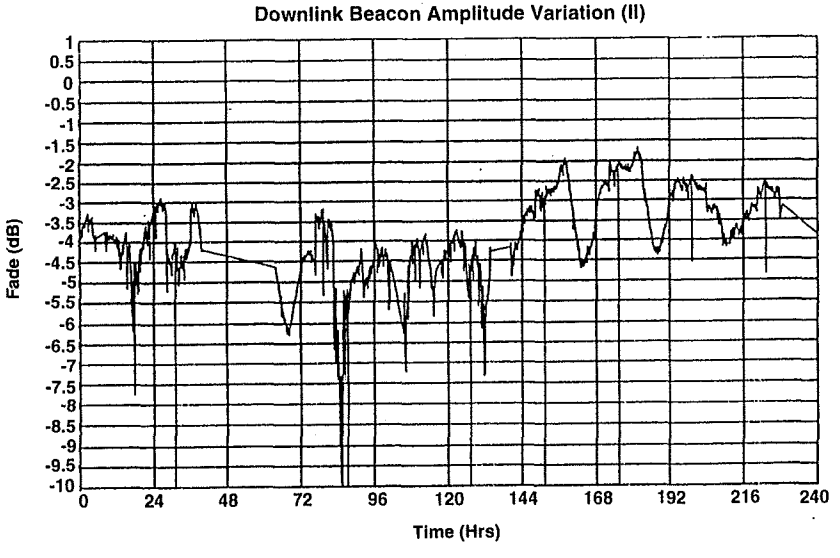

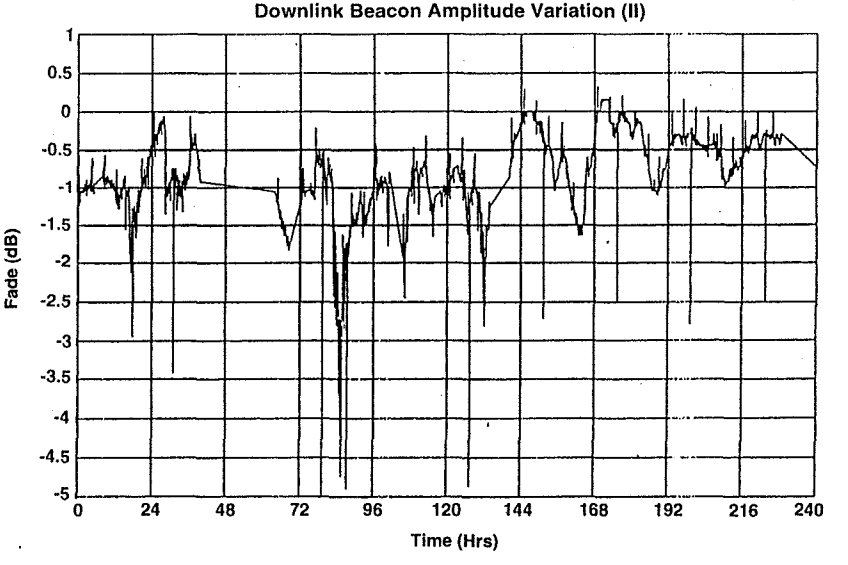

Beacon Frequency Analysis - 2 years data

Summary

- **Seasonal Frequency Drift :** **< 3,000 Hz @ 20 GHz**
  < 2,000 Hz @ 30 GHz
- **Diurnal Frequency Oscillation:** **+/- 250 Hz @ 20 GHz**
  +/- 1000 Hz @ 30 GHz
- **Transient Frequency:** **< 1500 Hz**

Beacon Anomalies Reported

Anomalies Reported:

- **Reported by ACSP (Feil):** **Dec 95: 15,20,21,22,23,24,25,26,27,30 and 31**
  Glitches on signal
- **Reported by Uof SF (Szkarz):** **Dec 95:22,27,29,30,31**
  Glitches on signal
- **Reported by OK + CO (Beaver):** **Dec 95: 24,25,26**
  Glitches cause by tear in feed horn

NASA LeRC ACTS Analysis:

- **Found no glitches during any time in Dec 95. (NASA data taken at 150 m sec)**

Page intentionally left blank

omit THIS PAGE

APSW IX

SESSION 2

EXPERIMENT STATUS REPORTS

L. Ippolito ***(Stanford Telecom)***

Page intentionally left blank

ELECTROMAGNETIC WAVES AND WATER ON A SURFACE: PARAMETERS AND RESULTS

by
Charles E. Mayer
Brad Jaeger
University of Alaska Fairbanks

I. INTRODUCTION

This report will start with an overview of the APT status, and then discuss the current scintillation models and compare measured data to models. Finally we will introduce the topic of water reactions on a surface and how this captive water will affect the propagation experiment.

The Alaska ACTS Propagation Terminal (APT) has continued to operate efficiently. A Global Positioning Satellite (GPS) system is now the primary clock of the APT, replacing the WWV receiver which often went for days without receiving the WWVH time signal. The Triplett UPS (Uninterruptible Power Supply) failed and has been replaced by an APC model UPS. A 20 W, 1.7 GHz transmitter is proposed to be installed on the Duckering Building roof, near the AK APT. It would only be installed on a noninterfering basis, but ascertaining interference may be a difficult and time consuming. One concern is that the transmitter, or its harmonics, could leak into the APT beacon or radiometer receivers. A second concern is that the 1.7 GHz signal would overload the front end of the 1.575 GHz GPS receiver, which is used for system timing information. This situation has been discussed with colleagues who have more GPS experience, namely Wolf Vogel, Geoff Torrence, and Dave Westenhaver.

II. SCINTILLATION STUDIES

A. Introduction

Atmospheric turbulence may seriously affect satellite-earth links at frequencies above 10 GHz. The turbulence in the troposphere yields small-scale and time-varying fluctuations of the refractive index along the propagation path, which causes amplitude, phase, and angle of arrival fluctuations, known as scintillation. Tropospheric scintillation effects increase in magnitude as the frequency increases, and as the elevation angle decreases.

The impact of rain-induced attenuation on satellite-earth communication links at frequencies above 10 GHz is generally predominant. However, for the design of low margin systems, especially those at high frequencies and low elevation angles, scintillation effects must be properly estimated for the link budget

B. Theory

Propagation through a turbulent medium has been extensively studied. The signal propagates through a turbulent layer, which is concentrated at the planetary boundary layer, the separation of the wet and dry atmosphere. Mixing, and the associated turbulence, occurs at this boundary, which is typically 1 to 1.5 km in altitude. The signal, after propagating through this turbulent layer can be considered a random variable with stationarity. This random variable can be described by its probability density function and its power spectrum. Theoretical studies yield models of these characteristic parameters based upon meteorological parameters that cannot be measured. The lack of knowledge of the these meteorological parameters along the propagation path length have

led to the development of semiempirical models representing the magnitude and characteristics of scintillations.

C. Measurement unit of scintillations

The intensity of the scintillations must be accurately portrayed by a measurement unit. The scintillation process is assumed to be a zero-mean process with fluctuations about that mean. The fluctuations can be represented in terms of their root mean square (rms). Since the mean of the process is zero, the standard deviation represents the rms of the process.

The measure of the intensity of scintillation used will be the standard deviation of the logarithm of the received signal, that is, the standard deviation of the received signal in decibels. The time duration of the standard deviation calculation will be one minute. For every minute of beacon data, we calculate a standard deviation to represent the magnitude of scintillations in that minute. We can then look at the distribution of these calculated one-minute standard deviations. We will look at the mean hourly standard deviation and compare this to two models; the CCIR model and the Karasawa model. These two models calculate the mean hourly value of the magnitude of scintillations over a monthly period. Both of these models have scaling terms for frequency, elevation angle, and size of the antenna. These models also contain a parameter of measured wet refractive index, Nwet, to account for the local water vapor density during the scintillation measurements. These two models are delineated in Figs. 1 and 2.

D. Seasonal Variations

Figs. 3 and 4 show the variation in the mean hourly standard deviation over the experiment length at Fairbanks. Also shown are predicted values of mean hourly standard deviation calculated from the CCIR model and the Karasawa model. These models make a prediction of standard deviation in a month based on wet refractivity (calculated from the average temperature and relative humidity in a month). This prediction is then scaled to frequency, elevation angle, and aperture size.

E. Kolmogorov-Smirnov Goodness of Fit Tests

Part of the basis of the prediction of signal fading due to scintillation is an integral of the area beneath a joint probability density function to obtain a cumulative distribution function. (The other part of the basis for the prediction is the determination of a reference standard deviation from local wet refractivity. This will be discussed in the next section.) The signal fading due to scintillation is typically assumed to have a Gaussian distribution given a constant standard deviation. The distribution of standard deviation is typically assumed to have one of two distributions; the lognormal distribution or the gamma distribution. The product of the conditional distribution of signal fading and the distribution of standard deviation forms the joint distribution required to find the cumulative distribution of signal fading.

Fig. 5 shows how well monthly observed distributions of standard deviation at Fairbanks fit the lognormal distribution or the gamma distribution. The Kolmogorov-Smirnov (K-S) test uses as its statistic the largest difference between an observed distribution and a theoretical distribution. The test is applicable to unbinned distributions so it was performed on the collection of hourly standard deviations for each month. The p-value is the conditional probability of observing the K-S statistic given that the observed distribution came from the theoretical distribution, which was assumed. If the p-value is smaller than a chosen probability threshold (typically 0.05) then the assumption of the theoretical distribution is said to be in error. The lognormal distribution fit is generally better than the gamma distribution fit, as indicated in Fig. 5.

February, March, and April had very low levels of humidity in the air, and hence very low magnitudes of scintillations.

F. Karasawa's Simplification

To calculate the area beneath the joint probability density function of signal fading and signal standard deviation, one further assumption is necessary. Karasawa found that the mean squared of standard deviation and the variance of standard deviation were related by $m^2=10\cdot\sigma^2_{\sigma x}$. The integral

$$p'(X>X_0)=\int_{X_0}^{\infty}\int_{0}^{\infty}P_1(X|\sigma_x)P_2(\sigma_x)d\sigma_x dx$$

involves four parameters. The Gaussian distribution, P_1, has parameters m and σ^2_x and the Gamma distribution, P_2, has parameters ς and β. Since ς and β are functions of m and σ^2_x we can use Karasawa's relation to simplify the integral. Figs. 6 and 7 show that the corresponding relation for Fairbanks is $m^2=7\cdot\sigma^2_{\sigma x}$.

G. Relation to Wet Refractivity

The main tool the Karasawa and CCIR models use to account for regional and seasonal variations is the prediction of a reference standard deviation, $\sigma_{x,REF}$, from monthly averaged wet refractivity. Karasawa found this relation to be $\sigma_{x,REF}=0.15+0.0052\cdot$Nwet, where Nwet is the monthly average wet refractivity. Figs. 8 and 9 show that in Fairbanks this becomes $\sigma_{x,REF}=0.0635+0.0033\cdot$Nwet at 20 GHz and $\sigma_{x,REF}=0.0678+0.0033\cdot$Nwet at 27 GHz.

H. Frequency Dependence

Models of standard deviation use an experimental station as a reference prediction and then provide scaling terms for other frequencies, elevation angles, and aperture sizes. The CCIR model uses frequency scaling consistent with the Tatarski model for the diffraction case, $f^{7/12}$. The elevation angle (path length) scaling used by the CCIR model, $\text{cosec}^{1.2}(\theta)$, is a compromise between the diffraction case, $\text{cosec}^{11/12}(\theta)$, and the geometrical optical case, $\text{cosec}^{3/2}(\theta)$. The Karasawa model uses experimentally derived scaling terms which are a compromise between the diffraction case and the geometrical optical case, $f^{0.45}\text{cosec}^{1.3}(\theta)$. With known station frequencies, elevation angle, and aperture size the CCIR scaling relation can be solved for the frequency exponent. The only unknown, the ratio of standard deviations, can be obtained by averaging the ratio of equal probability points on cumulative distribution functions. The frequency scaling exponent for the first year of data is 0.44.

I. CDF of Scintillation Magnitude

Figs. 10 and 11 show the cumulative distribution functions of the magnitude of scintillations for the first year of the experiment for 20 and 27 GHz, respectively. A best fit curve is also indicated on the plots.

III. FEED WETTING STUDIES

A. *Introduction*

Water on the surface of the reflector antenna or on the membrane covering the feed horn affects the electromagnetic wave propagation in several ways. The first way is absorption. The water absorbs microwave energy, reducing the magnitude of the wave after it propagates through the lossy dielectric medium of water. The second mechanism for signal loss is phase shift, as the wave propagates through the dielectric medium of water, which has a high dielectric constant. The wave front changes from the shape before it encountered the water, and now does not focus properly to a point. A third mechanism for signal loss is scattering of electromagnetic energy as the propagating electromagnetic wave experiences an impedance discontinuity at the air-water boundary. Water, with a high dielectric constant ($\varepsilon_r \sim 80$), has an impedance much different from that of free space, and will cause reflections or scattering from that different impedance surface.

The problem is further complicated because the water is not a uniform thickness across the wavefront. Hence the problem cannot be reduced to a simple one-dimensional electromagnetic dielectric slab boundary condition problem. Also, since the water droplets are generally small with respect to a wavelength ($\lambda_{27} = 1.1$ cm, $\lambda_{20} = 1.5$ cm in free space), Mie scattering coefficients must be used to estimate the amount of energy scattered by each droplet, as a function of droplet size.

B. *Experimental Results*

The receiving antenna in the ACTS propagation terminals is a 1.2-m offset parabolic reflector manufactured by Prodelin. Precipitation can wet or bead up on two surfaces, which will then affect the propagation measurements, as outlined above. The two surfaces are the surface of the offset parabolic reflector and a radome membrane covering the feed horn of the receiver. The angle of the feed membrane with respect to the horizon is approximately 36° plus the elevation angle of the line of sight to the ACTS satellite. Because of the low elevation angle of the Alaska APT (8°), the offset reflector is concave downward and vertically falling water cannot reach its surface. The feed membrane is at approximately 44° from the horizontal. Therefore, only wetting of the feed horn membrane will be considered. The problem is outlined in the following Powerpoint slides, and experimental results are shown in the last figure. The experimental feed wetting resulted in signal losses of 0.6 dB and 1.2 dB at each frequency for two different conditions of the feed membrane. The first condition was cold, resulting in a low surface tension. The feed membrane was then warmed, resulting in a higher surface tension.

SURFACE REACTIONS OF THE SESSILE DROP OF WATER ON A PLANE

- GOAL IS TO FIND THE ANGLE OF REPOSE (α) AS A FUNCTION OF THE MATERIAL OF THE PLANE

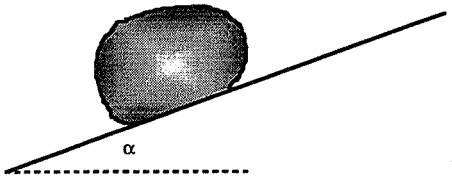

FORCE BALANCE ON THE SESSILE DROP

- TANGENTIAL COMPONENT OF GRAVITY FORCE = TANGENTIAL COMPONENT OF THE ADHESIVE FORCE BETWEEN THE SESSILE DROP AND THE MATERIAL OF THE PLANE
- THE FIRST FORCE IS THE TANGENTIAL GRAVITATIONAL FORCE, WHICH IS SIMPLY REPRESENTED AS $F_{grav,\ tangential} = F_{grav}\ \sin(\alpha)$

THE SECOND FORCE IS THE ADHESIVE FORCE = SURFACE TENSION FORCE

- SURFACE TENSION FORCE = SURFACE TENSION (γ in N/m) TIMES THE CIRCUMFERENCE OF THE CONTACT AREA (in m)

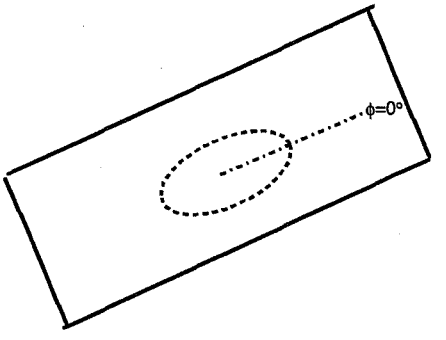

Alaska ACTS Propagation

TANGENTIAL SURFACE TENSION FORCE

- THE SURFACE TENSION FORCE TANGENTIAL TO THE PLANE IS THE SURFACE TENSION FORCE · COS(Θ), WHERE Θ IS THE CONTACT ANGLE
- CONTACT ANGLE $\Theta = \cos^{-1}[(\gamma_S - \gamma_{SL})/\gamma_L]$
  - γ_S = SURFACE TENSION OF THE SOLID PLANE
  - γ_L = SURFACE TENSION OF THE LIQUID (WATER)
  - γ_{SL} = INTERFACIAL TENSION BETWEEN SOLID AND LIQUID

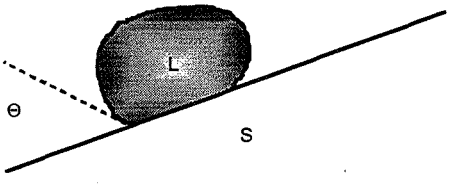

Alaska ACTS Propagation

CONTACT ANGLE

- CONTACT ANGLES Θ_r AND Θ_a, THE RECEDING AND ADVANCING CONTACT ANGLES RESPECTIVELY, ARE DIFFERENT DUE TO SURFACE ROUGHNESS AND SURFACE HETEROGENEITY. IF THE SURFACE IS VERY SMOOTH, THEN $\Theta_r = \Theta_a$, WHICH RESULTS IN VERY LITTLE TANGENTIAL SURFACE TENSION FORCE, AND THE DROPLET READILY RUNS OFF OF THE PLANE.

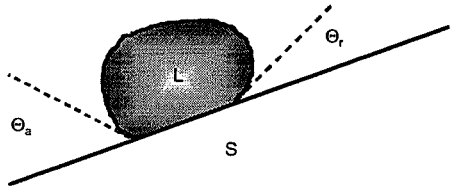

TANGENTIAL FORCE BALANCE EQUATION

- THE OVERALL TANGENTIAL ADHESIVE FORCE ON THE DROP IS THE INTEGRAL OF THE SURFACE TENSION FORCE AROUND THE 2π BOUNDARY CIRCUMFERENCE DOTTED WITH THE UNIT VECTOR ALONG THE SURFACE, a_ρ

$$F_{\text{adhesive, tang. } (\phi = 0 \text{ dir})} = \int_0^{2\pi} F_{ST}(\phi) \cdot \cos\Theta(\phi) \cdot \cos\phi \, d\phi \, a_{\rho o}$$

- THE ADHESIVE TANGENTIAL FORCE IS BALANCED WITH THE GRAVITATIONAL TANGENTIAL FORCE
  - IF THE SURFACE TENSION IS VERY STRONG, THE DROP MAY TEAR AS IT GETS LARGER AND RUN DOWN THE PLANE
  - IF THE SURFACE TENSION IS WEAKER, THE DROP "ROLLS" OR "SLIDES" DOWN THE PLANE

BOTTOM LINE

- DROPLET HEIGHT AND VOLUME AT THE ANGLE OF REPOSE ARE A FUNCTION OF THE CONTACT ANGLE
- AS THE HYDROPHOBIC MEMBRANE ON THE FEED HORN AGES, THE SURFACE BECOMES ROUGHER, THE SURFACE TENSION INCREASES, AND WATER STARTS TO BEAD ON THE MEMBRANE
- A THIN FILM OF WATER IS NOT THE PROBLEM
- MUCH THICKER BEADS OF WATER ARE THE PROBLEM

Alaska ACTS Propagation

EXPERIMENTAL MEASUREMENTS

- WATER WAS APPLIED TO FEED RADOME MEMBRANE 3 TIMES (INDICATED BY THE 3 ARROWS ON THE NEXT PLOT), AND DRIED OFF IN BETWEEN.
- THE SURFACE TENSION OF THE FEED MEMBRANE WAS THEN CHANGED (INCREASED) BY HEATING THE MEMBRANE, AND THE WATER WAS APPLIED 2 TIMES (INDICATED BY THE 2 ARROWS).
- 20 AND 27 BEACONS ARE ON TOP AND THE RADIOMETERS ON THE BOTTOM WITH THE 20 BEING THE TOP CURVE IN BOTH CASES.

Alaska ACTS Propagation

Fig. 1. The CCIR Scintillation Model

$$\sigma_{pre} = \frac{\sigma_{ref} \cdot f^{\frac{7}{12}} \cdot g(x)}{\sin(\theta)^{1.2}}$$

with

$$\sigma_{ref} = 0.0036 + 0.00013 \cdot N_{wet}$$

$$g(x) = \sqrt{3.86 \cdot (x^2+1)^{\frac{11}{12}} \cdot \sin\left(\left(\frac{11}{6}\right) \cdot \arctan\left(\frac{1}{x}\right)\right) - 7.08 \cdot x^{\frac{5}{6}}}$$

$$x = 0.00584 \cdot D_{eff}{}^2 \cdot \frac{k}{L}$$

$$D_{eff} = \sqrt{\eta} \cdot D$$

$$L = \frac{2 \cdot h}{\sqrt{\sin^2(\theta) + \left(\frac{2 \cdot h}{r_e}\right)} + \sin(\theta)}$$

$$N_{wet} = \frac{3730 \cdot H \cdot e_s}{(273+t)^2}$$

$$e_s = \frac{5854 \cdot \left(10^{\left(20 - \frac{2950}{(273+t)}\right)}\right)}{(273+t)^5}$$

σ_{pre}	is the predicted monthly average standard deviation of signal amplitude (dB)
L	is the effective turbulent path length (m)
h	is the turbulence height (m)
θ	is the elevation angle
D_{eff}	is the effective antenna diameter (m)
D	is the antenna diameter (m)
k	is the wave number (m^{-1})
η	is the antenna efficiency
r_e	is the effective earth radius=$8.5 10^6$ (m)
N_{wet}	is the wet refractivity (N units)
e_s	is the monthly average saturated water vapor pressure (mb)
t	is the monthly average surface temperature (°C)

Fig. 2. The Karasawa Scintillation Model

$$\sigma_x = \sigma_{x,ref} \cdot \eta_f \cdot \eta_\theta \cdot \eta_{D_a}$$

with

$$\sigma_{x,ref} = 0.15 + 0.0052 \cdot N_{wet} \qquad \eta_f = \left(\frac{f}{11.5}\right)^{0.45} \qquad \eta_\theta = \left(\frac{\cos ec(\theta)}{\cos ec(6.5°)}\right)^{1.3} \quad \theta > 5°$$

$$\eta_{D_a} = \sqrt{\frac{G(D_a)}{G(7.6)}}$$

$$N_{wet} = \frac{3730 \cdot H \cdot e_s}{(273+t)^2}$$

$$e_s = 6.11 \cdot \exp\left(\frac{19.7 \cdot t}{(t+273)}\right)$$

$$R = 0.75 \cdot \left(\frac{D_a}{2}\right)$$

$$G(R) = 1.0 - 1.4 \cdot \left(\frac{R}{\sqrt{\lambda \cdot L}}\right) \quad \text{for} \quad 0 \le \frac{R}{\sqrt{\lambda \cdot L}} \le 0.5$$

$$L = \frac{2 \cdot h}{\sqrt{\sin^2(\theta) + \left(\frac{2 \cdot h}{r_e}\right)} + \sin(\theta)}$$

σ_x	is the predicted monthly average standard deviation of signal amplitude (dB)
$\sigma_{x,ref}$	is the unscaled predicted monthly average standard deviation of signal amplitude (dB)
N_{wet}	is the wet refractivity (N units)
η_f	is the frequency scaling, f is the frequency (GHz)
η_θ	is the elevation angle scaling, θ is the elevation angle
η_{Da}	is the antenna diameter scaling, D_a is the antenna diameter (m)
H	is the monthly average relative humidity (%)
e_s	is the monthly average saturated water vapour pressure (mb)
t	is the monthly average surface temperature (°C)
G(R)	is the antenna aperture averaging factor
R	is the effective radius of circular aperture (m)
L	is the effective turbulent path length (m)
h	is the turbulence height (2000 m)
r_e	is the effective earth radius=$8.5 10^6$ (m)

Fig. 3. Variation in Mean Hourly Standard Deviation
December, 1993 to November, 1994

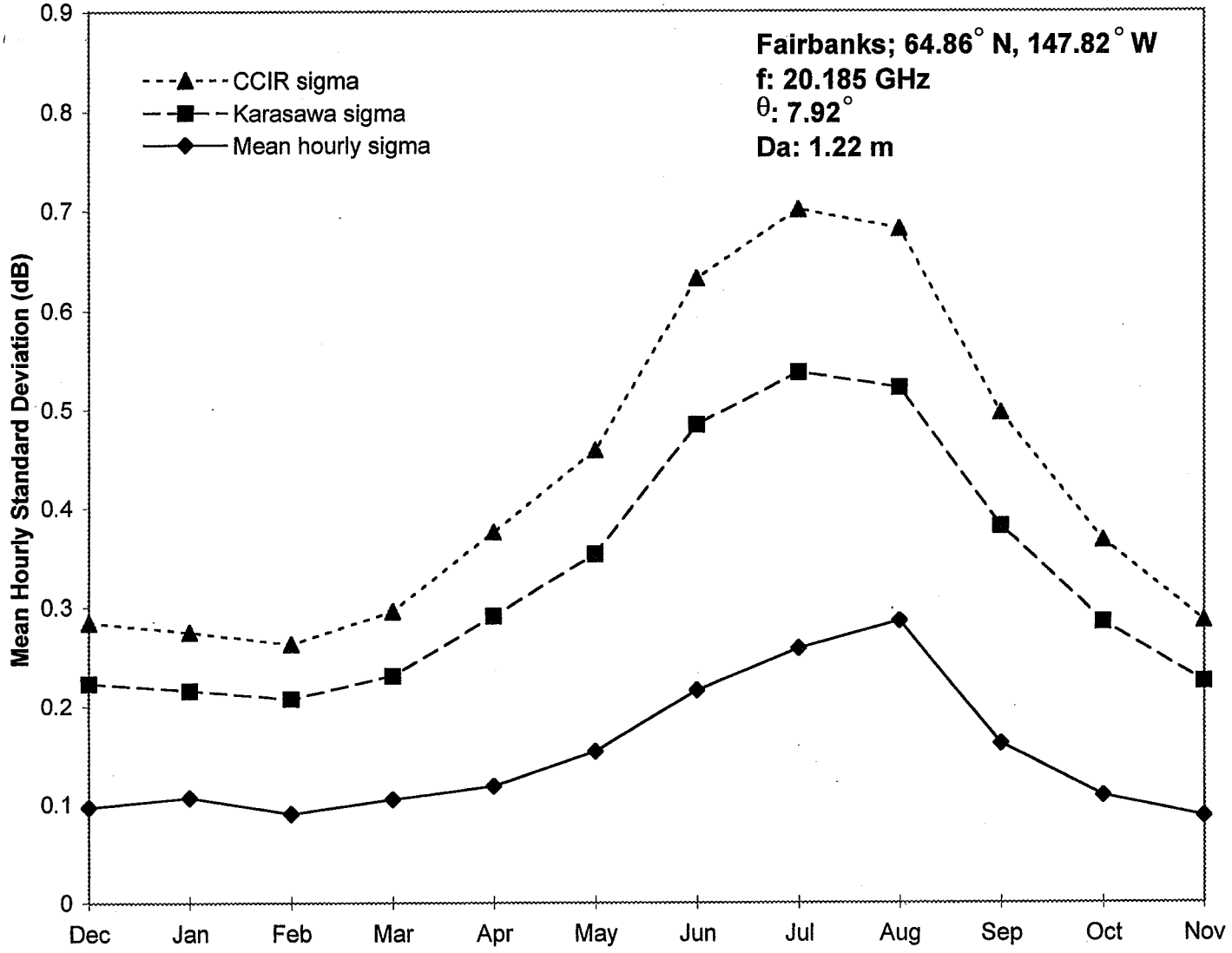

Fig. 4. Variation in Mean Hourly Standard Deviation
December, 1993 to November, 1994

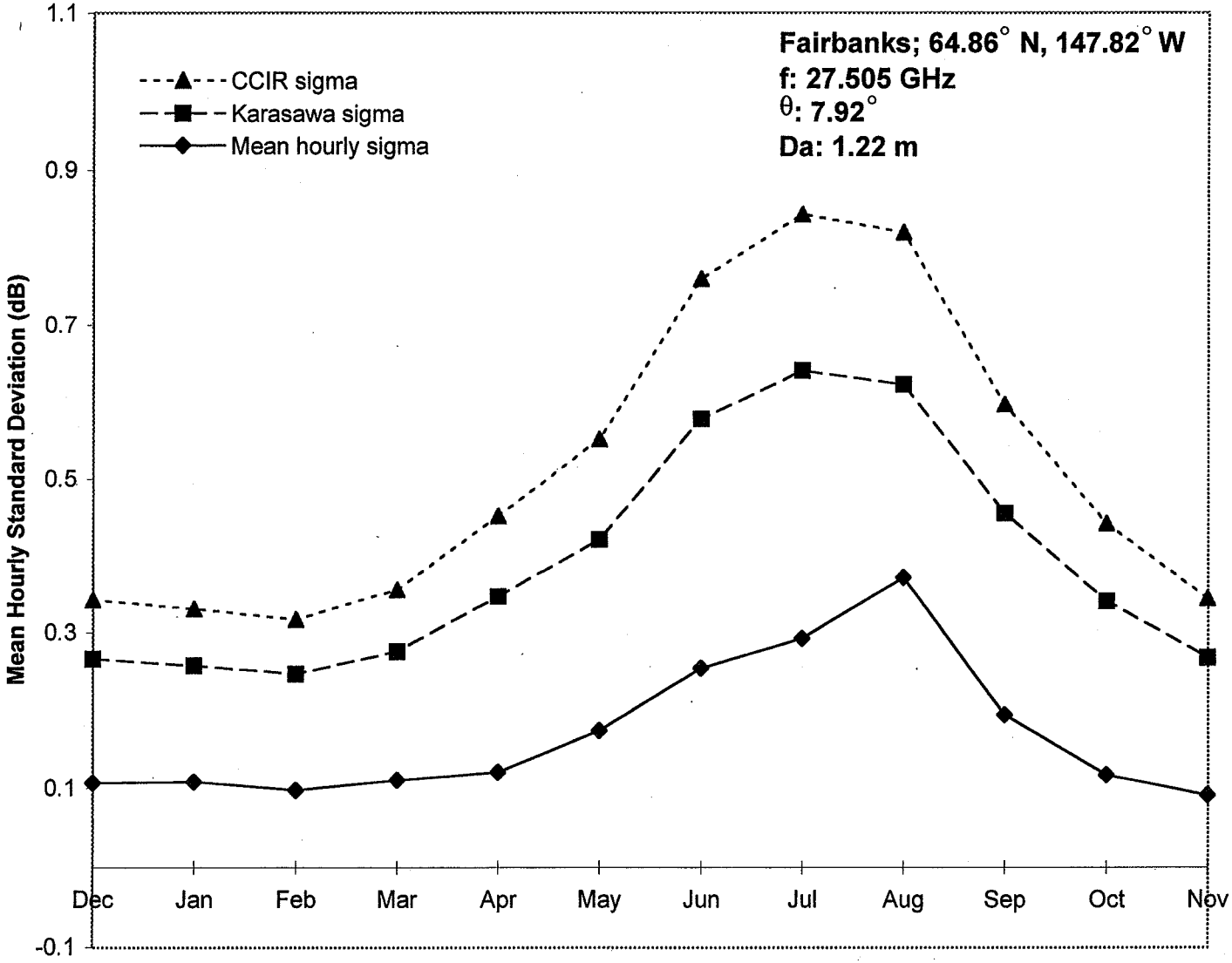

Fig. 5. Kolmogorov-Smirnov Test Significance Level
December, 1993 to November, 1994

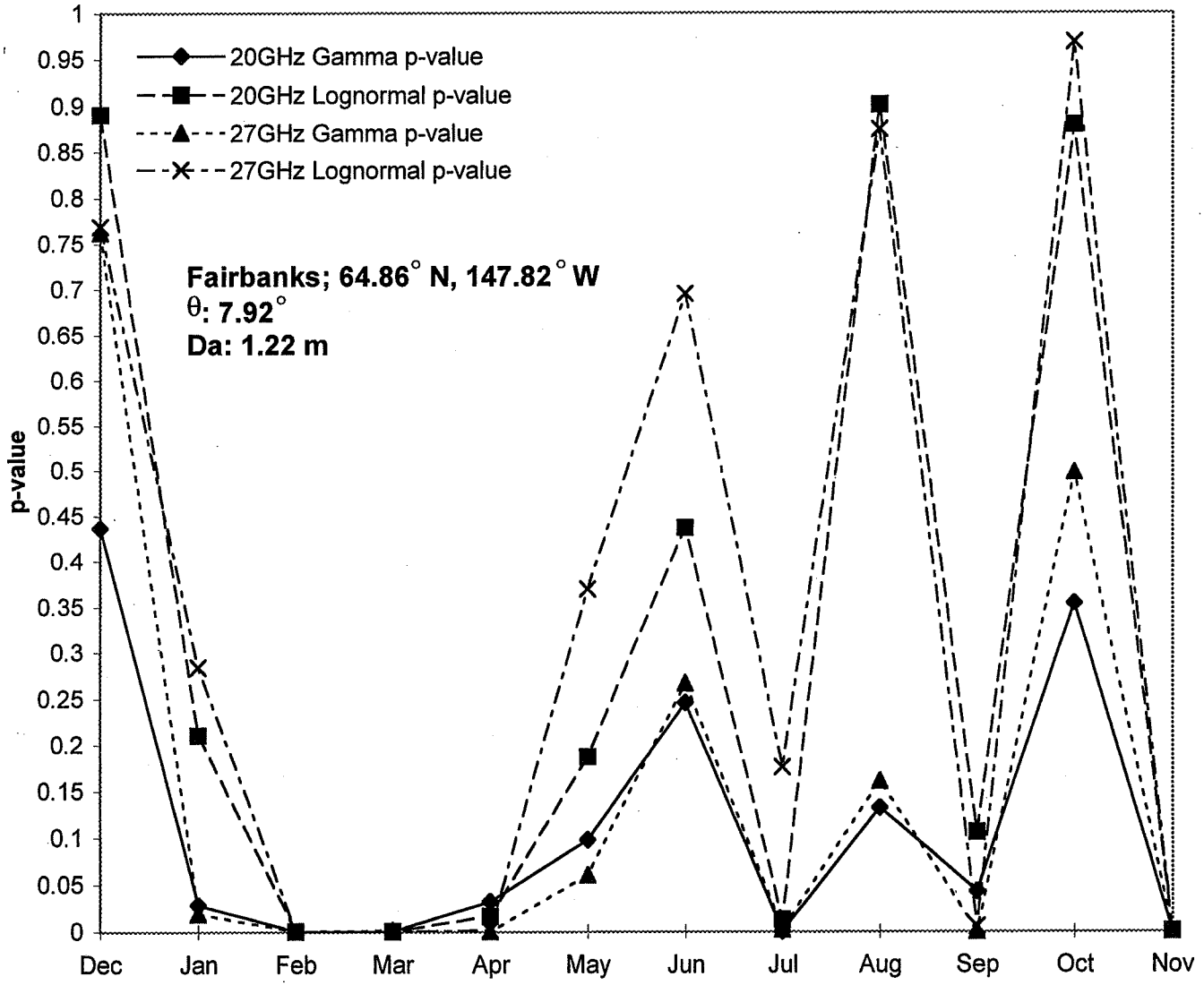

Fig. 6. Relationship Between Mean Squared and Variance of Hourly Standard Deviation December, 1993 to November, 1994

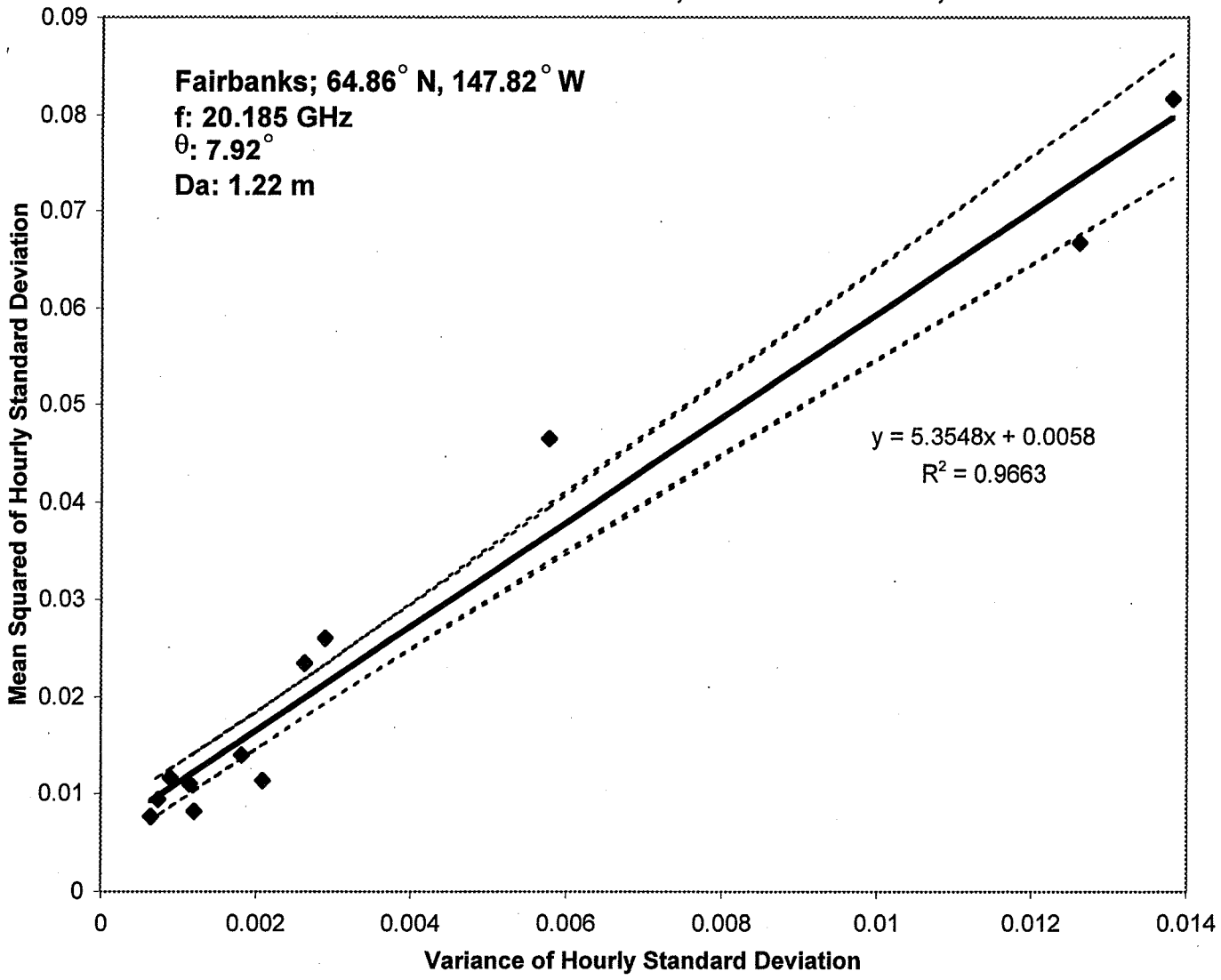

Fig. 7. Relationship Between Mean Squared and Variance of Hourly Standard Deviation December, 1993 to November, 1994

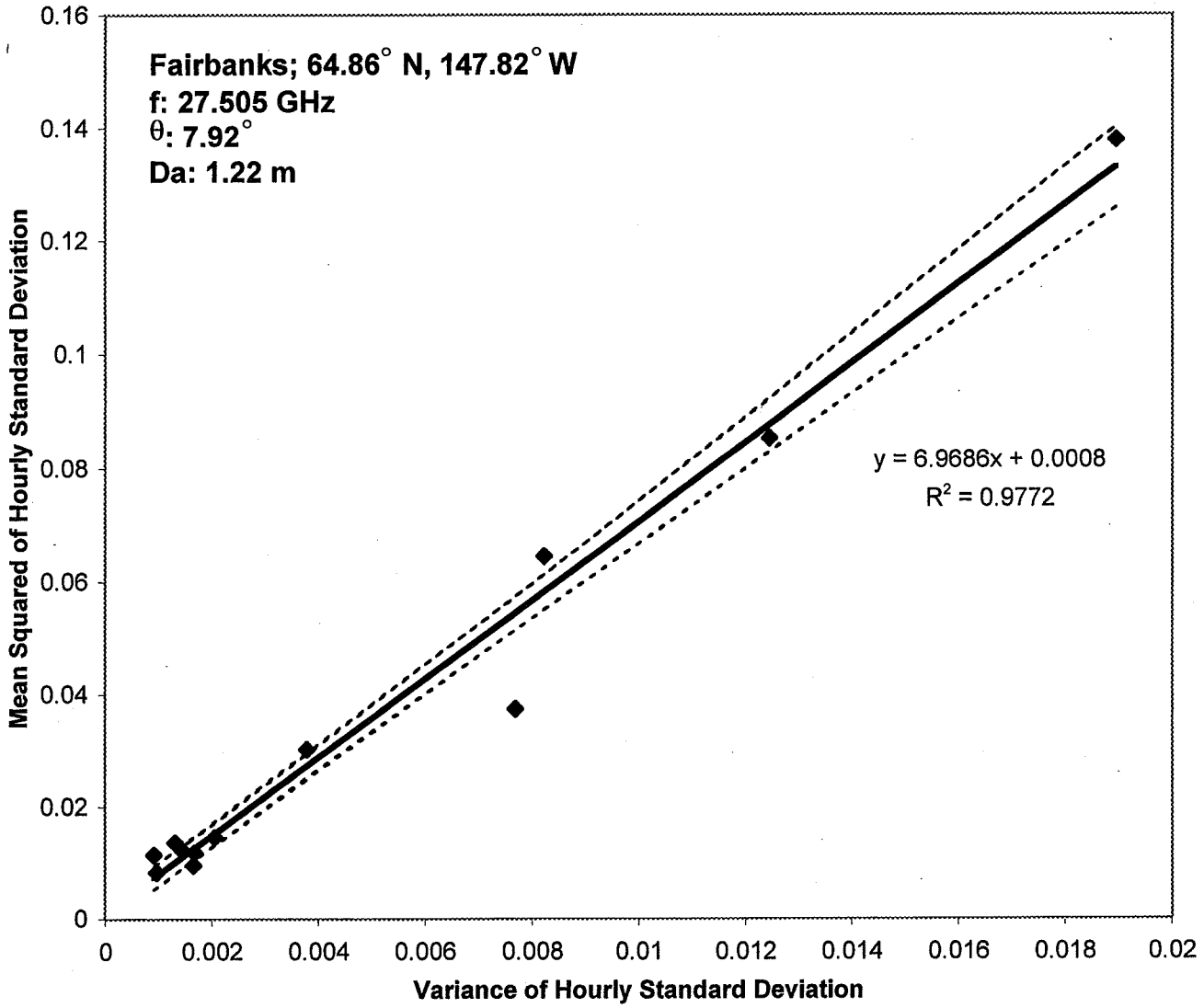

Fig.8. Linear Regression of Nwet and Mean Hourly Standard Deviation
December, 1993 to November, 1994

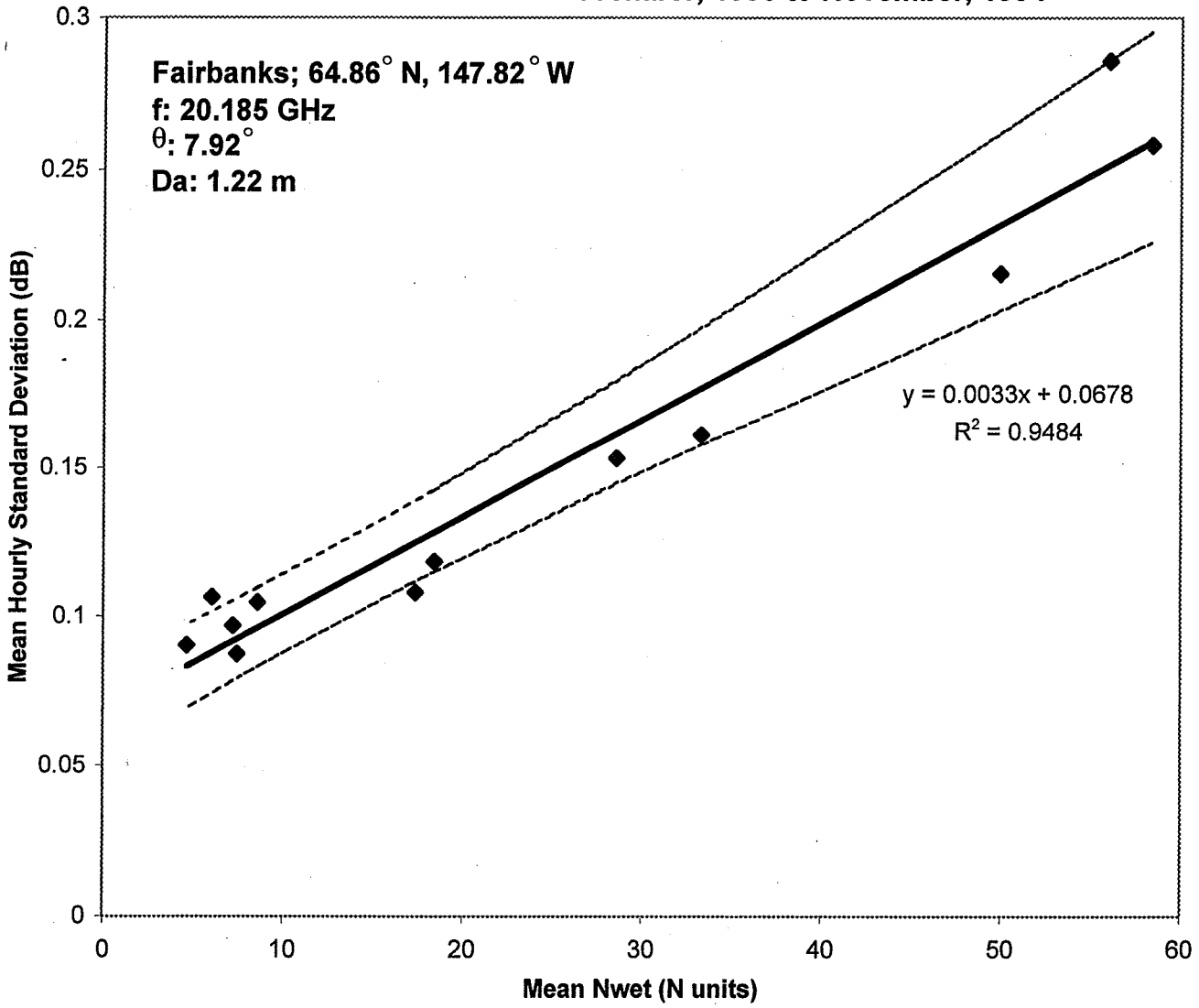

Fig. 9. Linear Regression of Nwet and Mean Hourly Standard Deviation December, 1993 to November, 1994

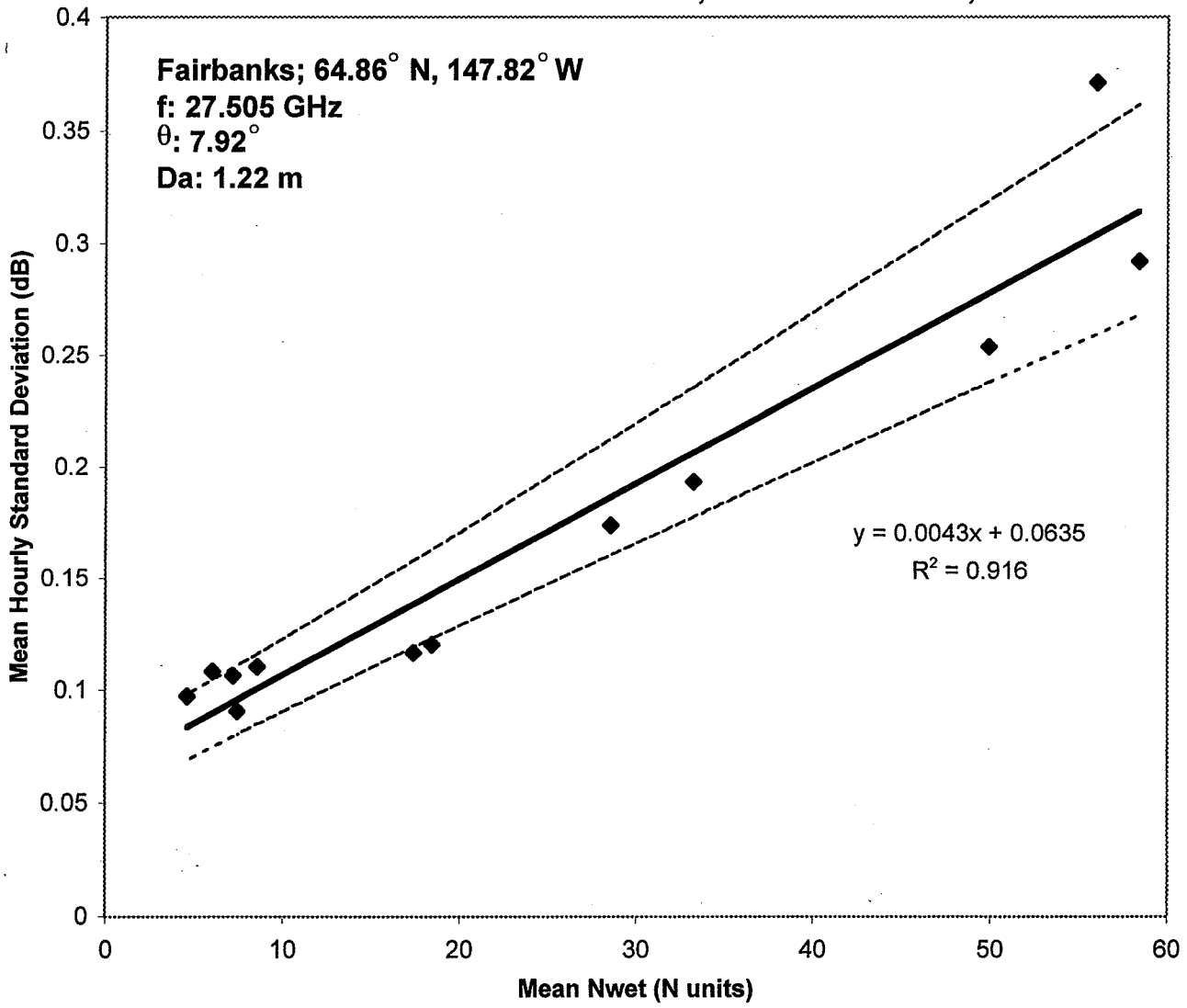

Fig.10. One Minute Standard Deviation Percent of Time Function
December, 1993 to November, 1994

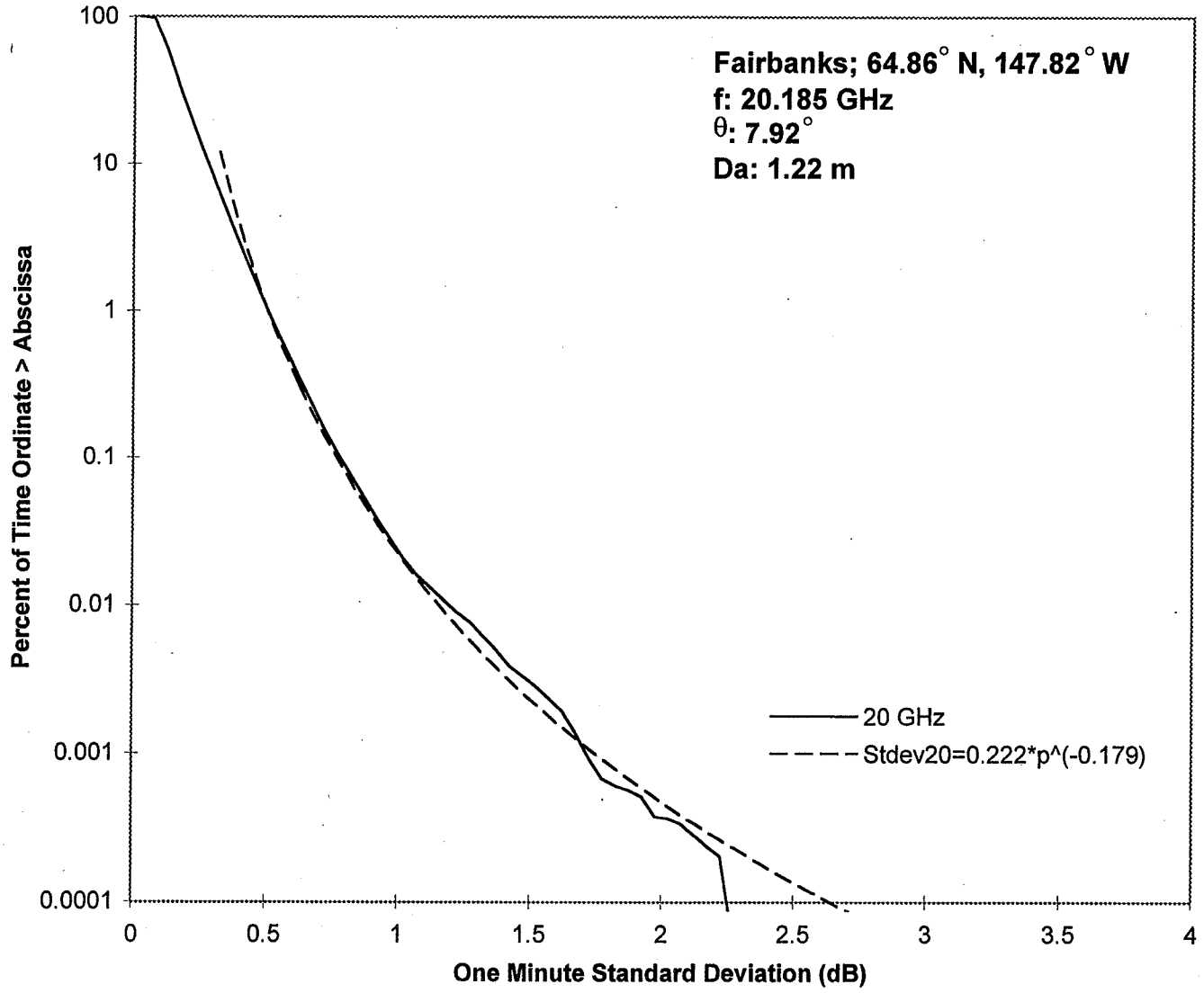

Fig. 11. One Minute Standard Deviation Percent of Time Function
December, 1993 to November, 1994

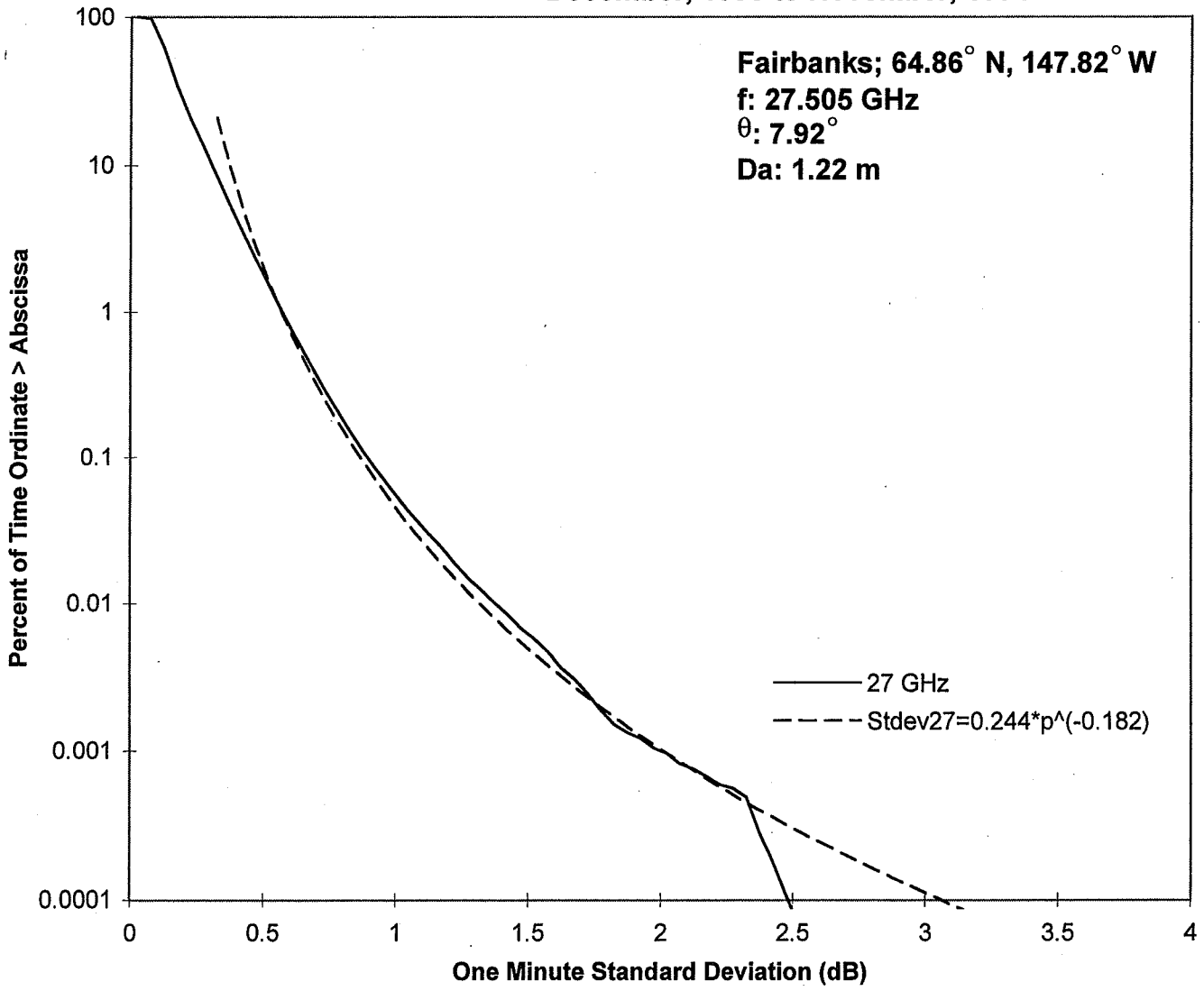

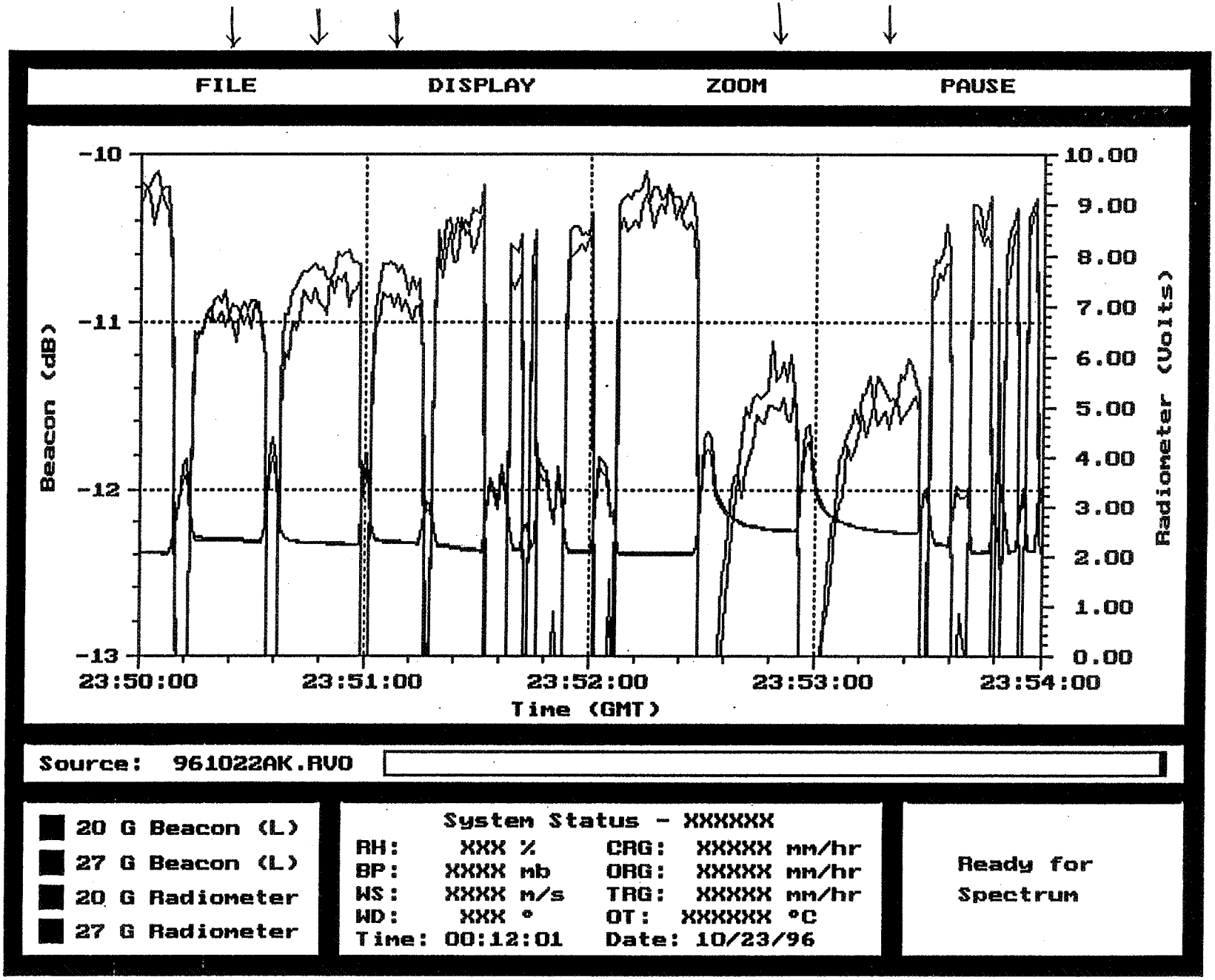

TOP = 27
BOTTOM = 20

THE UBC/ACTS EXPERIMENT

Status Report

November, 1996

by: M. Kharadly
B. Dow

DEPARTMENT OF ELECTRICAL ENGINEERING

FACULTY OF APPLIED SCIENCE

THE UNIVERSITY OF BRITISH COLUMBIA

OUTLINE

I. SUMMARY

Operation of Terminal
Moisture on Antenna Surfaces

II. BACKGROUND

Initial Investigations
Initial Model
Discussion

III. RECENT ACTIVITIES

Augmenting Adjusted Data Base
Wetting Experimentation
New Approach

IV. FUTURE ACTIVITIES

I. SUMMARY

Operation of Terminal

There is little to report concerning the operation and maintenance of the ACTS terminal apart from a most recent failure of the (new) feed horn membrane. This, of course, requires immediate action, as moisture inside the membrane means inaccurate data and probably unreliable calibration.

Moisture on Antenna Surfaces

The most pressing issue, requiring much attention, has been that of the effect of moisture on the antenna surfaces during rain events. The conclusion we have reached is that the attenuation data so far collected are inherently flawed, and seriously so. The data are flawed in the sense that they do not represent path attenuation, but inseparably include a random and significant component due to moisture on the antenna surfaces during rain events. This component is dependent on antenna type and elevation angle, amongst other factors. Analysis of these data as they stand, which we have done, is in our opinion of no use; such analysis necessarily yields meaningless results, which could be very misleading.

The type of antenna used in the receiving terminals, a parabolic dish with off-axis feed horn, where both dish and horn apertures are facing upwards and subject to being wetted during rain events, is clearly unsuitable for this type of experiment. Most of the excess attenuation due to antenna surface wetting results from the wet membrane covering the aperture of the feed horn.

The exact instantaneous values pertaining to path attenuation alone are irretrievable. It may be possible to obtain approximate corrected values. Some initial effort has been done in this direction; we do not consider it to be entirely satisfactory, however. Further work is needed and is currently under way.

The effect of moisture on the antenna surfaces on calibration has not yet been studied.

It is stressed that, in using the ACTS data for modeling or system design, it would be unwise to ignore the aforementioned effect in the ACTS propagation experiments. This is particularly important at lower values of measured attenuation (less than 10 dB), where these values could be grossly in error, if path attenuation alone is desired or if a different type of antenna is used.

II. BACKGROUND

At the Oklahoma meeting, last November, John Beaver reported significant discrepancies between rain attenuation derived from measurements using the CHILL radar and those derived using the Colorado ACTS terminal.

The ensuing discussions at that meeting were unsatisfactory. Because of the seriousness of the matter and its implications, however, I decided, on my own initiative, to investigate the matter further — did some calculations, and in early 1996, installed a system for wetting antenna surfaces with showers simulating rain of various intensity and drop size, conducted some initial experiments and performed preliminary analysis.

Initial Investigations

The calculations, which used simplifying assumptions, revealed that indeed significant attenuation could occur due to water films on the antenna surfaces, most of it from the membrane covering the feed horn aperture. This was confirmed experimentally, where the average attenuation reached maximum values of approximately 3 & 4 dB at the 20 GHz and 27 GHz, respectively, with much higher instantaneous attenuations values. These average values decreased as the shower intensity was reduced.

Initial Model

In a first attempt to correct for this effect, the results of these initial experiments were incorporated in a model that related the average attenuation due to antenna surface wetting, A_w, to the instantaneous measured (total) attenuation in a rain event, A_t. The model is of the form:

$$A_w = \alpha (1 - e^{-\beta A t})$$

where α and β are adjustable parameters. A rather rough, but nearer to the truth estimate of path attenuation, A_p, is given by

$$A_p = A_t - A_w$$

The adjusted instantaneous attenuation values using this model (with $\alpha = 3$ & 4 and $\beta = 1/3$ & 1/4 for the 20 GHz and 27 GHz, respectively) were established for the first two years of data.

Discussion

Although the above procedure for "correcting" the measured data was a step in the right direction, it is by no means entirely satisfactory:

(i) Relating the attenuation due to the effect of antenna surface wetting to the total measured attenuation (a reasonable measure) involves certain uncertainties, the most obvious of which is that the "degree" of antenna wetting (at the terminal) may not be representative of the rain characteristics along the path.

(ii) The correction is based on adjusting the instantaneous attenuation data by using estimated average attenuation values due to antenna surface wetting.

(iii) The model used may not provide the best description of the dependence of A_w on A_t. In addition, its parameters are based on initial experiments which were not decisive and whose values are only approximate.

Thus, there appears to be a need to devise other procedures for the purpose of correcting the measured data.

III. RECENT ACTIVITIES

Augmenting Adjusted Data Base

The first activity was to augment the adjusted data according to the above model by also working out those for worst-month characteristics. All adjusted and unadjusted characteristics were presented at the Fairbanks meeting in June.

Wetting Experiment

The second activity has been to improve the "wetting" experimentation. For this purpose, new, more controllable sprayers have been installed together with a pump to boost the pressure in the water line. Extensive wetting experiments have been conducted under various conditions of shower intensity and drop size, and wind speed and direction. It is virtually impossible however, to quantize the results of these experiments because of their very nature. It is, however, useful to study the results of these experiments and obtain some general characteristics of the attenuation due to wetting; this would help in understanding the mechanism of water collecting on the surfaces and hence how ot deal with the problem. We are in the process of analyzing these measurements.

New Approach

We are also pursuing a different approach, which has just been initiated, for correcting the measured data to circumvent some of the drawbacks of the previously used approach and model. It requires the detailed scrutiny and analysis of individual rain events (time consuming). It is based on: (a) comparing estimated average attenuation values over an event with average measured values, (b) comparing certain instantaneous attenuation values of the 20 and 27 GHz beacons, and (c) comparing short-period attenuation averages of the two beacons. Some assumptions, which have yet to be tested, are involved.

IV. FUTURE ACTIVITIES

(i) To find a satisfactory method to correct the three years of data we already have.

(ii) To investigate ways to circumvent the problem of wet antenna surfaces, including the development of new types of antennas for application at Ka-band and higher frequencies.

Page intentionally left blank

Ka-Band Propagation Studies Using the ACTS Propagation Terminal and the CSU-CHILL Multiparameter Radar

Experimenters

Colorado State University

Department of Electrical Engineering

Fort Collins, CO 80523

Investigators

V.N. Bringi, Professor

John Beaver

ACTS Propagation Studies Workshop

(APSW IX)

November 19-20, 1996

Herndon, VA

Outline

- CSU-APT Status Report
  - Terminal Update
  - Preprocessing Update
- CSU-APT Attenuation Data
  - 1996 Data
  - Comparisons with 1994 and 1995 data
- Results from Radar Propagation Model (1996)
  - July 5, 1996 (Stratiform event)
  - July 6, 1996 (Convective event)
- Antenna Wetting Results
  - Before applying hydrophobic solution
  - After applying hydrophobic solution
  - Maximum attenuation due to 'wetting effect'
  - Attenuation table

CSU-APT Status Report

- Terminal Update
  - CSU-APT was relocated on May 28, 1996, to a site 13 km south of the CSU-CHILL radar.
    * to avoid near field effects in radar data
    * to lower the elevation angles used by the radar
  - D. Westenhaver visited site on July 22, 1996
    * new hard drive installed
    * fan units were replaced in receiver box

- Preprocessing Update
  - December 1995 through August 1996 have been preprocessed using ACTSPP69
    * December 1995 - March 1996 have been sent to the data center in Texas
    * April 1996 through August 1996 are completed but have not yet been sent to the data center.

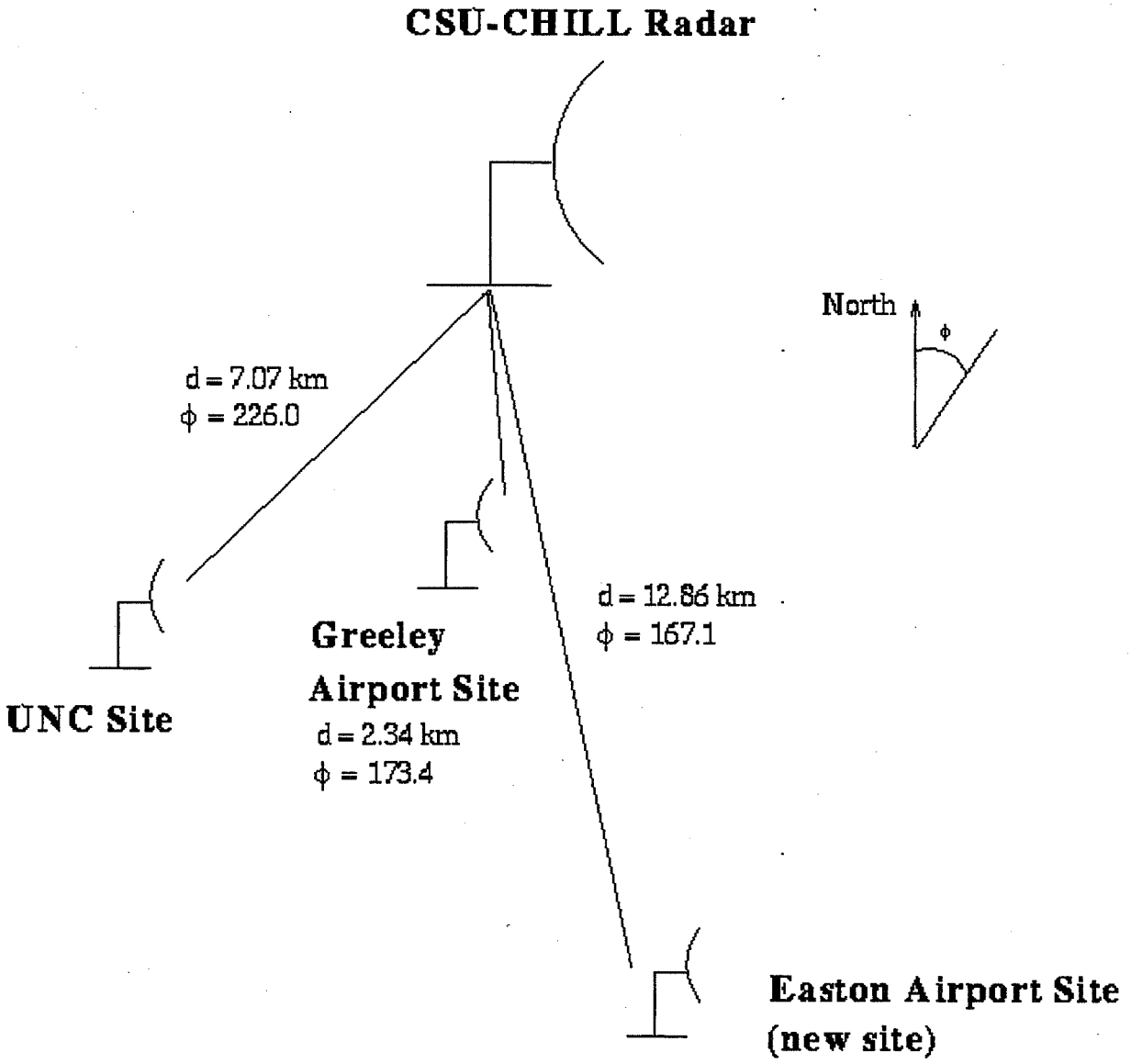
CSU-CHILL Radar
North
ϕ
d = 7.07 km
ϕ = 226.0
d = 12.86 km
ϕ = 167.1
UNC Site
Greeley
Airport Site
d = 2.34 km
ϕ = 173.4
Easton Airport Site
(new site)

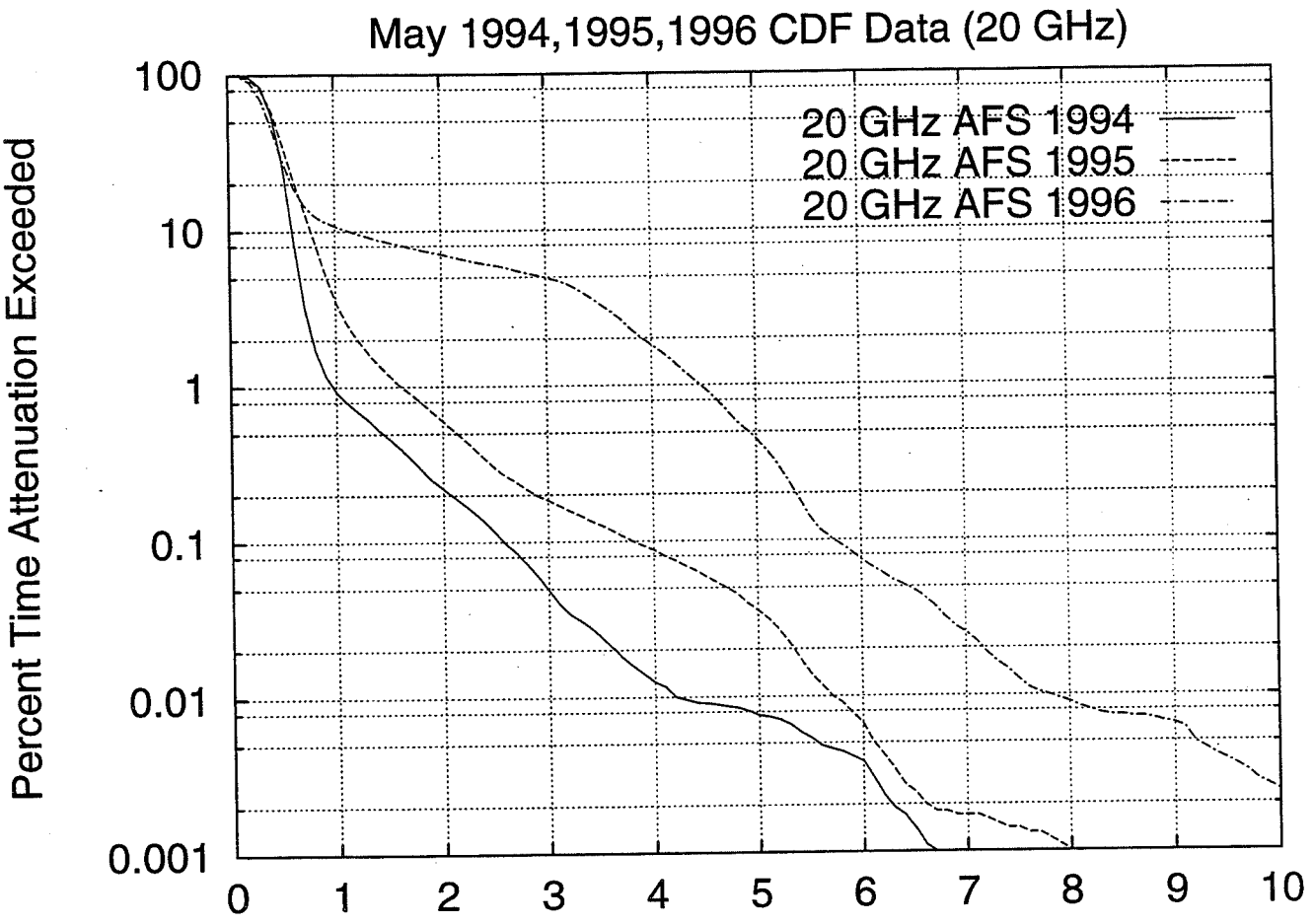
May 1994,1995,1996 CDF Data (20 GHz)
Percent Time Attenuation Exceeded
100
10
1
0.1
0.01
0.001
0
1
2
3
4
5
6
7
8
9
10
20 GHz AFS 1994
20 GHz AFS 1995
20 GHz AFS 1996

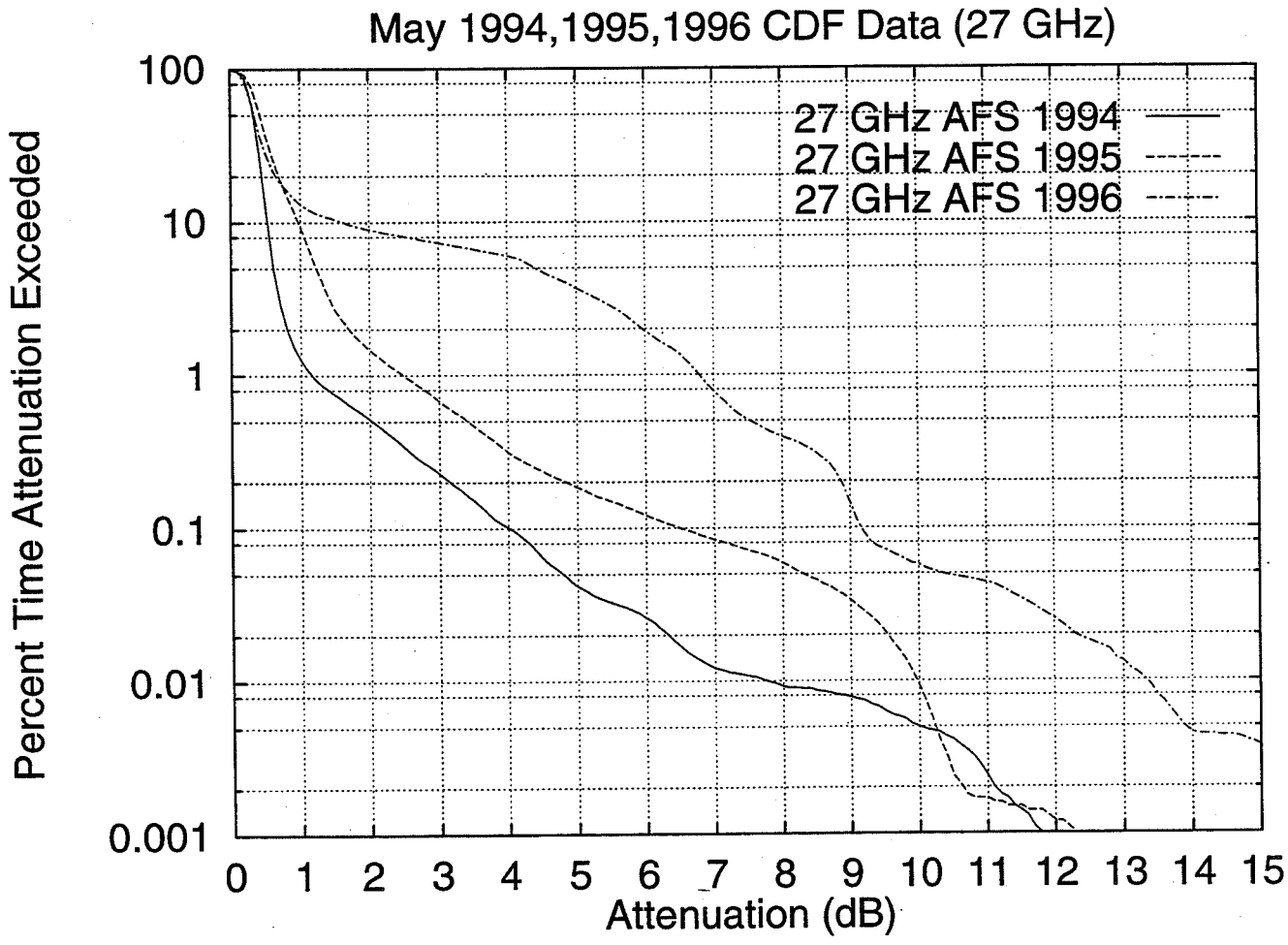
May 1994,1995,1996 CDF Data (27 GHz)
Percent Time Attenuation Exceeded
100
10
1
0.1
0.01
0.001
0
1
2
3
4
5
6
7
8
9
10
11
12
13
14
15
Attenuation (dB)
27 GHz AFS 1994
27 GHz AFS 1995
27 GHz AFS 1996

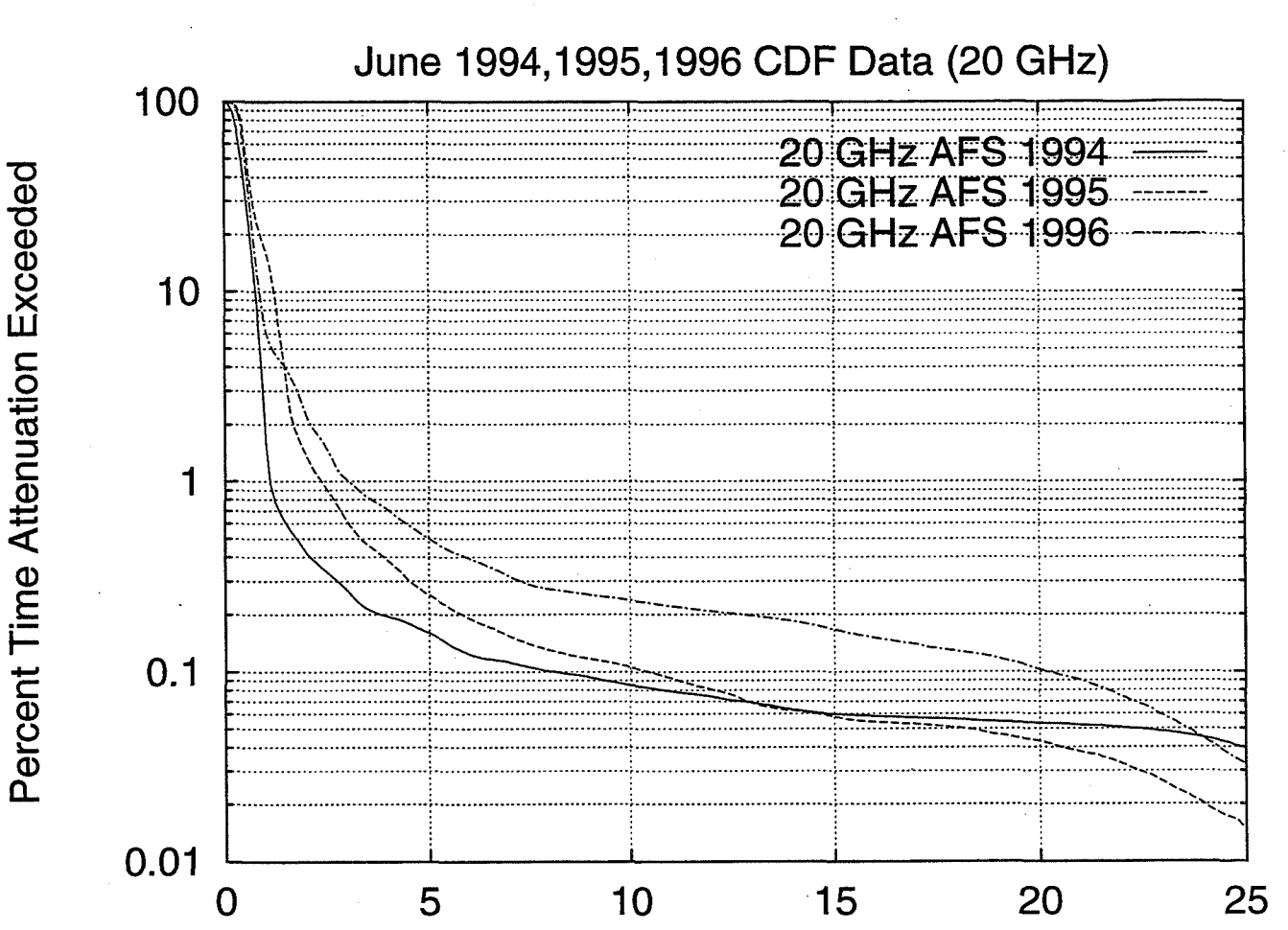
June 1994,1995,1996 CDF Data (20 GHz)
Percent Time Attenuation Exceeded
100
10
1
0.1
0.01
0
5
10
15
20
25
20 GHz AFS 1994
20 GHz AFS 1995
20 GHz AFS 1996

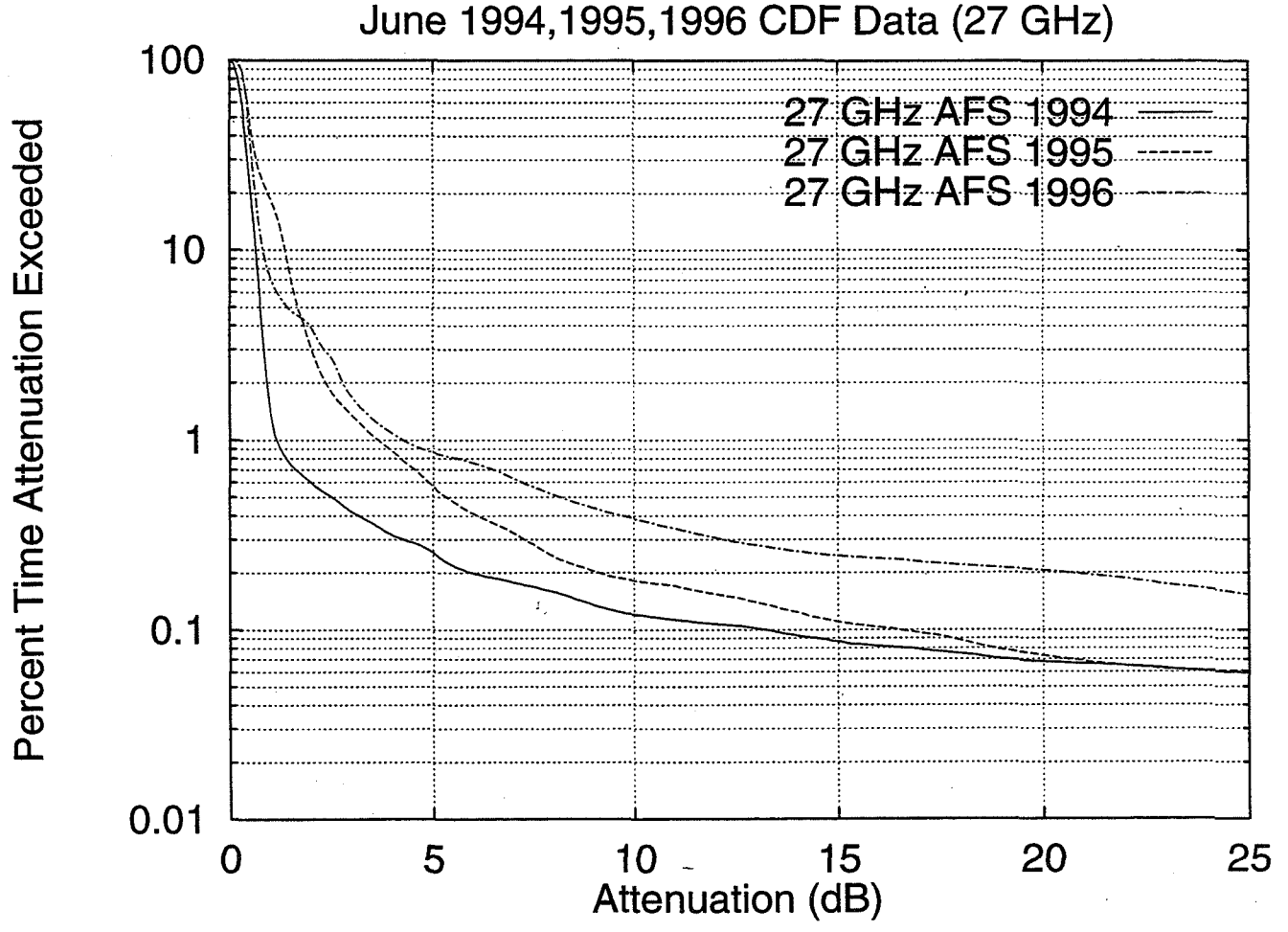
June 1994,1995,1996 CDF Data (27 GHz)
Percent Time Attenuation Exceeded
100
10
1
0.1
0.01
0
5
10
15
20
25
Attenuation (dB)
27 GHz AFS 1994
27 GHz AFS 1995
27 GHz AFS 1996

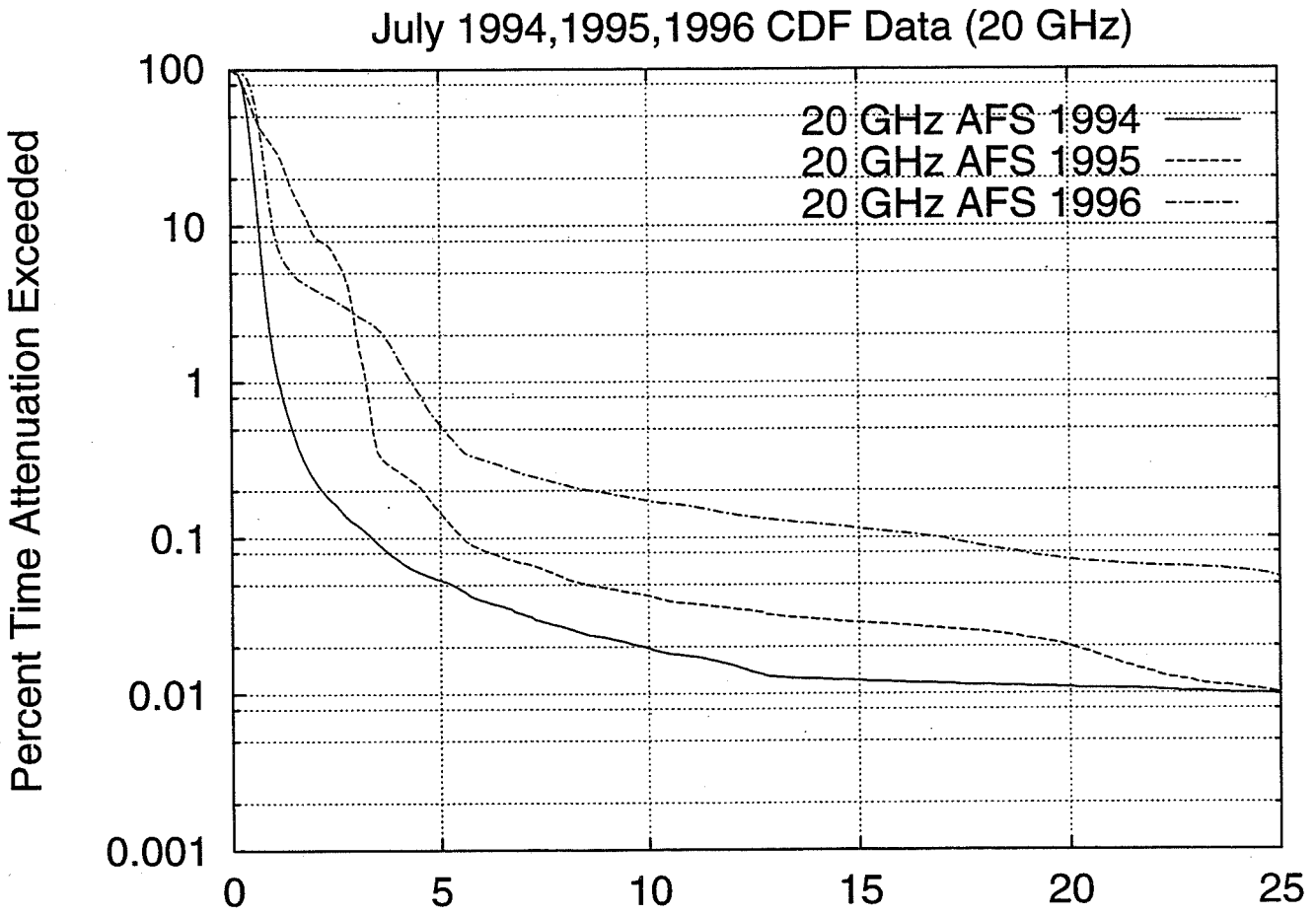
July 1994,1995,1996 CDF Data (20 GHz)
Percent Time Attenuation Exceeded
100
10
1
0.1
0.01
0.001
0
5
10
15
20
25
20 GHz AFS 1994
20 GHz AFS 1995
20 GHz AFS 1996

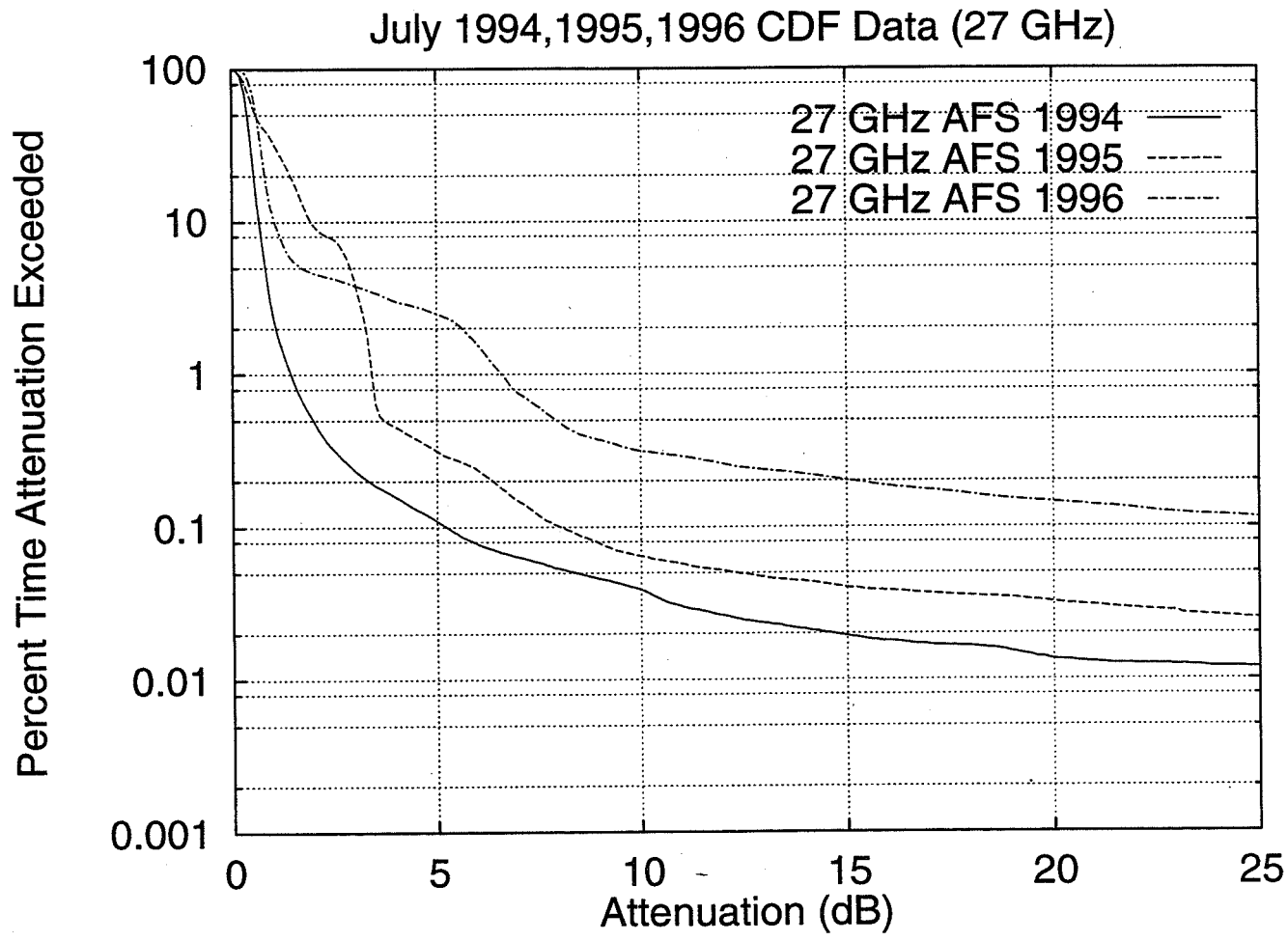
July 1994,1995,1996 CDF Data (27 GHz)
Percent Time Attenuation Exceeded
100
10
1
0.1
0.01
0.001
0
5
10
15
20
25
Attenuation (dB)
27 GHz AFS 1994
27 GHz AFS 1995
27 GHz AFS 1996

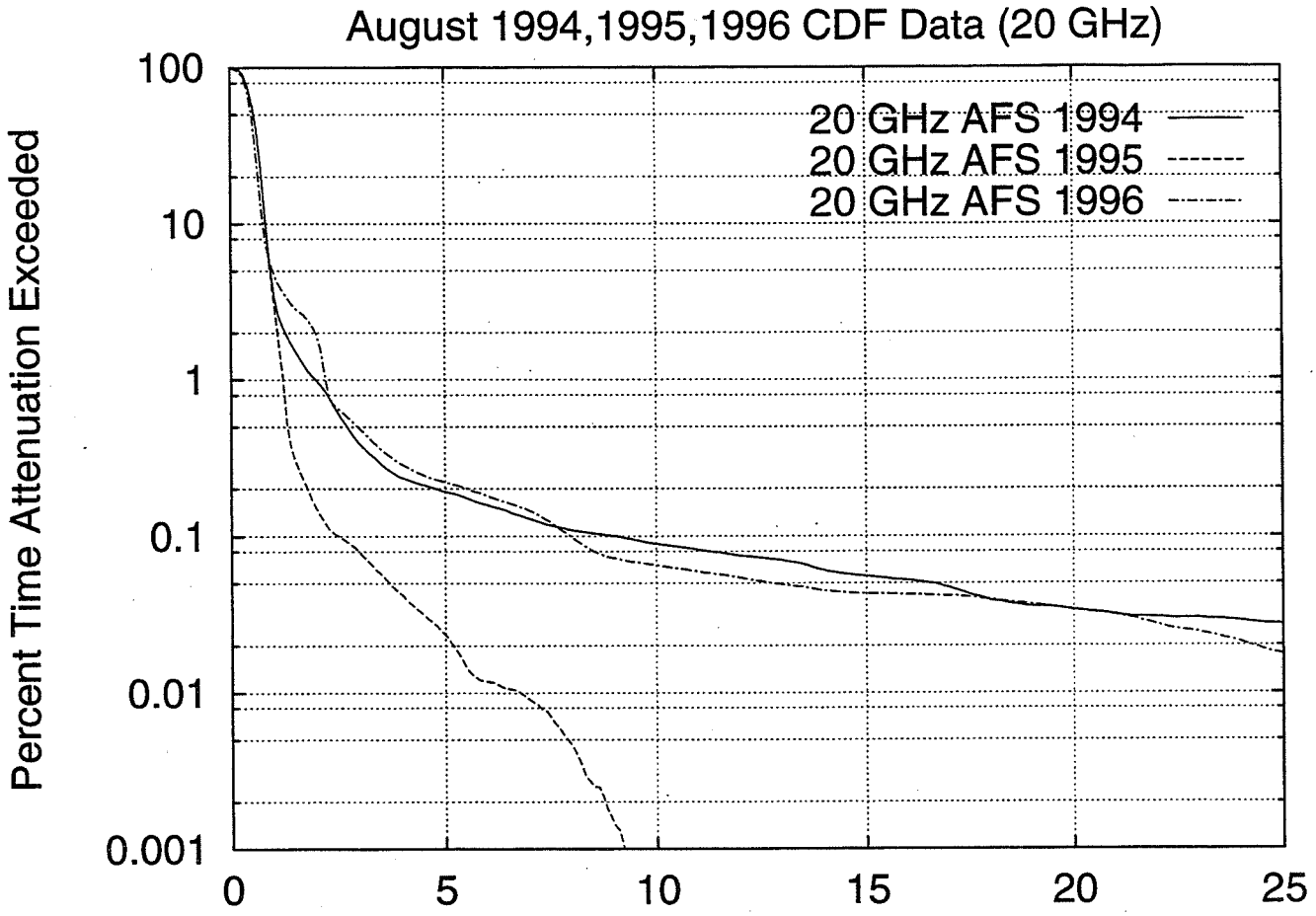
August 1994,1995,1996 CDF Data (20 GHz)
Percent Time Attenuation Exceeded
100
10
1
0.1
0.01
0.001
0
5
10
15
20
25
20 GHz AFS 1994
20 GHz AFS 1995
20 GHz AFS 1996

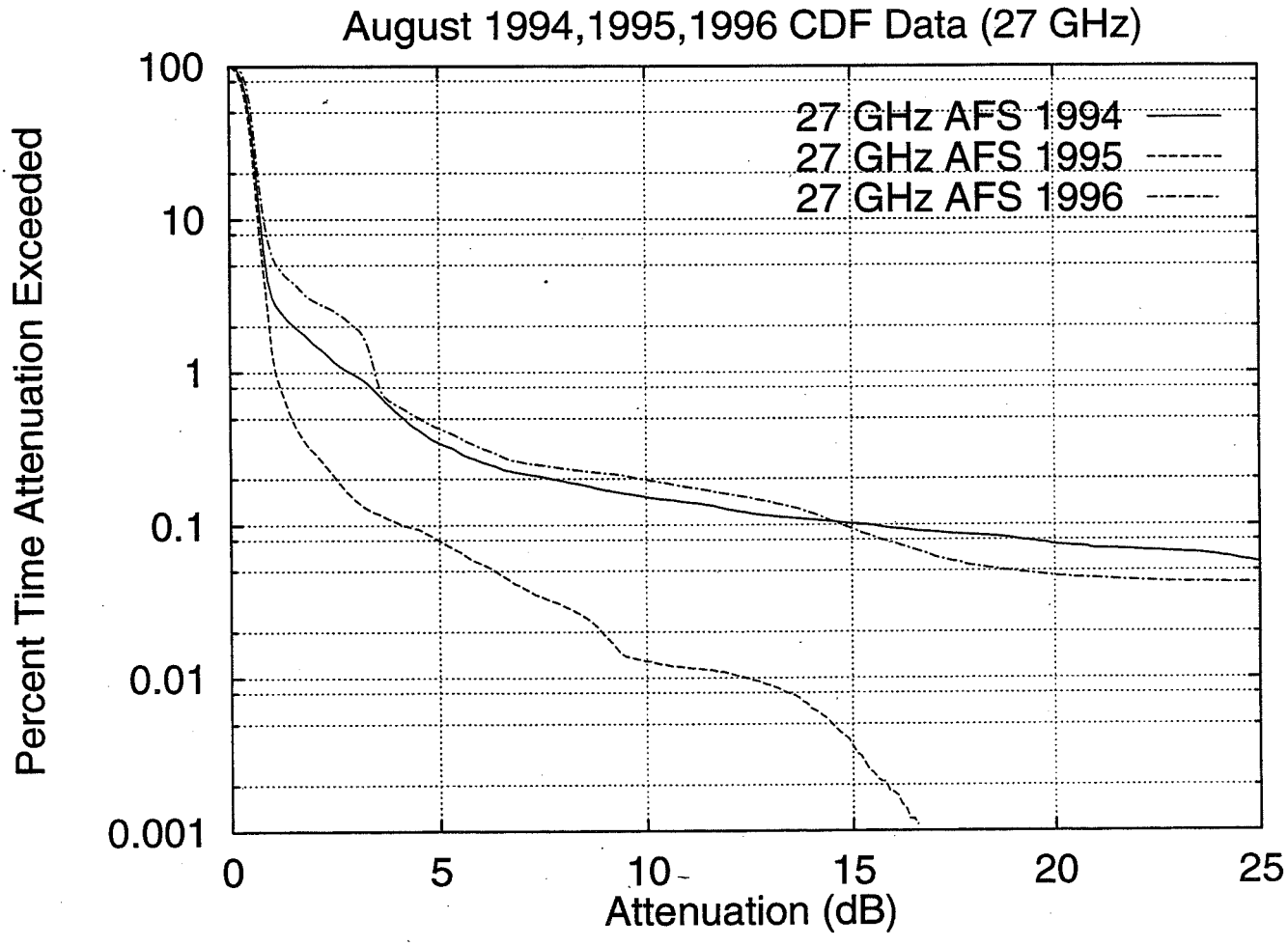
August 1994,1995,1996 CDF Data (27 GHz)
Percent Time Attenuation Exceeded
100
10
1
0.1
0.01
0.001
0
5
10
15
20
25
Attenuation (dB)
27 GHz AFS 1994
27 GHz AFS 1995
27 GHz AFS 1996

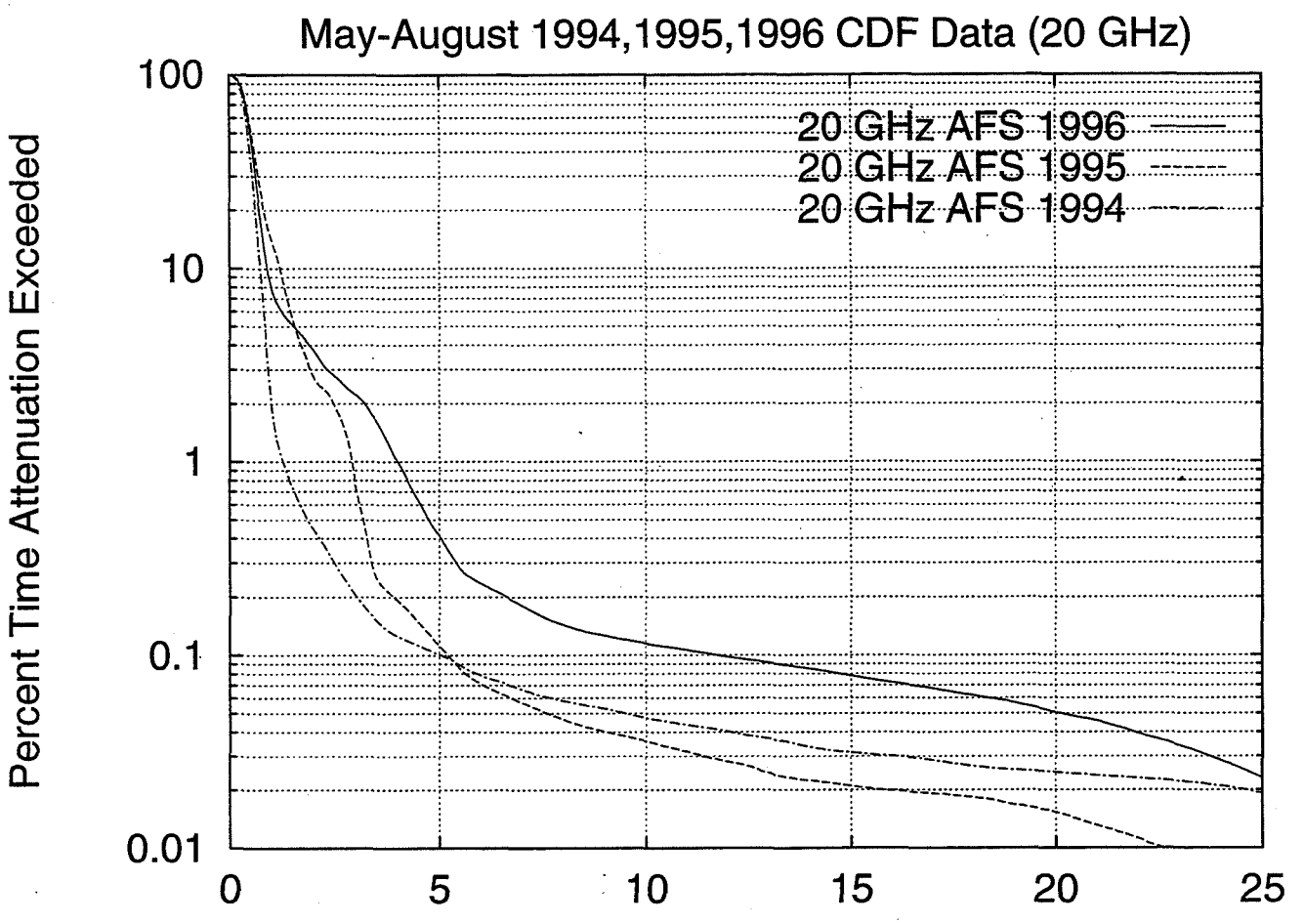
May-August 1994,1995,1996 CDF Data (20 GHz)
Percent Time Attenuation Exceeded
100
10
1
0.1
0.01
0
5
10
15
20
25
20 GHz AFS 1996
20 GHz AFS 1995
20 GHz AFS 1994

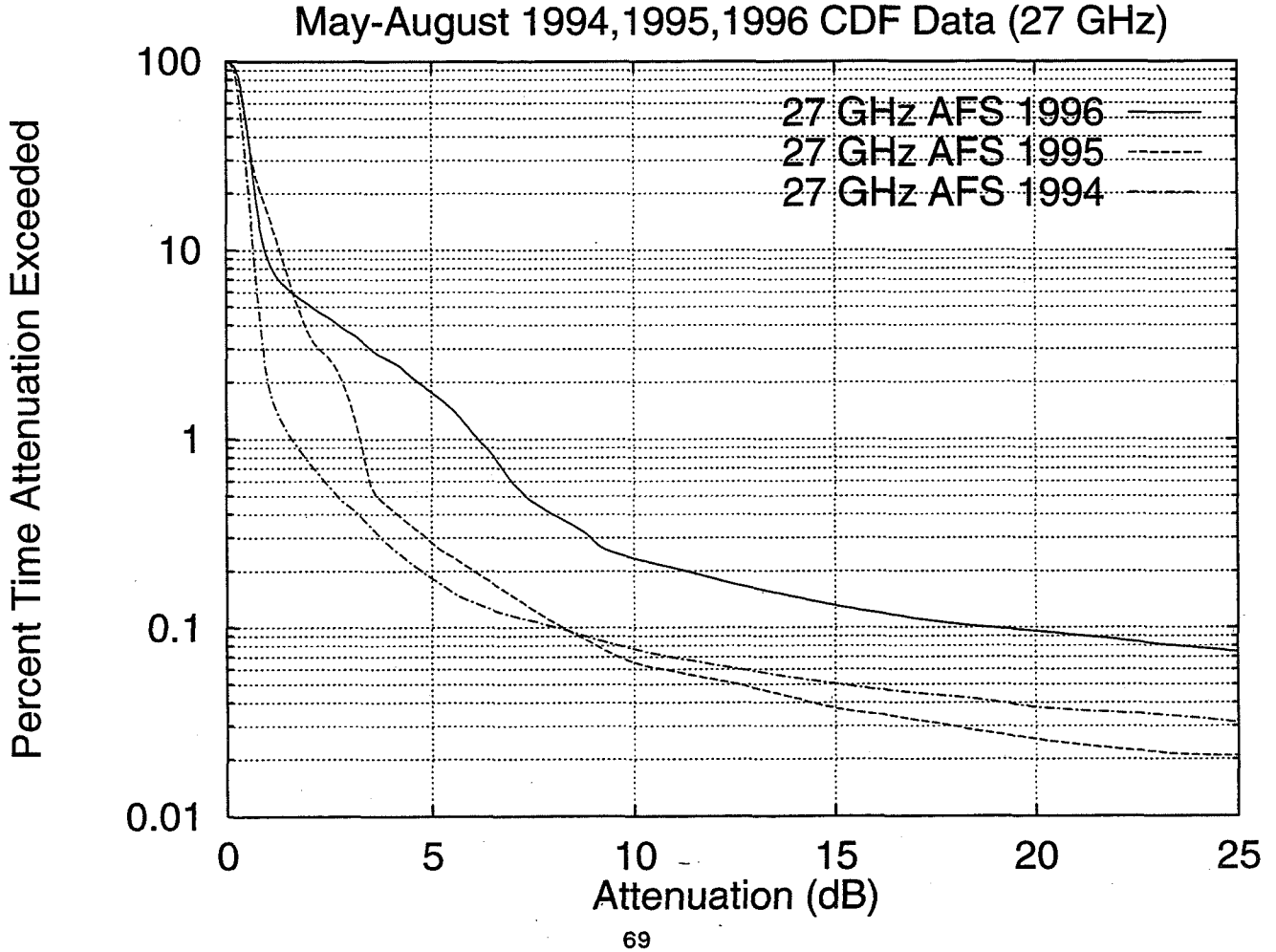
May-August 1994,1995,1996 CDF Data (27 GHz)
Percent Time Attenuation Exceeded
100
10
1
0.1
0.01
0
5
10
15
20
25
Attenuation (dB)
27 GHz AFS 1996
27 GHz AFS 1995
27 GHz AFS 1994

ACTS Data - Convective Case

7/6/96 ACTS Propagation Data (CO)

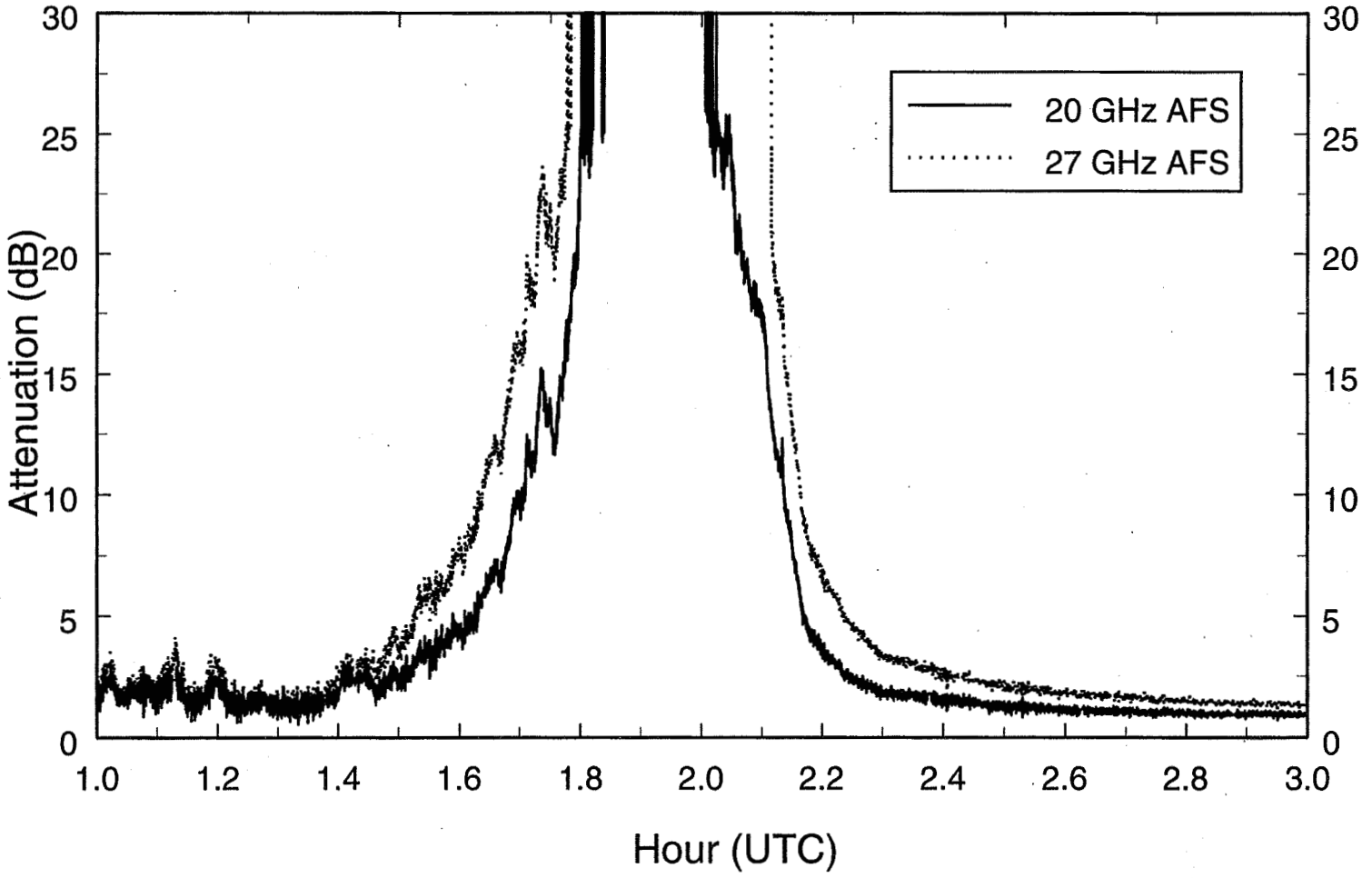

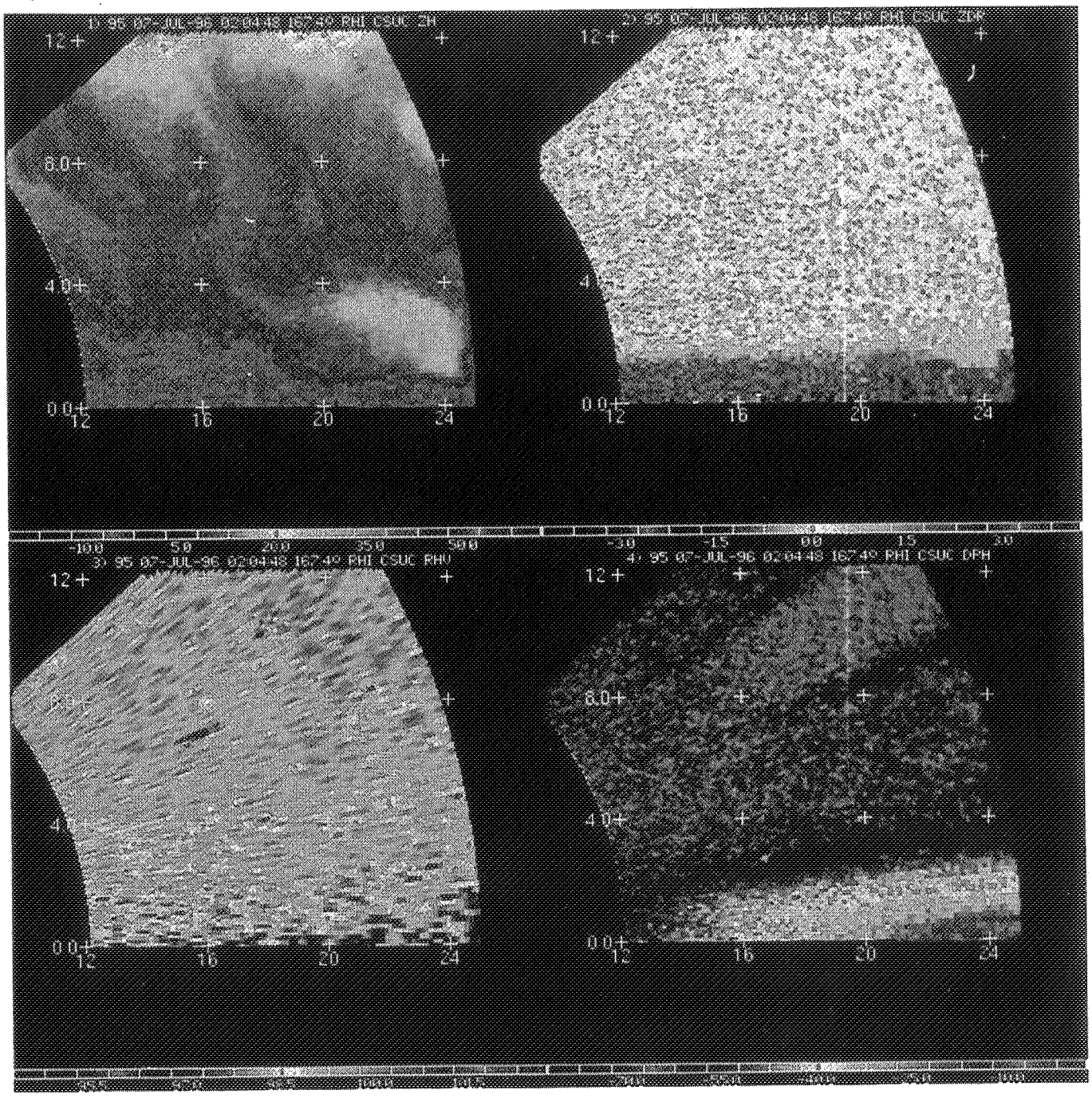
1) 95 07-JUL-96 02:04:43 167.4º RHI CSUC ZH
12
8.0
4.0
0.0
12
16
20
24
2) 95 07-JUL-96 02:04:43 167.4º RHI CSUC ZDR
-100
-5.0
-2.0
-.50
.50
3) 95 07-JUL-96 02:04:43 167.4º RHI CSUC RHO
-30
-15
0.0
.15
.30
4) 95 07-JUL-96 02:04:43 167.4º RHI CSUC DPH

July 6, 1996 Convective Case

Comparison of CSU-CHILL and CSU-APT Attenuation Estimates

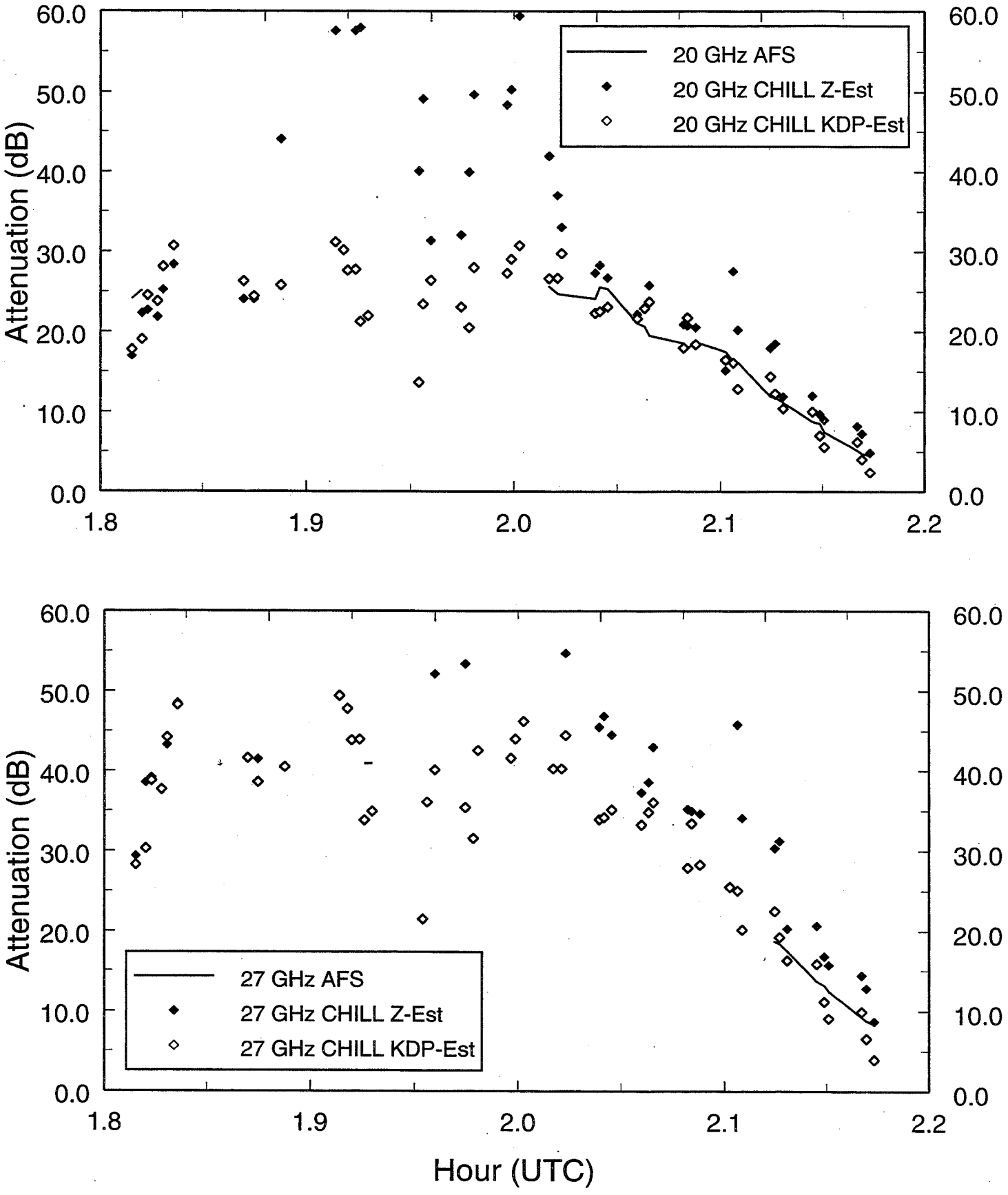

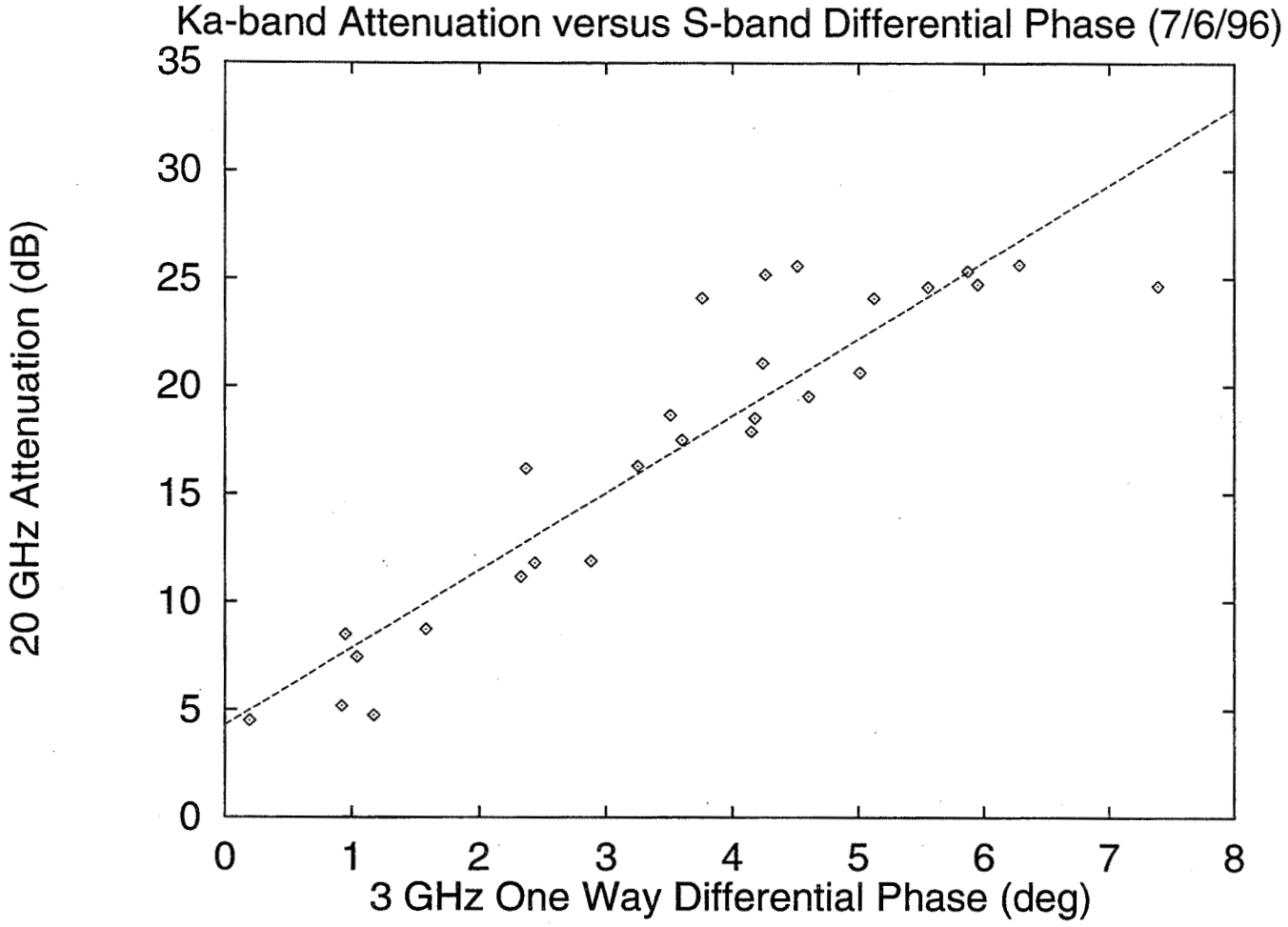
Ka-band Attenuation versus S-band Differential Phase (7/6/96)
20 GHz Attenuation (dB)
0
5
10
15
20
25
30
35
0
1
2
3
4
5
6
7
8
3 GHz One Way Differential Phase (deg)

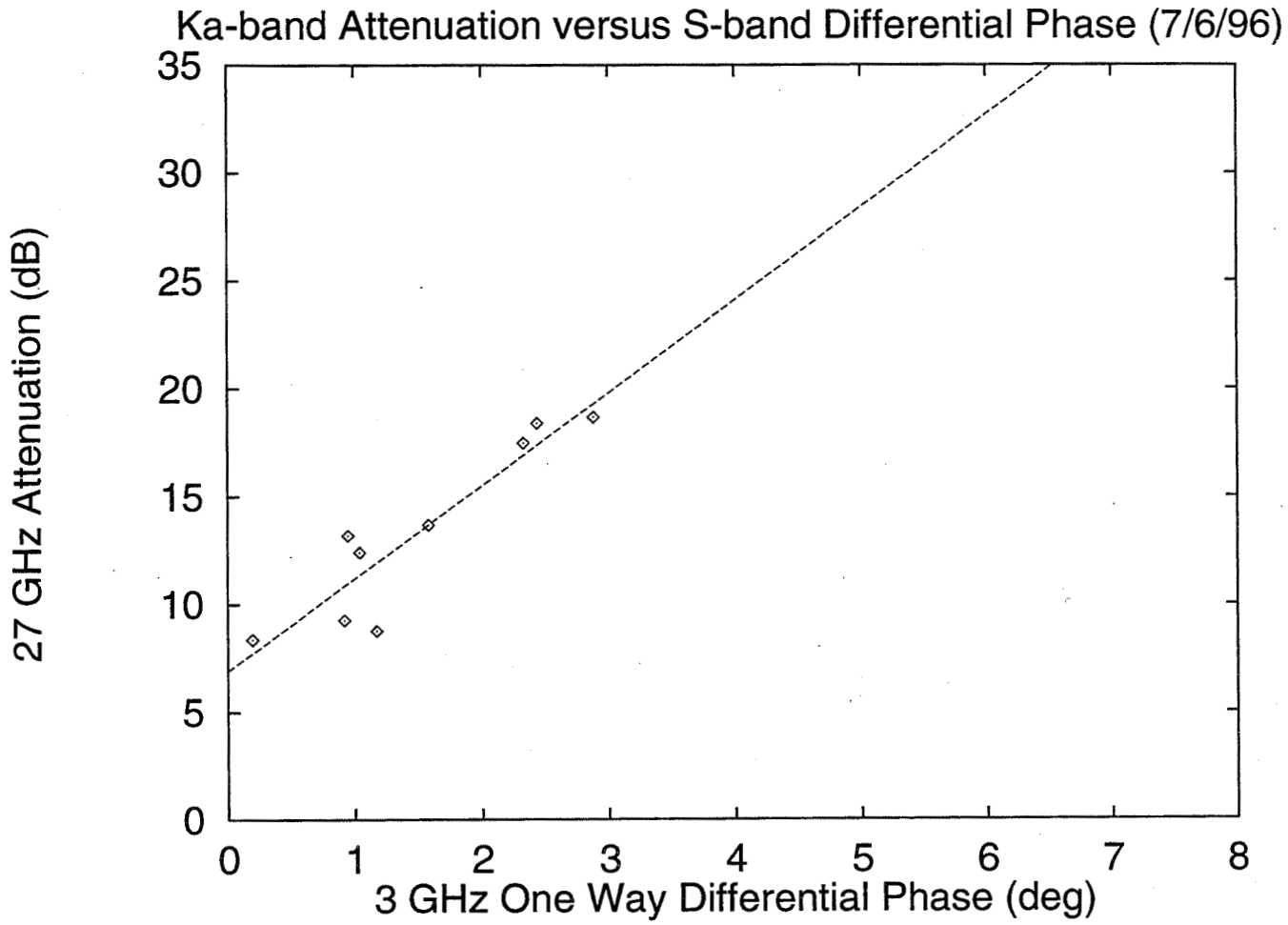
Ka-band Attenuation versus S-band Differential Phase (7/6/96)
27 GHz Attenuation (dB)
0
5
10
15
20
25
30
35
0
1
2
3
4
5
6
7
8
3 GHz One Way Differential Phase (deg)

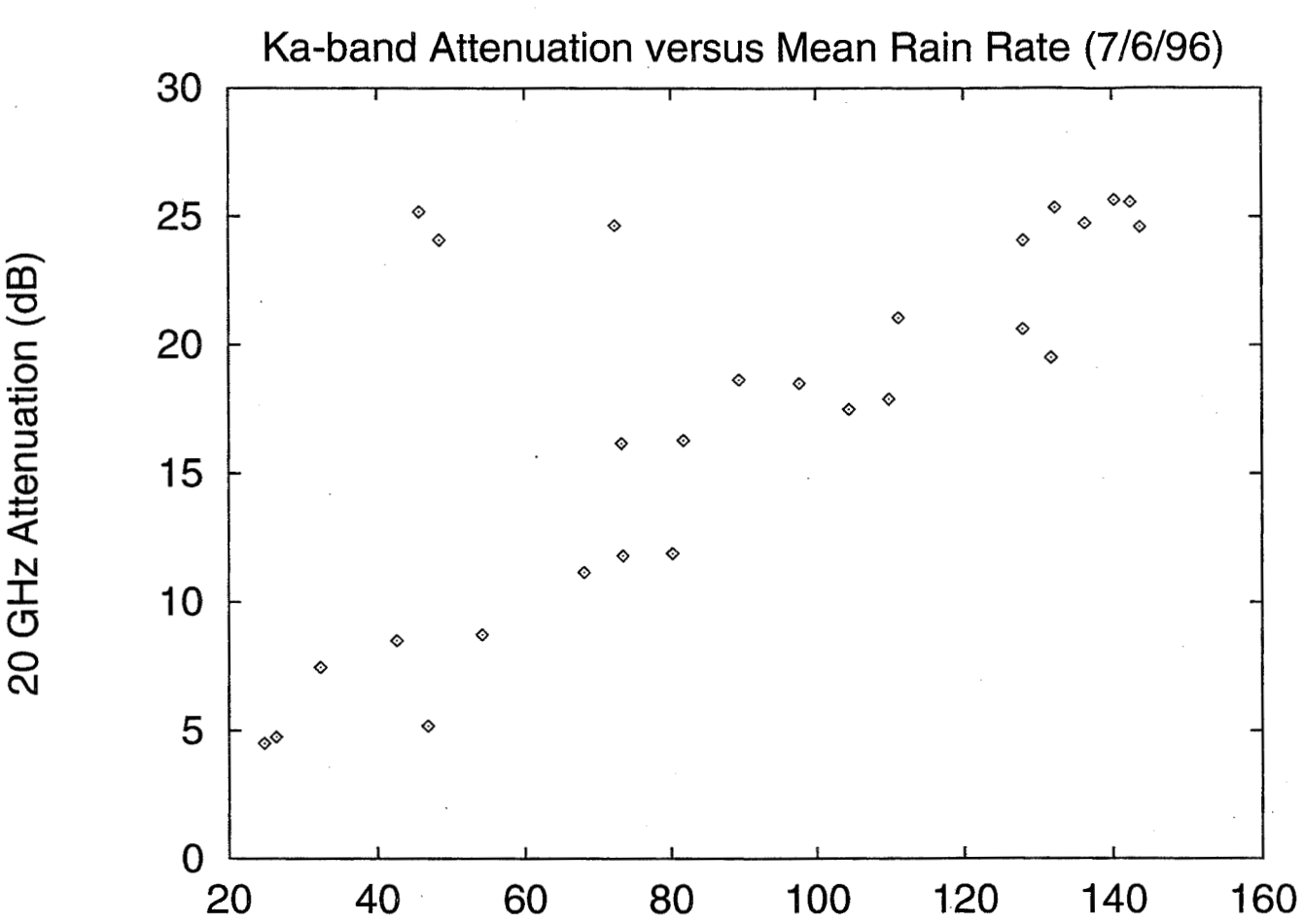
Ka-band Attenuation versus Mean Rain Rate (7/6/96)
20 GHz Attenuation (dB)
0
5
10
15
20
25
30
20
40
60
80
100
120
140
160

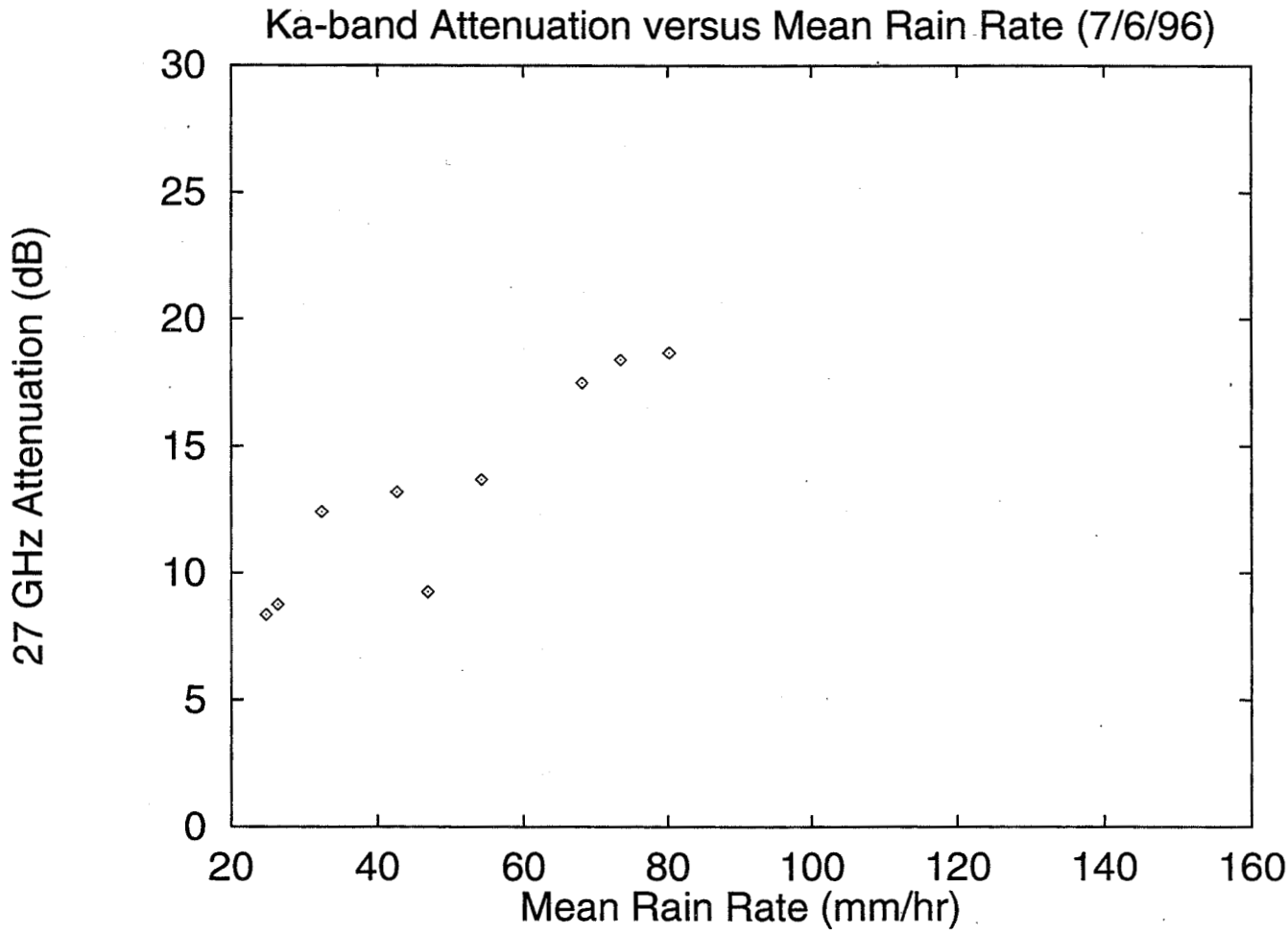
Ka-band Attenuation versus Mean Rain Rate (7/6/96)
27 GHz Attenuation (dB)
0
5
10
15
20
25
30
20
40
60
80
100
120
140
160
Mean Rain Rate (mm/hr)

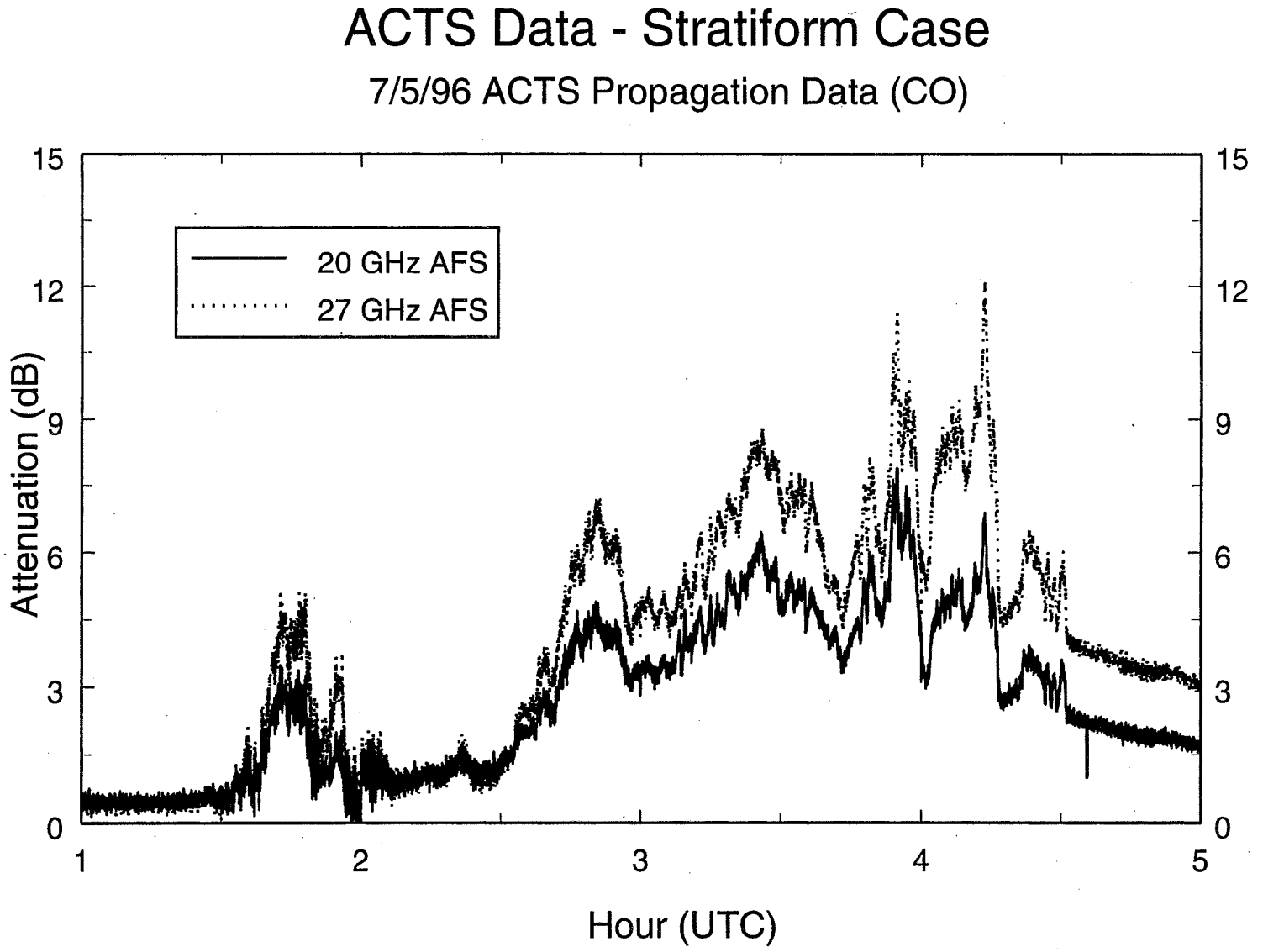
ACTS Data - Stratiform Case
7/5/96 ACTS Propagation Data (CO)
20 GHz AFS
27 GHz AFS
Attenuation (dB)
Hour (UTC)
0
3
6
9
12
15
1
2
3
4
5

July 5, 1996 Stratiform Case

Comparison of CSU-CHILL and CSU-APT Attenuation Estimates

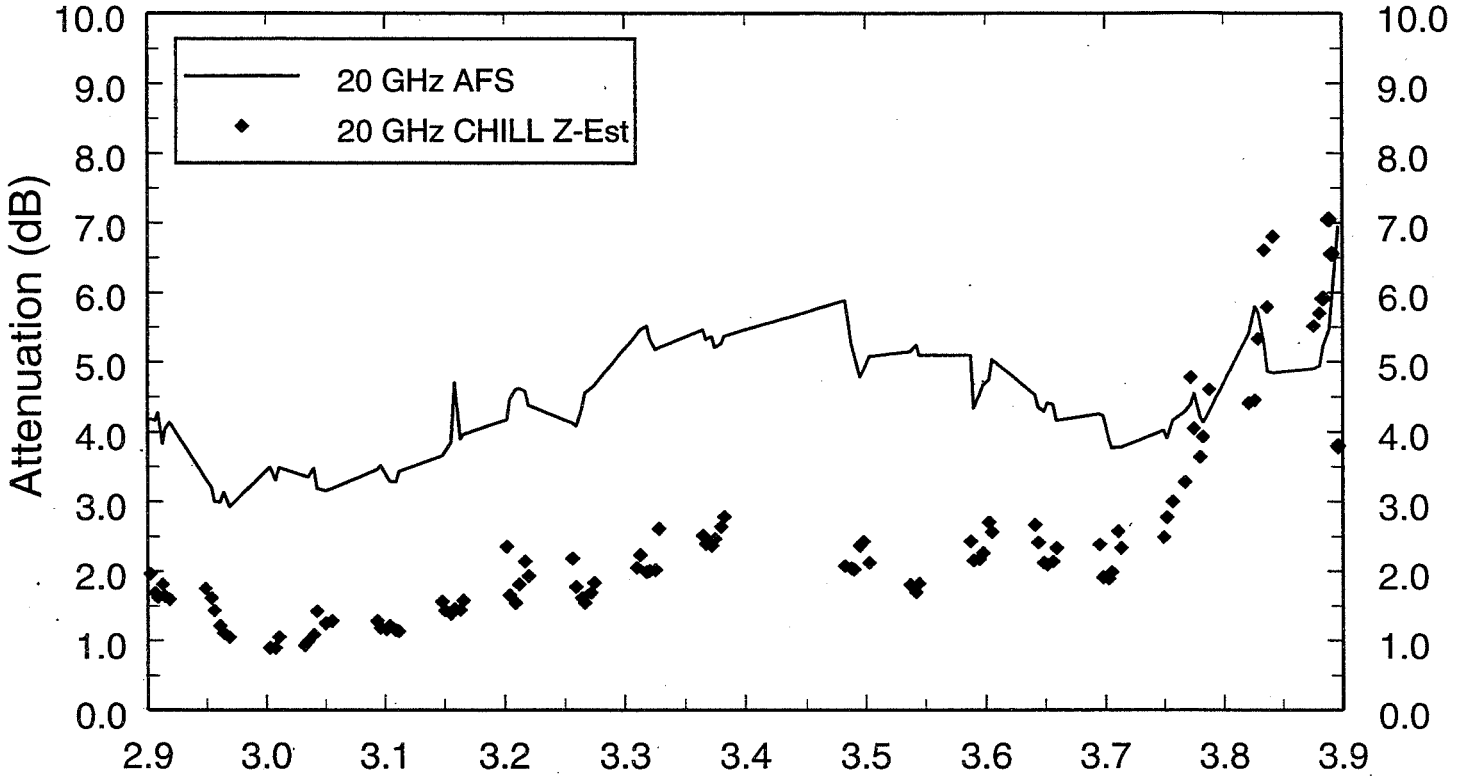

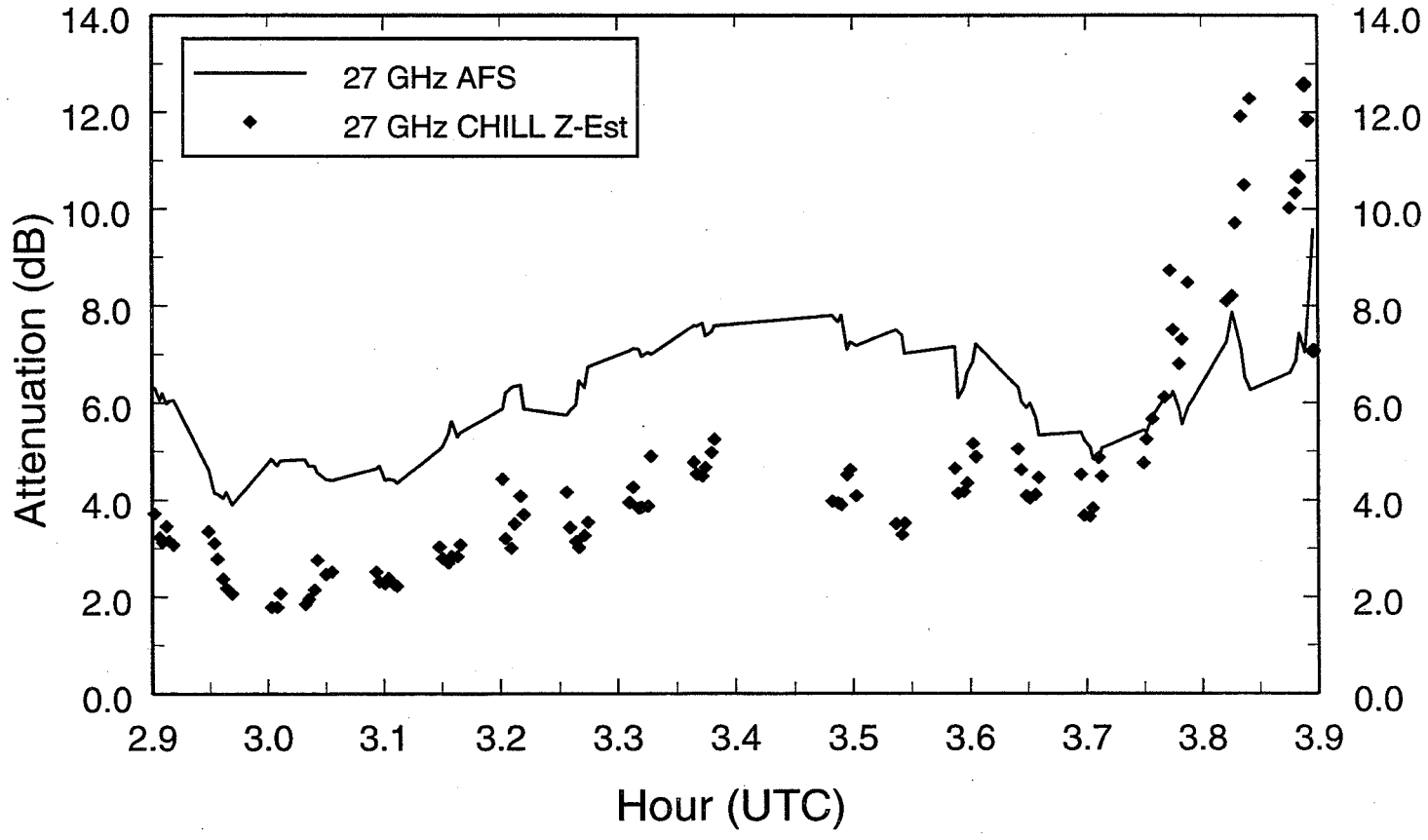

Antenna Wetting Test

Antenna Surface Alone

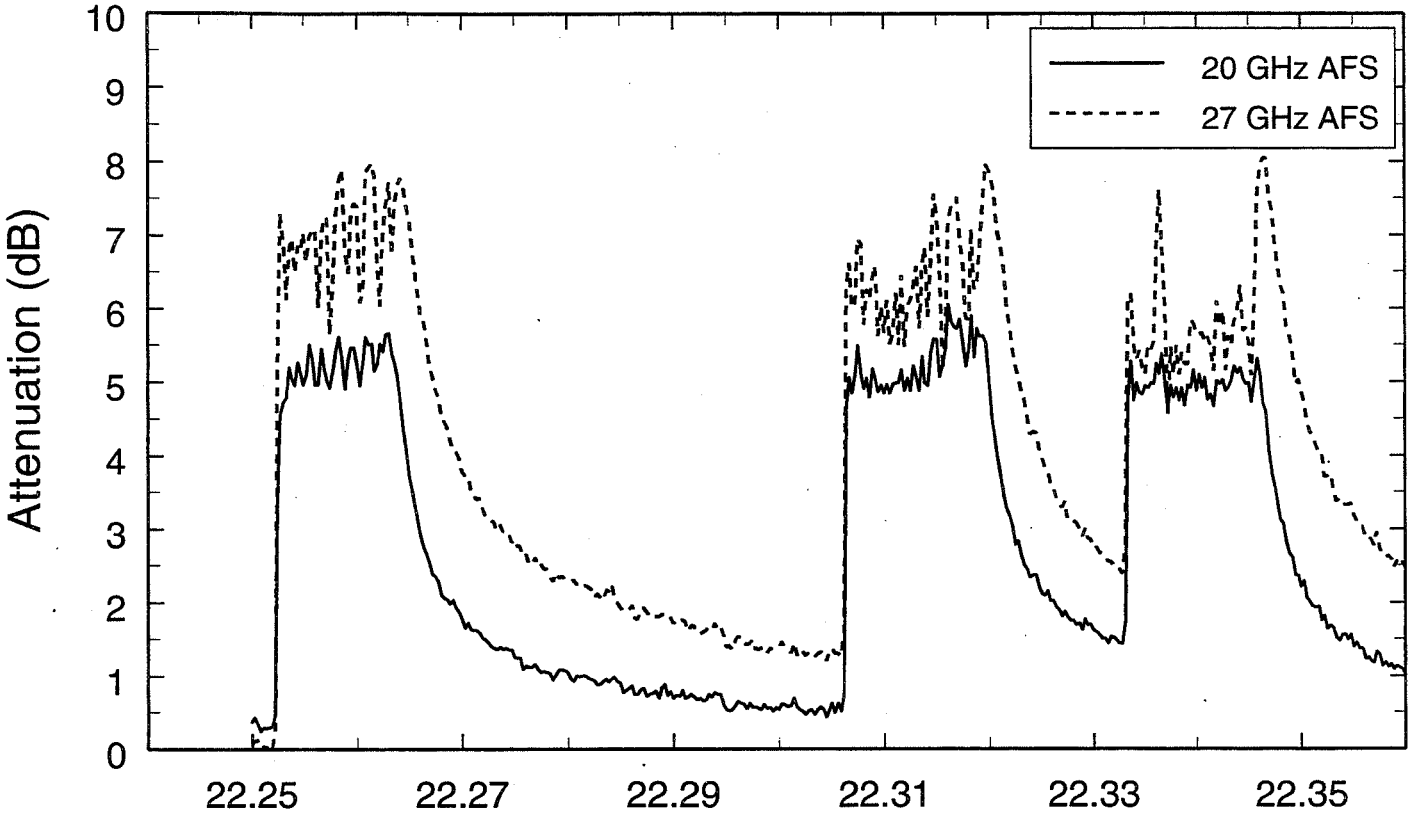

Feed Surface Alone

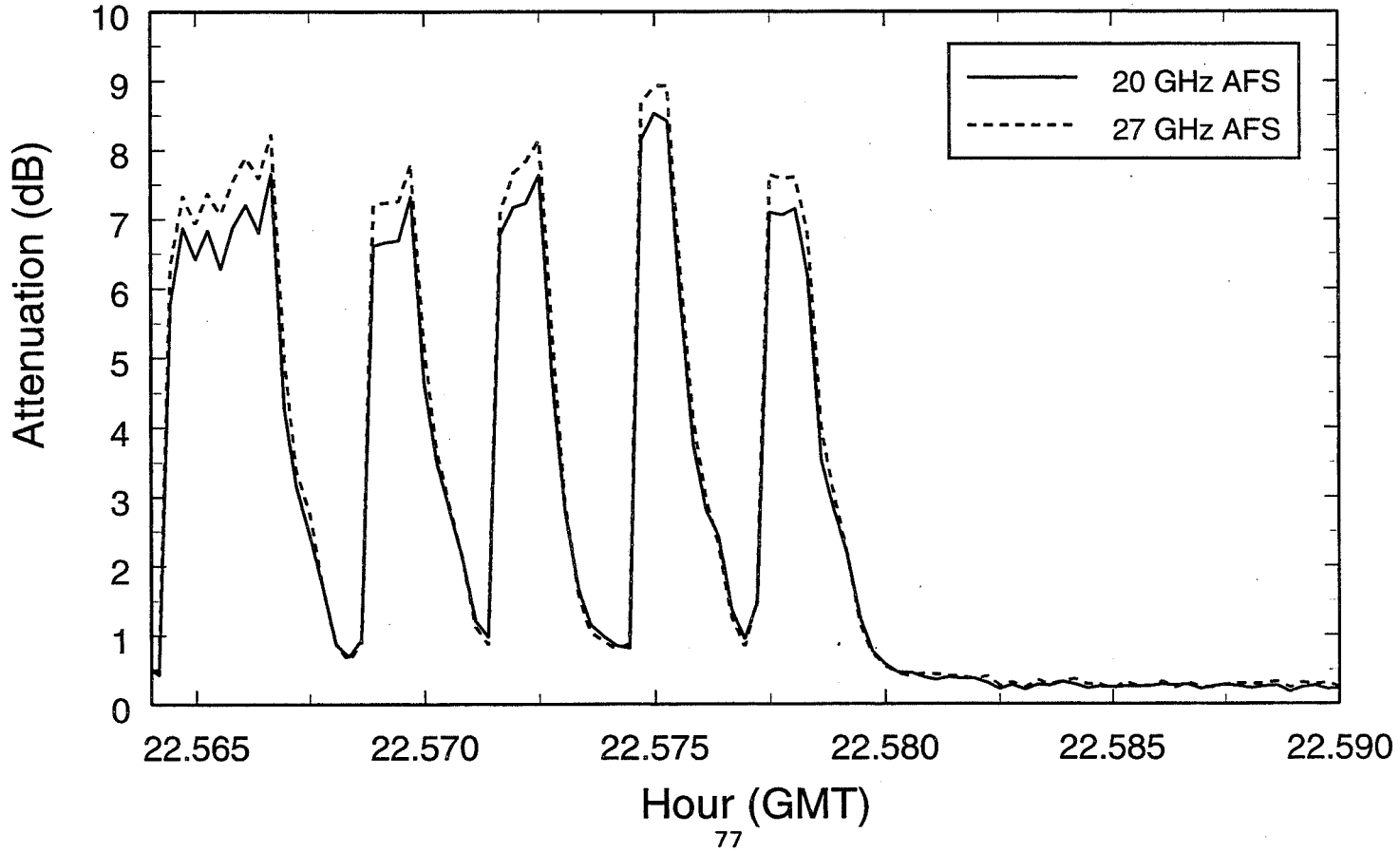

Antenna Wetting Test

Water Falling Between Feed and Antenna

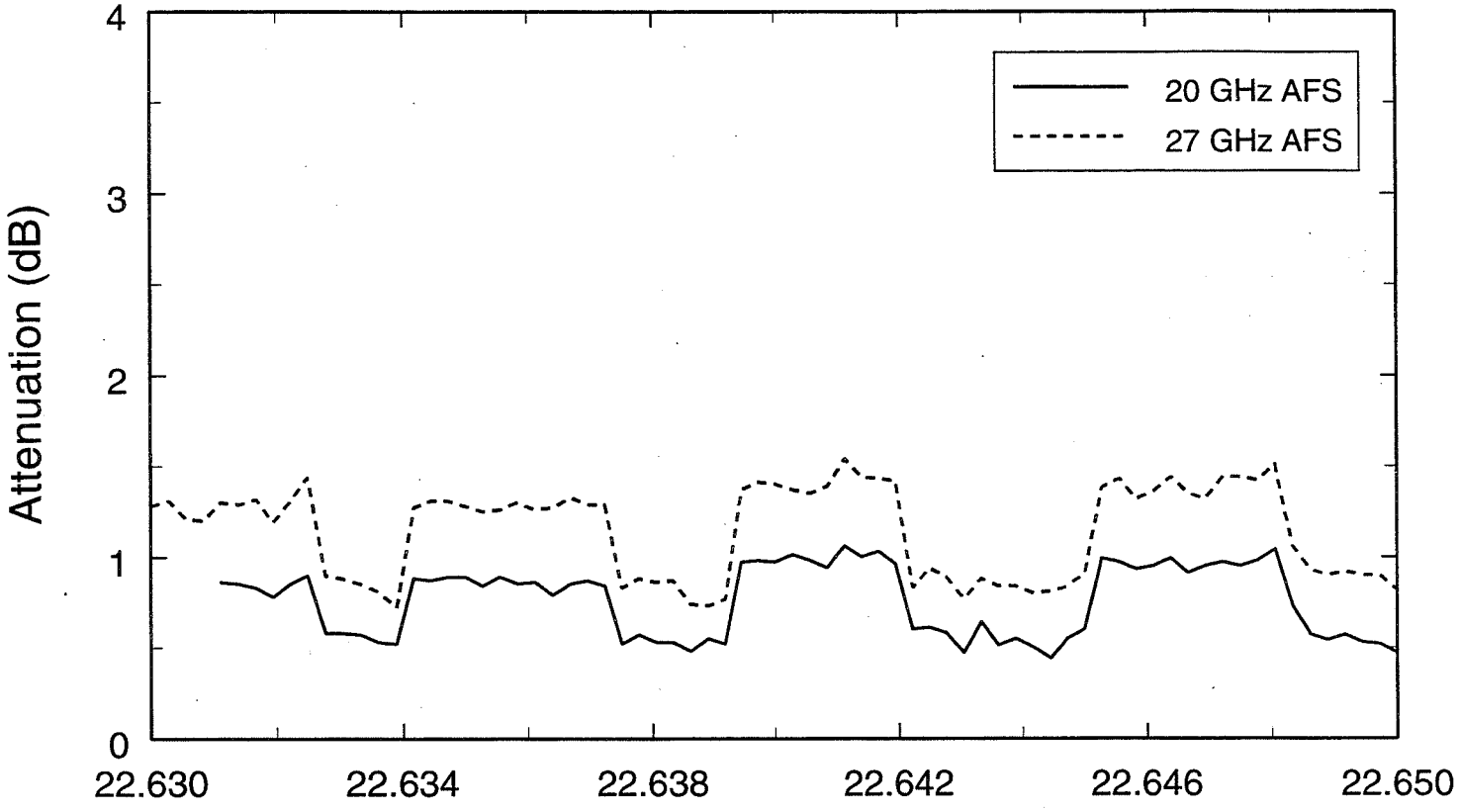

Water Sprayed Over Feed and Antenna Surface

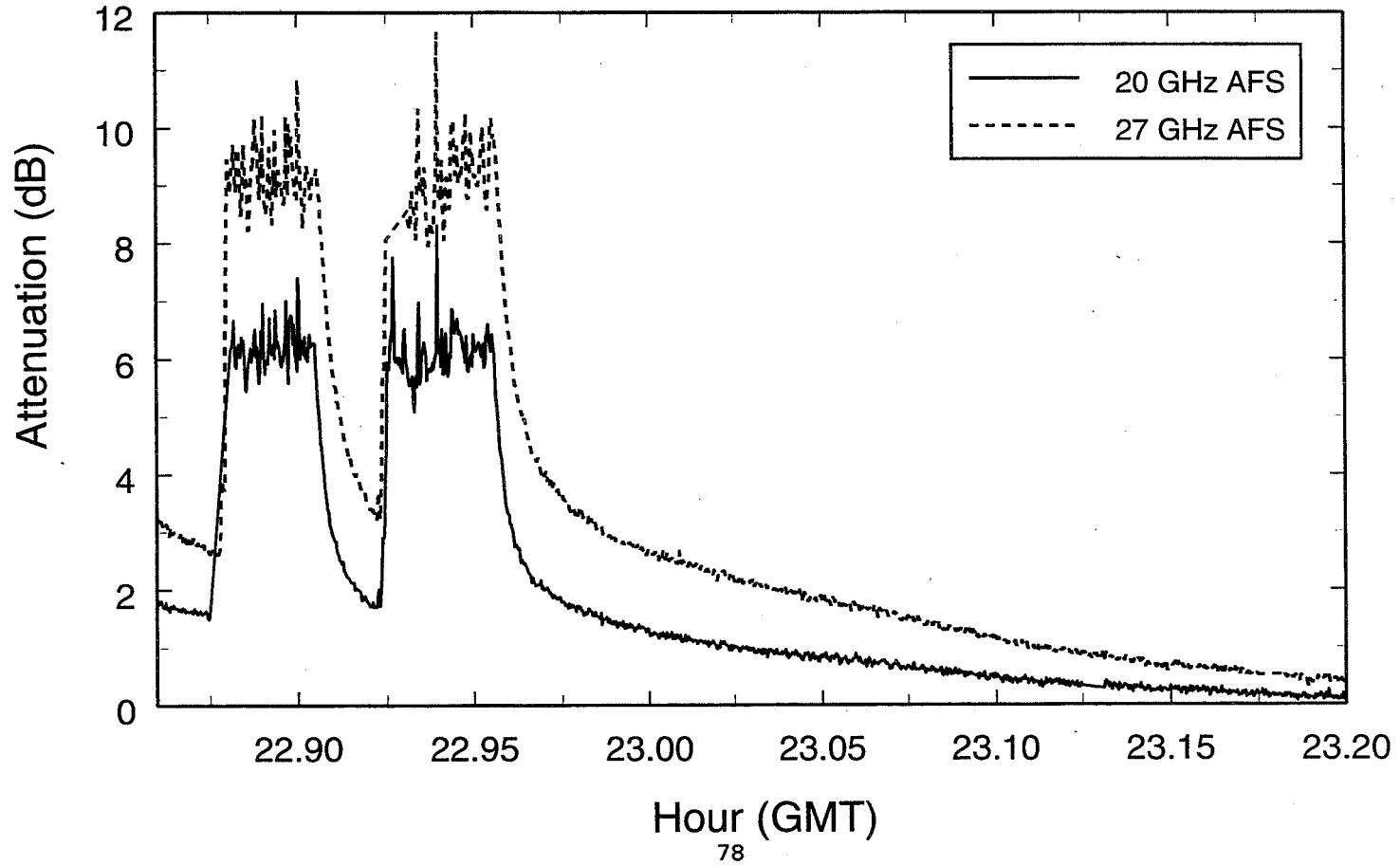

Antenna Wetting Test

Water Sprayed Over Feed and Antenna Surface

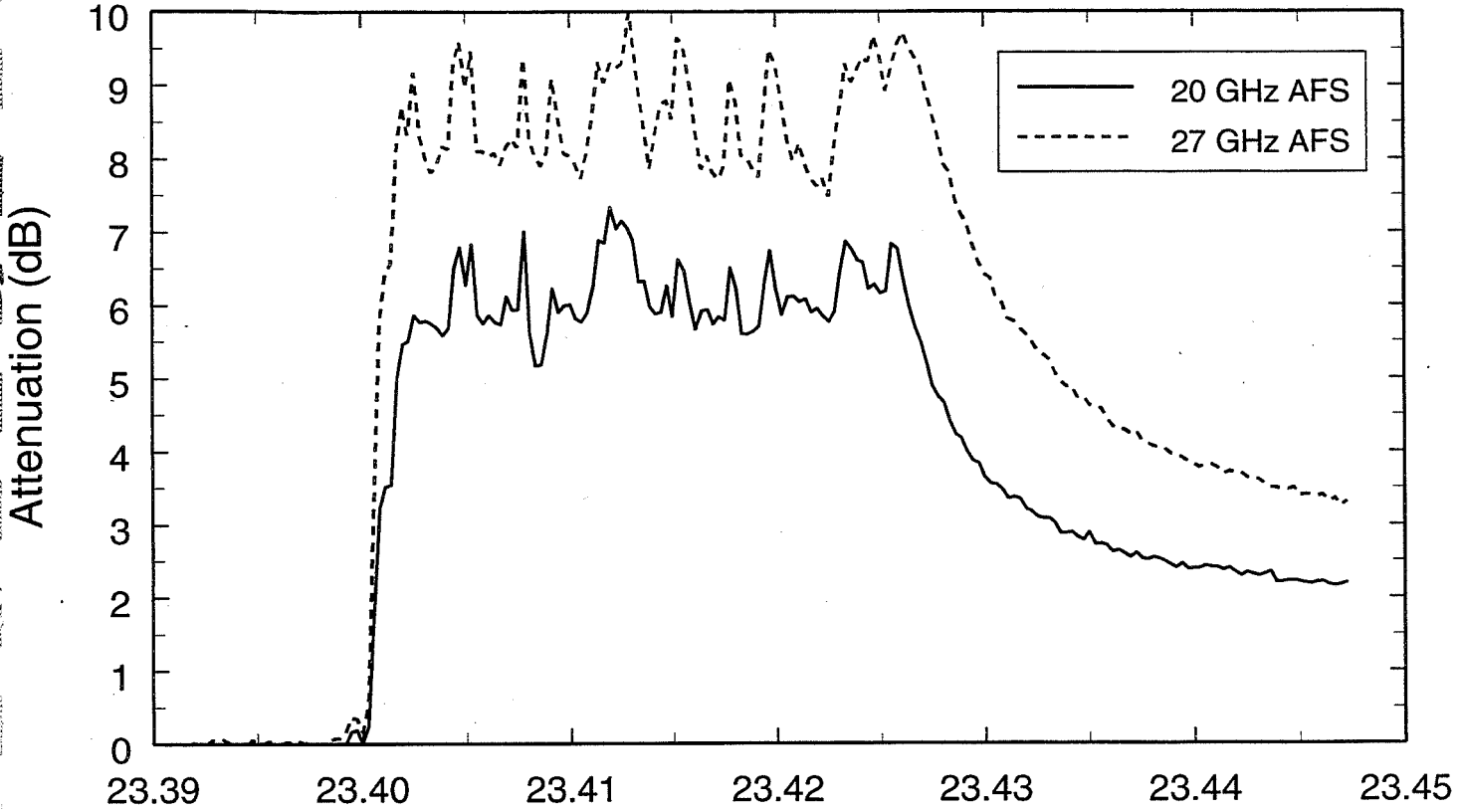

Rain Rate Data from Austrian 2D Video Disdrometer

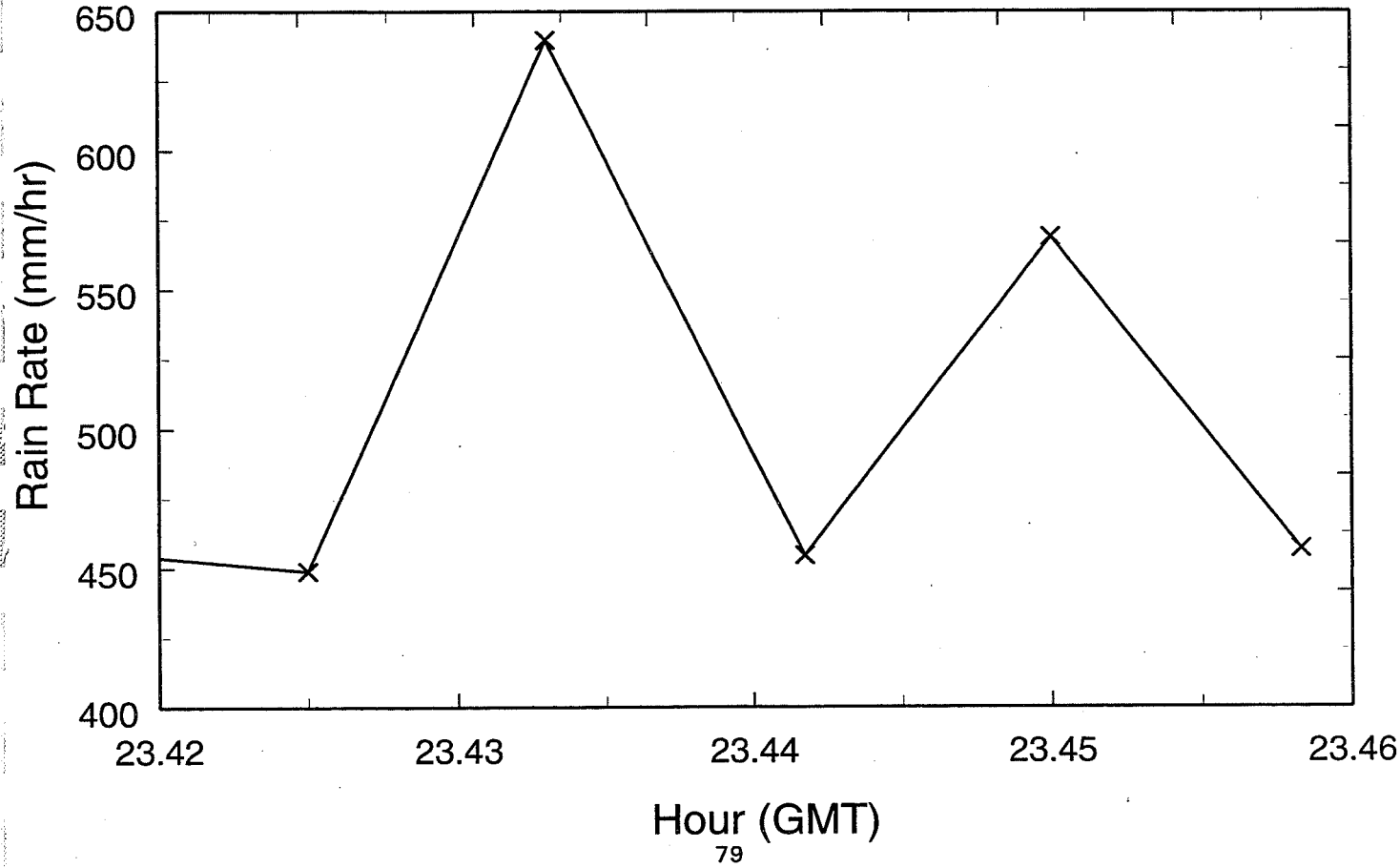

Antenna Wetting Test

Water Sprayed Over Feed and Antenna Surface

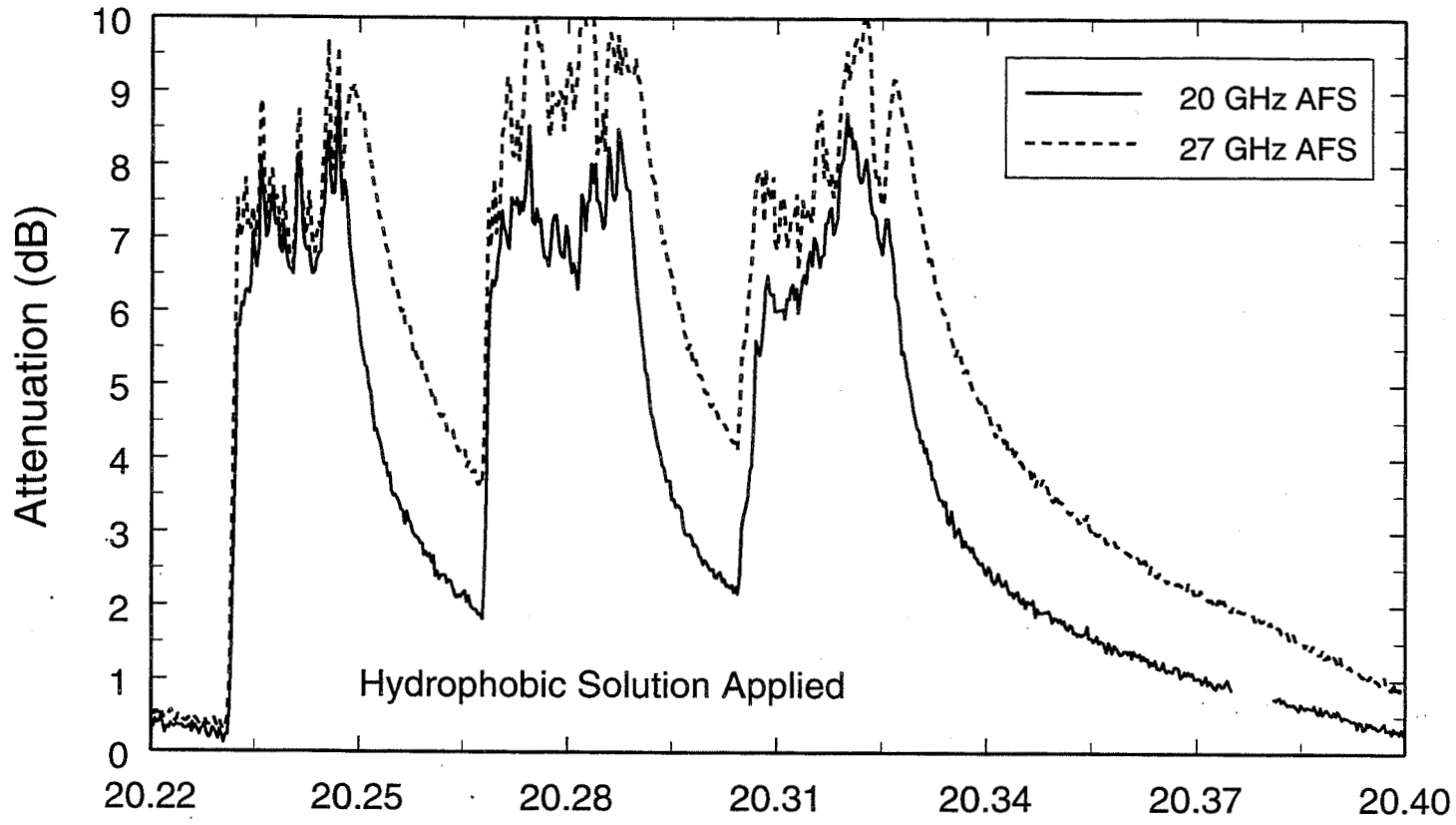

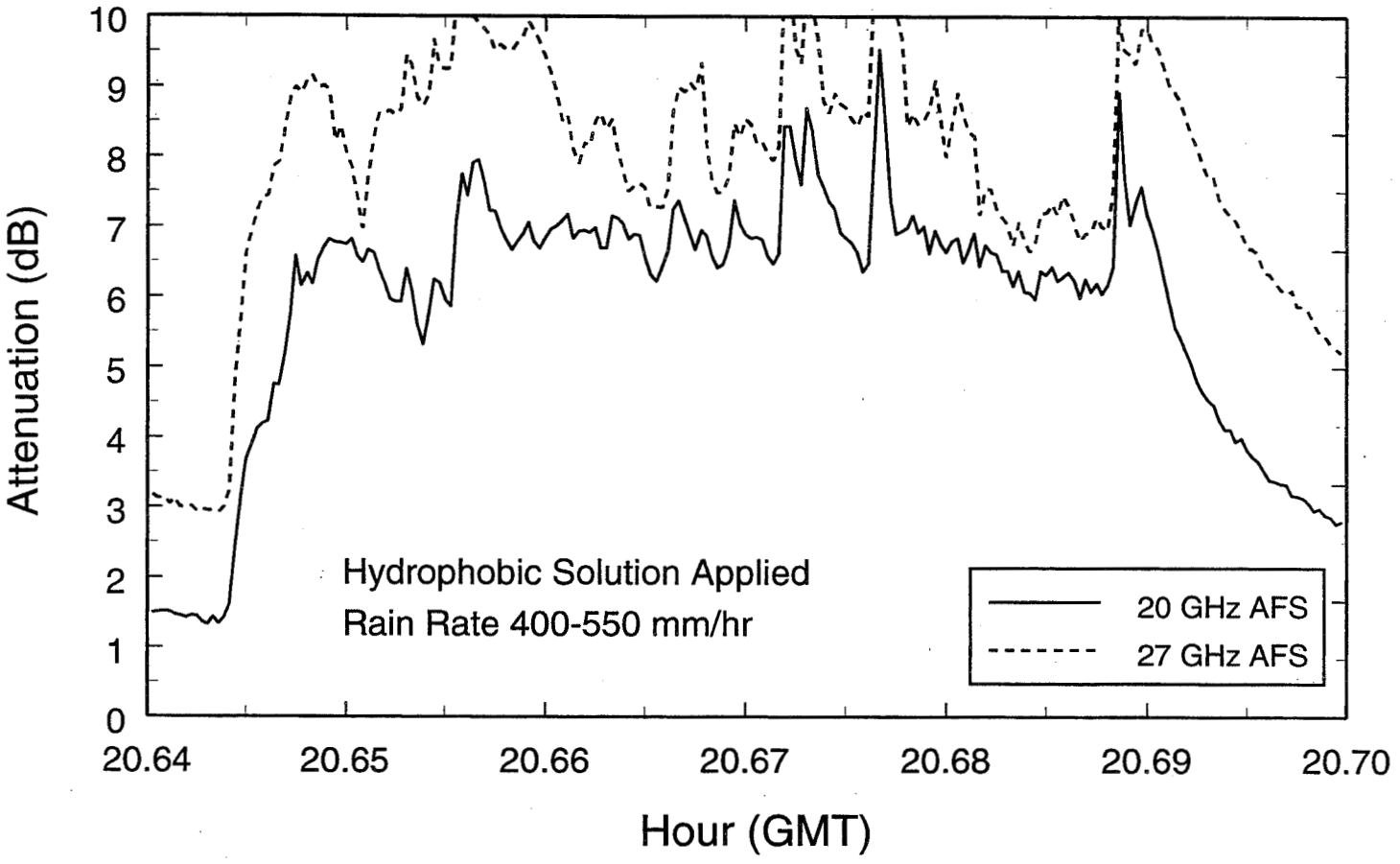

Antenna Wetting Test

Water Sprayed Over Feed and Antenna Surface

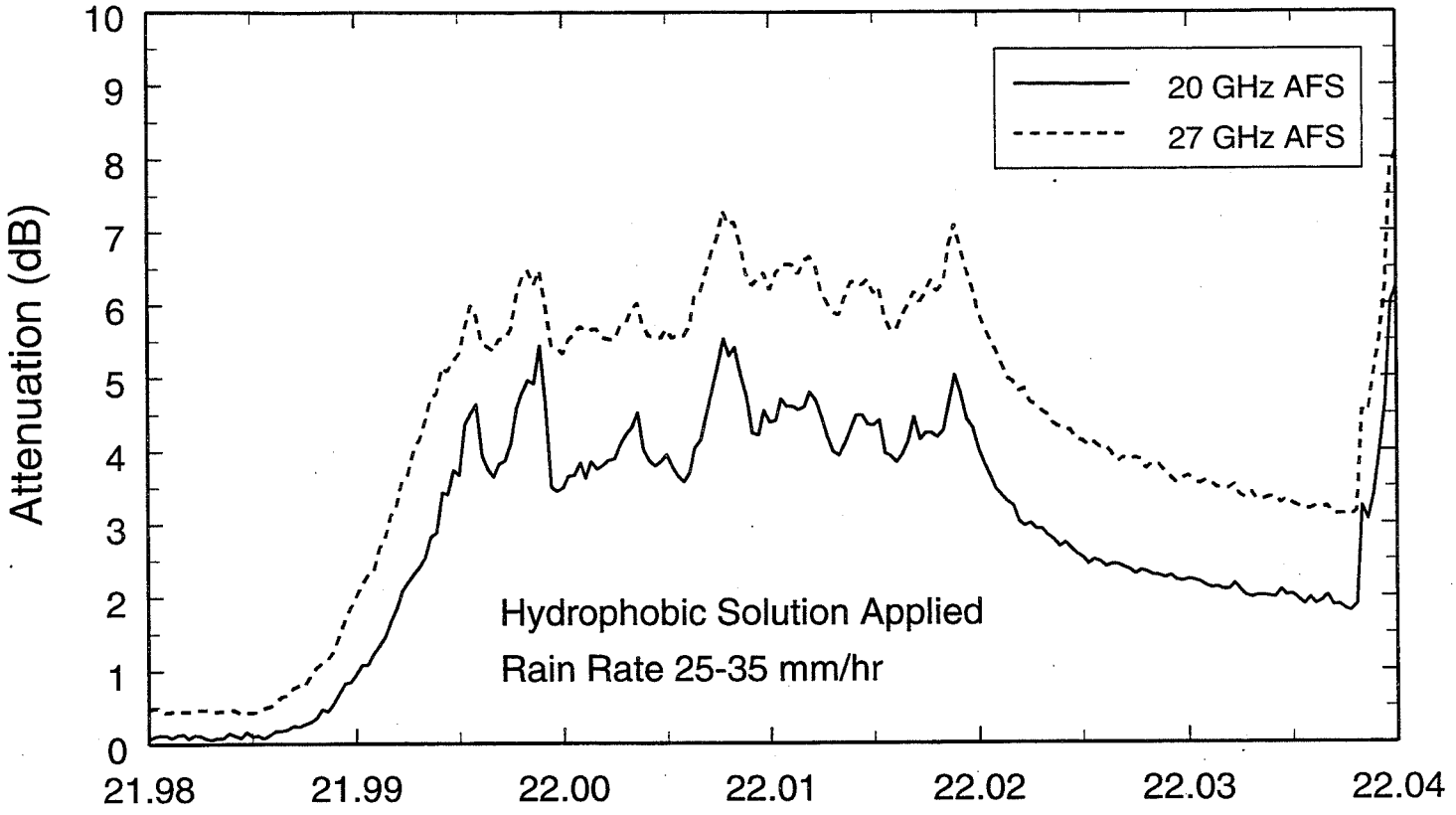

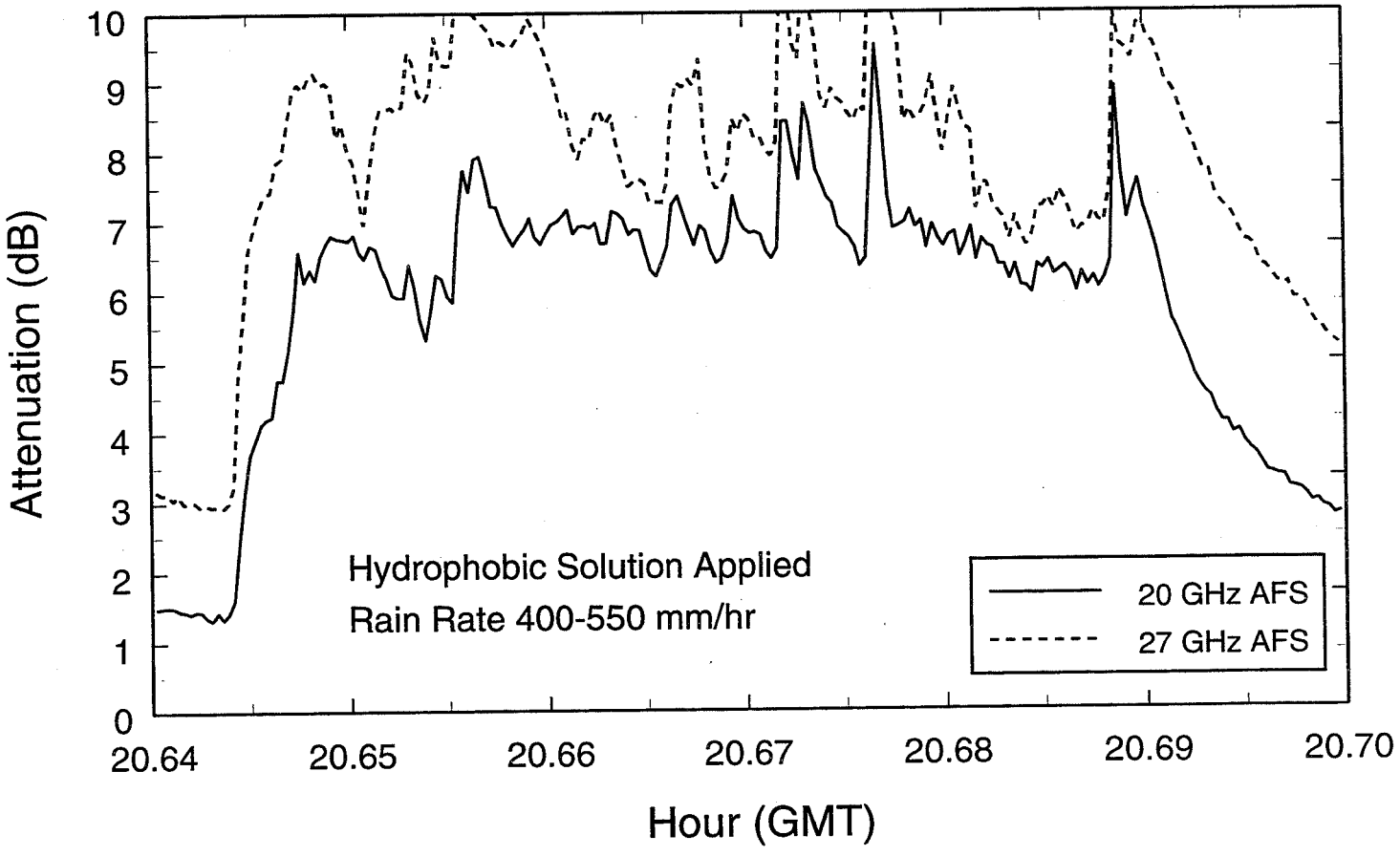

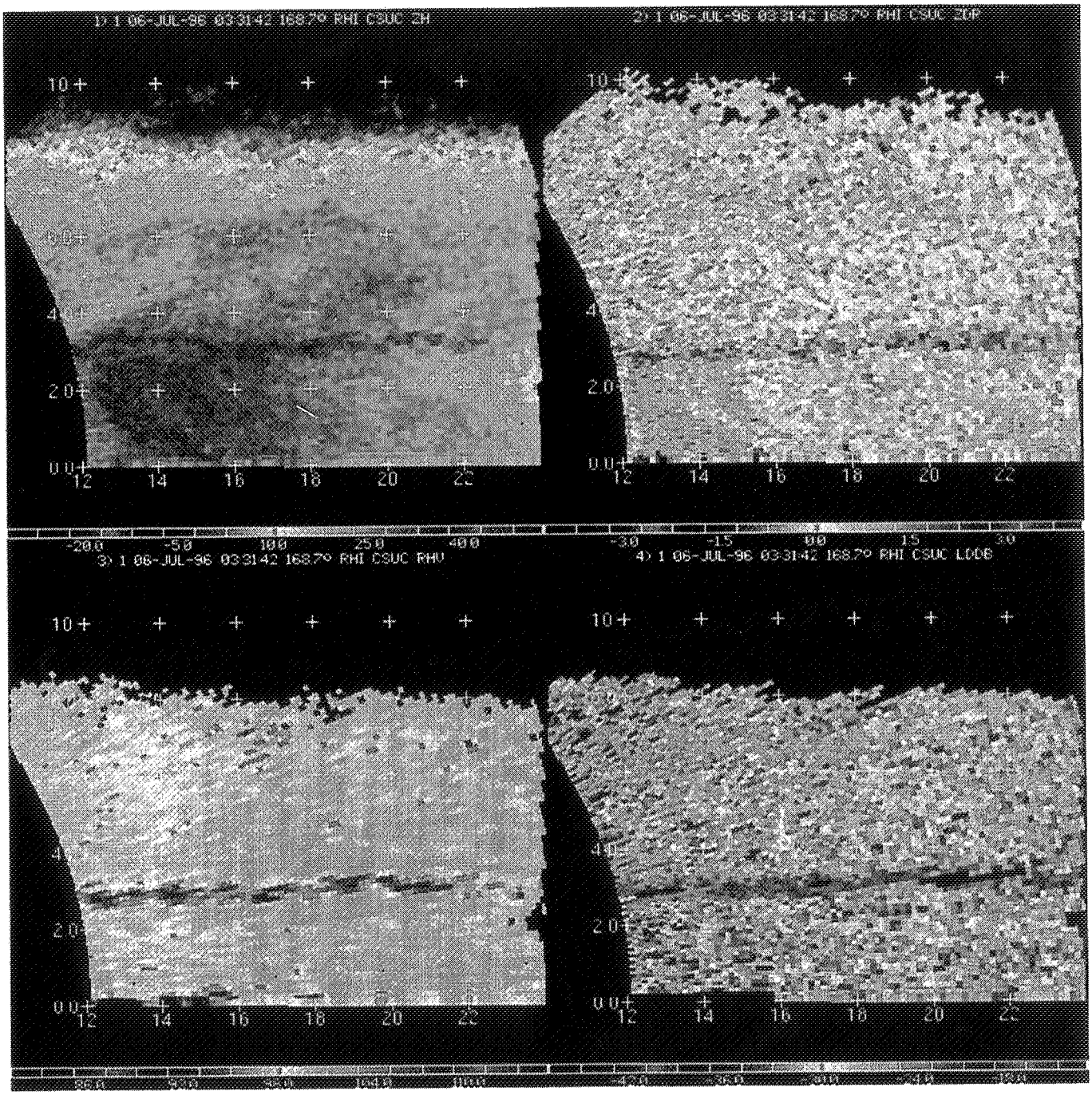
1) 1 06-JUL-96 033142 168.7° RHI CSUC ZH
2) 1 06-JUL-96 033142 168.7° RHI CSUC ZDP
-20.0 -5.0 10.0 25.0 40.0
3) 1 06-JUL-96 033142 168.7° RHI CSUC RHV
-3.0 -1.5 0.0 1.5 3.0
4) 1 06-JUL-96 033142 168.7° RHI CSUC LDRH
10
6.0
4.0
2.0
0.0
12 14 16 18 20 22

Estimation of Cloud Attenuation Using ACTS Beacon Measurements

Asoka Dissanayake

Introduction

- Cloud attenuation is an important consideration for low-margin operation of Ka-band satellite links.
- Models for cloud attenuation prediction must be included among propagation tools for Ka-band applications.
- Direct measurements of cloud attenuation are relatively scarce making it difficult to verify cloud attenuation prediction models.
- Measurements made using the ACTS beacon payload and ground terminals equipped with dual frequency radiometers may be used to estimate cloud attenuation.
- Cloud attenuation estimates for Clarksburg, MD, together with model comparisons are presented.

Introduction

- ACTS beacon measurements at 20.2 and 27.5 GHz provide estimates of total path attenuation which include:
  - gaseous absorption
  - cloud attenuation
  - rain attenuation
  - tropospheric scintillations
- Extraction of cloud attenuation from the total attenuation may be attempted by considering the frequency scaling and temporal properties of various propagation factors.

Propagation factors

- Gaseous absorption:
  - oxygen attenuation considered time invariant
  - fixed frequency scaling for water vapor absorption

- Cloud attenuation:
  - particles size < 0.01mm; Rayleigh scattering is applicable
  - frequency scaling ~ f^2; not expected to vary during the event

- Rain attenuation
  - frequency scaling depends on type of rain; tends to vary significantly during the event

Propagation Factors

- Tropospheric scintillations:
  - amplitude variations much faster than the those found with the other impairments. Can be separated from other factors using a high pass filter.
  - frequency scaling ~ $f^{7/12}$

- Other factors:
  - bulk refractive effects: negligible variation at moderate elevation angles
  - melting layer: present only during rain

Rain Event at Clarksburg, MD, on 1 July, 1995. Attenuation on 20.2 and 27.5 GHz ACTS Beacon Signal Shown.

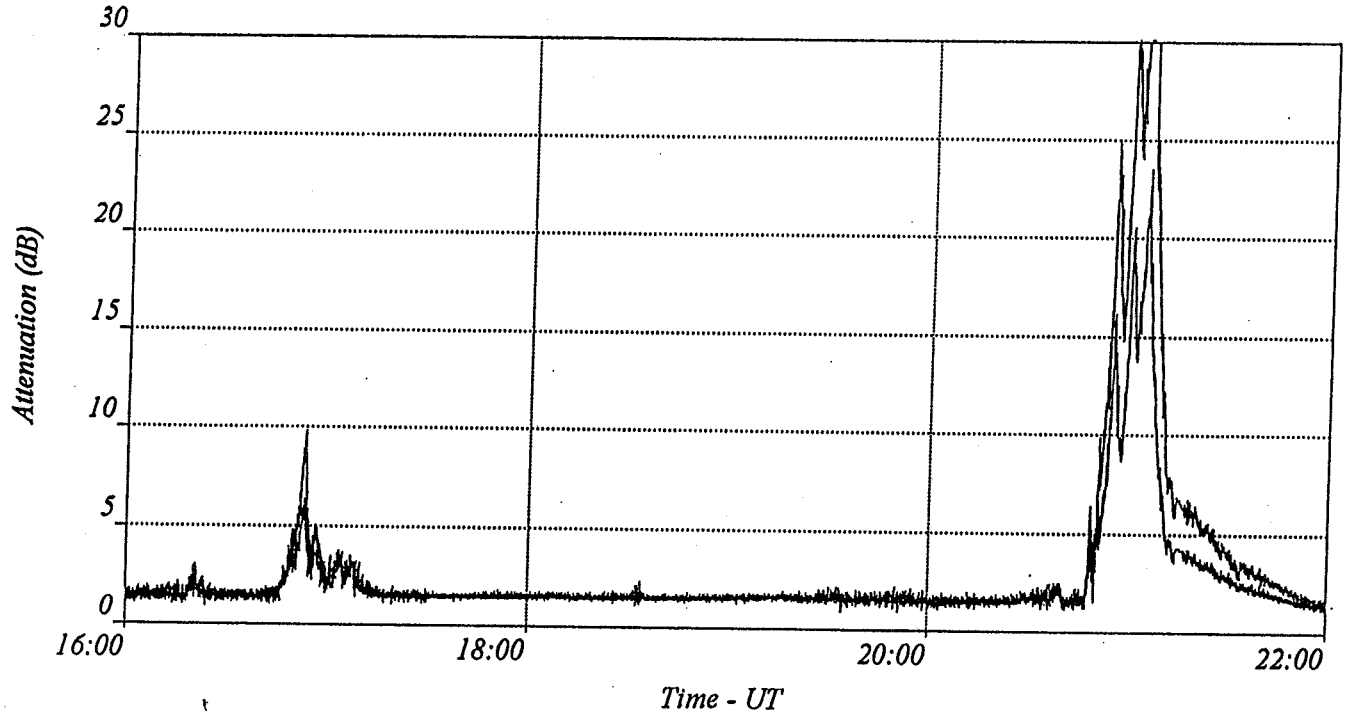

Identification of Different Propagation Factors

Power Spectrum of Fade Event on 7/1/95

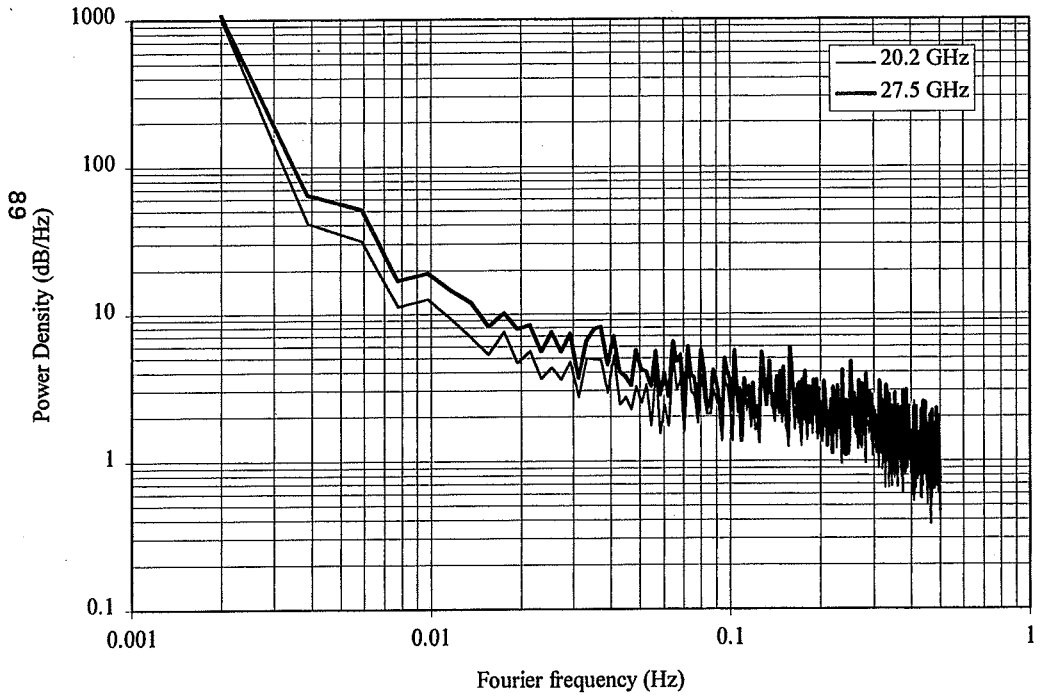

Frequency Scaling Ratio

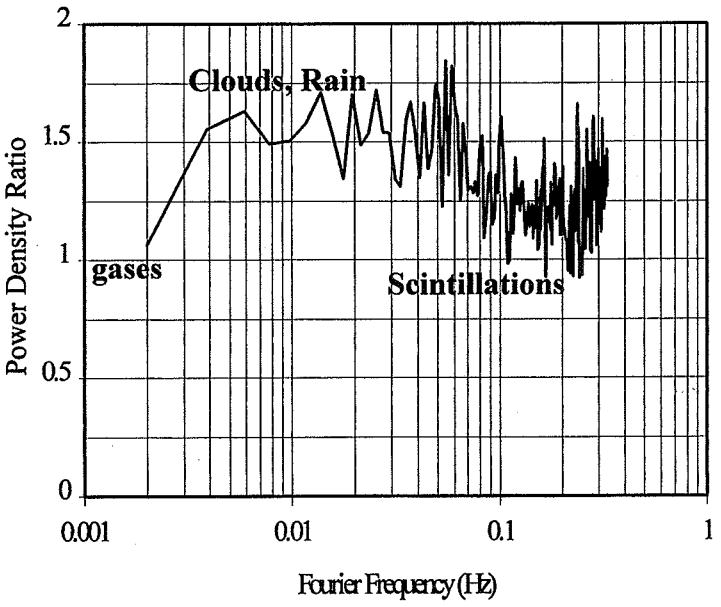

Cloud Attenuation Estimation Procedure

- Remove tropospheric scintillation using a suitable low-pass filter; filter time constant ~ 1 min.
- Identify fade events with rain on site and discard them.
- Select events which contain attenuation levels less than ~3 dB at 20.2 GHz.
- Calculate variance of fade ratio of the two beacon channels over 5 minutes; variance is used to detect the presence of rain and such events are also discarded.
- Remove oxygen absorption from the two beacon channels.
- Calculate contributions due to clouds and water vapor.

Cloud Attenuation Event on April 4, 1994

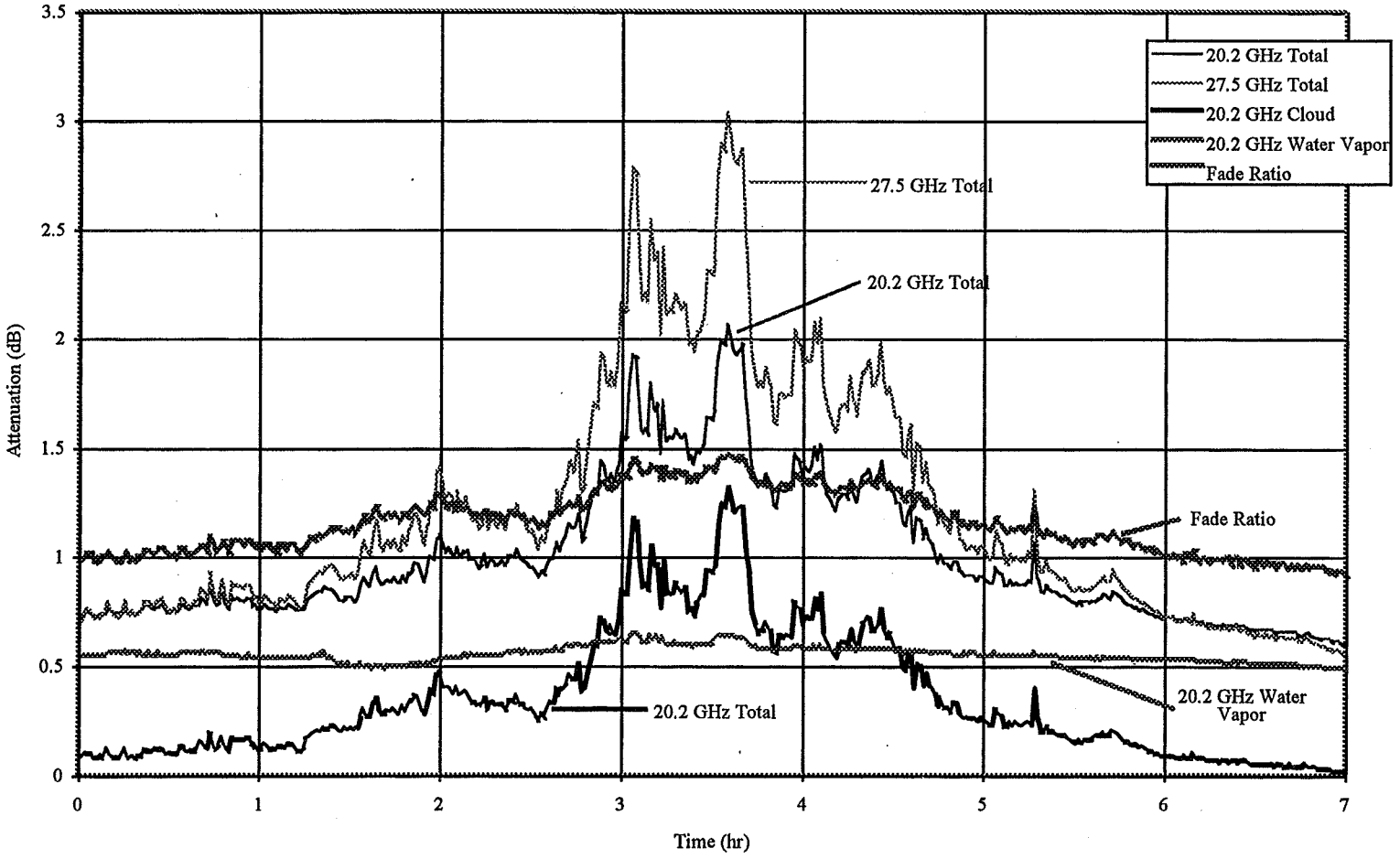

Cloud Attenuation Modeling

- Modeling based on cloud cover maps derived from synoptic weather data collected over a period of 10 years.
- Data available on six different cloud types; only water clouds are expected to produce significant attenuation.
- Occurrence probabilities of four cloud types (cumulus, cumulonimbus, stratus, and nimbo stratus) together with total cloud cover are used for the modeling.

Sample Cloud Cover Map for Cumulonimbus

Average Cloud Amount (%)

March, April, May (1971-1981)

Land Areas Only

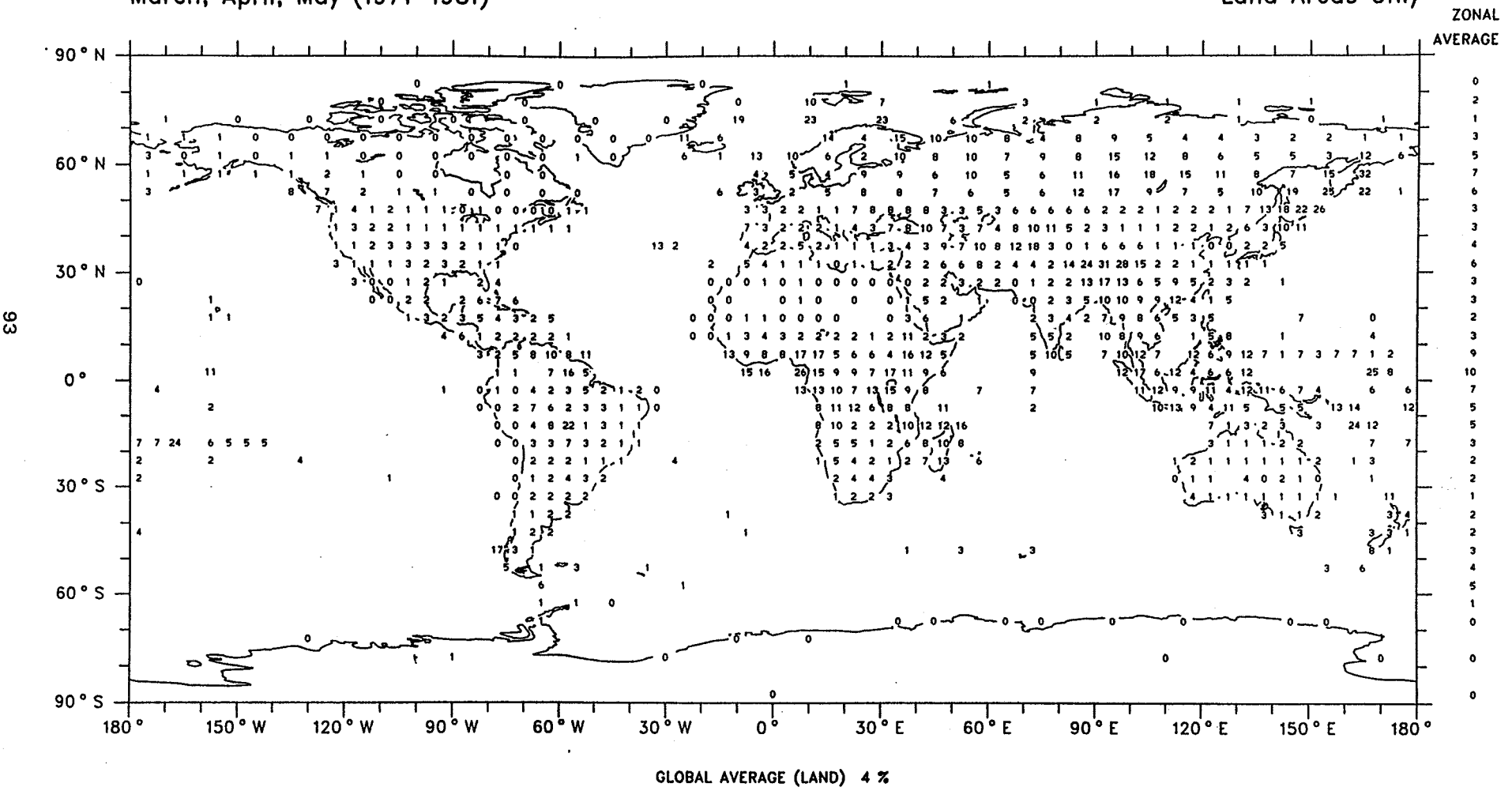

Cloud Attenuation Modeling

- Average properties of four cloud types:

Cloud Type	Vertical Extent (km)	Horizontal Extent (km)	Density (g/m3)
Cumulonimbus	3.0	4.0	1.0
Cumulus	2.0	3.0	0.6
Nimbostratus	0.8	10.0	1.0
Stratus	0.6	10.0	0.4

- Specific attenuation calculated assuming cloud temperature of 0°C (Rayleigh scattering).

- Attenuation statistics assumed to follow log-normal distribution.

Cloud Attenuation Distribution at 20.2 GHz

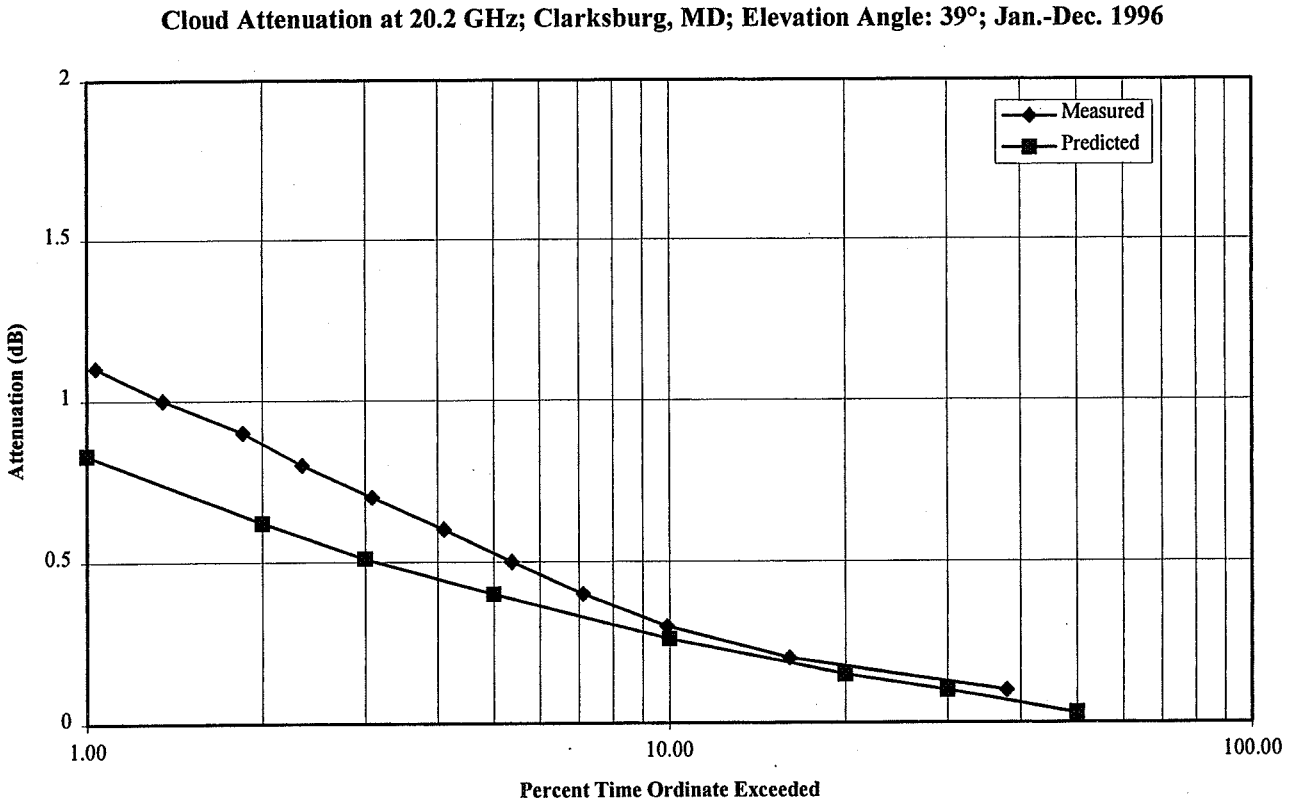

Cloud Attenuation Distribution at 27.5 GHz

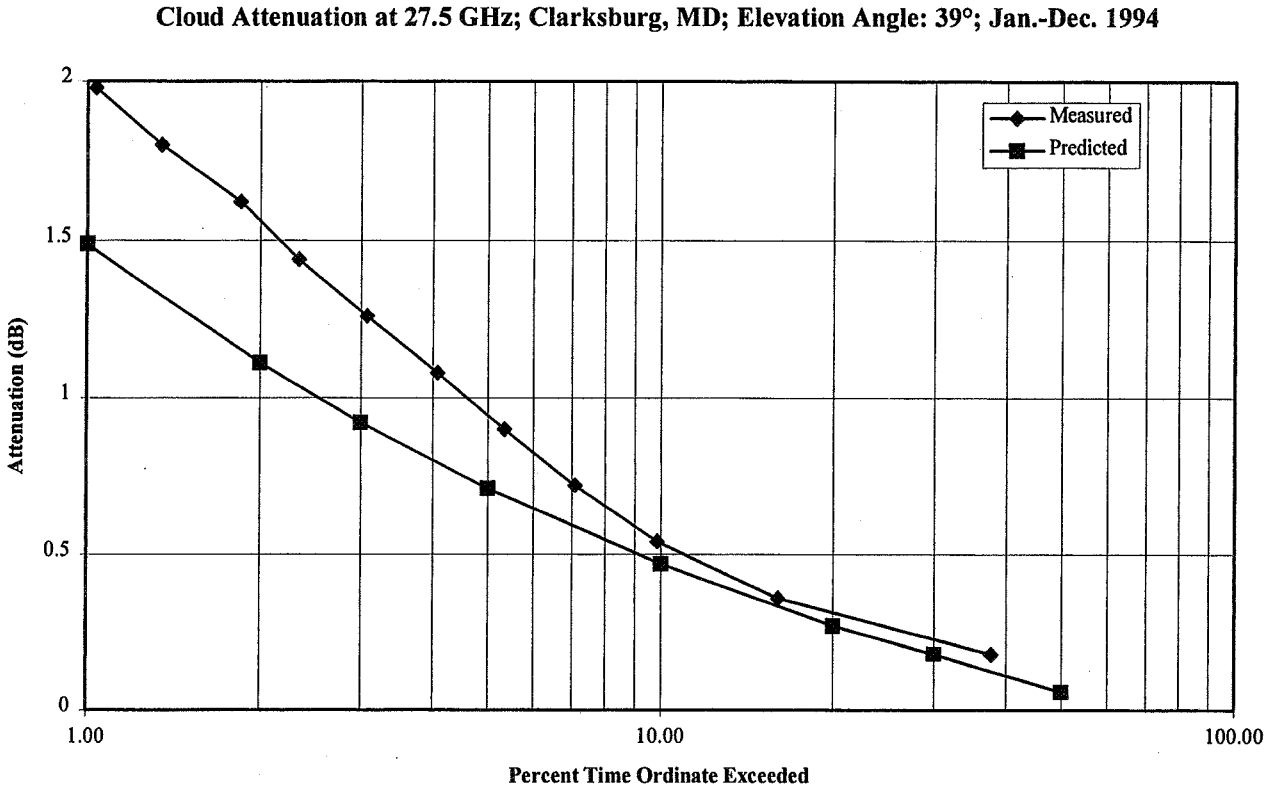

Conclusions

- Estimation of the cloud contribution towards the total path attenuation is feasible using the dual frequency ACTS measurements. Good stability of the measurement system and extra care in processing the data are required.

- Results presented are only preliminary; further processing is required to remove additional contributions from rain.

- Cloud model based on long-term cloud observations appears to provide reasonable results at lower percentage times. Some of the under estimation at higher percentage times may be attributed to incomplete processing of the data.

Page intentionally left blank

SPACE COMMUNICATIONS TECHNOLOGY CENTER

(SCTC)

ACTS Ka-BAND PROPAGATION MEASUREMENTS IN FLORIDA

HENRY HELMKEN
FLORIDA ATLANTIC UNIVERSITY (FAU)
&
RUDY HENNING
UNIVERSITY OF SOUTH FLORIDA (USF)

November 11 , 1996

OUTLINE

* **Florida ACTS Program Update**
* **Fade Duration Statistics**
* **ACA Estimation**
* **Short Baseline Diversity Experiment**
* **Conclusions**

ACTS PROPAGATION MEASUREMENTS

* NASA Propagation Terminal in Tampa, Florida
  University of South Florida (USF) Campus
  CCIR Rain Zone N, Global Rain Region E
  ACTS Elevation Angle: 52 Degrees
  ACTS Polarization: 43.6 Degrees
  33 Months of Data Pre-processed

* Diversity Experiments
  Extension of GTE Data Base
  COMSTAR Beacon Experiments 1978-80

FADE DURATION STATISTICS

* Conditional Probability

  $p(d) = p(d \mid a) * p(a)$

  $p(a)$ = Probability of Fade at Depth "a"

  $p(d \mid a)$ = Conditional Probability of Observing Fade of Duration "d" Given that "a" has Occurred

* Fade Duration Distributions
  Number of Duration "d" at Fade Depth "a"
  Total Time of Duration at Fade Depth "a"

* Cumulative Distribution Function
  Log-normal

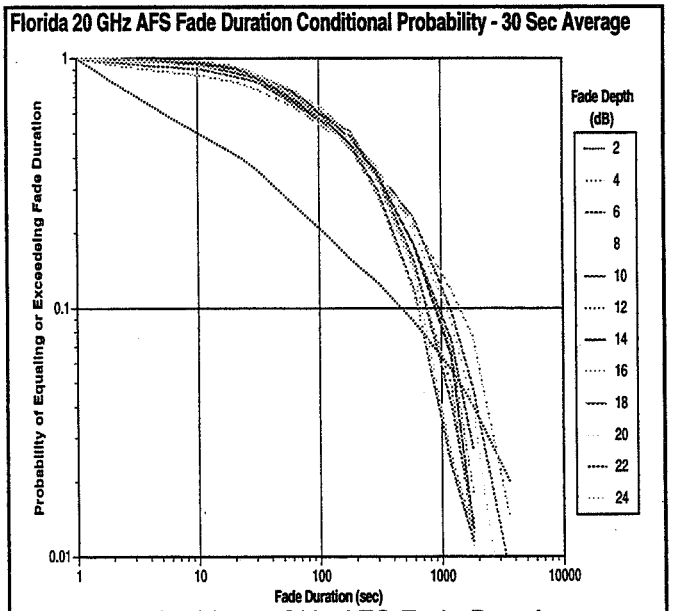

Figure 1. Florida 20 GHz AFS Fade Duration Distribution, Log-Log Scale, 30 Second Average

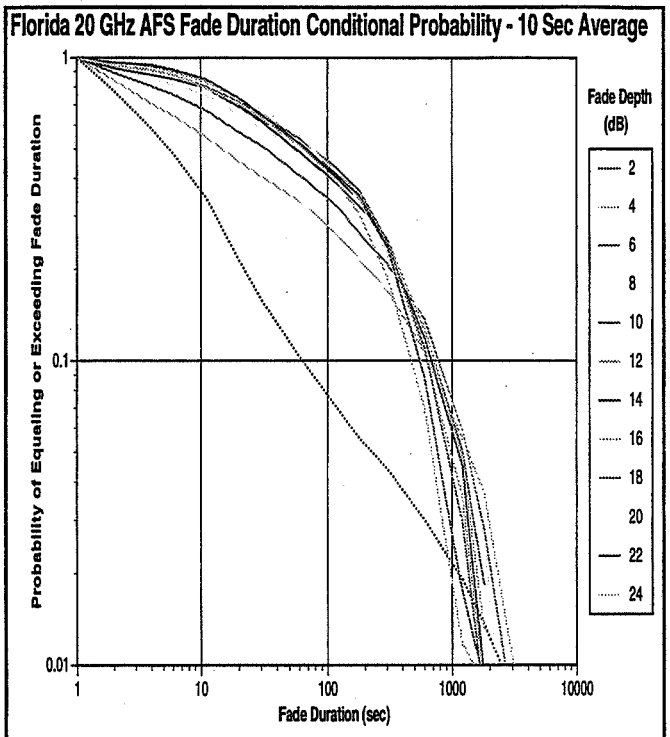

Figure 2. Florida 20 GHz AFS Conditional Fade Duration Distribution, 10 Second Averaging. All except 2 dB are tightly bundled

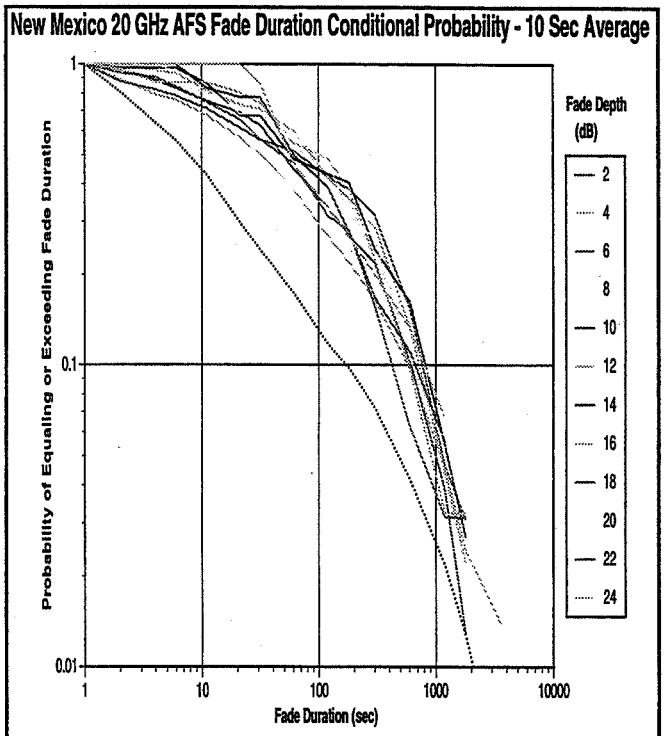

Figure 3. New Mexico 20 GHz AFS Conditional Fade Duration Distribution, 10 Second Averaging. All except 2 dB are tightly bundled.

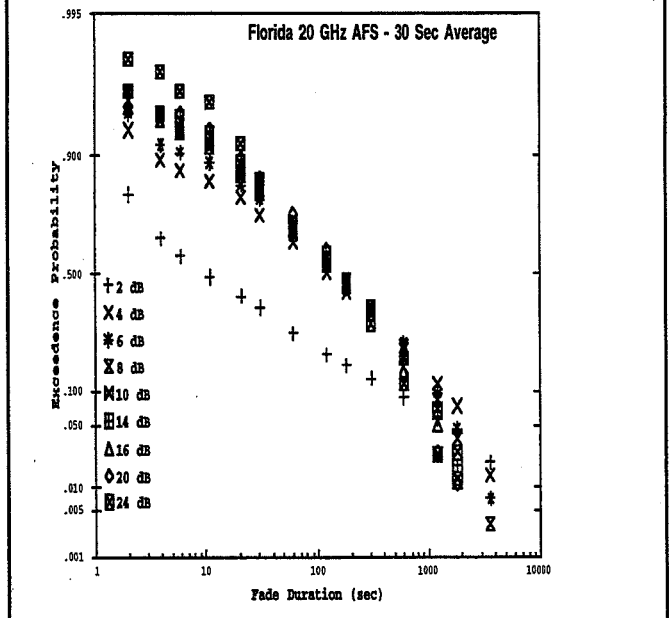

Figure 4. Log Normal plot of Florida AFS 20 GHz Conditional Fade Duration Distributions at Fade Depths from 2 dB to 24 dB, 30 second averaging. All except 2 dB are tightly bundled.

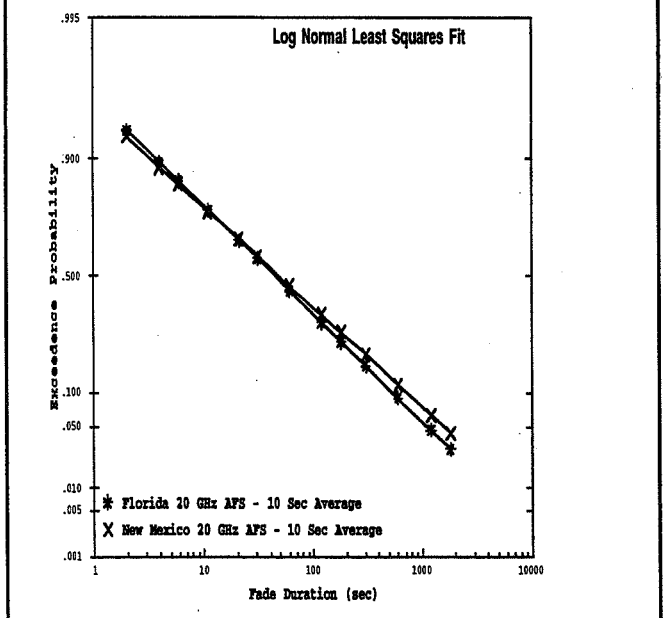

Figure 5. Comparison of Florida and New Mexico Log Normal least square fits of Conditional Fade Duration data, 10 second averaging. Florida and New Mexico have same elevation angle (52^{o})

SITE DIVERSITY EXPERIMENT

* Diversity Gain in the Florida sub-tropical Region
  - Focus on short baseline Diversity Gain
    - < 5km - greatest commercial interest
  - E-Systems Site at 42 km Baseline

* 20 GHz Transportable Diversity Terminal (TDT)
  - 1.2 m APT Dish
  - Downconvert to 70 MHz at Feed
  - APT Digital Receiver
  - 486 PC data recording in APT Format
  - Easily Replicated

* Operational Sites
  - Adjacent to APT Terminal
  - 1.2 km USF "Village" Campus Site
  - 4.3 km Commercial Site at GTEDS

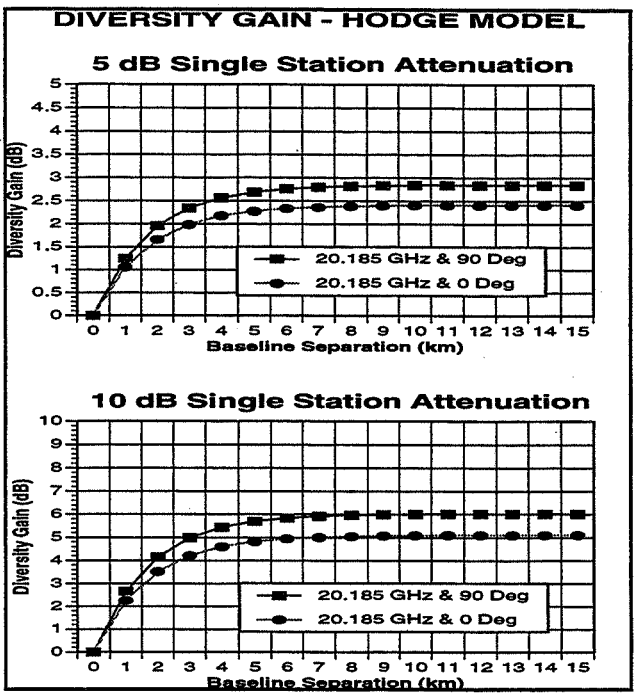

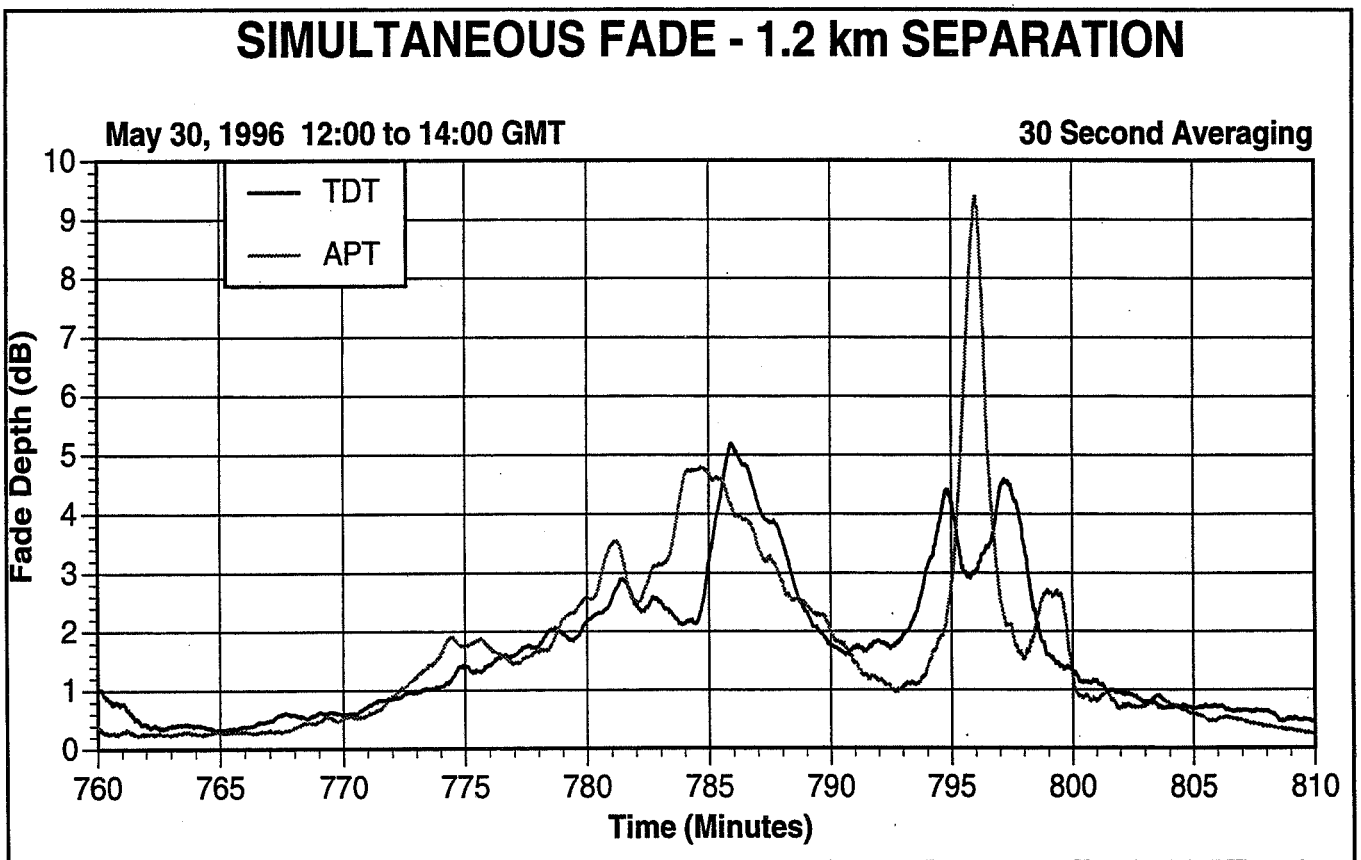

Figure 6. Comparison of Fade profiles observed simultaneously at the Acts Propagation Terminal (APT) and the Transportable Diversity Terminal (TDT) at a separation of 1.2 km.

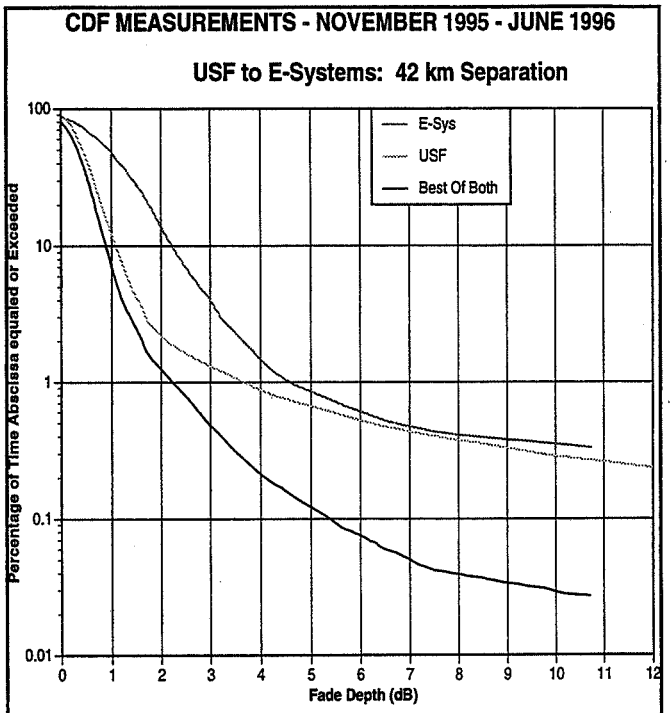

Figure 7. Measured CDF's at the E-systems remote terminal, the USF APT and best-of-both, 42 km separation.

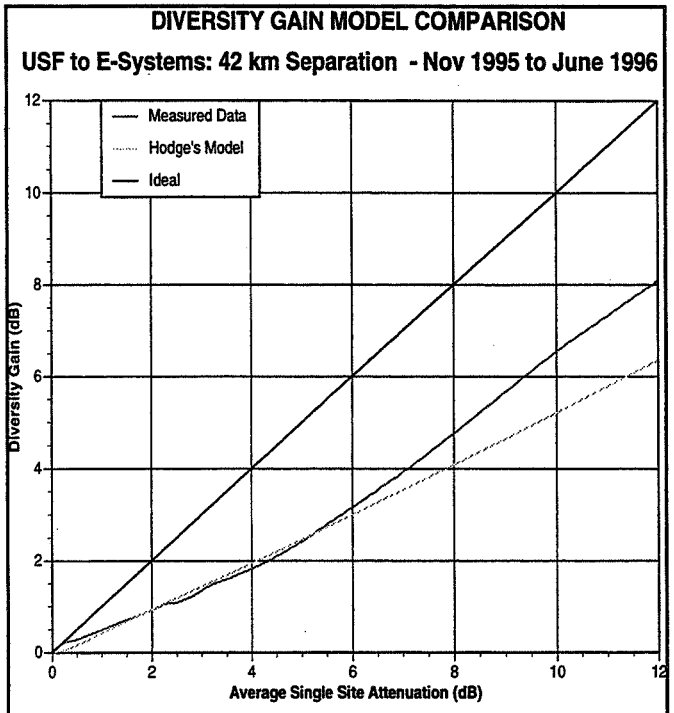

Figure 8. Comparison of Measured Diversity Gain and Hodge Model, 42 km separation.

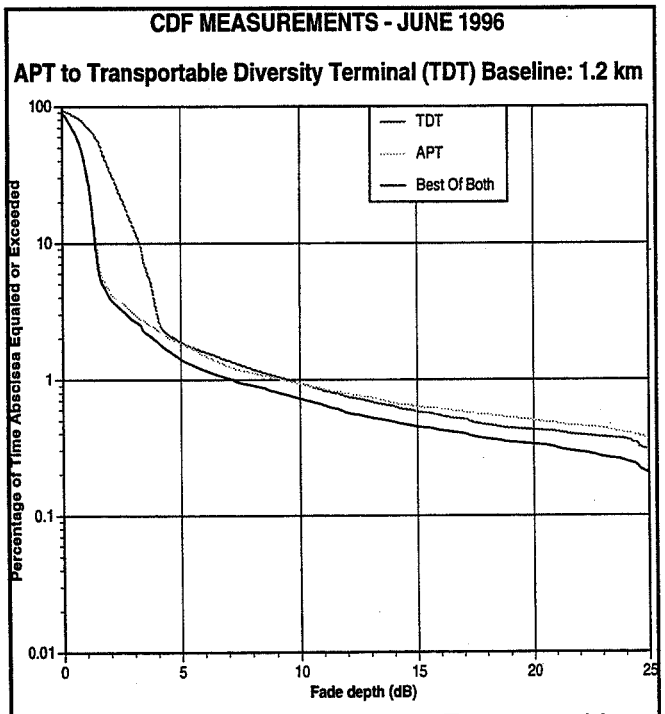

Figure 9. Measured CDF's at the Transporatable Diversity Terminal, the USF APT and best-of-both, 1.2 km separation.

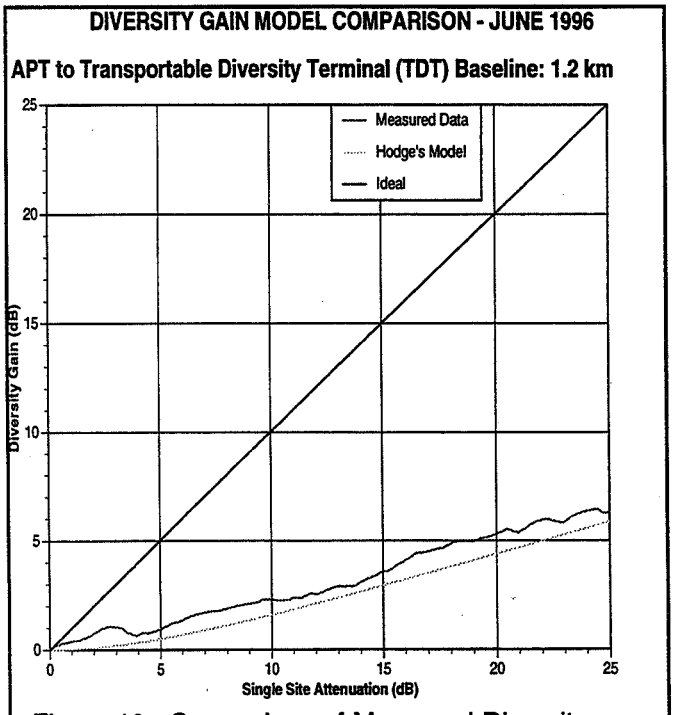

Figure 10. Comparison of Measured Diversity Gain and Hodge Model, 1.2 km separation.

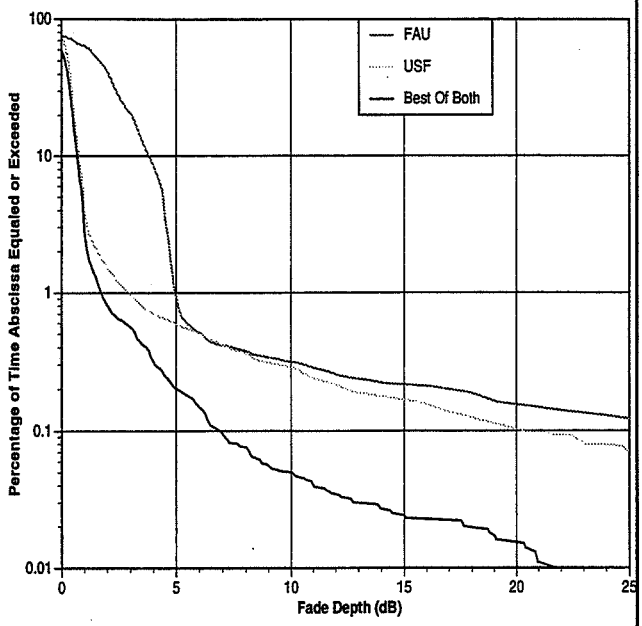

Figure 11. Measured CDF's at the Transporatable Diversity Terminal, the USF APT and best-of-both, 4.3 km separation.

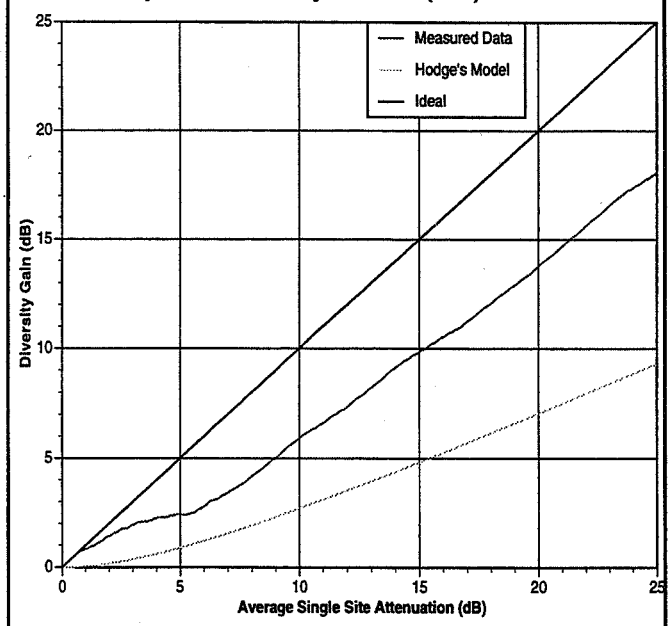

Figure 12. Comparison of Measured Diversity Gain and Hodge Model, 4.3 km separation.

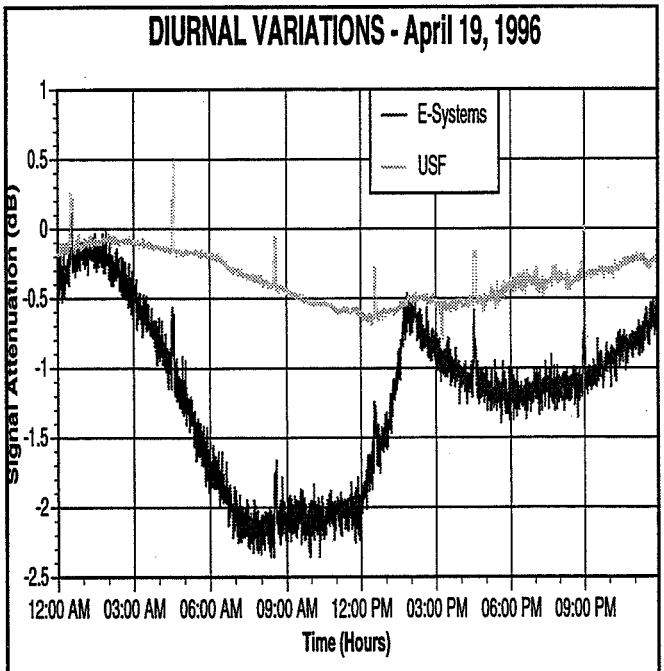

Figure 13. Diurnal Variations, comparison between APT Terminal at USF and E-System, 43 km separation.

CONCLUSIONS

*** 33 Months of Data Pre-processed**

*** Fade Duration Statistics**
Independent of Fade Depth

*** Conditional Probability Representation**
Underlying Log-Normal Distribution

*** Model dependencies**
Elevation Angle Dependence
Filter Dependence

*** Diversity Experiments**
Hodge Model May Underestimate Gain

*** Continue Diversity Experiments**
Viable Option in Sub-tropical Regions

Page intentionally left blank

New Mexico APT Status

June - November 1996

Stephen Horan
New Mexico State University
November 1996

Topics

- Equipment Status
- Maintenance Performed
- Glitches
- Rain Statistics

Equipment Status

Operational Statistics					
		Total Time			
Month	Status	Days	Hours	Minutes	% of Total
June	Up	30	0	0	100%
	Down	0	0	0	0%
July	Up	31	0	0	100%
	Down	0	0	0	0%
August	Up	27	4	6	87.65%
	Degraded	3	17	6	11.98%
	Down	0	2	48	0.38%
September	Up	30	0	0	100%
	Down	0	0	0	0%
October	Up	30	20	40	99.6%
	Down	0	3	20	0.4%
Total	Up	149	0	46	97.4%
	Degraded	3	17	6	2.4%
	Down	0	6	8	0.2%

Degraded performance due to 27 GHz receiver losing synchronization and meteorological sensors being offline after maintenance period.

Maintenance Performed

- In August, Dave Westenhaver replaced the APT computer hard disk and receiver hardware updates made
- In October, the feed horn was replaced

Glitches

- 20 GHz glitches appear on both the radiometer and beacon measurements at the same time
- Random events that seem to be most common in the winter months
- Cause is unknown

Sample Glitches

Example of a glitch event for September 1, 1995

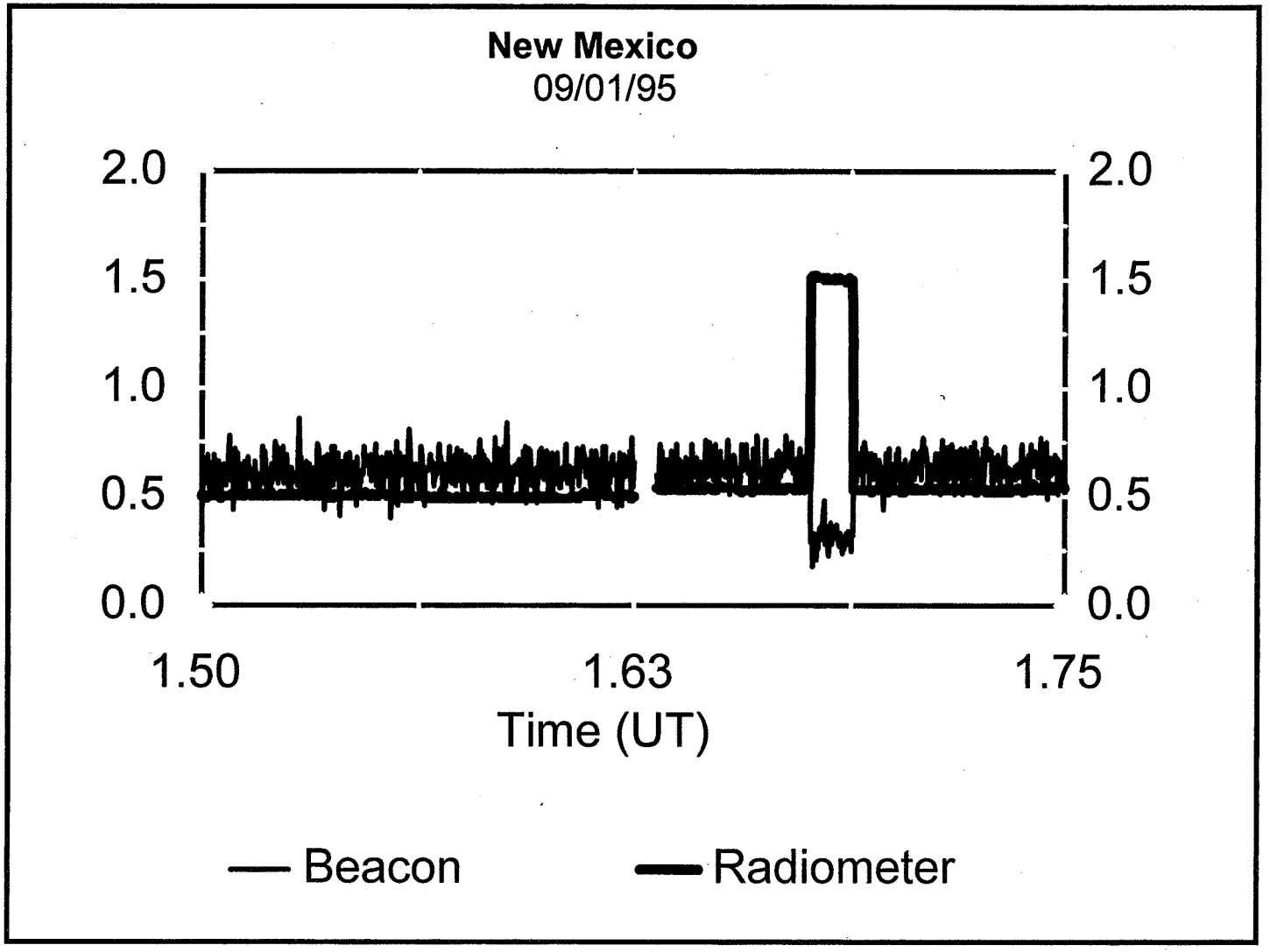

Stanford Telecom / New Mexico State University

ACTS Propagation Measurements Program

Data Analysis Summary

Julie H. Feil
Louis J. Ippolito
Stephen Horan
Jennifer Pinder
Frank Paulic

APSW X
November 19 & 20, 1996
Washington D.C.

Agenda

- **Introduction**
  - ➢ Experiment objectives & configuration
- **ACTS K_A band measurements and analysis**
  - ➢ Processing technique differences
  - ➢ Worst month attenuation and weather measurements
  - ➢ 33 month (12/1/93-8/31/96) propagation statistics
  - ➢ Model comparisons
- **Summary and future activities**
- **New Mexico State University**
  - ➢ Station Status

STel ACTS Propagation Experiment Objectives

- Measure and evaluate K_A band propagation effects and link performance for New Mexico
- Develop long-term statistics and prediction modeling techniques for New Mexico climate region for advanced satellite system planning and design
- Compare ACTS measurements (Ka band) to TDRS Space-to-Ground Link (Ku band) measurements
- Apply ACTS measurements to future satellite systems such as TDRS, Spaceway, Iridium, Odyssey, Teledesic, etc.

-3-

New Mexico Propagation Terminal

- Elevation angle: 51°
- Measured parameters
  - ➢ Beacons: 20.185 GHz and 27.505 GHz
  - ➢ Radiometers: 20 GHz and 27.505 GHz
  - ➢ Rain rate (CRG, TBG)
  - ➢ Temperature, Relative Humidity, Wind Vector
- Ancillary Measurements from TDRS
  - ➢ 13.5 GHz SGL delogged signal attenuation plots for identified weather events ('Raindance')
  - ➢ Coincident Steering Data: date, time, antenna azimuth and elevation
  - ➢ Lack of calibrated data

-4-

ACTS K_A Band Measurements Summary

- 33 months of data processed (2.75 years of statistics)
- Worst month (in 33 months): July 1996
- Cumulative weather measurements
- Comparison of old and new processing techniques for cumulative attenuation statistics
- Model comparisons
- 2 years of rain rate statistics (10/1/94-9/30/96)
- Attenuation Ratio
- Fade Duration
- Fade Slope

Worst Month: July 1996 Free Space Attenuation (AFS)

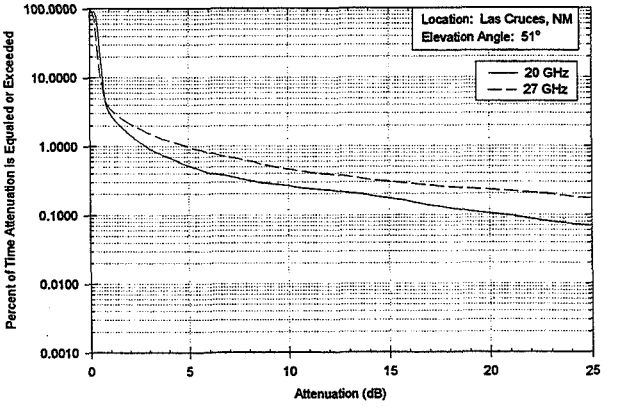

From *.pv2 files

July 1996 Radiometric Derived Attenuation (ARD)

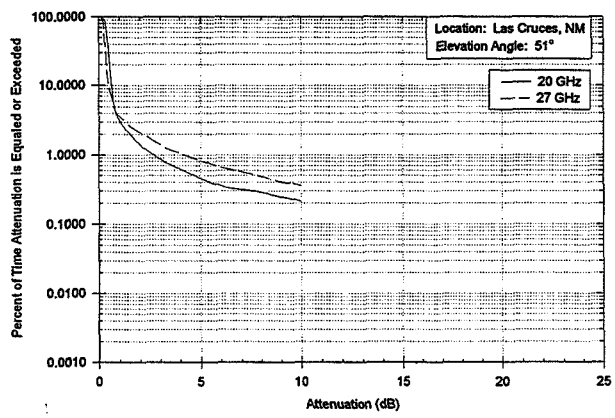

From *.pv2 files

- 7 -

July 1996 Clear Air Attenuation (ACA)

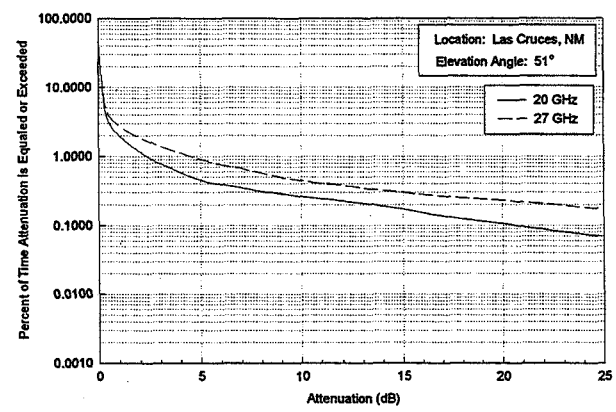

From *.pv2 files

- 8 -

Cumulative Surface Temperature

33 Months: December 1, 1993 through August 31, 1996

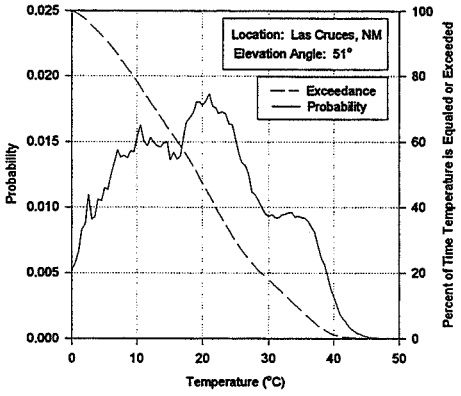

Cumulative Relative Humidity

33 Months: December 1, 1993 through August 31, 1996

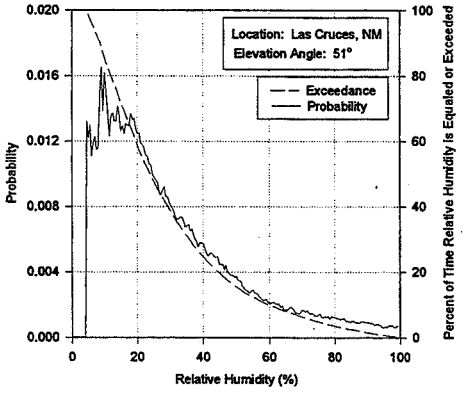

Comparison of Processing Techniques

- **33 Months Statistics: December 1993 -August 1996**
  - From *.pv0 processing (ACTSEDIT)
  - From *.pv2 processing (ACTSPP)
- **Minor differences between two processing techniques**
  - Monthly Statistics are within 1 dB
  - Gaseous absorption is less for *.pv2 than for *.pv0 processing
  - Rain Attenuation is almost identical

Attenuation wrt Free Space (AFS)

33 Months: December 1, 1993 through August 31, 1996

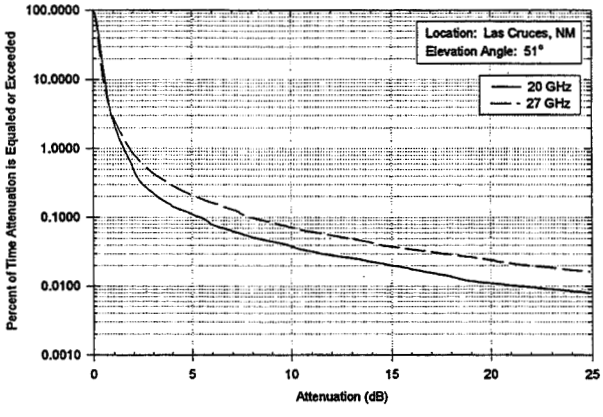

From *.pv2 files

Attenuation wrt Free Space (AFS)

33 Months: December 1, 1993 through August 31, 1996

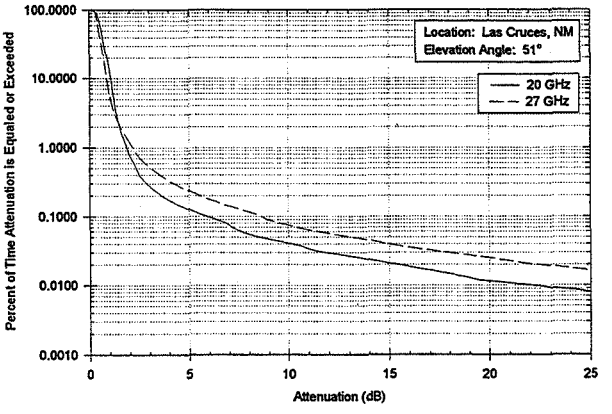

From *.pv0 files

- 13 -

Radiometric Derived Attenuation (ARD)

33 Months: December 1, 1993 through August 31, 1996

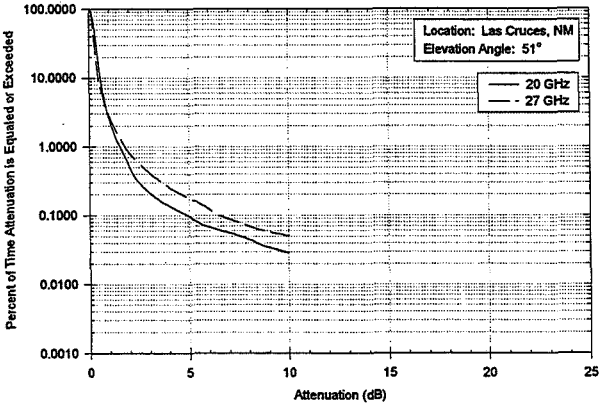

From *.pv2 files

- 14 -

Radiometric Derived Attenuation (ARD)

33 Months: December 1, 1993 through August 31, 1996

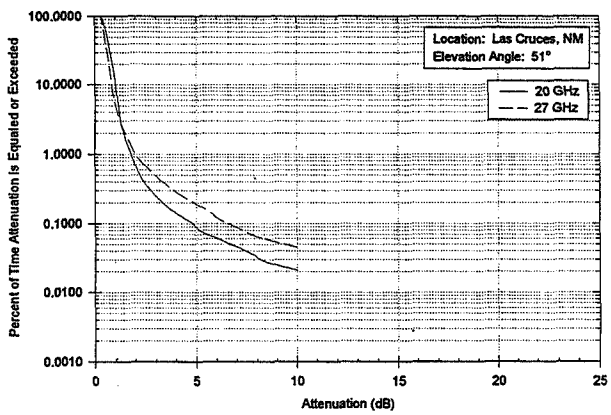

From *.pv0 files

- 15 -

Attenuation wrt Clear Air (ACA)

33 Months: December 1, 1993 through August 31, 1996

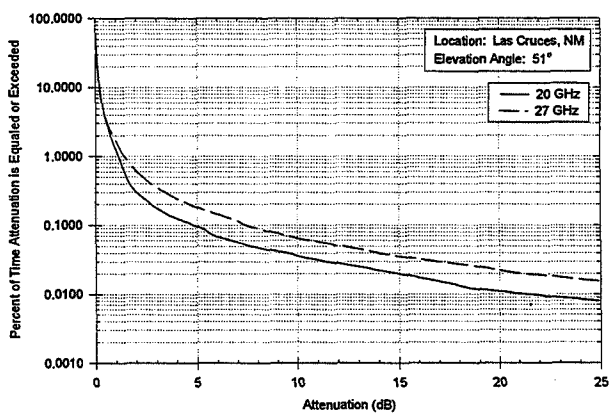

From *.pv2 files

- 16 -

Model Comparison of 20 GHz Cumulative Distribution

33 Months: December 1, 1993 through August 31, 1996

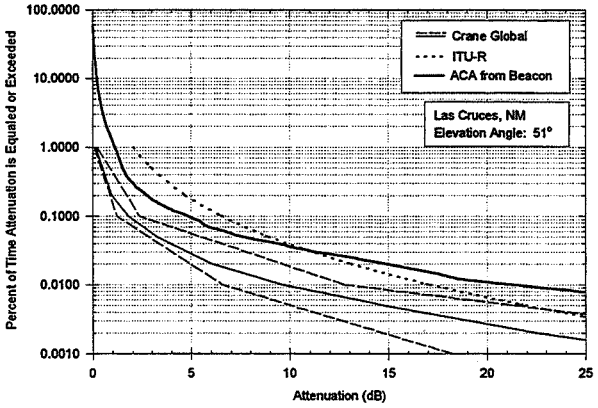

From *.pv2 files

- 17 -

Model Comparison of 27 GHz Cumulative Distribution

33 Months: December 1, 1993 through August 31, 1996

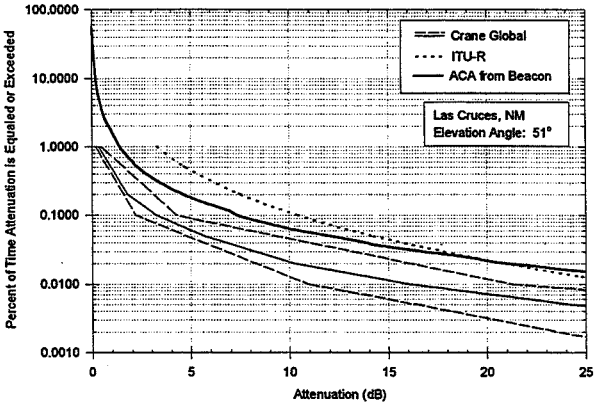

From *.pv2 files

- 18 -

2 Year Rain Rate Statistics

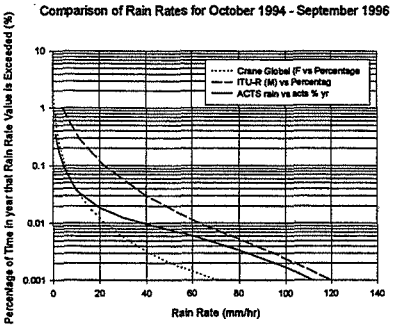

Comparison of 20 GHz ACA and Global Model with Local Rain Statistics

2 Years: October 1, 1994 through September 30, 1996

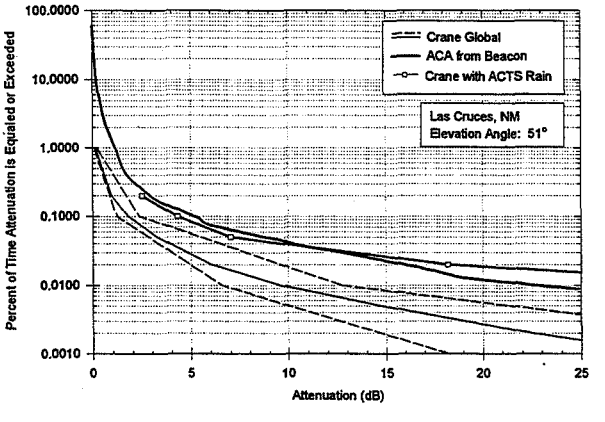

From *.pv2 files
10/1/94-9/30/96

Comparison of 27.5 GHz ACA and Global Model with Local Rain Statistics

2 Years: October 1, 1994 through September 30, 1996

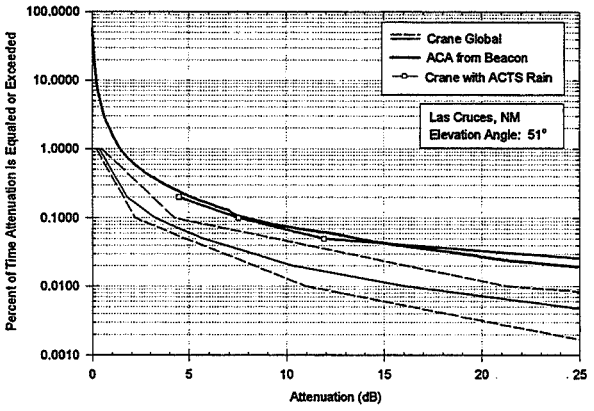

From *.pv2 files
10/1/94-9/30/96

- 21 -

Comparison of 20 GHz ACA and ITU Model with Local Rain Statistics

2 Years: October 1, 1994 through September 30, 1996

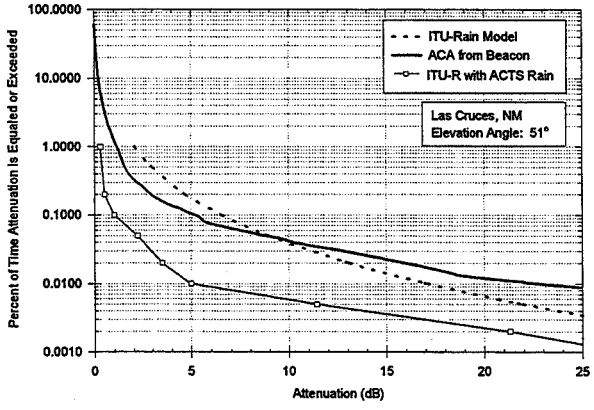

From *.pv2 files
10/1/94-9/30/96

- 22 -

Comparison of 27.5 GHz ACA and ITU Model with Local Rain Statistics

2 Years: October 1, 1994 through September 30, 1996

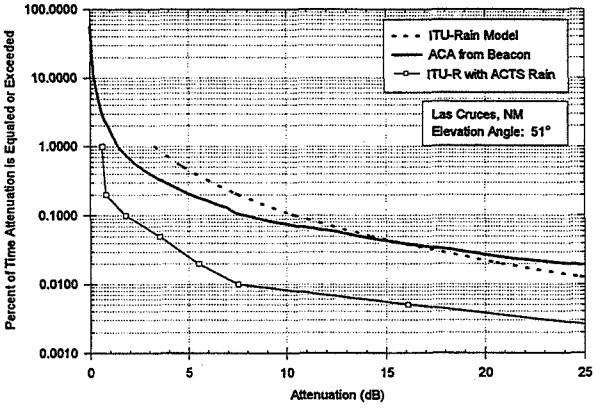

From *.pv2 files
10/1/94-9/30/96

Statistical Attenuation Ratio for ACA

33 Months: December 1, 1993 through August 31, 1996

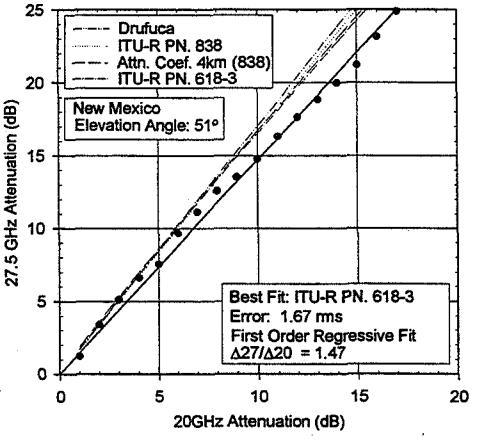

From *.pv2 files
12/1/93-8/31/96

Statistical Attenuation Ratio for AFS

33 Months: December 1, 1993 through August 31, 1996

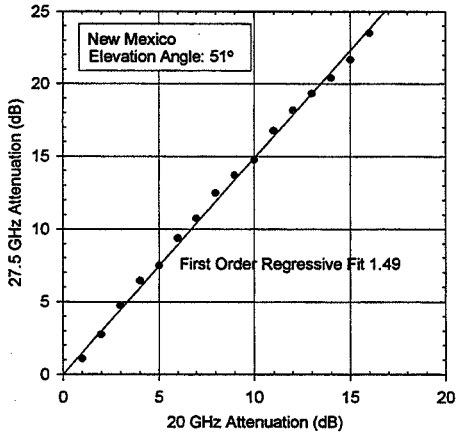

From either *.pv2 or *.pv0 files
12/1/93-8/31/96

20 GHz Fade Duration

33 Months: December 1, 1993 through August 31, 1996

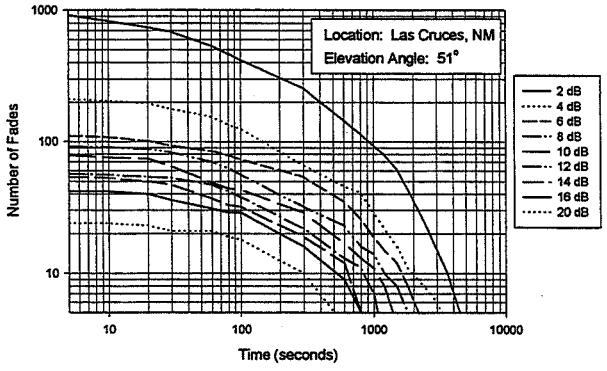

From *.pv2 files
12/1/93-8/31/96

27.5 GHz Fade Duration

33 Months: December 1, 1993 through August 31, 1996

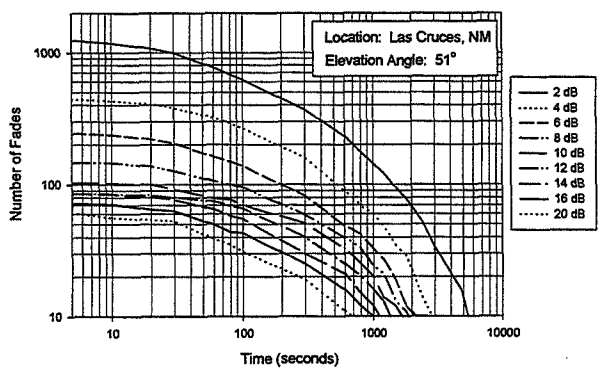

From *.pv2 files

20 GHz Fade Slope 2 Year Statistics

2 Years: December 1, 1993 through November 30, 1995

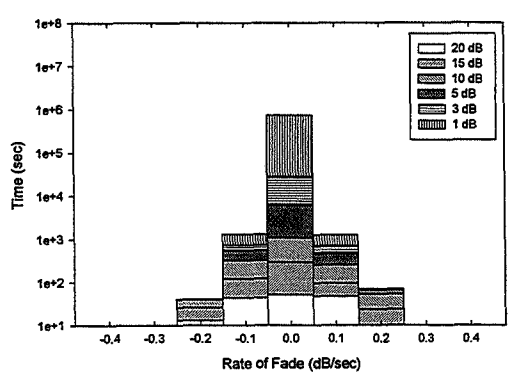

From *.pv2 files
12/1/93-11/30/96

27.5 GHz Fade Slope 2 Year Statistics

2 Years: December 1, 1993 through November 30, 1995

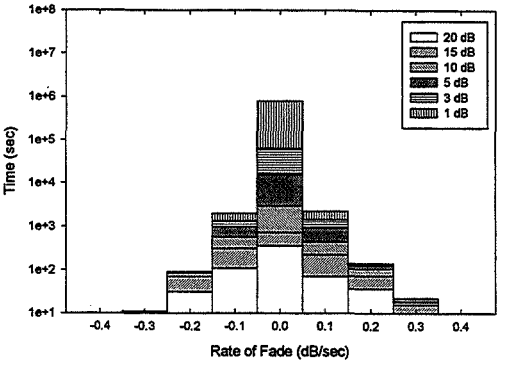

From *.pv2 files
12/1/93-11/30/96

2 Year Fade Slope Cumulative Statistics

For Attenuation greater than 1 dB.

(2 Years: December 1, 1993 through November 30, 1995)

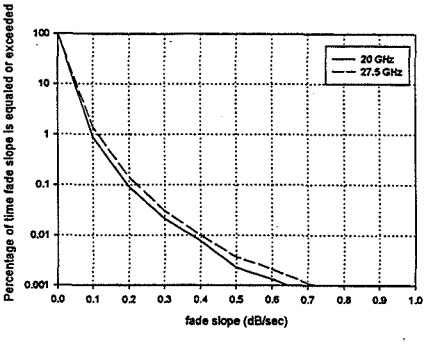

From *.pv2 files
12/1/93-11/30/96

New Mexico ACTS Statistics Summary

- **ACTSEDIT (.pv0) and ACTSPP (.pv2) processing have minor differences (< 1 dB) in attenuation distributions**
- **Measured link performance for 33 month period**

Annual Link Availability	20.185 GHz	27.505 GHz
99.90 %	5.4 dB	7.8 dB
99.95 %	8.2 dB	12.8 dB
99.99 %	21.4 dB	> 25 dB

New Mexico ACTS Statistics Summary (Cont.)

- **According to the National Climatic Data Center**
  - ➢ Above average temperature
  - ➢ Average humidity
  - ➢ Below average precipitation (60% of typical)
- **Rain Attenuation model prediction comparisons**
  - ➢ ITU-R model reasonable prediction
  - ➢ Crane global model under-predicts by 3-15 dB
  - ➢ Measured rain statistics improve prediction for global model
- **Attenuation ratio predicted well by models until 12 dB**
- **Secondary Statistics**
  - ➢ Fade Duration and slope statistics are reasonable

Future Activities

- Complete 3.75 year cumulative distributions from *.pv0 preprocessing
- Complete 3.75 year cumulative distributions from *.pv2 preprocessing
- Extend collection of raindance data for comparison to ACTS data
- Contract renewal to complete fourth year statistics and to start fifth year statistics

Page intentionally left blank

The Effects of Atmospheric Turbulence on the ACTS Beacon Signal Propagation: Data Analysis

By

Xuhe Wang and Robert K. Crane

School of Meteorology

University of Oklahoma

Norman, Oklahoma

December, 1996

Introduction

In this research we focused on the effects of tropospheric turbulence on electromagnetic wave propagation. Kolmogorov's hypothesis of locally isotropic turbulence was used as the theoretical basis for this research. The equations of electromagnetic wave propagation through a weakly turbulent atmosphere were solved to find the relationship between the power spectral density of microwave amplitude fluctuations and the atmospheric turbulence.

The ACTS beacon propagation data collected at different ACTS Propagation Experiments sites were analyzed. The results of spectral analyses on these data were consistent with the theoretical prediction of the relationship between scintillation (fast fluctuations in radio wave amplitude) power spectra and atmospheric turbulence spectra. The frequency and angle-of-arrival dependencies in the scintillation variance calculated from the ACTS propagation data were also in good agreement with the theoretical predictions. Radiosonde data from the upperair sounding station near our ACTS terminal were used to estimate the heights of turbulent layers and the turbulence fluctuation frequency corresponding to the transport of turbulence through the first Fresnel zone of the terminal antenna pattern. These estimates were then compared with the scintillation power spectra of the ACTS beacon signal. Good agreement was found in the comparison.

The research found that water vapor fluctuations in the turbulence occurring at the top of planetary boundary layer (1-1.5 km) contribute the most to the scintillation

we observed in ACTS beacon signal. There was a clear "-8/3" power law relationship between the signal fluctuation frequency and the scintillation power spectral density. Scintillation variance was proportional to the "7/6" power of the beacon frequency and close to the "-11/6" power of the sine of the elevation angle of the terminal antenna.

Following are the last two chapters of the thesis[1]. Theoretical reviews were given in previous chapters and are not included in here.

1 "The Effects of Atmospheric Turbulence on the ACTS Beacon Signal Propagation" - a Master Thesis by Xuhe Wang

CHAPTER 4

DATA ANALYSIS AND DISCUSSIONS

4.1 Data Processing

The methods for scintillation analysis appearing in the literature were high-pass filtering the time series of the received signal to separate the scintillation from other propagation phenomena. The variances of the scintillation are described by Mooulsley and Vilar, 1982; Karasawa et. al., 1988a; Karasawa and Mastsudo, 1991; Salonen et.al., 1996. The assumption underlying is that the lowest frequency of scintillation is in the range of 0.004 – 0.01 Hz, although the highest fluctuation frequency components of rain attenuation or gaseous absorption may also be found in this frequency range. In our study we will not perform filtering, since we are interested in the spectra of different scintillation events.

With the aid of the standard ACTS preprocessing software, daily summary plots were generated for the whole experiment period. These plots give information about the minute-averaged time series of beacon power level, estimates of attenuation, and fluctuations of attenuation within a minute. Also included in the plots is the surface meteorological data near the terminal. Figures 7–10 show the plots for 8/17/96.

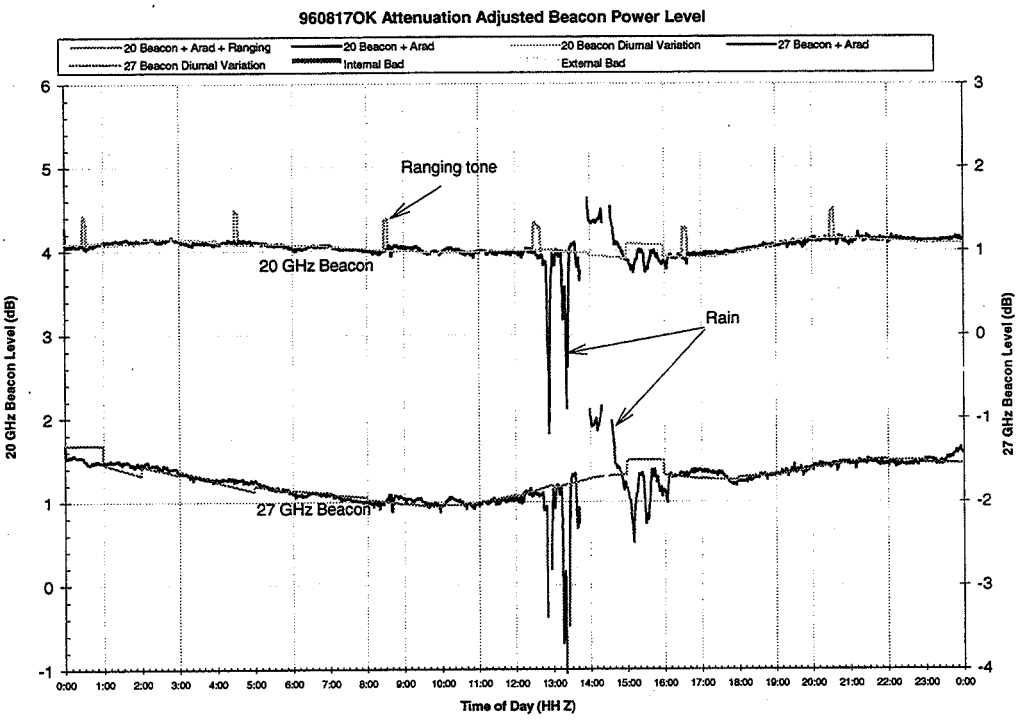

Figure 7. Attenuation removed beacon levels of 8/17/96, at Norman, OK

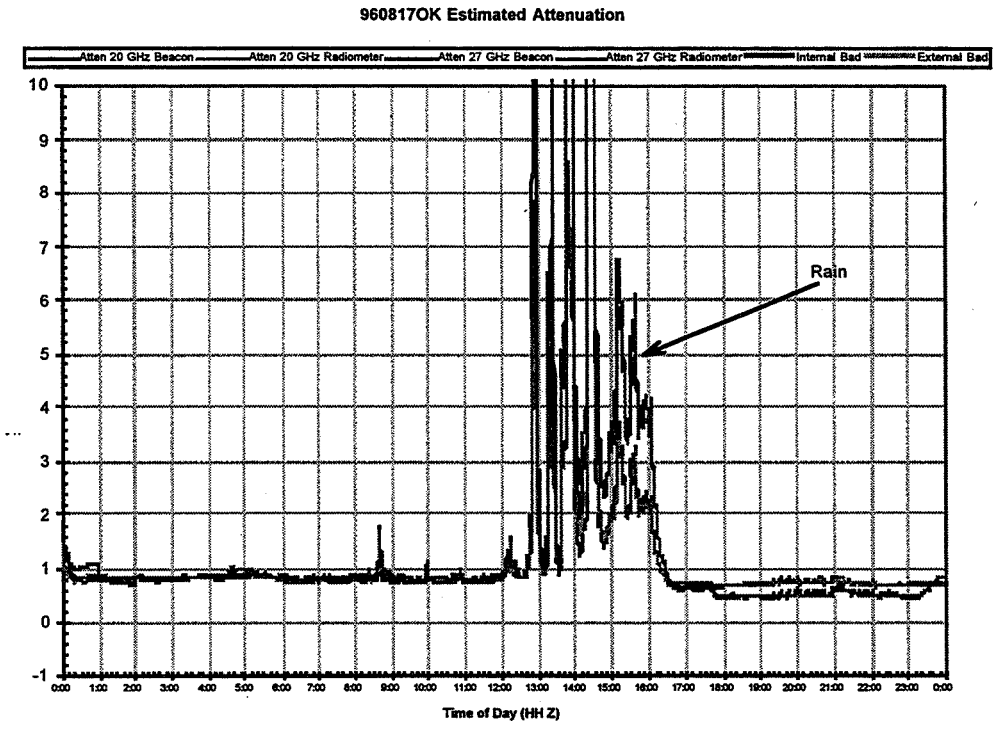

Figure 8. Estimated attenuation with respect to free sky of 8/17/96, at Norman, OK

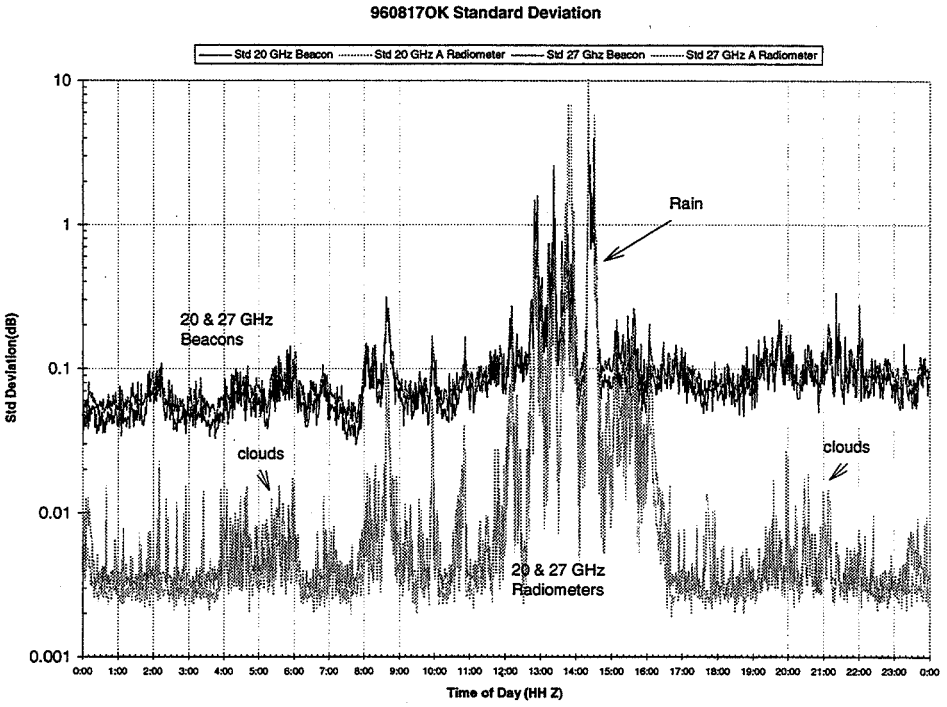

Figure 9. Standard deviation of attenuation within one minute of 8/17/96, Norman, OK

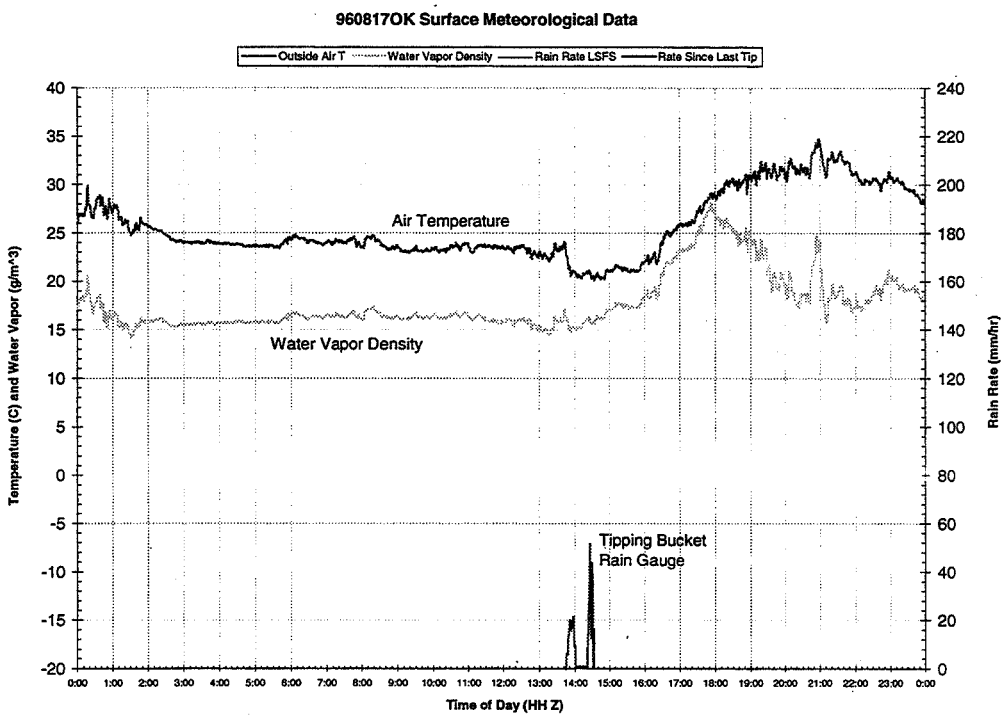

Figure 10. Surface meteorological data near the antenna of 8/17/96, Norman, OK

These charts provide a lot of valuable information as shown in the above figures. For example, the standard deviation chart can be used to detect the weather changes right along the beacon propagation path, Referring to Figure 9, we can see one rain event intersected the path between 12 Z to 17 Z, some cloud passages before, and after the rain (the clouds manifest themselves as increasing fluctuations in radiometer channels), and scintillation (not evident for this day). These charts serve as the guide line for us picking up different events.

For the 1 Hz data we first use the ACTS preprocessing software to extract the second-by-second beacon time series at the two frequencies for a selected time interval. During the radiometer autocalibration interval (during which the beacon receiver is turned to total power mode and the beacon signal at that frequency is no longer recorded, refer to Figure 11) the beacon power level at one frequency is calculated from that at the other frequency (we assume the beacon levels at the two frequencies are highly correlated). The resulting beacon time series is shown in Figure 12.

After filling the gaps caused by radiometer autocalibration we perform various points (128, 256, 512) FFTs on the resulting time series. Figure 13 gives one example of the FFT results.

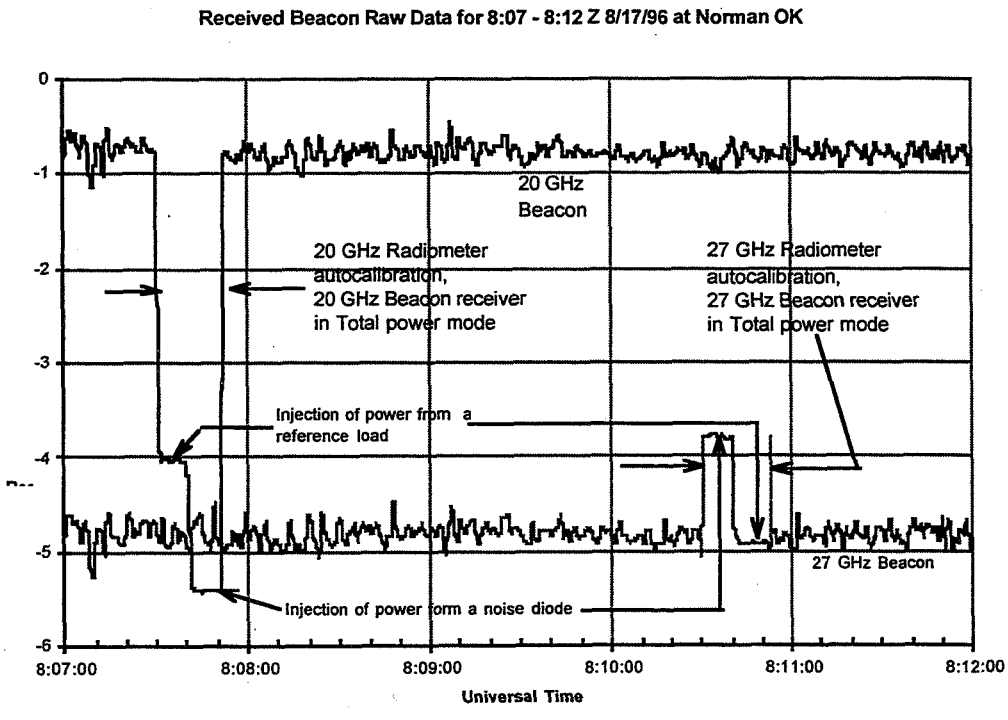

Figure 11. Radiometer autocalibration

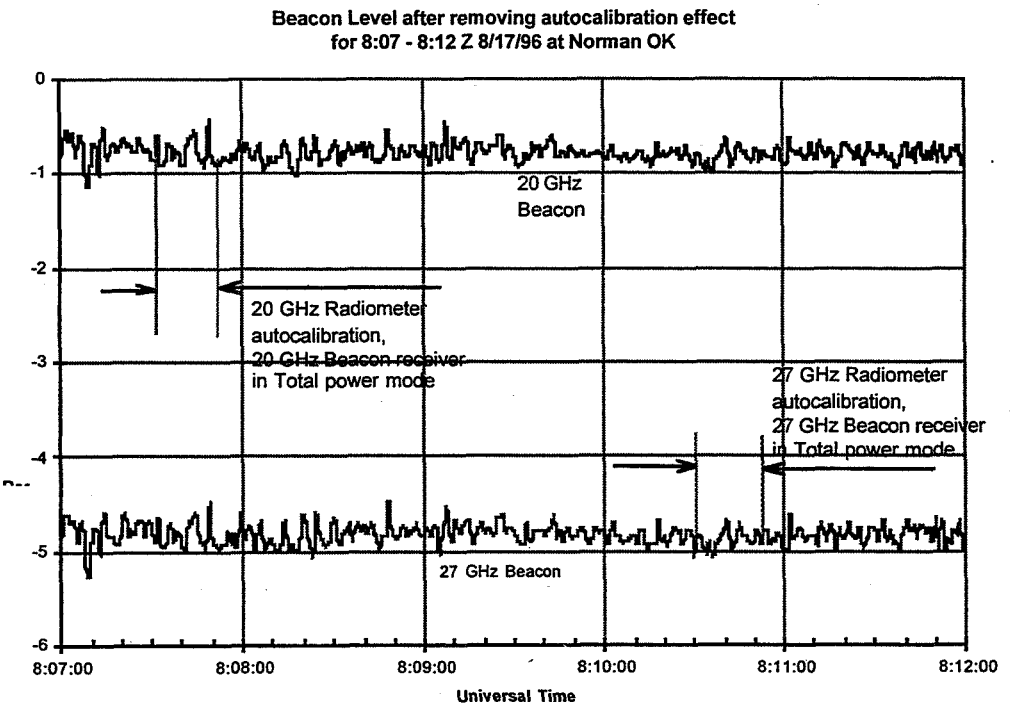

Figure 12. Removing the autocalibration effect on the received beacon data

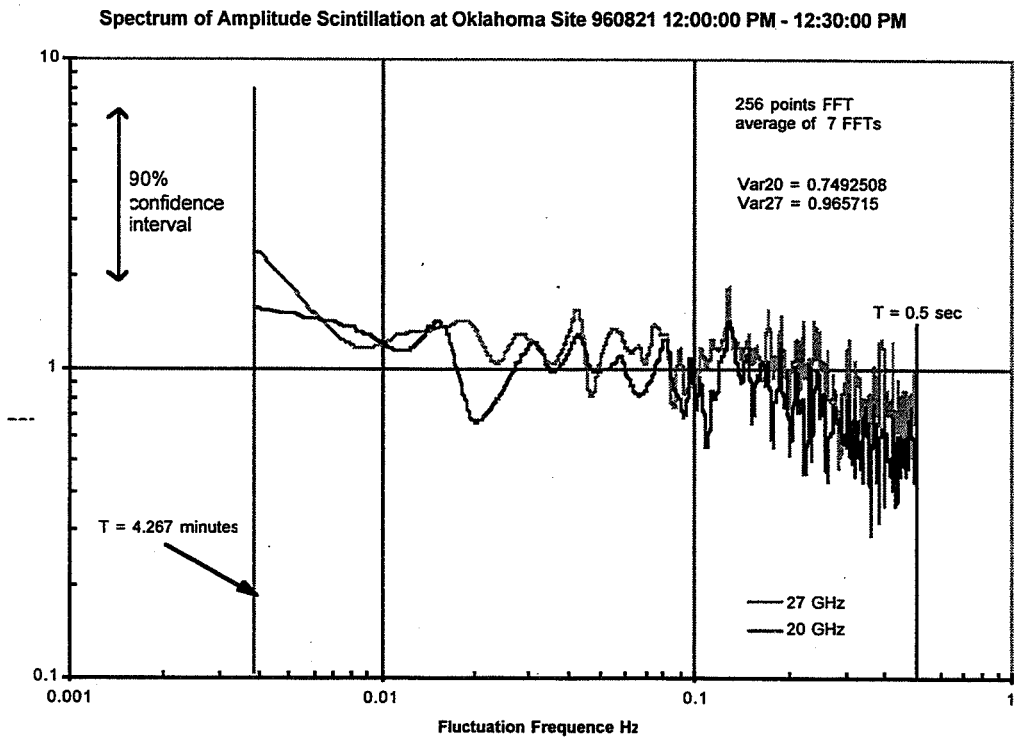

Figure 13 Spectrum of Amplitude Scintillation Calculated from ACTS 1 Hz Data

A special ACTS preprocessing program actshdr.exe is used to process the 20 Hz ACTS data, which provides the user with options to perform different length FFTs. The available lengths of FFTs are 512, 1024, 2048 and 4069 points. The Norman ACTS terminal began automatically collecting 20 Hz on February 17, 1996. Since then for every hour of observation, 10 minutes of 20 Hz data are recorded. Figure 13 shows the 1024 points FFT results for each hour of 8/17/96. The lowest frequency value corresponding to 1024 points 20 Hz data is 0.01953 Hz, with a period corresponding to 51.2 seconds. So with 10 minutes data we compute 11 FFTs, and the results in Figure 14 are the average of the 11 FFTs.

The profiles of vertical wind shear, vertical potential temperature gradient, and Richardson number at 0 Z and 12 Z can be calculated from radiosonde data near an ACTS terminal. The layer wind shear is estimated by using formula

$$\frac{\partial|\vec{u}|}{\partial z}=\frac{\sqrt{(u_2\cos\theta_2-u_1\cos\theta_1)^2+(u_2\sin\theta_2-u_1\sin\theta_1)^2}}{z_2-z_1} \qquad (4.1)$$

where u_i,θ_i,z_i are the wind speed, wind direction, and height at level i respectively, and $i=1,2$ stands for two adjacent layers in the sounding data. The vertical wind shear profile for 8/7/96 12 Z is shown in Figure 15 (discussion about this figure is given in Sec 4.3).

Parameters also indicated in the figure are the estimated fluctuation frequency corresponding to air motion through the first Fresnel zone (see Sec 4.2), the relative

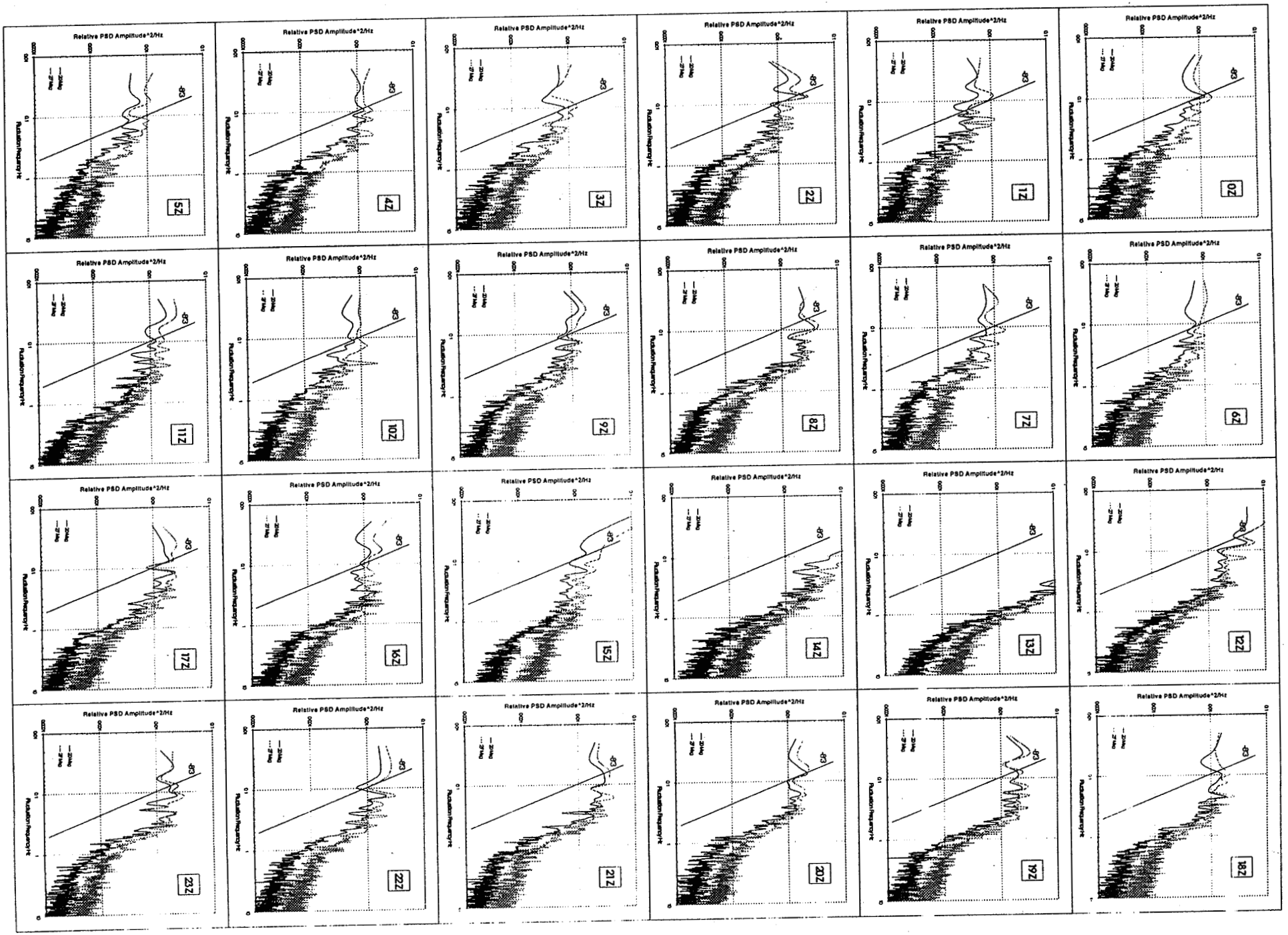

Figure 14. Spectra of ACTS 20 Hz data on 8/17/96, Norman, OK

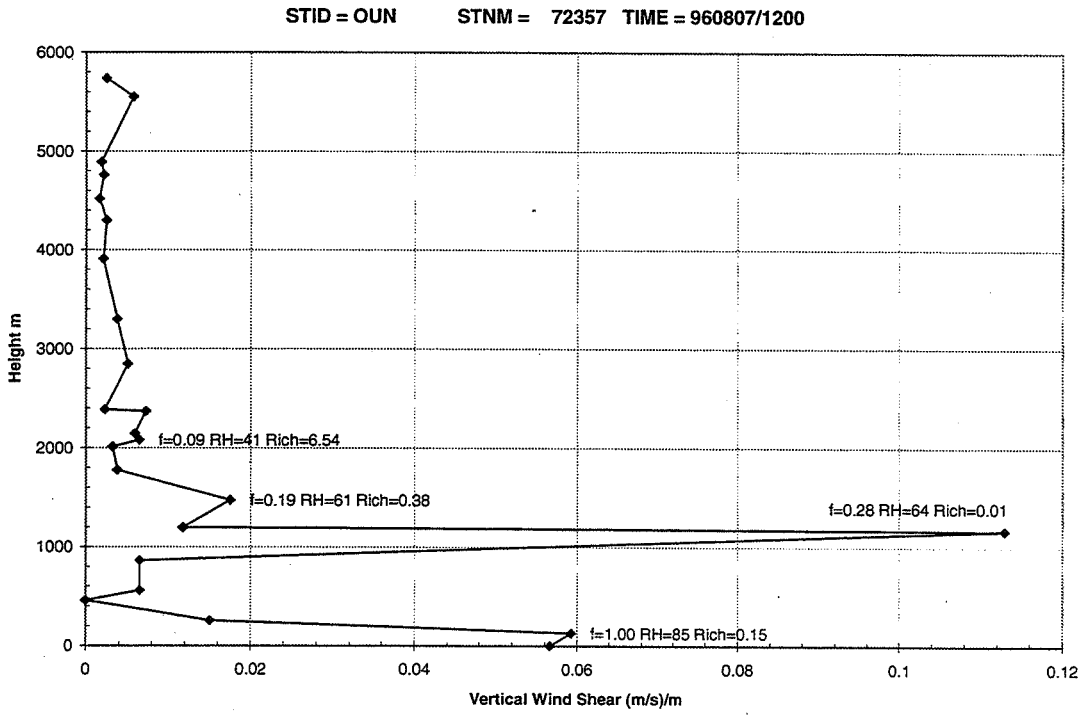

Figure 15. 8/7/96 12 Z Vertical Wind Shear Profile Calculated from the Upperair Sounding Data at Norman, OK

humidity, and the Richardson number at each significant level. The Richardson number is calculated from the following formula

$$R_i = \frac{\frac{g}{\bar{\theta}}\frac{\partial \theta}{\partial z}}{\left(\frac{\partial \vec{u}}{\partial z}\right)^2} = \frac{\frac{2g}{(\theta_1+\theta_2)}\frac{(\theta_2-\theta_1)}{(z_2-z_1)}}{\left(\frac{\partial \vec{u}}{\partial z}\right)^2} \qquad (4.2)$$

where θ_1 and θ_2 are potential temperature at two adjacent layer. The vertical profile of the Richardson number for 8/7/96 12 Z calculated from OUN (Norman) upperair sounding data is shown in Figure 15. The vertical profile of the buoyancy frequency is given in Figure 16.

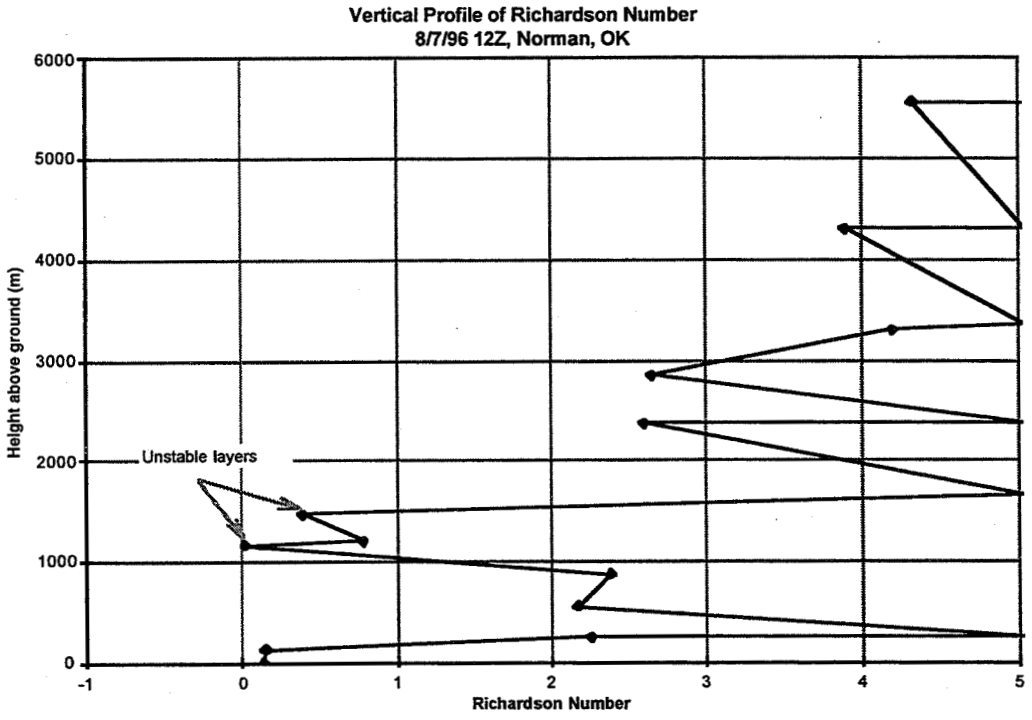

Figure 16. 8/7/96 12 Z Vertical Profile of Richardson Number

Calculated from Upperair Sounding Data form Station OUN

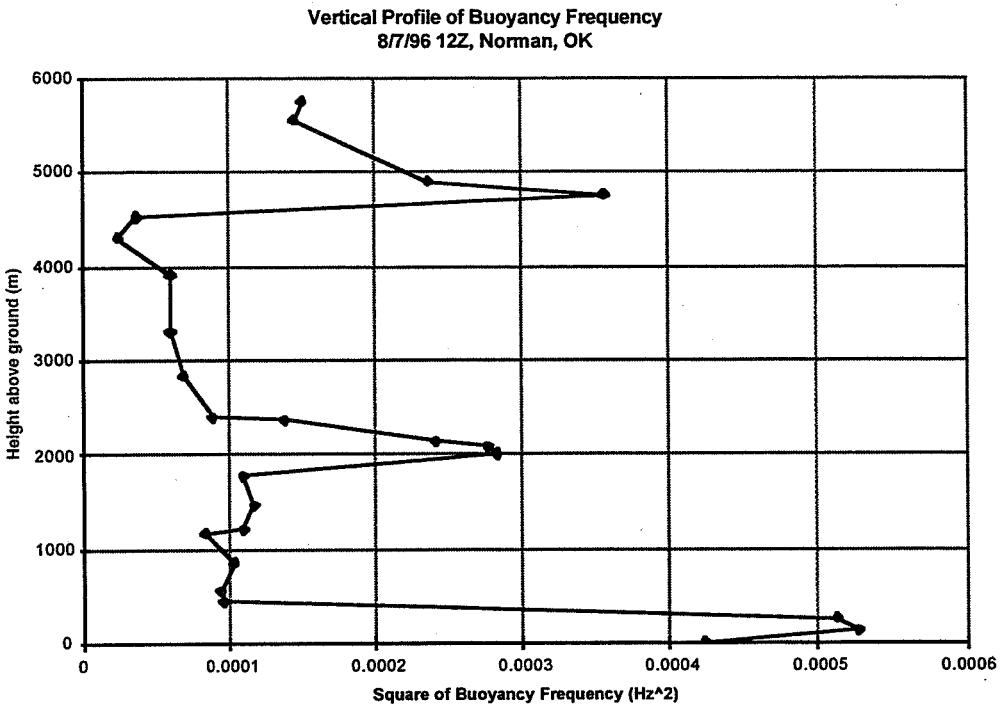

Figure 17. 8/7/96 12 Z Vertical Profile of Buoyancy frequency at Norman, OK

4.2 Main Characteristics of Scintillation Spectra

In Chapter 3 we have discussed wave propagation through a weak turbulent layer and made an assumption that the main contribution to the scintillation observed in the ACTS data is coming from the fluctuations of refractive index with scale size $l_o << l << L$ (i.e., inertial subrange). We also found from the theoretical derivation that the largest amplitude scintillations are produced by fluctuations on scale sizes of the order of the first Fresnel zone size. So it is important for us to first estimate these crucial parameters. The inner scale of fluctuations of refractive index in the first two kilometers of the troposphere has been estimated to be on the order of centimeters (Crane 1980, Doviak and Zrnic, 1993, pp. 474), while the outer scale is estimated to be on the order of 50 m - 100 m (Crane 1980). If the layer height is equal to 1 kilometer then the first Fresnel zone sizes are equal to 4.4 m and 3.8 m for 20 GHz and 27 GHz respectively. So we can expect that the spectra of our ACTS data should be consistent with what we have discussed in Chapter 3.

The general spectral shape of the ACTS 20 Hz data is shown in Figure 18, the data is recorded under clear sky. We see from Figure 18 that the spectral density peaks at 0.1 Hz; spectral regions confirming the "-8/3" law and "+1/3" law are separated by the peak. While the high frequency end of the "-8/3" part is mixed into noise at ~0.7 Hz. In most of cases, which include rain, clouds and clear sky, we observe the "-8/3" region in our spectra. The differences among spectra are the position of the spectral

peak (or sometime no peak can be observed) and the spectral shapes at low frequencies, which may deviate greatly from "+1/3" law.

Figure 19 is an example which has a different spectral shape than that in Figure 18, but the data is also recorded under clear sky. We see from Figure 19 the "-8/3" part still can be observed, while the peak in the spectrum shafts to higher frequency as compared to that in Figure 18 , the low frequency part no longer follows a "+1/3" law.

Most spectra of the data collected during clouds intersecting the propagation path have similar spectral shapes as Figure 19 (with even hard to distinguishable spectral peaks). Figure 20 shows one of them.

Figure 21 gives an example of the spectra of 20 Hz ACTS data recorded during rain (this rain event is also shown in Figures 7, 8, 9 and 10). We see the spectrum deviates significantly from "+1/3" at the low frequency end and no peak can be observed in the spectrum. Figure 22 shows the spectrum calculated from 1 Hz data during the same rain event in the time interval 13:00 - 14:00 Z. The spectrum in Figure 21 is expanded into to the lower frequency range. We find from Figure 22 the spectrum now follows a "-1" power law, which is in agreement with the spectral observation in cumulus or cumulonimbus (Zhou, 1991, pp. 265 - 268, Karasawa et. al., 1991) (see Sec 3.8).

Figure 23 is another example of the spectra of amplitude scintillation during rain, which also shows a "+1" power law relation. The physical processes behind this relation remain to be discovered.

The clear summer day diurnal changes in scintillation are evident in the ACTS data. Figure 24 shows the spectra for one of such days. It clearly indicates strong scintillation occurring during 16 - 23 Z (local time 11 AM - 6 PM).

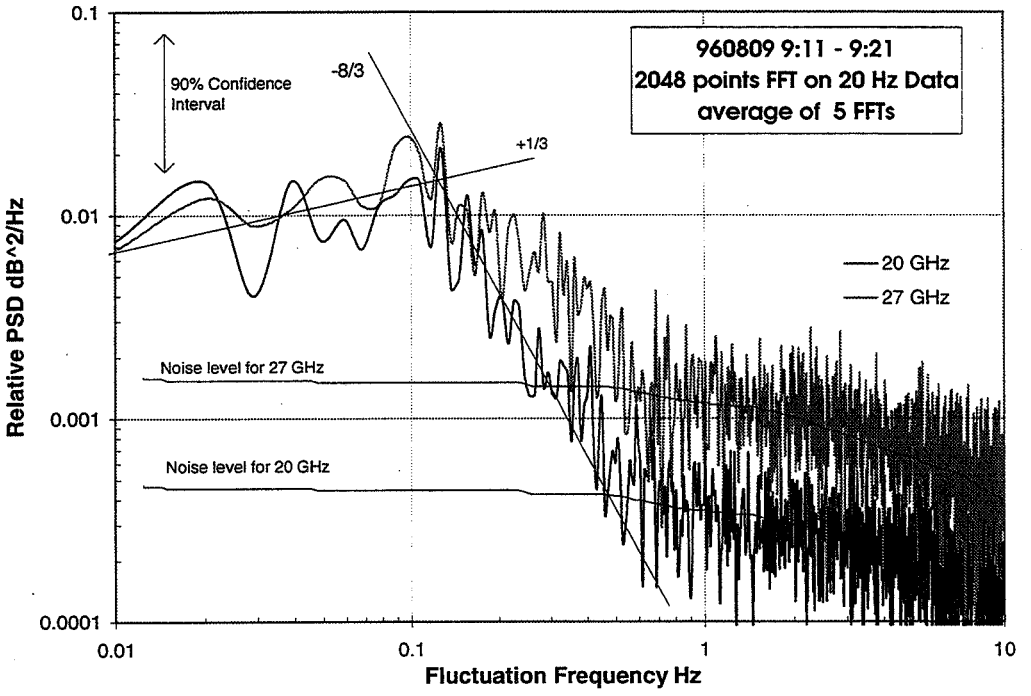

Figure 18 General Spectral Shape of ACTS 20 Hz Data

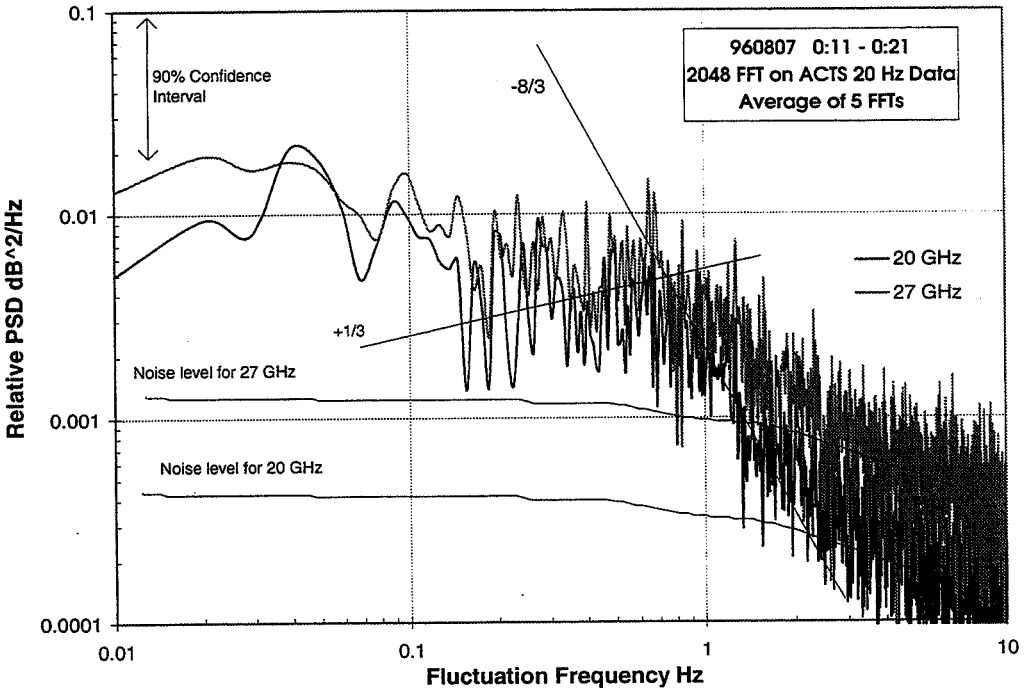

Figure 19 Spectrum of 8/7/96/ 0:11- 0:21 ACTS 20Hz Data

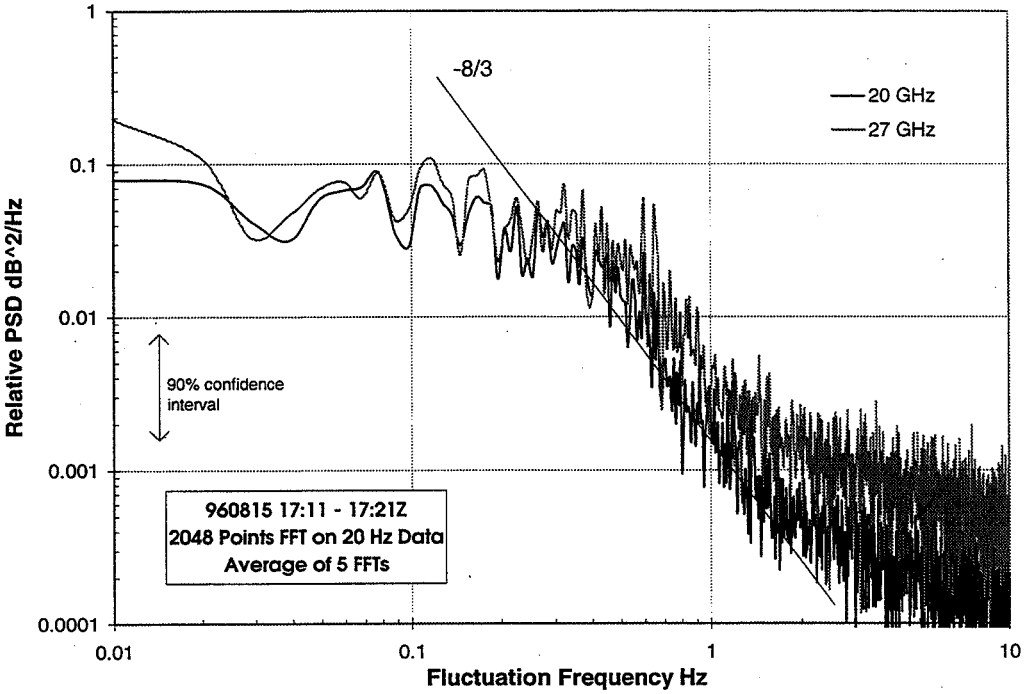

Figure 20 Spectrum of amplitude scintillation when clouds intersect the beacon propagation path, ACTS Norman site

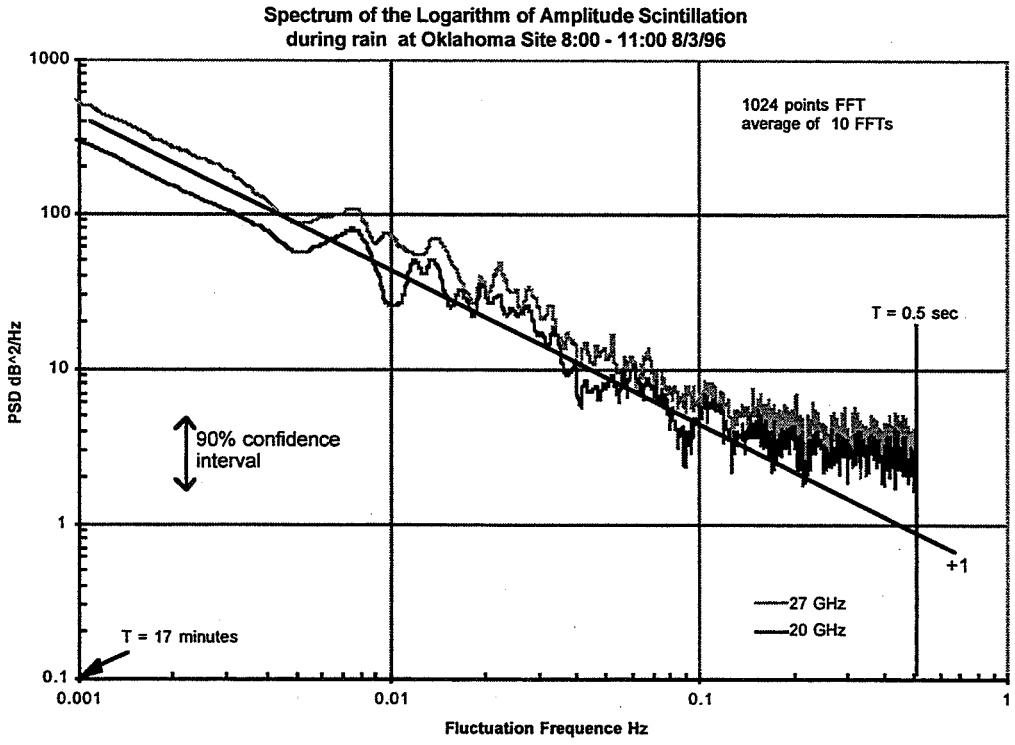

Figure 21 Scintillation Spectrum for a Rain Event

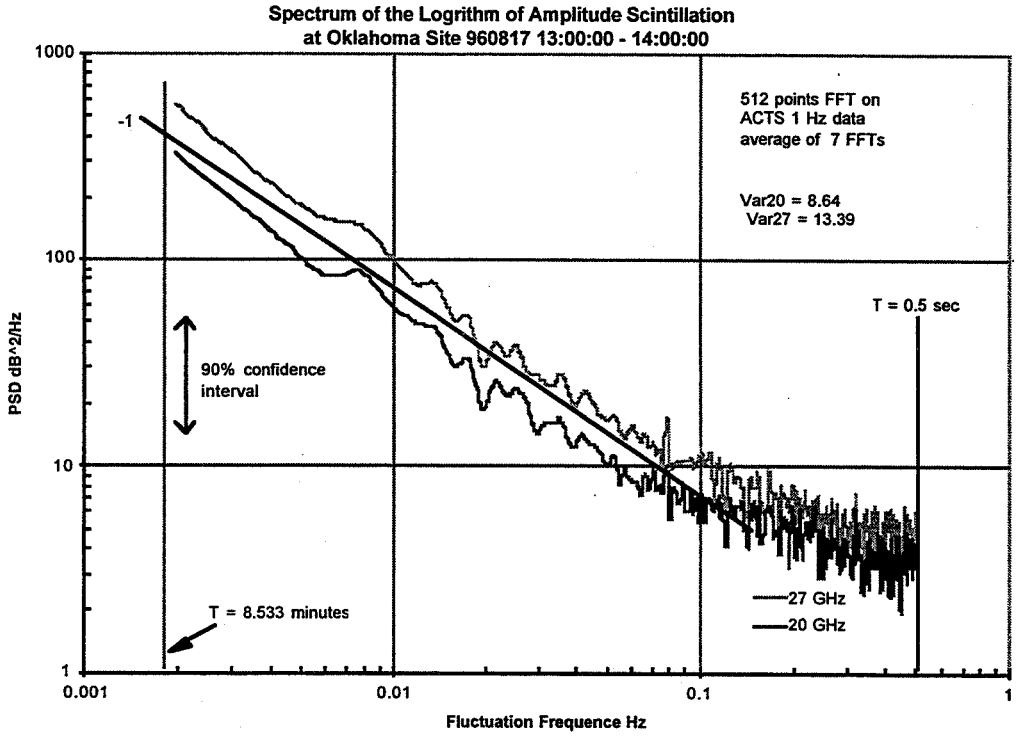

Figure 22 Scintillation spectrum calculated from ACTS 1 Hz data recorded during the same rain event as in Figure 21

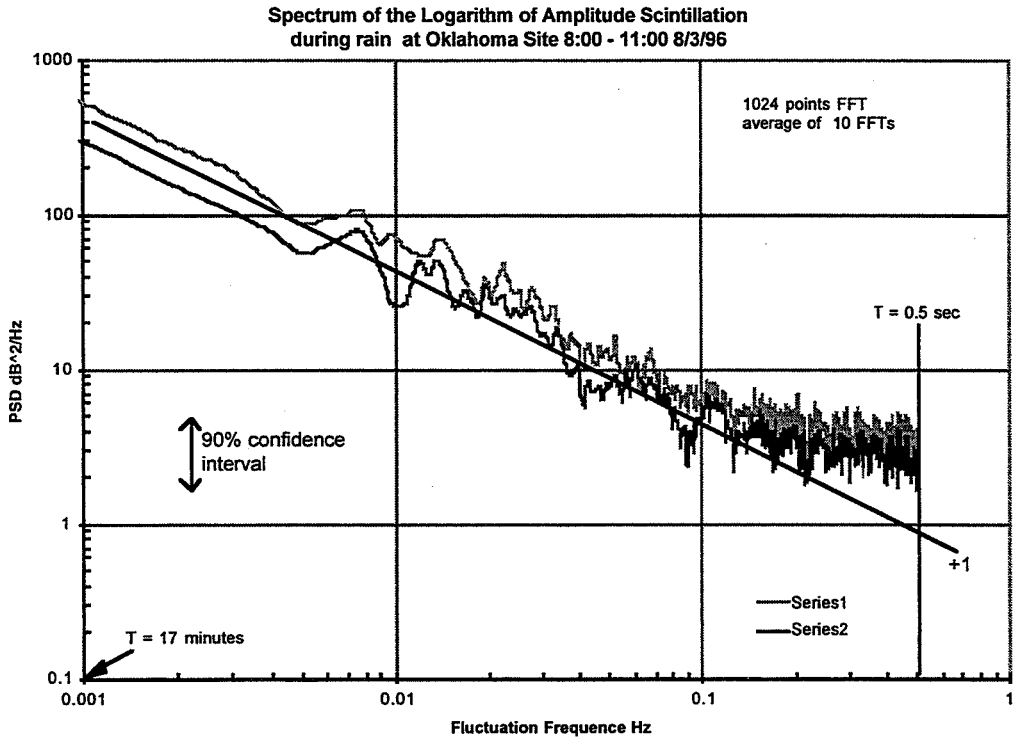

Figure 23 Spectrum of amplitude scintillation

during a rain event 8 - 11Z, 8/3/96, Norman, OK

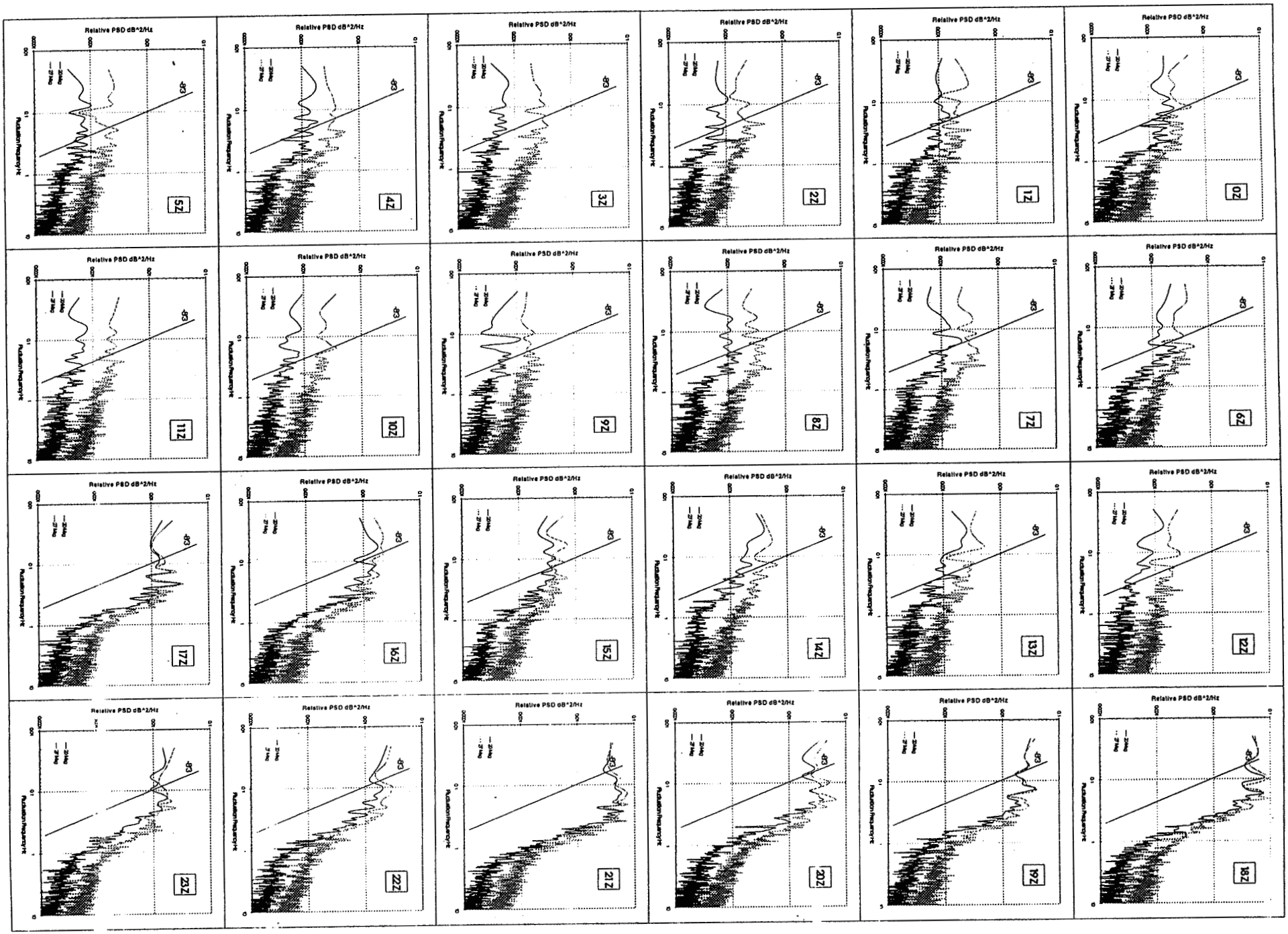

Figure 24 Diurnal changes of spectra during a clear summer day 8/13/96, Norman

4.3 Comparison Radiosonde Data and ACTS Scintillation Data

To make use of the radiosonde data we need to answer an important question about how we map the time domain fluctuations we observed in the ACTS beacon signal into the spatial domain refractive index fluctuations which, as supposed, intersect the ACTS beacon propagation path. To answer this question we make some crude assumptions:

(1) The spatial distribution of refractive index irregularities is stratiform, i.e. concentrated in layers;

(2) the refractive index irregularities in one layer are drifting along the mean flow at that layer.

To simplify the problem let us first consider the case in which there is only one layer of such irregularities of the refractive index. Then in order to find this layer we make a further assumption that the refractive index irregularities can be found concentrated in a turbulent layer which is characterized by a large vertical wind shear or small Richardson number (<1). Based on these assumptions we can calculate the first Fresnel zone of the ACTS antenna corresponding to this layer by using radiosonde data.

$$\sqrt{\lambda r} = \sqrt{\lambda \frac{H}{\sin \alpha}} \tag{4.3}$$

where α is the elevation angle, and H is the turbulent layer height above the ACTS terminal. The wave number corresponding to this fluctuation scale is

$$k = \frac{2\pi}{\sqrt{\lambda r}}. \tag{4.4}$$

Then the fluctuation frequency with this characteristic length is equal to

$$f = \frac{2\pi v}{k} = \frac{v}{\sqrt{\lambda \frac{H}{\sin\alpha}}}, \tag{4.5}$$

where v is the average translation speed in the layer, which can be found from sounding data. Examples for estimated fluctuation frequencies are shown in Figure 15 (indicated in the figure as $f = 0.28$, etc.).

In using radiosonde data to estimate the peak scintillation frequencies in the spectra of ACTS beacon signal, some cautions should be kept in one mind:

(1) the vertical resolution in the sounding is poor, usually the vertical sampling interval is ~ 300 m, which hardly gives good estimates about real atmospheric turbulence;

(2) to make the situation worst, the sounding balloon may shaft with wind to a great extent;

(3) the sounding station is not collocated with the ACTS terminal;

(4) radiosonde instruments may give false readings about actual meteorological parameters. This is especially true for humidity sensor;

(5) the launch time of the radiosonde is not the best time for turbulence observation.

We will also restrict ourselves to only consider the first 2 km of sounding data with the assumption that contributions to scintillation from higher level layers are small enough to be safely neglected.

Now let us first consider Figures 15, 16 and 17, in which two turbulent layers can be seen at heights just above 1 km (top of boundary layer), which are characterized by strong vertical wind shear, less static stability and small Richardson number (<1). The relative humidity measured (refer to Figure 15) at those two levels indicated that the layers are not the boundaries of cloud. So this is a very good case of clear sky turbulence. We should expect scintillation can be observed in the ACTS data. The spectrum of 20 Hz ACTS beacon signal recorded during 12:11 - 12:21Z is shown in Figure 25. By examining the spectrum carefully we see the spectral density reaches maximum right at the fluctuation frequencies we have calculated from sounding data at these two layers (refer to Figure 15). This observation is consistent with our previous discussion that the largest beacon signal fluctuations are produced by fluctuations of refractive index on scale sizes of the order of first Fresnel zone size.

Figure 26 and 27 are another comparison between the sounding data and the scintillation spectrum measured by ACTS terminal. There is a strong vertical wind shear layer around the top of boundary level as indicated in Figure 26. Although the Richardson number is not very small at that level, in Figure 27 we still can locate the spectral peak around 0.38 Hz, which coincides with the estimation indicated in Figure 26.

Figures 28 and 29 give one more comparison. In this case the frequency corresponding to the first Fresnel zone is very low. So we need to calculate the spectrum from 1 Hz data, which is shown in Figure 29. The peak frequency is also close to that estimated from the sounding data. Note in this scintillation spectrum we no longer observe "-8/3" and "+1/3" power laws. The possible reason is that for a longer time period (in this case ~1 hour) the beacon signal is no longer a random variable with stationary first increment and after we average over 7 FFTs, the statistics of the signal fluctuations may deviate greatly from the statistics of a random variable with stationary first increment.

All the above comparisons indicates that the largest scintillation components come from locations near the top of the boundary layer. This is what we expected, since large vertical wind shear and a rapid decrease in absolute humidity is most probably found at this height.

Due to limitations in making use of the sounding data as mentioned above, there are many cases in which the vertical profiles calculated from sounding data are totally irrelevant to the ACTS scintillation spectra. Figures 30 and 31 give one such occurrence. In the vertical wind shear profile we can find a well defined layer just above 1000 m, but the estimated peak frequency (0.19 Hz) cannot be found in the spectrum. Nevertheless, at present the sounding data are the only long term data available for the purpose of estimating vertical profiles of various meteorological parameters.

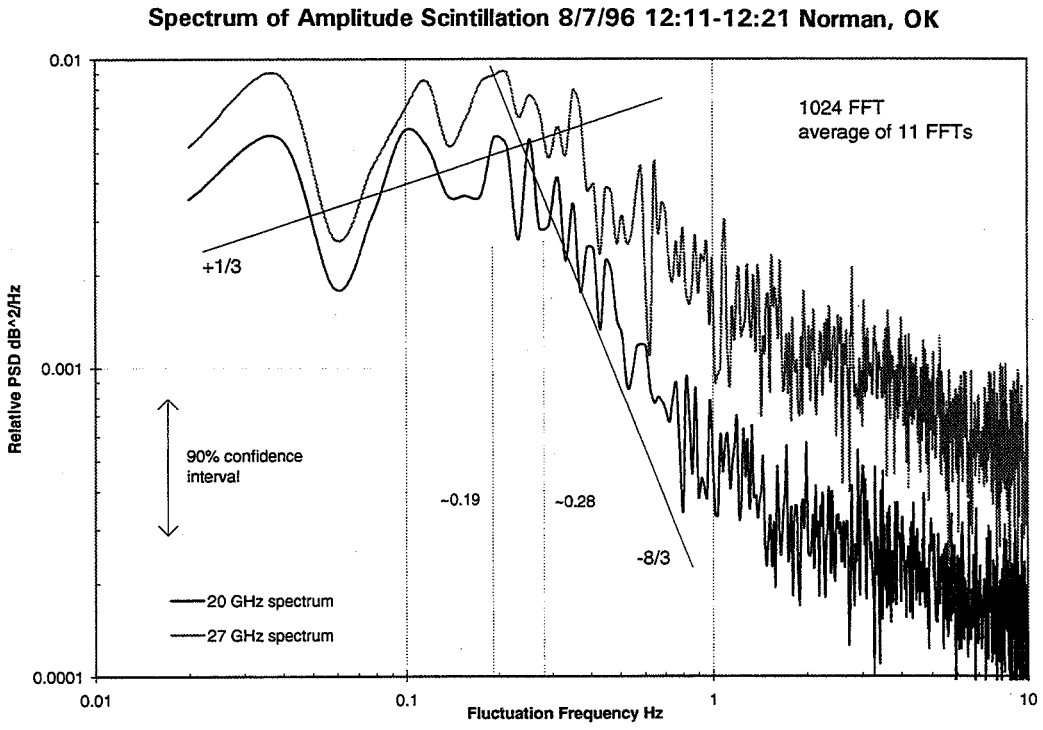

Figure 25. Spectrum of Amplitude Scintillation during 12:11 - 12:21 Z, 8/7/96

Calculated from Norman ACTS 20 Hz Data

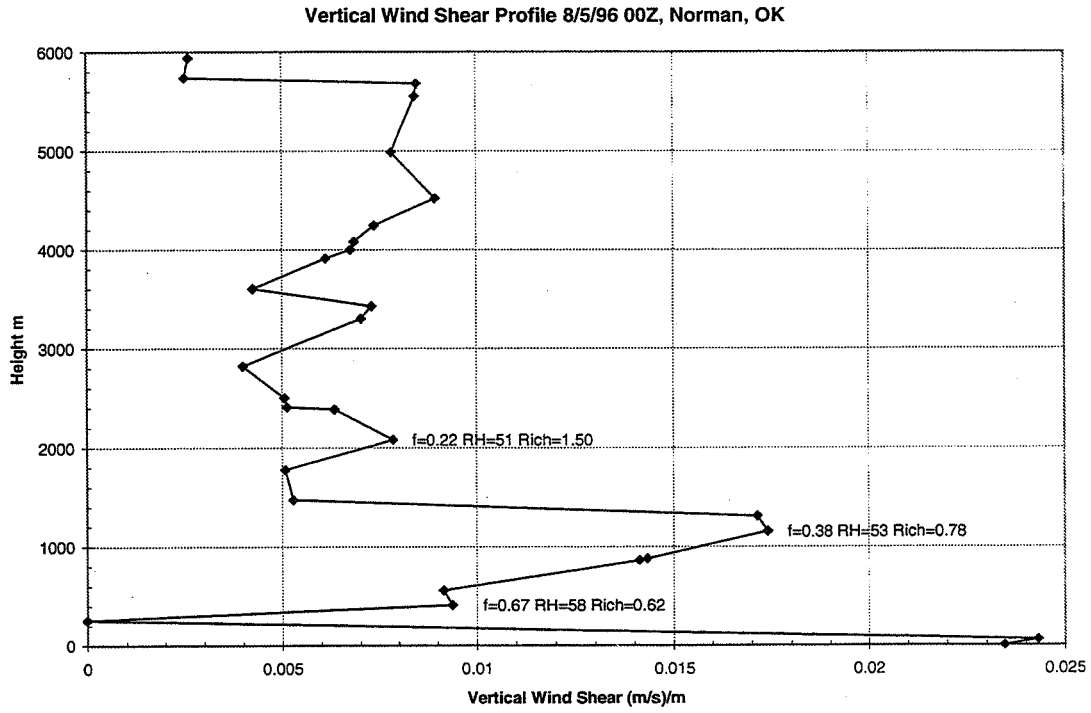

Figure 26 Vertical wind shear profile form radiosonde data of

8/5/96 00Z, OUN (Norman, OK)

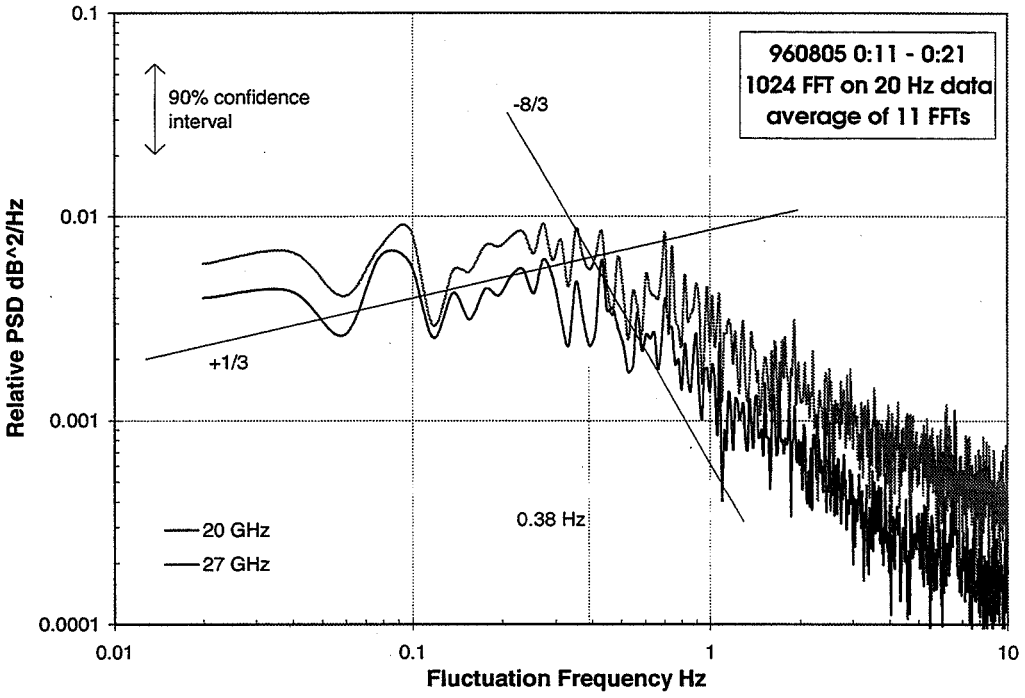

Figure 27 Scintillation spectrum of 8/5/96 0:11-0:21, Norman, OK

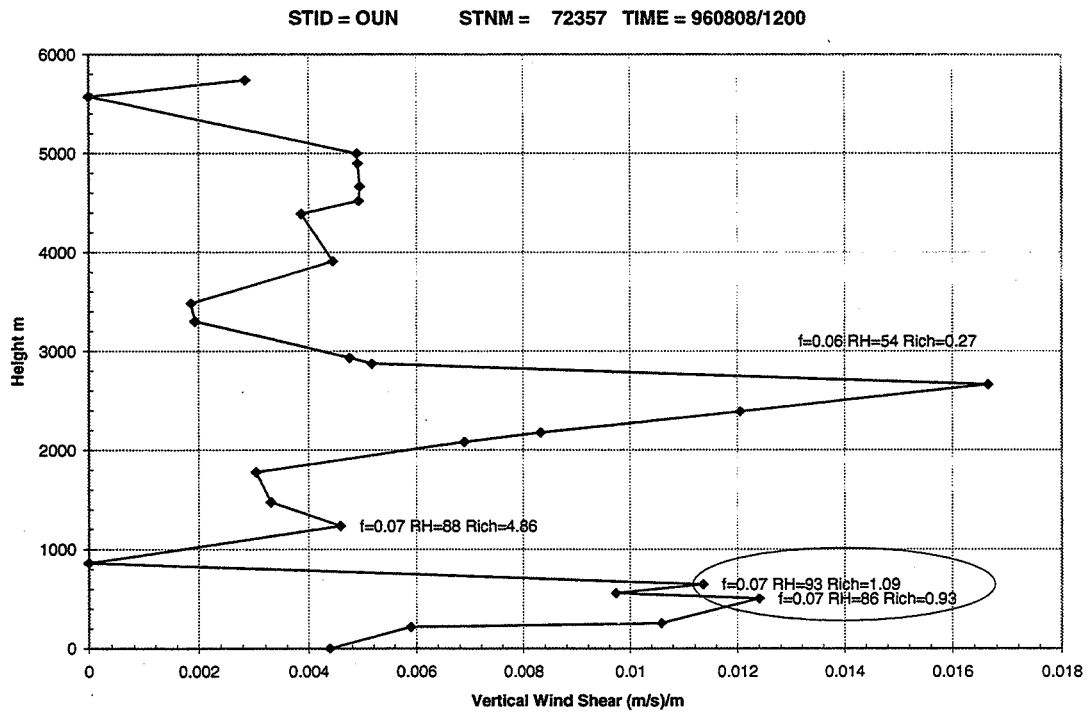

Figure 28 Vertical Wind Shear Profile 8/8/96 12Z, Norman, OK

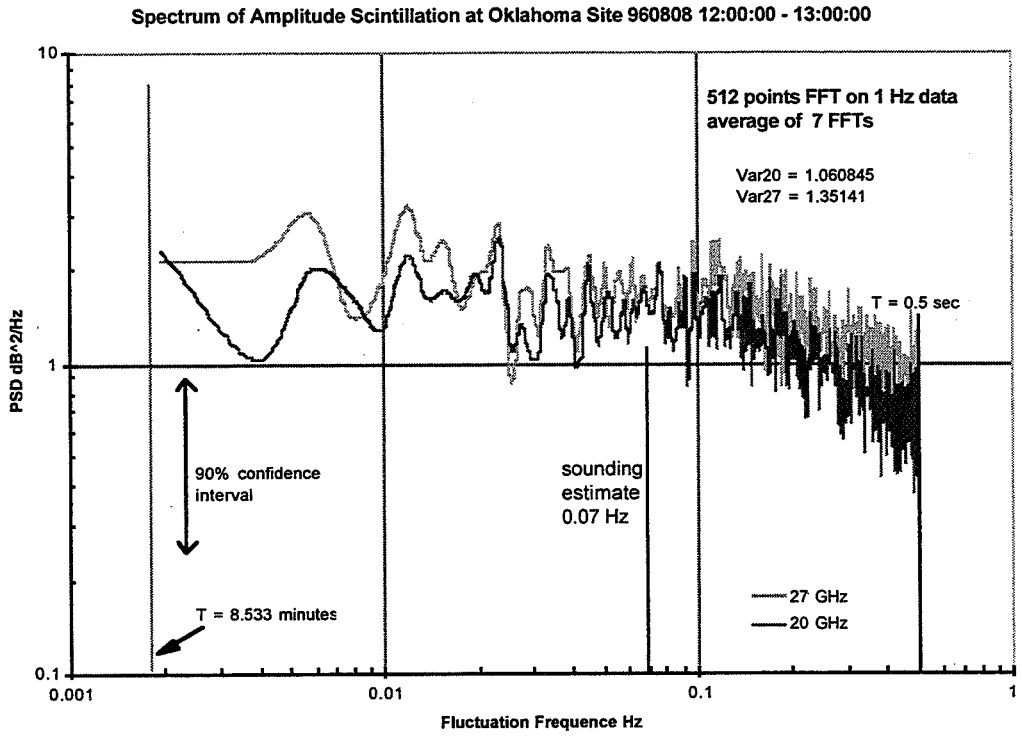

Figure 29 Scintillation spectrum calculated

from ACTS 1 Hz data 8/8/96 12-13Z, Norman, OK

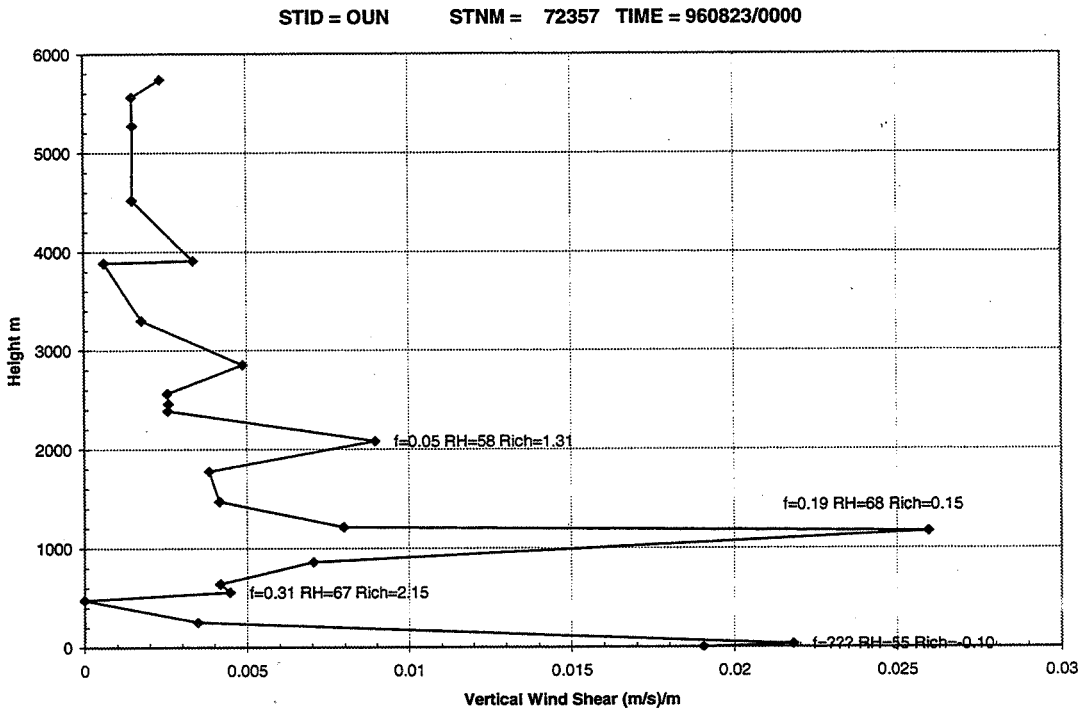

Figure 30 Vertical wind shear profile of 8/23/96 00Z over Norman, OK

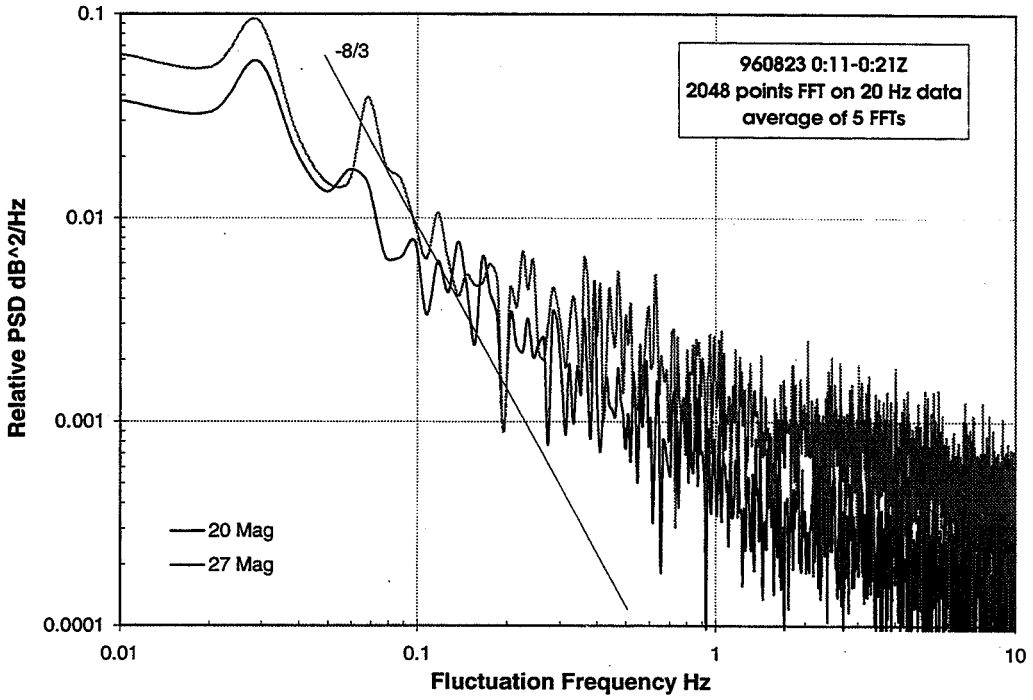

Figure 31 Scintillation spectrum which has no relation with the vertical profile estimated from sounding data

4.4 Variance of the Logarithm of the Amplitude Scintillation

The frequency dependence of the variance of the logarithm of the amplitude scintillation measured at the two beacon frequencies is in surprisingly good agreement with the theoretical prediction. As we discussed in Sec 3.7 the variance of the logarithm of the amplitude fluctuation is

$$\overline{\chi^2} = 0.31 C_n^2 k_o^{7/6} r^{11/6}. \tag{3.54}$$

From this equation we see that the variance is proportional to $f^{7/6}$. With two frequencies operating in parallel, we can easily make comparison between the variance measured in the two frequencies. Figure 32, 33, 34 and 35 give the frequency dependence of the scintillation variance measured at four ACTS propagation experiments sites (Oklahoma, Alaska, Colorado, and Florida). The variances are calculated by first performing 1024 points FFT on 20 Hz ACTS data then sum the spectral density estimates (except the DC component) over the frequency domain. The slopes in these figures are very close to the expected theoretical value

$$\left(\frac{f_{27GHz}}{f_{20GHz}}\right)^{7/6} \frac{g_{27GHz}^2(x)}{g_{20GHz}^2(x)}$$

where $g(x)$ is the antenna averaging factor (Crane, 1979, pp.46, CCIR 1990, pp.175)

In order to study the elevation angle dependence of the scintillation variance, we adopted the CCIR model (CCIR 1990, pp. 174-175).

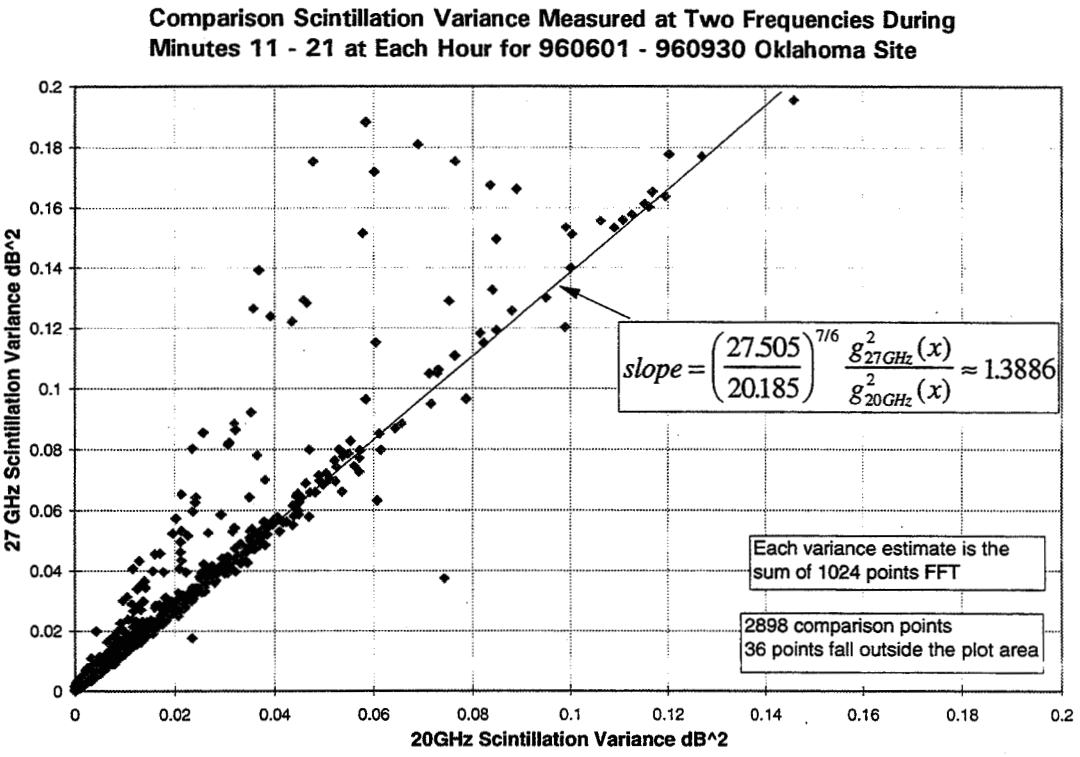

Figure 32 Frequency dependence of the scintillation variance measured at ACTS Oklahoma site during 960601 - 960930

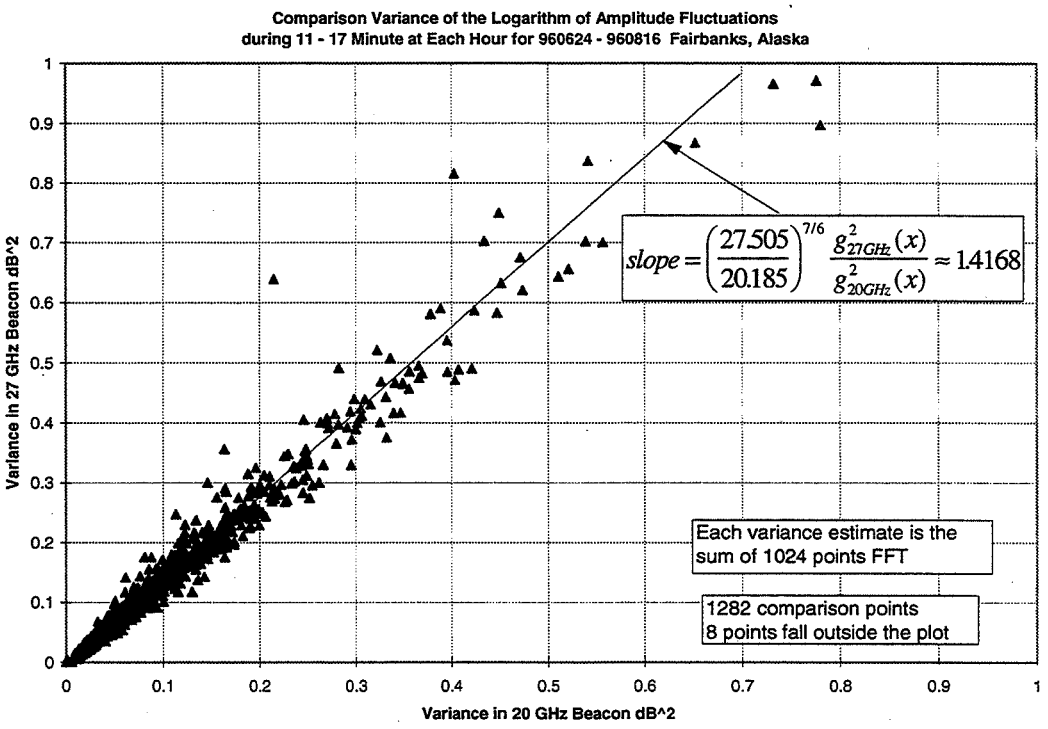

Figure 33. Frequency dependence of the scintillation variance measured at ACTS Alaska site during 960624 - 960816

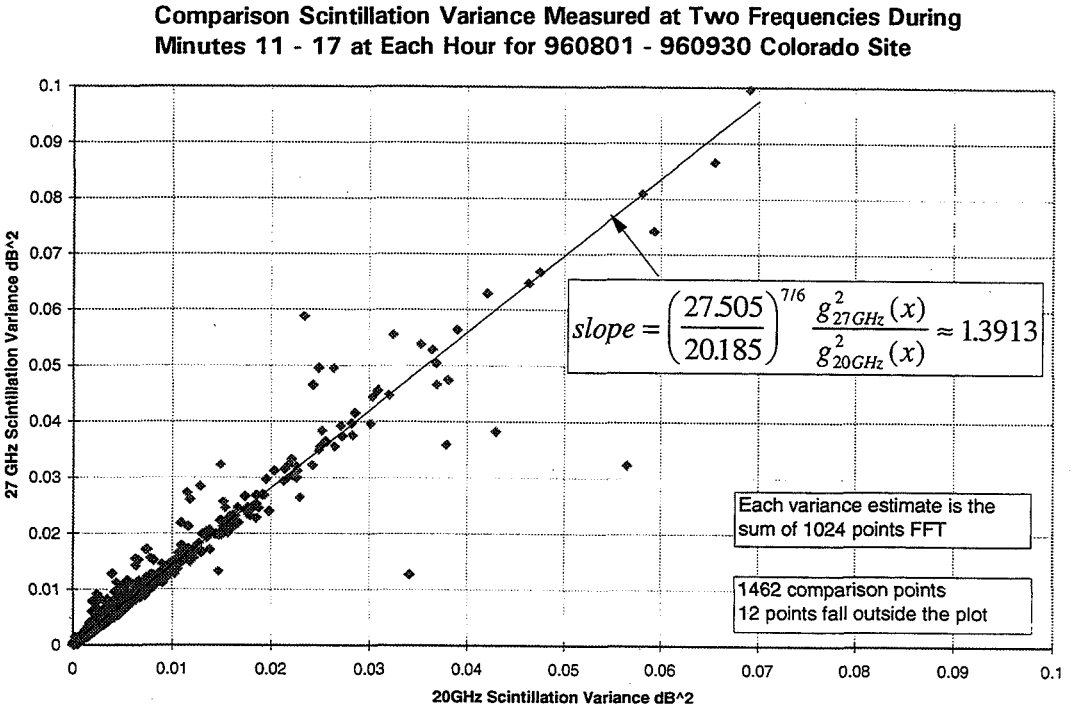

Figure 34 Frequency dependence of the scintillation variance measured at ACTS Colorado site during 960801 - 960930

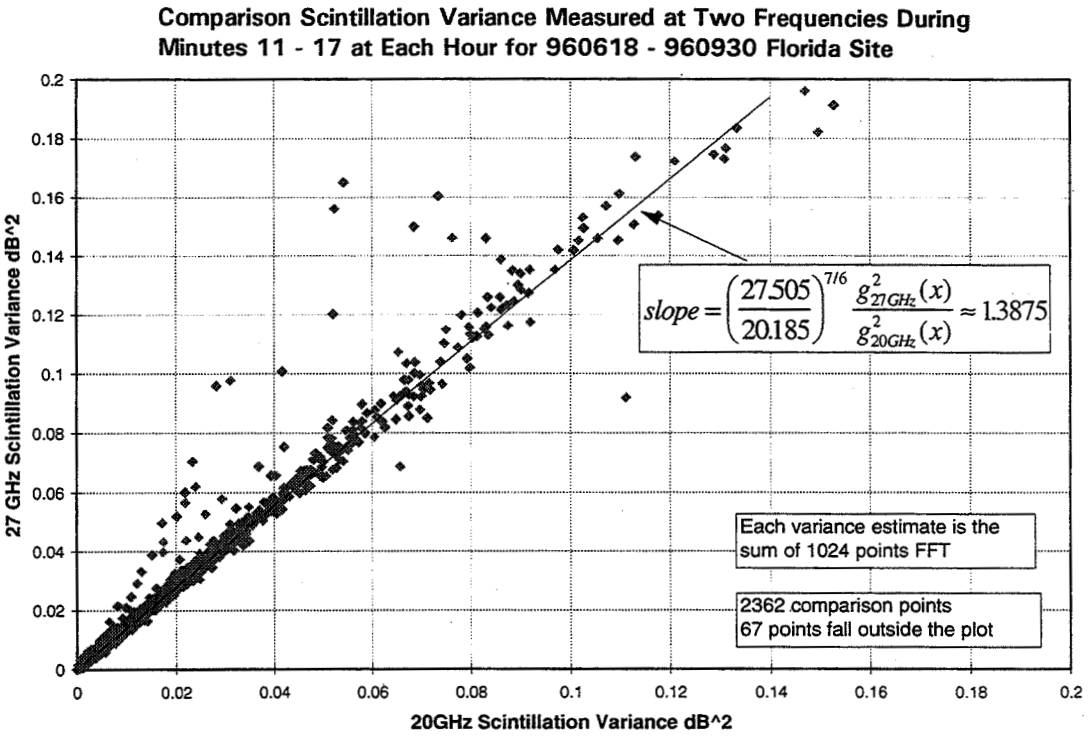

Figure 35 Frequency dependence of the scintillation variance measured at ACTS Florida site during 960618 - 960930

CCIR model:

$$\overline{\chi^2} = \frac{\overline{\chi^2_{ref}} f^{7/6} g^2(x)}{(\sin\theta)^b}$$

$b = 2.4$ (CCIR); $b = 11/6$ (also tested)

$g^2(x)$ antenna averaging factor (Crane, 1979, pp.46)

The height of turbulence is set to 1000m

$$\chi_{ref} = 3.6 \times 10^{-3} + 1.03 \times 10^{-4} N_{wet}$$

where N_{wet} is climatological average (following values were adopted from Bean et. al. 1996, pp. 39)

Alaska: $N_{wet} = 50N$

Colorado: $N_{wet} = 80N$

Oklahoma: $N_{wet} = 90N$

Florida: $N_{wet} = 120N$

The medians of the scintillation variance measured at four sites during the three summer months of 1996 were compared with the model prediction as shown in Table 2. From the table we see that

1) original CCIR model ($b = 2.4$) overestimates the variance especially for the Alaska site,

2) even with $b = 11/6$ the model's predictions are still larger than the medians of measured variance, but better than that of the original model,

3) the medians of measured variance at the Colorado site are the smallest among the four sites and also differ from model prediction greatly, which might be due to the specific geological location of that site (on the lee side of the Rocky Mountains, where it is usually dry and the boundary layer may be shallower than 1 km)

Since the four sites are located in different climate zones it is hard to statistically determine elevation dependency of the scintillation variance by only using the three months 20 Hz data and one model. But qualitatively we still can see that the elevation angle dependency is closer to the $(\sin\theta)^{-1\,1/6}$ law rather than $(\sin\theta)^{-2.4}$.

Table 2

Elevation angle dependency of scintillation variance

(where b as given in pp. 73)

	20 GHz	27 GHz
AK elevation = 8.1		
Median of measured	0.06363	0.08596
CCIR (b=11/6)	0.08888	0.12618
CCIR (b=2.4)	0.26982	0.38306
CO elevation = 43.1		
Median of measured	0.00314	0.00473
CCIR (b=11/6)	0.00824	0.01144
CCIR (b=2.4)	0.01022	0.01420
OK elevation = 49.1		
Median of measured	0.00514	0.00804
CCIR (b=11/6)	0.00801	0.01110
CCIR (b=2.4)	0.00939	0.01301
FL elevation = 52.0		
median of measured	0.00730	0.01108
CCIR (b=11/6)	0.01136	0.01573
CCIR (b=2.4)	0.01301	0.01801

CHAPTER 5 CONCLUSION

In this research we have studied the effect of the atmospheric (or more specifically tropospheric) turbulence on electromagnetic wave propagation. The 1 Hz and 20 Hz ACTS beacon propagation data collected at different ACTS Propagation Experiments sites were utilized in our analysis. Radiosonde data from sounding station OUN were used to compare with the scintillation data observed at the ACTS Propagation Experiment Oklahoma site.

Spectral analysis of the scintillation data is consistent with the theoretical prediction made by Tatarski in 1965. The "-8/3" power relation (which corresponding to Kolmogorov "-5/3" law) between the spectral density and fluctuation frequency is observed in most of spectra calculated from ACTS 20 Hz beacon data. Comparison between the radiosonde data and the scintillation spectra revealed that the largest scintillation components come from locations near the top of the boundary layer (in some cases that is not true, the possible reasons are that there exist some limitations, as stated in Sec 4.3, in applying radiosonde data to scintillation estimation). The frequency dependency in scintillation variance was found being proportional to $f^{7/6}$. The angle-of-arrival dependency in scintillation variance was found being close to $(\sin\theta)^{-1\,1/6}$. Both are in agreement with the theoretical value. While the elevation angle dependency differs greatly from CCIR model ($(\sin\theta)^{-2.4}$).

Radiosonde data might be useful in determining long term statistics properties of the tropospheric turbulence, which then can be incorporated into the scintillation prediction model for satellite communication system design.

Long term meteorological data, such as airborne turbulence measurements or radar clear sky observations, with better vertical resolution than the radiosonde data can greatly help the scintillation estimation.

Due to the time limitation, in this research we have only studied about 12 station months of scintillation data (3 summer months data from 4 sites). The scintillation data analysis was only based on two frequencies (20 GHz and 27 GHz). The analysis is far from complete. With more scintillation data accumulated in the future (all the 7 ACTS Propagation Experiments sites will keep operating for the next 2 years), we hope more accurate scintillation statistics can be obtained.

BIBLIOGRAPHY

Bean, B. R. , B. A. Cahoon, C. A. Samson, and G. D. Thayer 1966 A World Atlas of Atmospheric Radio Refractivity, U. S. Dept. of Commerce/Envir. Sci. Admin. Washington D. C.

Browand, F. K., and Ho, C. M., 1983, "The mixing layer: an example of quasi two-dimensional turbulence", Two-dimensional turbulence, J. Mec. Ther. Appl. Suppl., R. Moreau ed., pp 99-120

CCIR Report 563-4, 1990, "Effects of the atmosphere (radiometeorology)"

Champagne, F. H., Friehe, C. A., LaRue, J. C. and Wyngaard, J. C., 1977, J. Atmos. Sci., Vol. 34, pp 515

Crane, R. K., 1976, Low elevation angle measurement limitations imposed by the troposphere; An analysis of scintillation observation made at Haystack and Millstone. MIT, Lincoln Lab. Tech. Rep. 518, Lexington, Mass

Crane, R. K., 1977, "Stratospheric turbulence" Rep. No. AFGL TR 77-0207, Air Force Geophys. Lab., MIT, Lexington, Mass

Crane, R. K., and Blood, David W., 1979, "Handbook for the estimation of microwave propagation effect - link calculation for earth-space paths (path loss and noise estimation)", ERT Tech. Report No.1 P-7376-TR1, Environmental Research & Technology, Inc., Concord, Mass

Crane, R. K., 1980, "A review of radar observations of turbulence in the lower stratosphere", Radio Sci., Vol. 15, pp. 177-193

Crane, R. K., Wang, X., Westenhaver, D. B. and Vogel, W. J., 1996 "ACTS Propagation Experiments: experiment design, calibration, data preparation and archival", to appear in a Proceedings of IEEE in 1997

Doviak, R. J. and Zrnic, D. S., 1993, Doppler Radar and Weather Observations, second edition, Academic Press, CA

Gargione, F., 1989, "ACTS spacecraft beacon characteristics", Presentations of the First ACTS Propagation Studies Workshop, JPL, CIT, California, pp. 35-66

Gibson, M. M., 1963, "Spectra of turbulence in a round jet", J. Fluid Mech., Vol. 15, pp. 161-173

Gossard. E. E., 1977, "Refractive index variance and its height distribution in different air mass", Radio Sci., Vol. 12, No. 1, pp. 89-105

Grant, H. L., Stewart, R. W. and Moilliet, A., 1962, "Turbulent spectra from a tidal channel", J. Fluid Mech., Vol. 12, pp 241 - 268

Gunderman. R. J., 1992, "ACTS project update", Presentations of the Fourth ACTS Propagation Studies Workshop, JPL, CIT, California, pp. 11-22

Haddon, J., Lo, P., Moulsley, T. J. and Vilar, E., 1980, "Spectra of amplitude scintillation in X-band satellite down-link", Electron. Lett., Vol. 16, pp. 619-620

Karasawa, Y., Yasukawa, K. and Yamada, M., 1988a, "Tropospheric scintillation in the 14/11-GHz Bands on earth-space paths with low elevation angles", IEEE Trans. On Ant. And Propagation, Vol. 36, No. 4, pp. 563-569

Karasawa, Y., Yamada, M. and Allnutt, J. E. 1988b, "A new prediction method for tropospheric scintillation on earth-space paths", IEEE Trans. On Ant. And Propagation, Vol. 36, No. 11, pp. 1608-1614

Karasawa, Y., and Matsudo, T., 1991, "Characteristics of fading on low-elevation angle earth-space path with concurrent rain attenuation and scintillation", IEEE Trans. On Ant. And Propagation, Vol. 39, No. 5, pp. 657-661

Moulsley, T. J. and Vilar, E., 1982, "Experimental and theoretical statistics of microwave amplitude scintillations on satellite down-link", IEEE Trans. On Ant. And Propagation, Vol. AP-30, No. 6, pp. 1099-1106

Ortgies, G., 1993, "Frequency dependence of slant-path amplitude scintillations", Electr. Lett., Vol. 29, No. 25, pp 2219-2220

Rabin, R. M. and Doviak, R. J. 1989, "Meteorological and astronomical influences on radar reflectivity in the convective boundary layer", J. Appl. Meteor. Vol. 28, pp. 1226-1235

Salonen, T. E., Tervonen, J. K. and Vogel, W. J., 1996, "Scintillation effects on total fade distributions for earth-satellite links", IEEE Trans. On Ant. And Propagation, Vol. 44, No. 1, pp. 23-27

Stutzman, W., 1992, "ACTS propagation terminal update", Presentations of the Fourth ACTS Propagation Studies Workshop, JPL, CIT, California, pp. 25-40

Tatarski, V. I., 1961, Wave Propagation in a Turbulent Medium, New York, McGraw-Hill

Tatarski, V. I., 1971, The Effects of the turbulent atmosphere on Wave Propagation, U. S. Dept. of Commer., NSF, Nat. Tech. Infrom. Serv.

Zhou, X. J. 1991, Advanced Atmospheric Physics (in Chinese), Meteorology Press, Beijing, P. R. China

Frequency Scaling at 20 GHz and 12 GHz from the ACTS and Digital Satellite System

Julius Goldhirsh, Bert H. Musiani
Applied Physics Laboratory, The Johns Hopkins University
julius_goldhirsh@jhuapl.edu

Wolfhard J. Vogel
Electrical Engineering Research Laboratory, The University of Texas at Austin
wolf_vogel@mail.utexas.edu

Figure 1: Background

During the year period September 1, 1995 through August 31, 1996, simultaneous measurements of transmissions at 20 GHz from the ACTS and 12.5 GHz transmissions from the Direct Satellite System were made at the Applied Physics Laboratory located in central Maryland. The receiving antennas were approximately collocated being approximately 18 m from one another and the pointing angles were approximately the same. They differed by little over 1° in azimuth and 0.5°.

The 12 GHz direct satellite system was suggested as a relatively inexpensive resource by Wolf Vogel who set up a similar system at Austin, Texas. Wolf provided the software and information regarding, calibration and assisted in the analysis of the data.

Figure 2: Objectives

The objectives of the measurements were first, to determine cumulative fade distributions over simultaneous periods at the two frequencies, and secondly to examine different frequency scaling models. The scaling models are reviewed here. The models considered are the ITU-R model, an empirical model derived from the data, and a model which relies on the rain rate and the drop size distribution. The ITU-R and rain rate model were also adjusted using antenna wetting considerations.

Figure 3: Link Parameters

As mentioned, the pointing angles of both systems are approximately the same (38.7° for ACTS versus 38.2° for DSS in elevation) and (214° for ACTS versus 215.3° for DSS in azimuth). The receiver dynamic ranges are 22 and 10 dB, and the sampling times are 0.5 s for ACTS and 10 s for DSS. The DSS receiver is low noise and the output of the data acquisition system is given in terms of the carrier to noise ratio in dB. Since the receiver has a relatively low noise figure, the noise added by the fading medium was considered in arriving at the resultant rain fade.

Figure 4: Rain Fade Versus Decrease in Carrier to Noise Ratio

In this figure is shown a nominal calibration curve giving the rain attenuation versus the decrease in the receiver carrier to noise ratio. The receiver tended to lose lock at rain fades ranging from 5 dB to 7 dB or decreases of carrier to noise ratios of 10 dB and greater.

Figure 5: Analysis Methodology

We summarize here the salient methodology from which the distributions were obtained.

(1) The signal level or carrier to noise level before and after each rain fade resulted in a threshold level relative to which the rain fade was calculated. In this way, the effects of atmospheric absorption and clouds are mitigated and we predominantly arrive at the fading effects caused by rain.

(2) Only simultaneous measurement periods were used in the analysis. Hence, if one system was down, data from the other measurements were not used. The joint time over which both systems were up was relatively high; being of the order of 97% of the time.

(3) Equal probability levels were examined in arriving at the individual models

Figure 6: Simultaneous Distributions at 12 GHz and 20 GHz

In this figure are shown plotted the 12 GHz DSS cumulative fade distribution (square points), the ACTS 20 GHz distributions for the first year (September 1, 1994 through August 31, 1995; circular points) and second year (September 1, 1995 through August 31, 1996; triangular points). We note the following salient features:

1. The 20 GHz ACTS fades for the first and second years are generally within 1 dB of one another.
2. The 20 GHz fades are approximately 3 to 4 times larger than the 12 GHz fades over the percentage range (0.4% to 0.02%).

Figure 7: ITU-R Model Formulation

In this figure is shown the ITU frequency scaling formulation. I'll not go into details other than to point out that the formulation is relatively complicated as shown. It is approximately given by the product of the fade at frequency f_1 times the ratio of the frequency squared.

Figure 8: Empirical Model Scaling

In this figure is given a plot of the ACTS 20 GHz versus the DSS 12.5 GHz fades. Also shown is a curve predicted from the data where the vertical scale represents the dependent variable and the abscissa the independent variable. Agreement between the best fit curve and the data points are within a small fraction of a dB. Another best fit relation was derived where the dependent variable was 12.5 GHz and the independent variable was 20 GHz.

Figure 9: Empirical Methods Upscaling and Downscaling

Shown in this figure are the resultant empirical formulations giving residuals within a small fraction of a dB for upscaling and downscaling cases

Figure 10: Frequency Upscaled Distributions - ITU-R and Empirical Fits

In this figure are given the ITU-R upscale distribution using the 12.GHz case. We note fade differences near 4 dB (P = 0.08%) exist when comparing the ITU-R model with the measured 20 GHz distribution. The empirical fit is shown to agree within a small fraction of a dB. The frequency squared case gives larger dB values ranging between 0.1 dB (P = 0.4%) to 1 dB (P = 0.02%) vis-à-vis the ITU-R model.

Figure 11: Frequency Downscaling Distributions - ITU-R Model

In this figure is shown the ITU-R downscaling case. Here, the maximum dB difference between the ITU-R and measured distribution is around 2 dB at p = 0.07%. The empirical model shows agreement to within a few tenths of a dB.

Figure 12: Frequency Scaling Using Measured Rain Rate and M-P Drop Size Distribution

Here, we describe the attenuation in terms of equal probability values of rain rate and effective path lengths using the relations shown in the first two equations, where $A(f_1)$, and $A(f_2)$ are the equal probability attenuations at frequencies f_1 and f_2 occurring at the equal probability effective rain rate R. Also, l_e is the effective path length over which the effective rain rate is uniform. The parameters a_1, a_2, b_1, b_2 are frequency and to some extent drop size distribution dependent. These are tabulated for the M-P distribution in a paper by Olsen, Rogers and Hodge. Dividing the second equation by the first, we obtain the third equation which is independent upon the path length.

Using a rain rate distribution derived for the mid-Atlantic coast employing a rain gauge network of 10 gauges over an eight year period and the 12.5 GHz equal probability fades, a resultant attenuation distribution was derived at 20 GHz.

Figure 13: Rain Rate Distribution

In this figure is shown the rain rate distribution for the mid-Atlantic coast employing a rain gauge network of 10 gauges over an eight year period. The distribution represents the equivalent of approximately 80 site-years of measurements.

Figure 14: Fade Distribution at 20 GHz Using the Rain Rate Method

The dashed curve in this figure gives the rain rate method which is does better than the ITU-R distribution by 0.5 dB at P = 0.4% and 1.5 dB at P = 0.02%.

Figure 15: Apparent Fade Depth Caused by Wetting of 20 GHz Antenna and Feed

In this figure is shown the results of an antenna wetting experiment associated with the 20 GHz system. The wetting was carried out by spraying the antenna employing a hose and showering the dish and antenna feed from above. The corresponding figure represents an apparent fading versus time for different spray conditions of the antenna and feed. An eyeball estimate of the rain rate was approximately 20 mm/h. The apparent fading ranged from 1 to 6 dB. Even when the sustained wetting was halted, the residual wetted surface gave a 1 dB apparent fade.

Figure 16: Scale Distribution at 20 GHz Adjusted for Antenna Wetting

When the ITU-R and the rain rate scaled distributions are adjusted for antenna wetting by simply adding 2 dB at each percentage level, the predicted levels agree more respectably with the measured levels. In fact, the rain rate method shows general agreement to within $\pm$ 1 dB.

Figure 17: Summary and Conclusions

The salient experimental results are as follows: (1) The 12.5 GHz fade interval between 1 dB and 5 dB resulted in probabilities from 0.4% to .02%, respectively. (2) The 20 GHz fades were larger by a factor of 3 (at P = 0.02%) to 4 (at P = 0.4%) relative to the 12.5 GHz fades. (3) The 20 GHz distribution for the second year of 20 GHz measurements was within +/- 1 dB of that of the first year. (4) The ITU-R method gave a maximum deviation which was approximately 4 dB relative to the 20 GHz measured case and within 2 dB when adjusted for antenna wetting. (5) The rain rate method gave closer predictions than the ITU-R model and was within $\pm$ 1 dB of the measured levels when adjusted for antenna wetting. (6) In all cases empirical fits which intrinsically have antenna wetting levels built into them were within a small fraction of a dB of the measured levels.

Frequency Scaling at 20 GHz and 12 GHz from ACTS and the Digital Satellite System

Julius Goldhirsh, Bert H. Musiani
Applied Physics Laboratory
The Johns Hopkins University
Applied Physics Laboratory

Wolfhard J. Vogel,
Electrical Engineering Research Laboratory
The University of Texas at Austin

Figure 1

Background

- Simultaneous measurements at APL (central-Maryland)
  - September 1, 1995-August 31, 1996
  - 12.5 GHz Direct Satellite System
  - ACTS 20 GHz Beacon
  - Pointing Angles Near Coincidence
  - Receiver Antennas Collocated

Figure 2

Objectives

- ♥ Determine cumulative fade distributions
  - ♠ ACTS 20 GHz beacon
  - ♠ DSS at 12.5 GHz
- ♥ Examine frequency scaling models
  - ♠ ITU-R
  - ♠ Empirical
  - ♠ Rain rate and drop size distribution
- ♥ Adjust models for antenna wetting
- ♥ Effort elaborated in Technical Report: APL/JHU A2A-96-U-001, October 96

Figure 3

Link Parameters for ACTS and DSS Receiver Systems

Parameter	Both	ACTS	DSS
Latitude	39°10'7.5"		
Longitude	76°53'55.5"		
Satellite Location		100°W	101°W
Elevation Angle (°)		38.7	38.2
Azimuth (°)		214.0	215.3
Frequency (GHz)		20.185	12.5
Antenna Dia. (m)		1.2	0.46
Beamwidth (°)		0.85	3.6
Carrier to Noise (dB)		28	14
Receiver Dynamic Range (dB)		22	10
Sampling Rate (s)		0.5	10

Figure 4

Rain Fade Measured with DSS Receiver Versus Decrease in Carrier to Noise Ratio

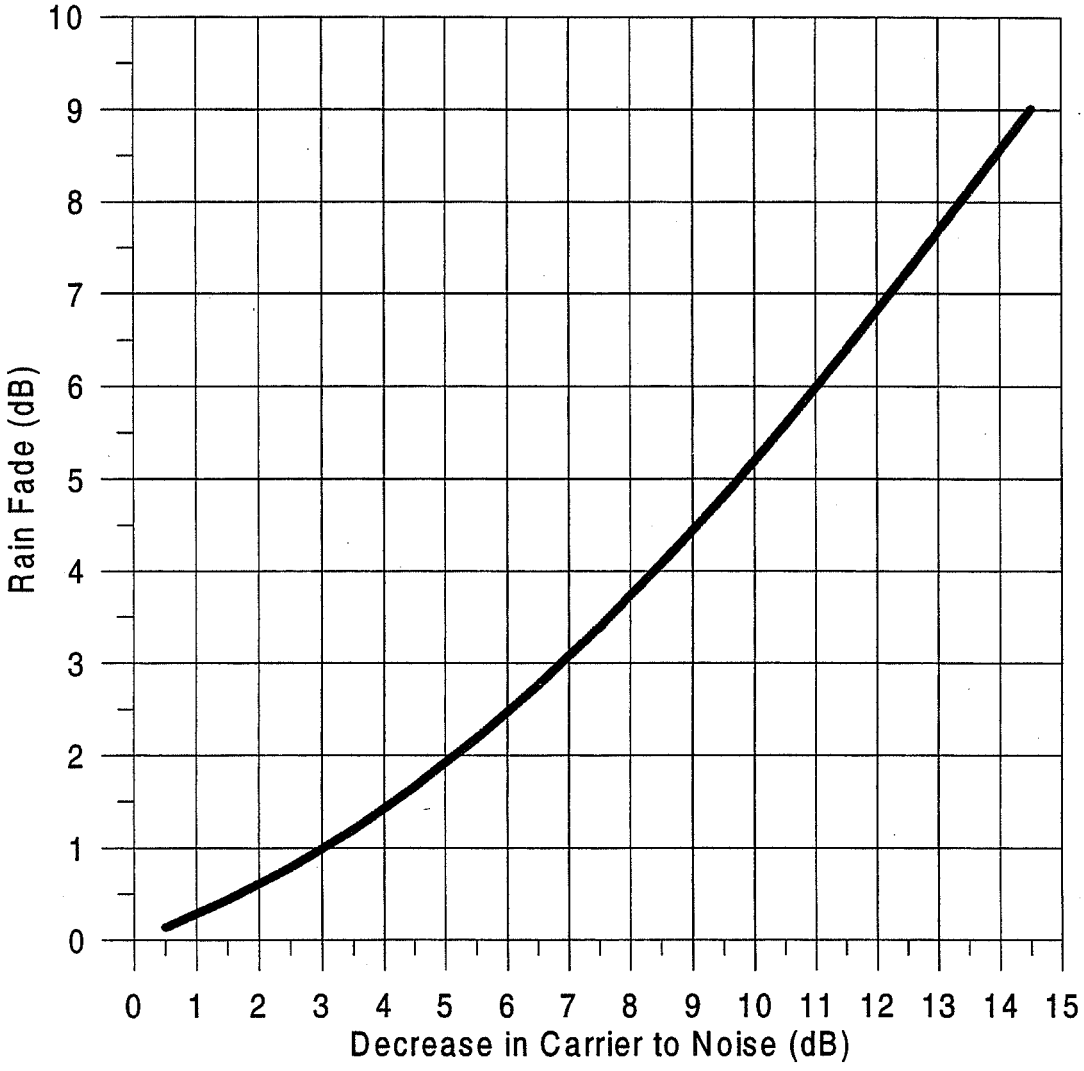

Figure 5

Analysis Methodology

- ♥ Rain fade relative to power levels before and after each rain period
  - ♠ Effect of atmospheric gas absorption mitigated
  - ♠ Effect of clouds mitigated
- ♥ Simultaneous periods of measurements examined
- ♥ Equal probability levels examined for model determination

Figure 6

Simultaneous Distributions at 12 GHz and 20 GHz over Period 9/1/95-8/31/96 Comparison with First Year of Measurements

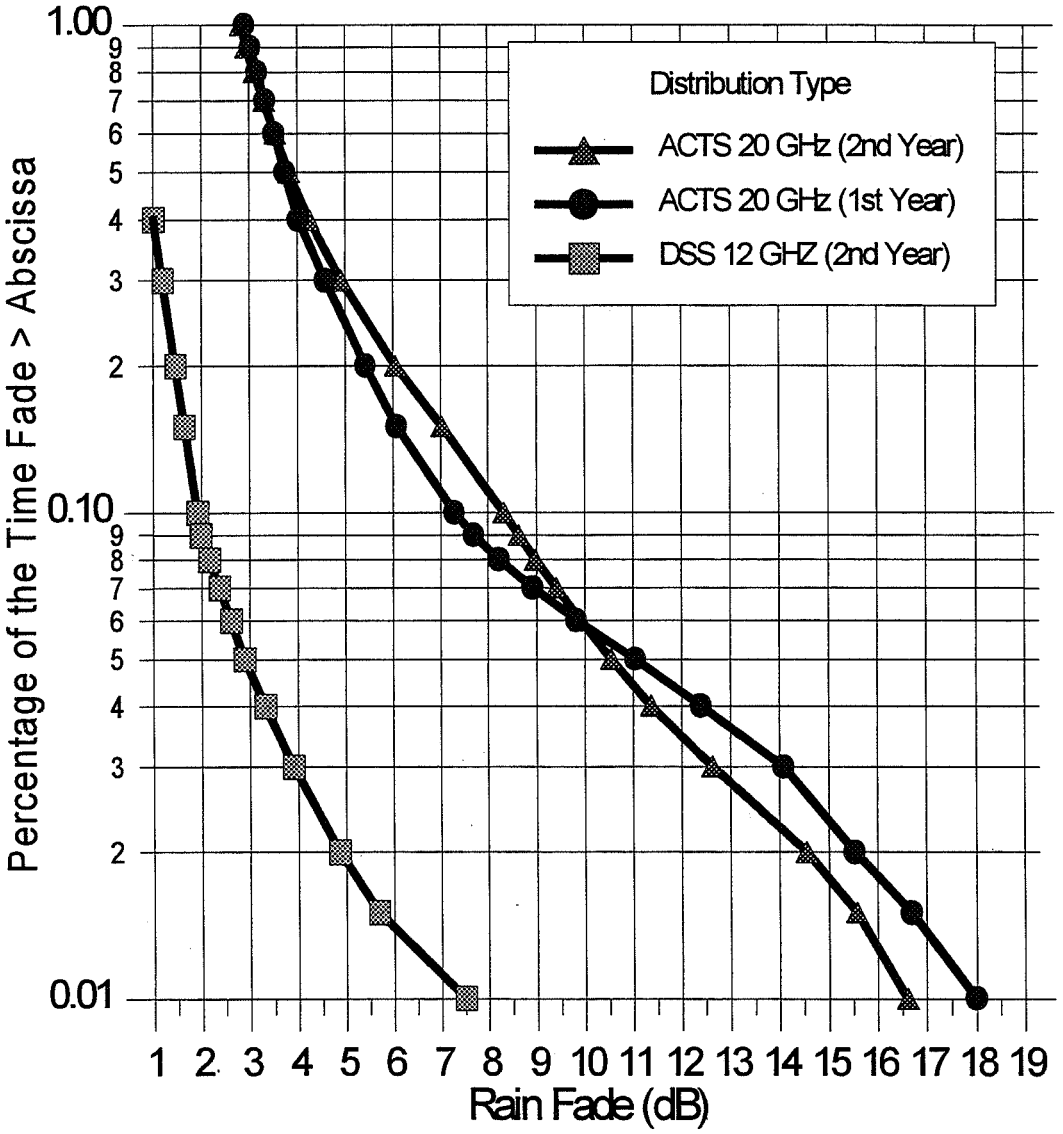

Figure 7

ITU-R Model Formulation

ITU-R Doc 5/BL/46-E
15 March 1994

$$\phi(f) = \frac{f^2}{1+10^{-4} f^2}$$

$$H = 1.12x10^{-3}\left(\frac{\phi_2}{\phi_1}\right)^{0.5} (\phi_1 A_1)^{0.55}$$

$$A_2 = A_1\left(\frac{\phi_2}{\phi_1}\right)^{1-H}$$

Frequency Square Formulation

$$A_2 = A_1(f_2/f_1)^2$$

Figure 8

Equal Probability Measured Fades at 20 GHz Versus 12 GHz Empirical Scaling Method

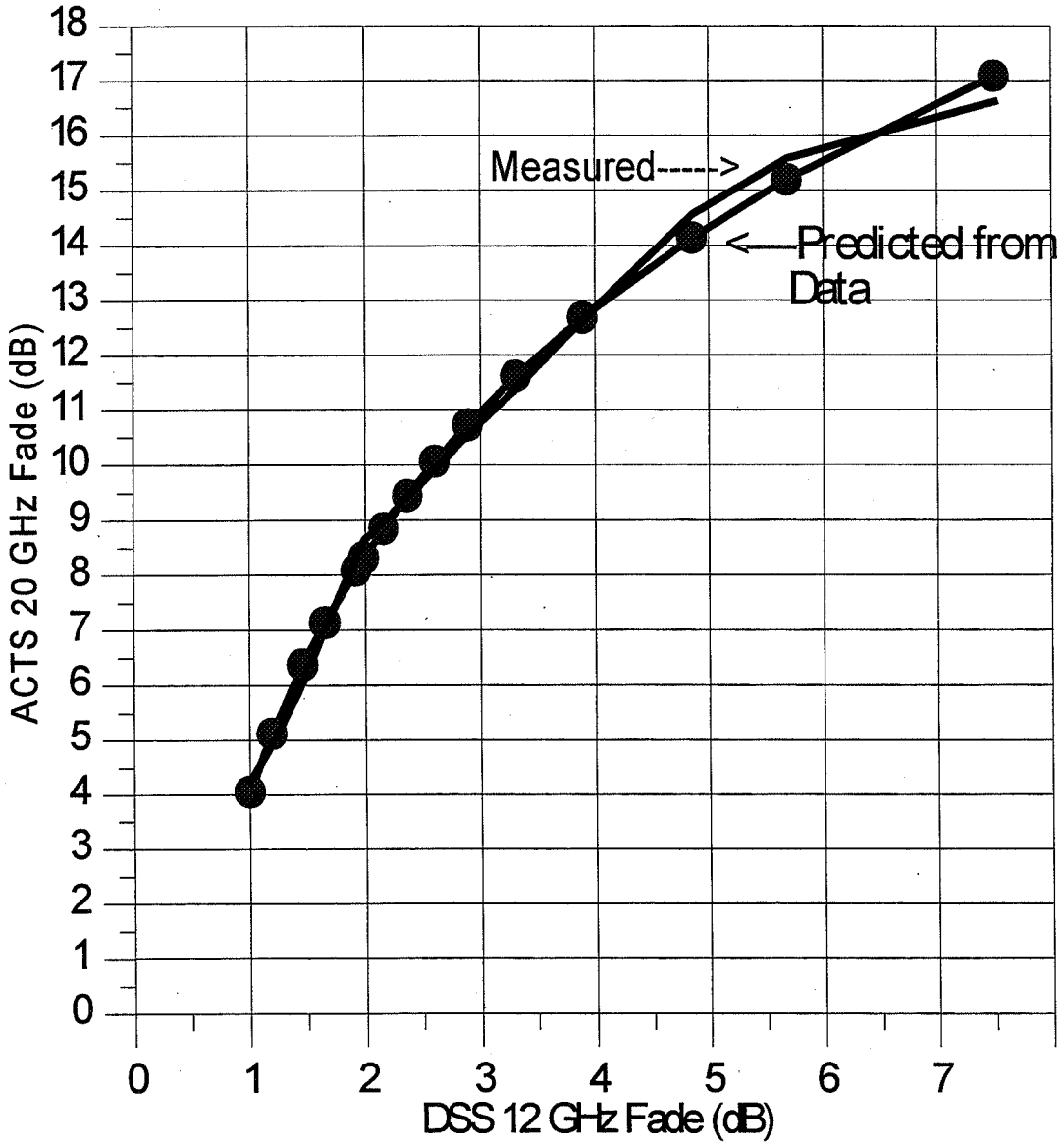

Figure 9

Empirical Method - Upscaling

$$A(f_2) = a + bA(f_1)^c$$

$$f_2 = 20.185 \quad GHz$$

$$f_1 = 12.5 \quad GHz$$

$$a = 106.35$$

$$b = 110.34$$

$$c = 0.0556$$

Empirical Method - Downscaling

$$A(f_2) = \frac{1}{a + bA(f_1)^{-0.5}}$$

$$f_1 = 20.185 \ GHz$$

$$f2 = 12.5 \quad GHz$$

$$a = -0.72895$$

$$b = 3.530$$

Figure 10

Frequency Scaled Distributions at 20 GHz from Measurements at 12 GHz ITU-R and Empirical Methods

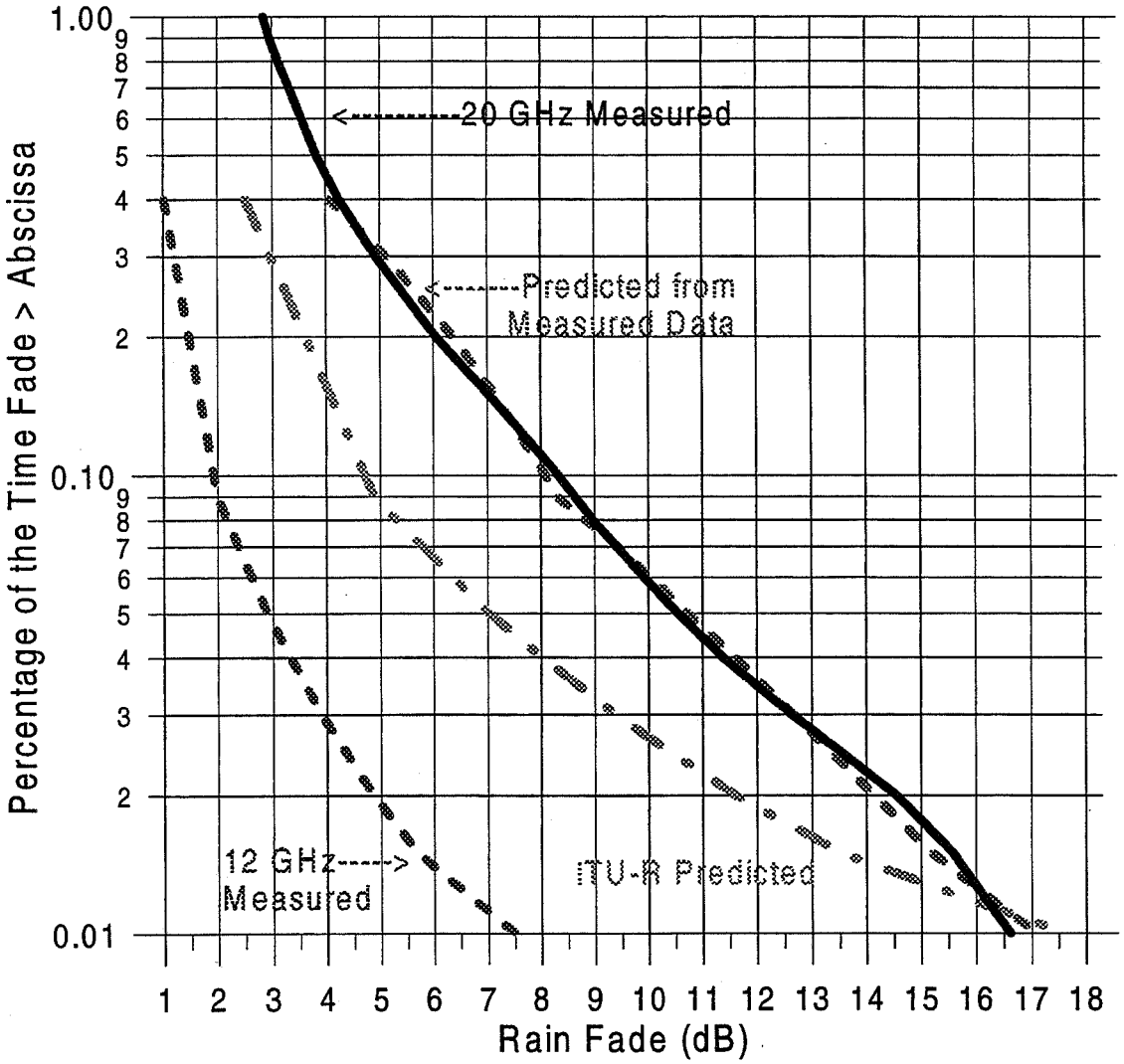

Figure 11

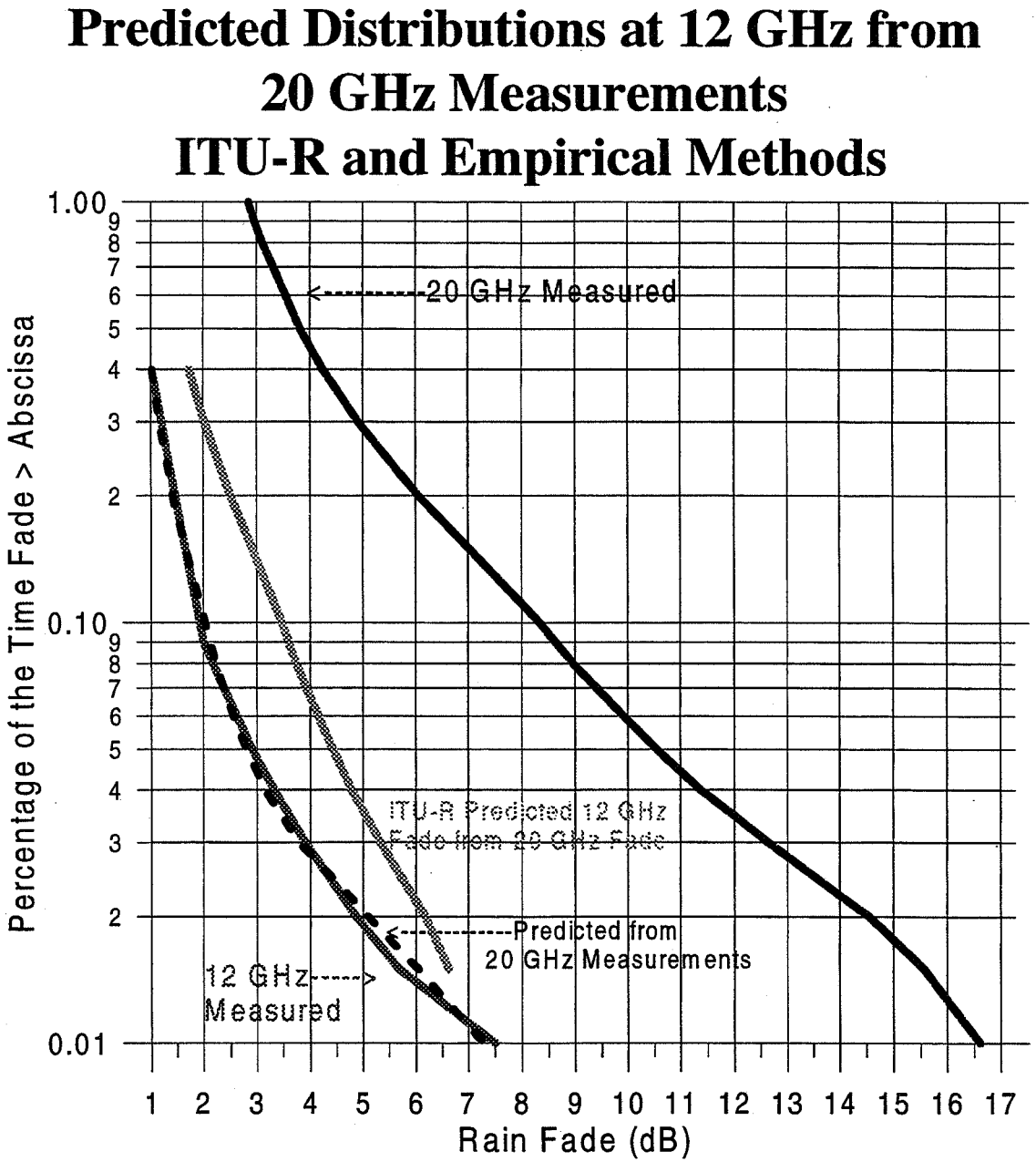
Predicted Distributions at 12 GHz from 20 GHz Measurements ITU-R and Empirical Methods
Percentage of the Time Fade > Abscissa
1.00
0.10
0.01
20 GHz Measured
ITU-R Predicted 12 GHz Fade from 20 GHz Fade
Predicted from 20 GHz Measurements
12 GHz Measured
1 2 3 4 5 6 7 8 9 10 11 12 13 14 15 16 17
Rain Fade (dB)

Figure 12

Frequency Scaling Using Measured Rain Rate and M-P Drop Size Distribution

$$A(f_1) = a_1 R^{b_1} l_e$$
$$A(f_2) = a_2 R^{b_2} l_e$$

$$A(f_2) = A(f_1) \frac{a_2}{a_1} R^{b_2 - b_1}$$

$$a_1 = 2.3685\text{X}10^{-2}$$
$$a_2 = 2.2262\text{X}10^{-2}$$
$$b_1 = 1.1306$$
$$b_2 = 1.1326$$

Figure 13

Cumulative Rainrate Distribution for Mid-Atlantic Coast of U.S.

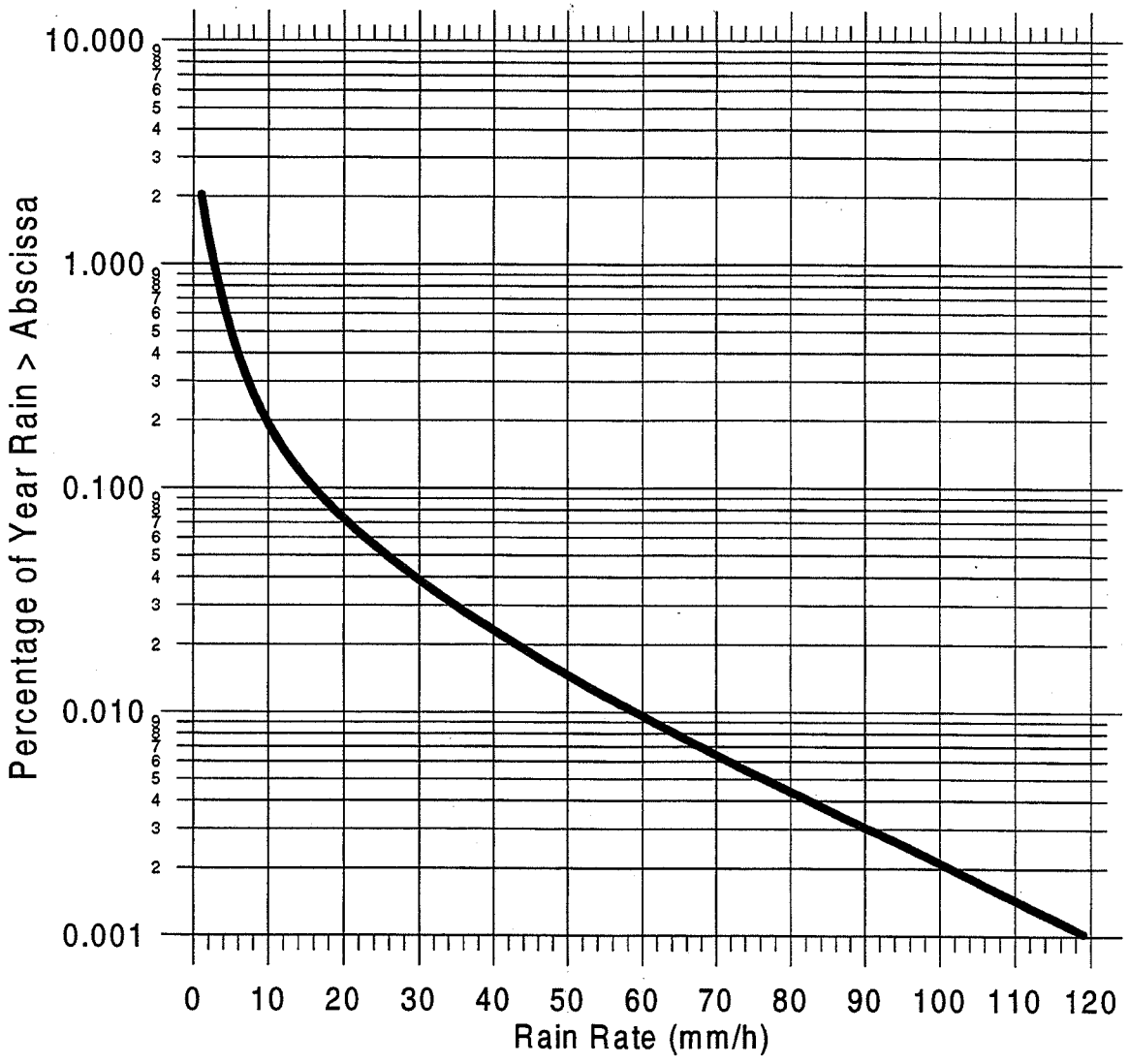

Figure 14

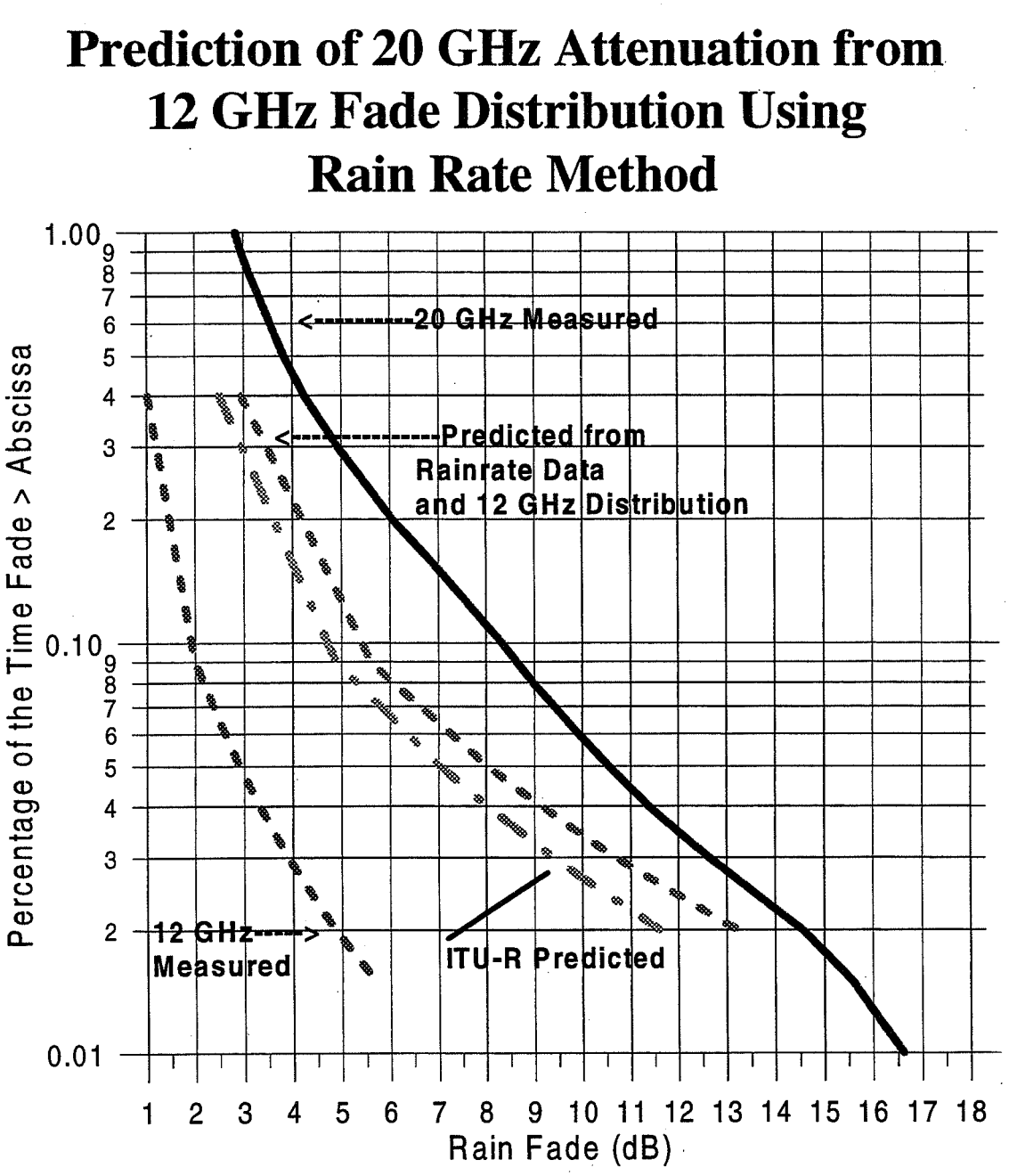
Prediction of 20 GHz Attenuation from 12 GHz Fade Distribution Using Rain Rate Method
Percentage of the Time Fade > Abscissa
1.00
0.10
0.01
20 GHz Measured
Predicted from Rainrate Data and 12 GHz Distribution
12 GHz Measured
ITU-R Predicted
1 2 3 4 5 6 7 8 9 10 11 12 13 14 15 16 17 18
Rain Fade (dB)

Figure 15

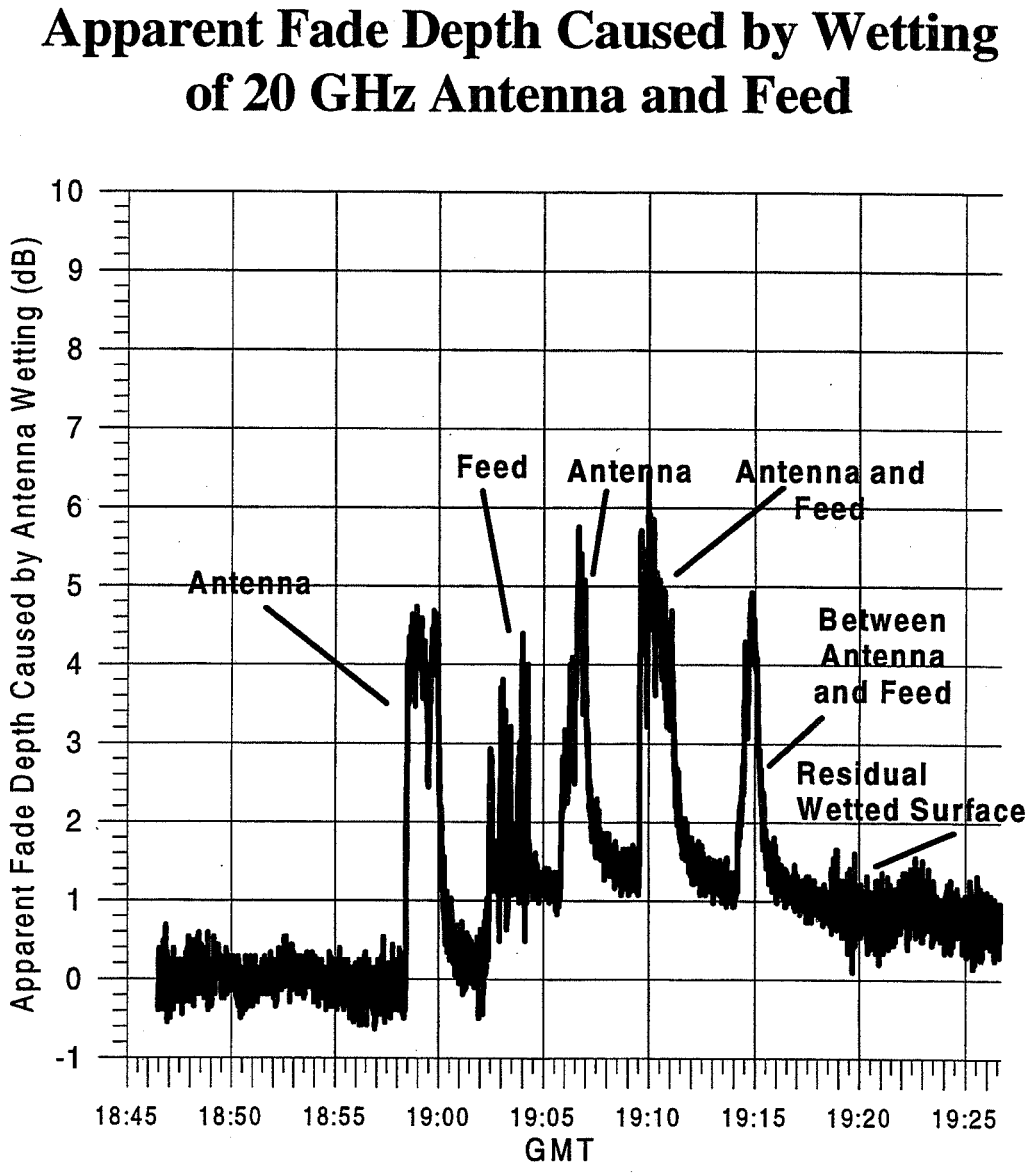
Apparent Fade Depth Caused by Wetting of 20 GHz Antenna and Feed
Apparent Fade Depth Caused by Antenna Wetting (dB)
10
9
8
7
6
5
4
3
2
1
0
-1
Feed
Antenna
Antenna and Feed
Antenna
Between Antenna and Feed
Residual Wetted Surface
18:45
18:50
18:55
19:00
19:05
19:10
19:15
19:20
19:25
GMT

Figure 16

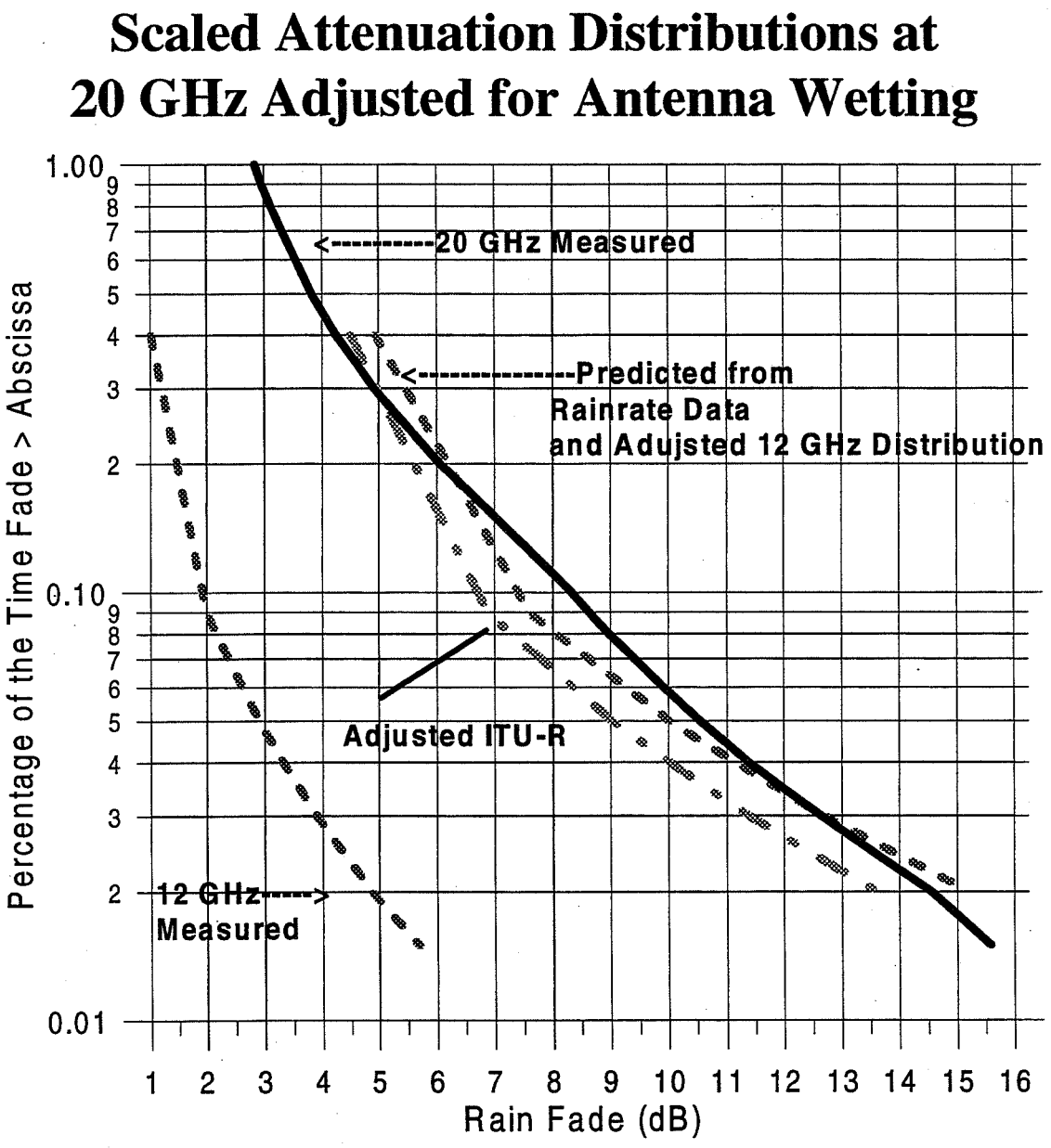
Scaled Attenuation Distributions at
20 GHz Adjusted for Antenna Wetting
Percentage of the Time Fade > Abscissa
1.00
0.10
0.01
<----------20 GHz Measured
<----------Predicted from
Rainrate Data
and Adujsted 12 GHz Distribution
Adjusted ITU-R
12 GHz----->
Measured
1 2 3 4 5 6 7 8 9 10 11 12 13 14 15 16
Rain Fade (dB)

Figure 17

Summary and Conclusions

- 12 GHz rain fades from 1 dB to 5 dB resulted in P = 0.4% to 0.02%
  - 20 GHz rain fades 3 (0.02%) to 4 times (0.4%) larger
- 20 GHz distribution for second year was within +/- 1 dB of first year
- ITU-R frequency scaling
  - Maximum deviation was 4 dB relative to20 GHz measured case
  - 2 dB maximum deviation when adjusted for antenna wetting
- Rainrate frequency scaling
  - Gave 0.5 dB to 1.5 dB closer fade levels
  - Within +/- 1 dB when adjusted for antenna wetting
- Empirical fits frequency scaling
  - Within small fraction of dB

Figure 17

Summary and Conclusions

- ♥ 12 GHz rain fades from 1 dB to 5 dB resulted in P = 0.4% to 0.02%
  - ♠ 20 GHz rain fades 3 (0.02%) to 4 times (0.4%) larger
- ♥ 20 GHz distribution for second year was within +/- 1 dB of first year
- ♥ ITU-R frequency scaling
  - ♠ Maximum deviation was 4 dB relative to 20 GHz measured case
  - ♠ 2 dB maximum deviation when adjusted for antenna wetting
- ♥ Rainrate frequency scaling
  - ♠ Gave 0.5 dB to 1.5 dB closer fade levels
  - ♠ Within +/- 1 dB when adjusted for antenna wetting
- ♥ Empirical fits frequency scaling
  - ♠ Within small fraction of dB

Page intentionally left blank

omit to p209

EERL / Univ. of Texas

ACTS Data Center Status

Geoffrey W. Torrence

Electrical Engineering Research Laboratory
The University of Texas at Austin

Presented at APSW IX
Herndon, VA
November 19-20, 1996

1

EERL / Univ. of Texas

Raw Data Received

RV0 Files as of 11-15-1996

Year	Month	AK	BC	CO	FL	MD	NM	OK
95	Dec	31	31	31	31	31	31	31
96	Jan	31	31	31	31	31	31	31
96	Feb	29	29	27	29	29	27	29
96	Mar	31	31	30	31	31	24	31
96	Apr	30	30	30	30	20	30	30
96	May	31	31	31	31	31N	31	31
96	Jun	30	30	30	30	30N	30	30
96	Jul	31	31	31*	31	31N	31	31
96	Aug	31	31	31	31R	31N	31	31
96	Sep	..	30N	..	28	..	30N	..
96	Oct	..	..	..	..	..	31N	..
96	Nov	..	..	..	..	..	..	..

2

EERL / Univ. of Texas

PV2 Data Received

PV2 Files as of 11-15-1996

Year	Month	AK	BC	CO	FL	MD	NM	OK
95	Dec	..	31	..	31	..	31N	31
96	Jan	..	31	..	31	..	31	31
96	Feb	..	29	..	29	..	27	29
96	Mar	..	..	..	31	..	24	31
96	Apr	..	..	..	30	..	30	30
96	May	..	..	..	31	..	31	31
96	Jun	..	..	..	..	..	30	30
96	Jul	..	..	..	..	..	..	31
96	Aug	..	..	..	..	..	..	31
96	Sep	..	..	..	..	..	..	..
96	Oct	..	..	..	..	..	..	..
96	Nov	..	..	..	..	..	..	..

3

EERL / Univ. of Texas

Miscellaneous Files as of 11-15-1996

Year	Month	AK	BC	CO	FL	MD	NM	OK
95	Dec	.....	.LDSRE	.....	.LDSRE	.....	.LDSRE	.LD..E
96	Jan	.....	.LDSRE	.....	.LDSRE	.....	.LDSRE	.LD..E
96	Feb	.....	.LDSRE	.....	.LDSRE	.....	.LDSRE	.LD..E
96	Mar	.....	.....	.....	.LDSRE	.....	.LDSRE	.LD..E
96	Apr	.....	.....	.....	.LDSRE	.....	.LDSRE	.LD..E
96	May	.....	.....	.....	.LDSRE	.....	.LDSRE	.LD..E
96	Jun	.....	.....	.....	.....	.....	.LDSRE	.LD..E
96	Jul	.....	.....	.....	.....	.....	.....	.LD..E
96	Aug	.....	.....	.....	.....	.....	.....	.LD..E
96	Sep	.....	.....	.....	.....	.....	.....	.....
96	Oct	.....	.....	.....	.....	.....	.....	.....
96	Nov	.....	.....	.....	.....	.....	.....	.....

Key: C=CAL, L=LOG, D=DFC, S=SRF, R=RTN, E=EDF

4

EERL / Univ. of Texas

CD-ROM Requests fulfilled: original 2-year set

- School of Communication System Management, Ohio University
- Hughes Communications
- Hughes Space Communications
- EMSAT (Advanced Technology for Emergency Medical Services)

5

EERL / Univ. of Texas

Plans for CD-ROM distribution: at end of current year

- Raw data to each site which requests it
- Correction for the original 2-year set
  - several sites have substantially redone PV2
  - upgrades of software
- Third year PV2 for all sites
  - 2 CD-ROM's
  - distribute to all doers

6

EERL / Univ. of Texas

Plans for CD-ROM distribution: at end of forth (final?) year

- 4 years of compressed data is 7 CD-ROM's (~24 uncompressed)
- make a new set with one site per CD

7

EERL / Univ. of Texas

Suggestions for future

- We suggest ARCADA BACKUP for use with the original tape drives if switching to Windows 95
  - Colorado Software seems to have too many problems with reading back the tapes.
  - ARCADA format is incompatible so let us know if you switch.

8

EERL / Univ. of Texas

Suggestions for future

- We will be happy to accept data on IOMEGA "Zip" Drive
  - cost < $300 for drive and a year's supply of floppies
  - up to 100 Mbytes of data
- We will also accept data on IOMEGA "Jaz" Drive or CD ROM's

9

Page intentionally left blank

Acts Propagation Terminals

Engineering Support and Systems Upgrades

David Westenhaver

Westenhaver Wizard Works, Inc.

November 19-20, 1996

Software Status / Deficiencies and Known Problems

Data Collection (DRX) software status:

Current version 17 of 4/25/96.

Need to open beacon acquisition constraints.

Data Acquisition and Control System (DACS) software status:

Current version 10 of 4/01/96.

Need to add force beacon reacquisition.

Need to prevent repeating radiometer setups.

Terminate and Stay Resident (TSR) software status:

Current version 11 of 7/16/96.

Will automatically collect high data rate data.

Data missing from RV0; defragment disk.

ActsView software status:

Current version 3 of 9/26/94.

Need to be able to read CD directly.

Need to add display of tipping bucket gauge.

Change color scheme.

Actspp PreProcessing software status:

Current version 6.9 of 5/22/96.

Need to lower memory requirements.

Need to add optical rain gauge to EDF file.

Software Hardware Status / Deficiencies and Known Problems

System cooling fans have been replaced at all sites.

New low vibration fan installed in DRX.

Replacement fans installed in DACS and Receiver Enclosure Cooler.

New hard discs have been installed in all sites data collection PC.

Low-Noise Block (LNB) Failures.

20 GHz LNB at OU and USF replaced.

Have unstable 20 GHz LNB at CSU.

Selecting vender for replacement units.

Radiometer 0.25 -0.5 Volt Jumps

This effect is seen at several sites.

Cause is being investigated. It may be due to LNB.

Feed Horn Widow.

Problem: The windows crack and leak water.

Solution: Replace the feed horn.

Uninterruptable Power Supply (UPS):

Problems: 2 sites had batteries failures, 2 sites had electronics failures.

Solution: Batteries replaced, units replaced.

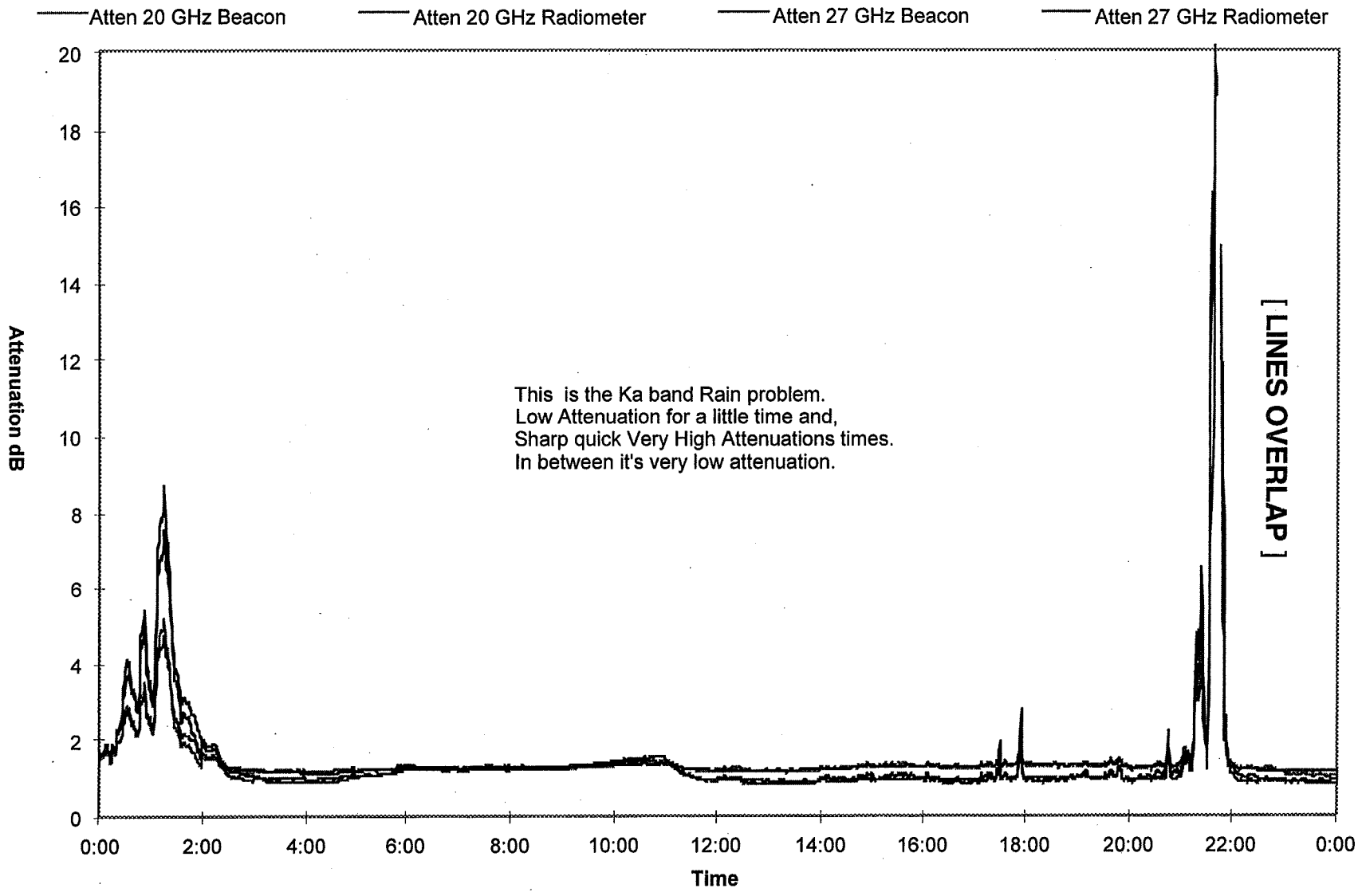
Atten 20 GHz Beacon
Atten 20 GHz Radiometer
Atten 27 GHz Beacon
Atten 27 GHz Radiometer
Attenuation dB
20
18
16
14
12
10
8
6
4
2
0
0:00
2:00
4:00
6:00
8:00
10:00
12:00
14:00
16:00
18:00
20:00
22:00
0:00
Time
This is the Ka band Rain problem.
Low Attenuation for a little time and,
Sharp quick Very High Attenuations times.
In between it's very low attenuation.
[LINES OVERLAP]

Summary Plots of LNB Gain Loss

Summary Plots of Feed Horn /Antenna Water Effects

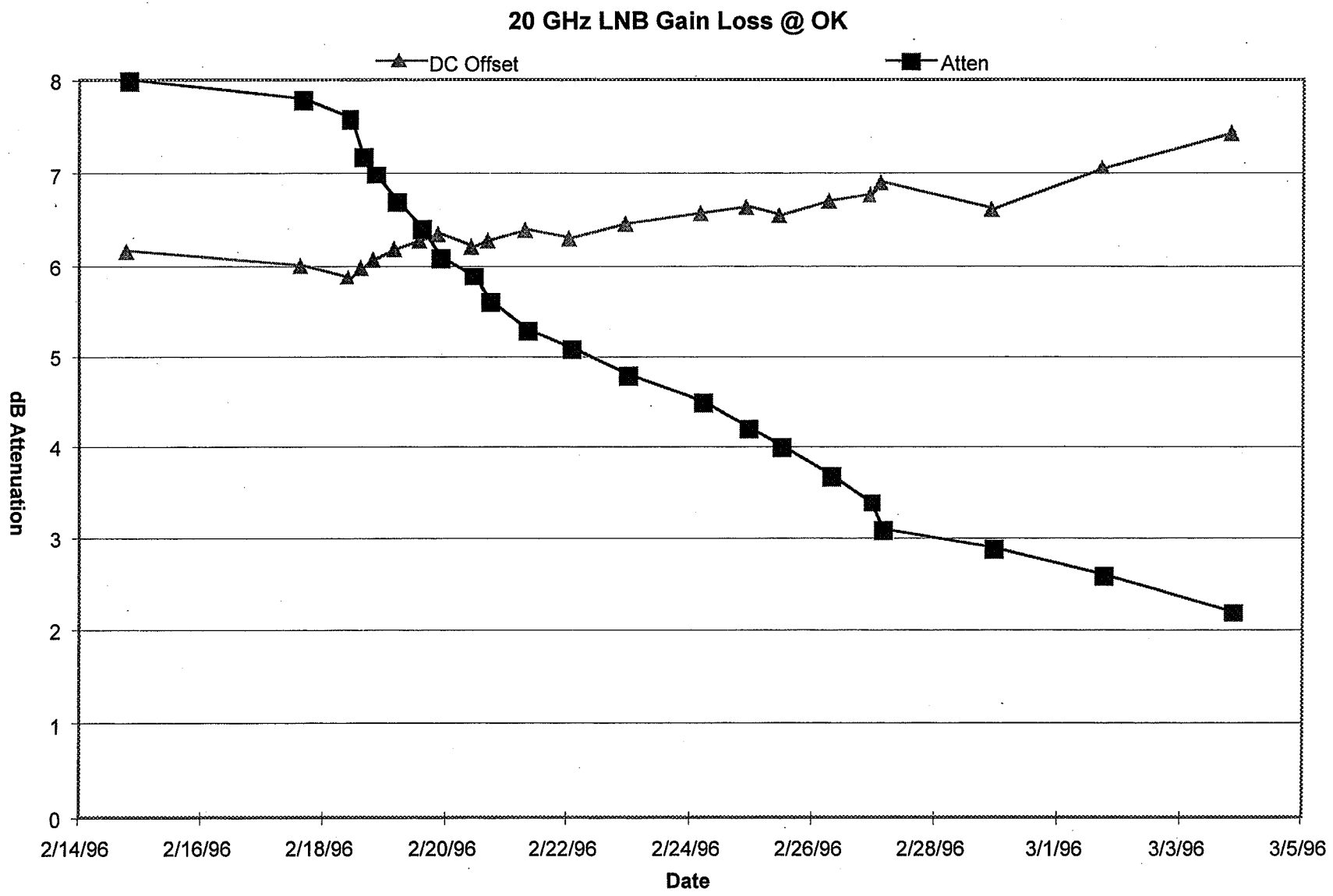
20 GHz LNB Gain Loss @ OK
DC Offset
Atten
dB Attenuation
0
1
2
3
4
5
6
7
8
2/14/96
2/16/96
2/18/96
2/20/96
2/22/96
2/24/96
2/26/96
2/28/96
3/1/96
3/3/96
3/5/96
Date

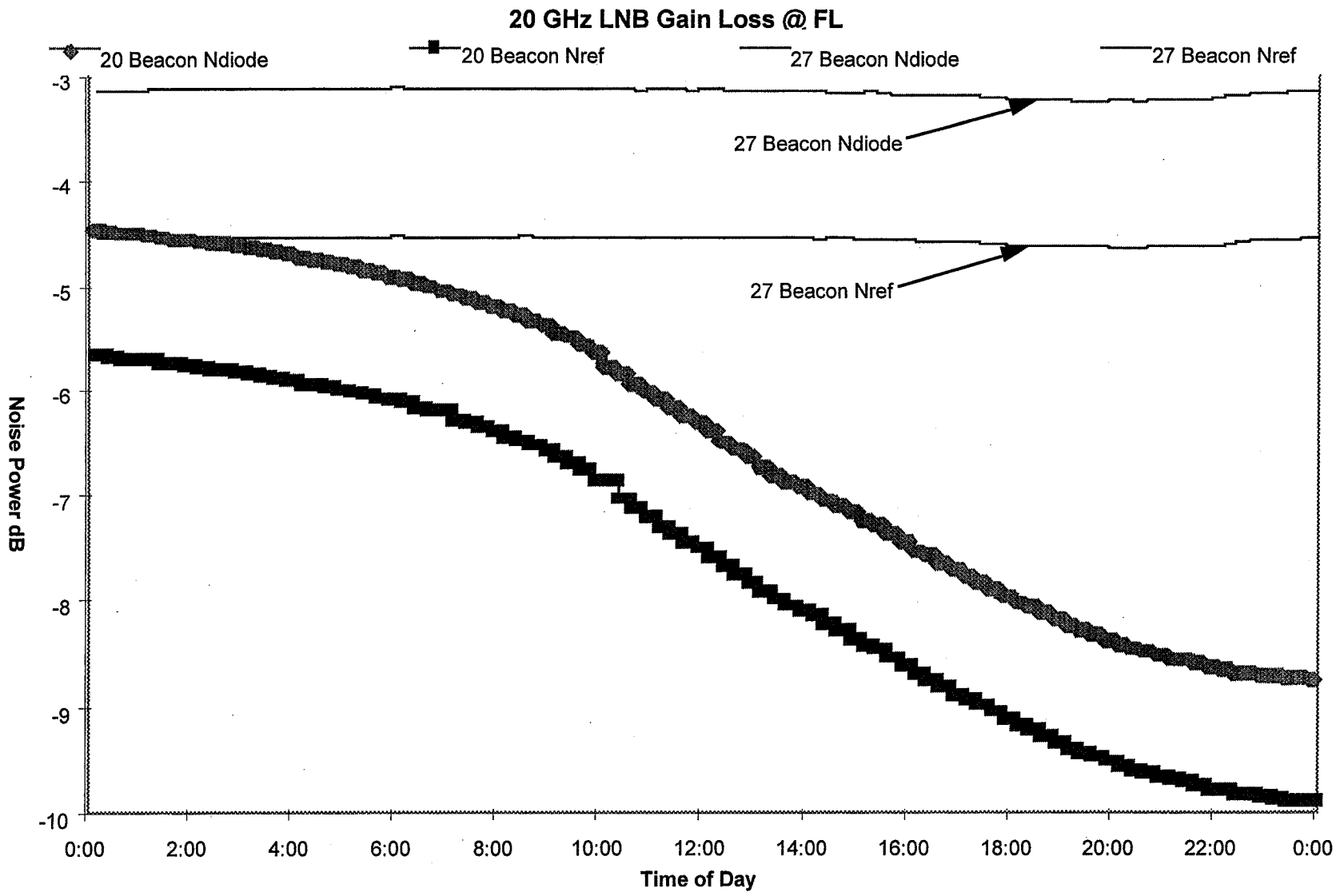
20 GHz LNB Gain Loss @ FL
20 Beacon Ndiode
20 Beacon Nref
27 Beacon Ndiode
27 Beacon Nref
27 Beacon Ndiode
27 Beacon Nref
-3
-4
-5
-6
-7
-8
-9
-10
Noise Power dB
0:00
2:00
4:00
6:00
8:00
10:00
12:00
14:00
16:00
18:00
20:00
22:00
0:00
Time of Day

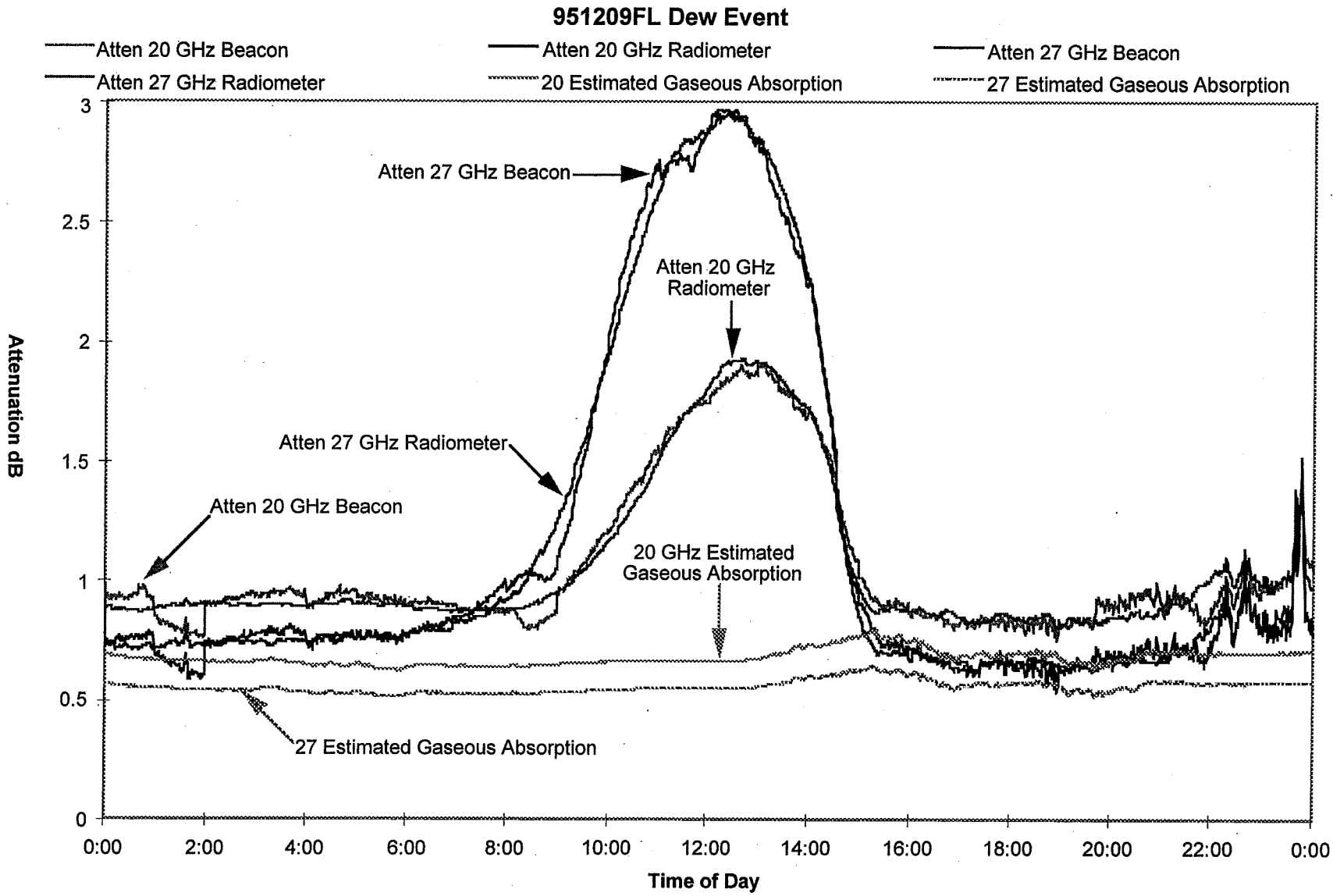
951209FL Dew Event
Atten 20 GHz Beacon
Atten 20 GHz Radiometer
Atten 27 GHz Beacon
Atten 27 GHz Radiometer
20 Estimated Gaseous Absorption
27 Estimated Gaseous Absorption
Attenuation dB
Time of Day
0
0.5
1
1.5
2
2.5
3
0:00
2:00
4:00
6:00
8:00
10:00
12:00
14:00
16:00
18:00
20:00
22:00
0:00
Atten 27 GHz Beacon
Atten 20 GHz Radiometer
Atten 27 GHz Radiometer
Atten 20 GHz Beacon
20 GHz Estimated Gaseous Absorption
27 Estimated Gaseous Absorption

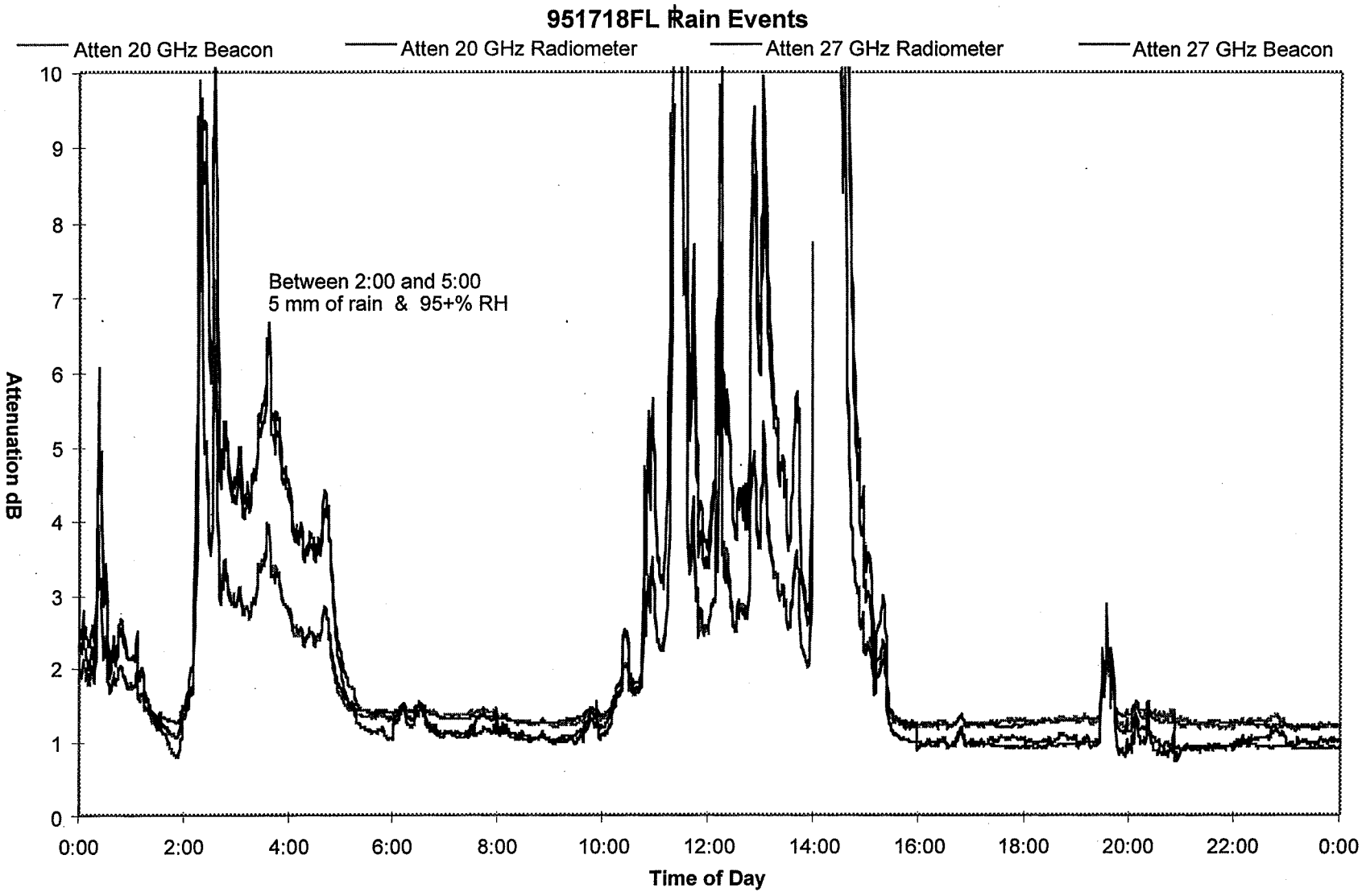
951718FL Rain Events
Atten 20 GHz Beacon
Atten 20 GHz Radiometer
Atten 27 GHz Radiometer
Atten 27 GHz Beacon
Between 2:00 and 5:00
5 mm of rain & 95+% RH
Attenuation dB
Time of Day
0
1
2
3
4
5
6
7
8
9
10
0:00
2:00
4:00
6:00
8:00
10:00
12:00
14:00
16:00
18:00
20:00
22:00
0:00

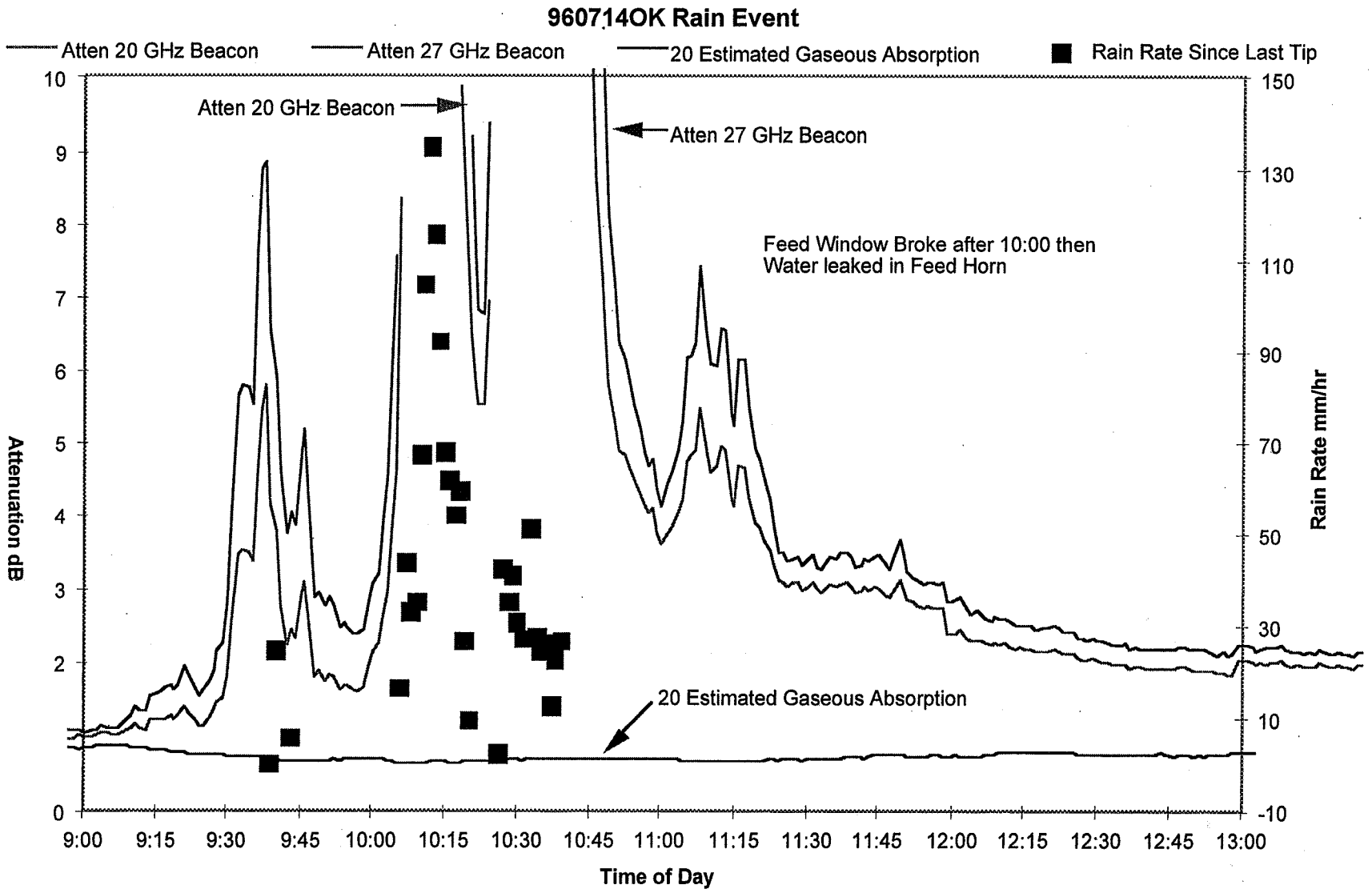
960714OK Rain Event
Atten 20 GHz Beacon
Atten 27 GHz Beacon
20 Estimated Gaseous Absorption
Rain Rate Since Last Tip
Atten 20 GHz Beacon
Atten 27 GHz Beacon
Feed Window Broke after 10:00 then
Water leaked in Feed Horn
20 Estimated Gaseous Absorption
Attenuation dB
Rain Rate mm/hr
Time of Day
0
2
3
4
5
6
7
8
9
10
-10
10
30
50
70
90
110
130
150
9:00
9:15
9:30
9:45
10:00
10:15
10:30
10:45
11:00
11:15
11:30
11:45
12:00
12:15
12:30
12:45
13:00

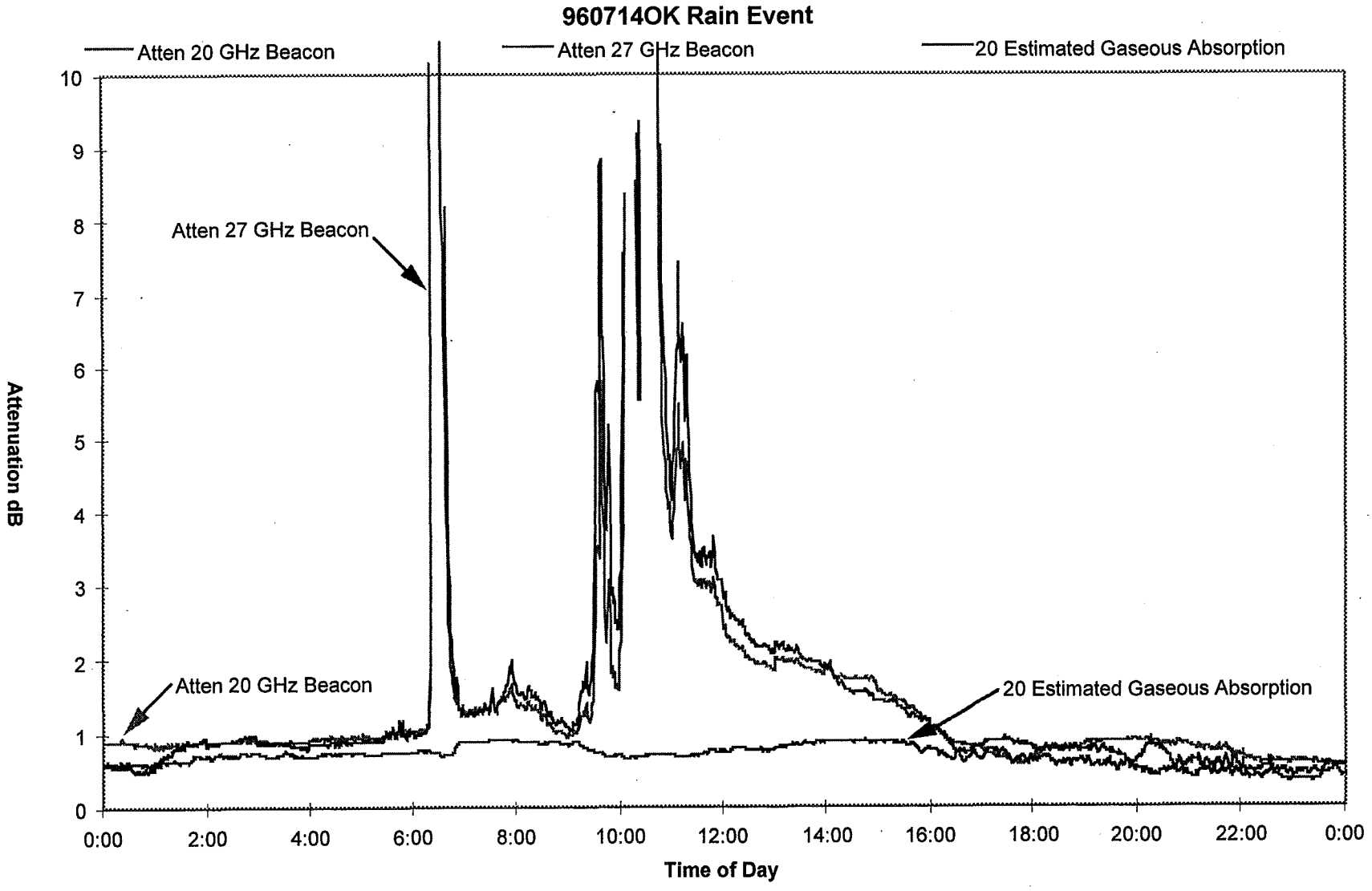
960714OK Rain Event
Atten 20 GHz Beacon
Atten 27 GHz Beacon
20 Estimated Gaseous Absorption
Atten 27 GHz Beacon
Atten 20 GHz Beacon
20 Estimated Gaseous Absorption
Attenuation dB
Time of Day
0
1
2
3
4
5
6
7
8
9
10
0:00
2:00
4:00
6:00
8:00
10:00
12:00
14:00
16:00
18:00
20:00
22:00
0:00

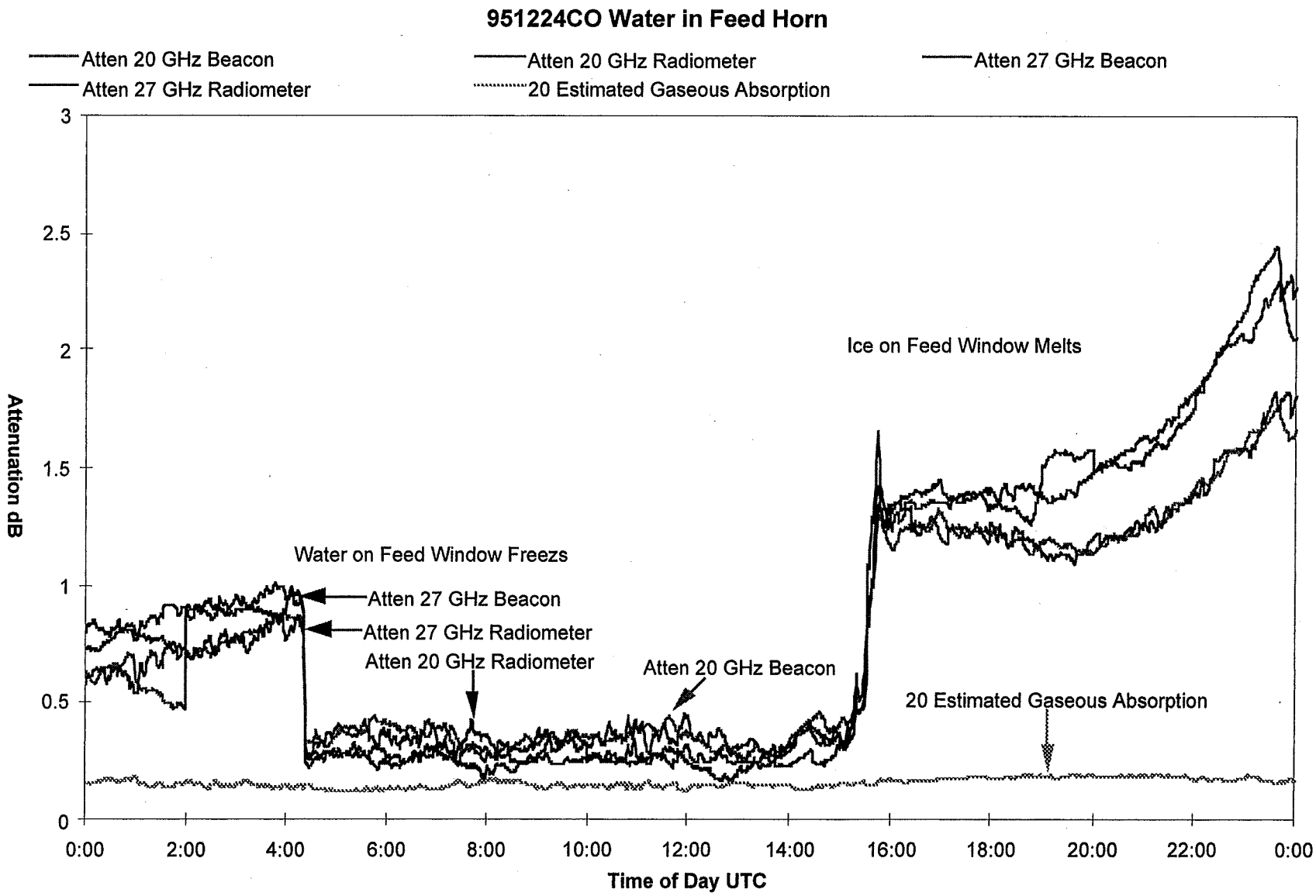
951224CO Water in Feed Horn
Atten 20 GHz Beacon
Atten 20 GHz Radiometer
Atten 27 GHz Beacon
Atten 27 GHz Radiometer
20 Estimated Gaseous Absorption
Attenuation dB
3
2.5
2
1.5
1
0.5
0
Ice on Feed Window Melts
Water on Feed Window Freezs
Atten 27 GHz Beacon
Atten 27 GHz Radiometer
Atten 20 GHz Radiometer
Atten 20 GHz Beacon
20 Estimated Gaseous Absorption
0:00
2:00
4:00
6:00
8:00
10:00
12:00
14:00
16:00
18:00
20:00
22:00
0:00
Time of Day UTC

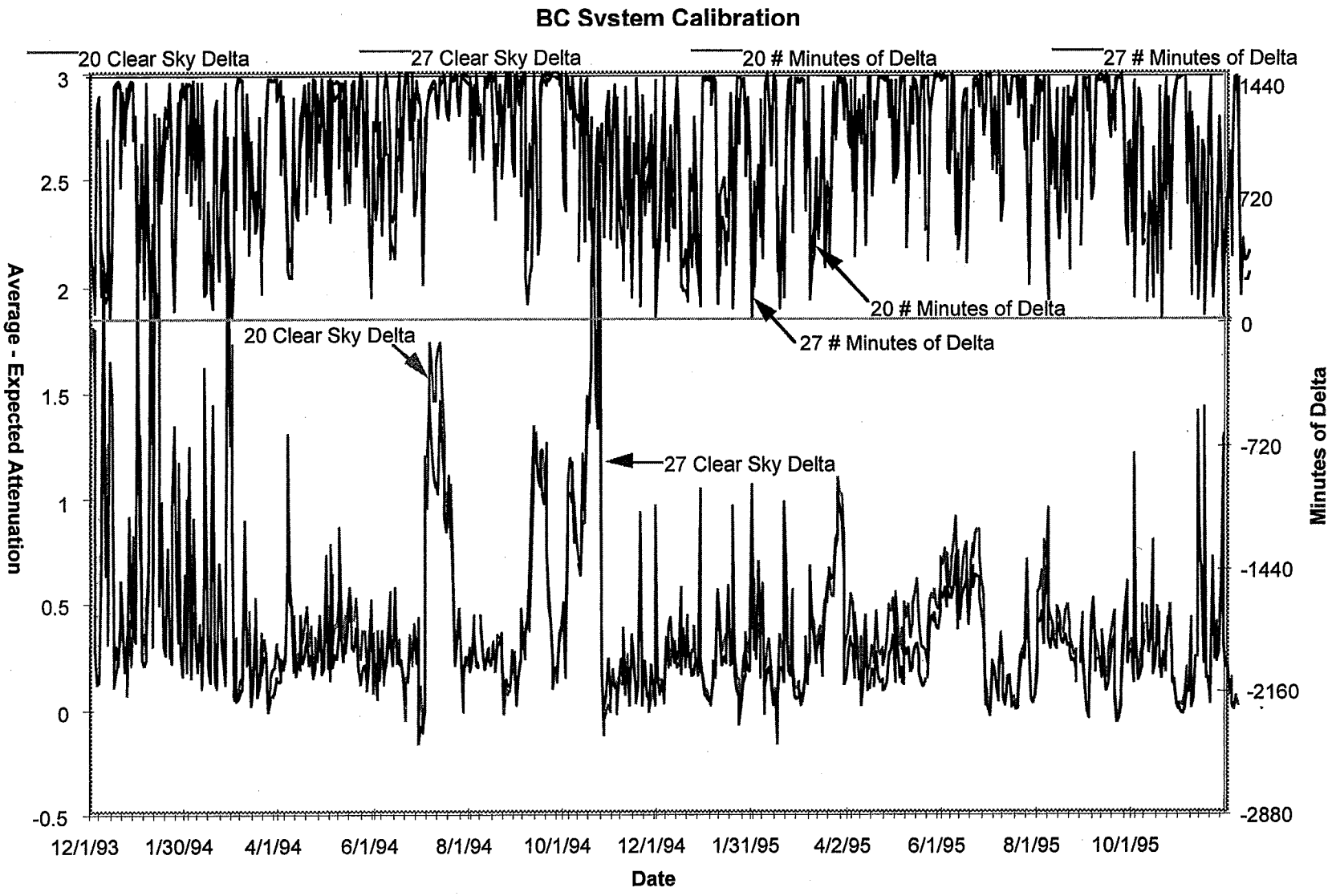
BC Svstem Calibration
20 Clear Sky Delta
27 Clear Sky Delta
20 # Minutes of Delta
27 # Minutes of Delta
Average - Expected Attenuation
Minutes of Delta
Date
3
2.5
2
1.5
1
0.5
0
-0.5
1440
720
0
-720
-1440
-2160
-2880
12/1/93
1/30/94
4/1/94
6/1/94
8/1/94
10/1/94
12/1/94
1/31/95
4/2/95
6/1/95
8/1/95
10/1/95

Page intentionally left blank

OMIT THIS PAGE

SESSION 3

SPECIAL TOPICS

W. Vogel ***(U. TX)***

Page intentionally left blank

ACTS Propagation Experiment:

Rain-Rate Distribution Observations and Prediction Model Comparisons

R.K. Crane and P. Robinson

School of Meteorology
University of Oklahoma
Norman, OK 73019

November 30, 1996

Revised February 1, 1997

to be published in the

Proceedings of the IEEE

Abstract

Empirical distribution functions for one-minute average rain-rate values were compiled for 9 station years of observations at five of the ACTS Propagation Experiment terminal sites. The empirical distribution functions were compared with cumulative distribution functions generated by three different rain-rate distribution prediction models. On the basis of the expected differences between model predictions and experimental measurements, not one of the model combinations provided good predictions.

1.0 Introduction

The NASA Advanced Communications Technology Satellite (ACTS) Propagation Experiment was designed to obtain slant-path beacon attenuation statistics at frequencies of 20.2 and 27.5 GHz [1]. The primary atmospheric phenomenon contributing to attenuation at these frequencies is attenuation by rain. Two years of observations are now available from seven experiment sites in the United States and Canada. The sites are displayed on the map in Figure 1 of [2]. The locations and propagation path parameters for each site are listed in Tables 1 and 2 of [2] (included). These sites were chosen to sample the rain attenuation process in six rain-rate climate regions. The map shows the boundaries of two rain-rate climate models, the ITU-R model [3] and the Crane Global model [4]. Two of the sites are on or near the boundaries of one or both models. The site in New Mexico lies on the ITU-R model boundary, whereas the site in Oklahoma is near a boundary of the ITU-R model and is close to several boundaries of the Global model. (Rain-rate distribution prediction errors should be largest when the site is on or near a climate region boundary.)

All the available prediction models for the statistics of attenuation by rain base their predictions on rain-rate distribution models. The attenuation prediction models are generally of two types: 1) regression models that provide the best match between observed attenuation distributions and predicted or observed rain-rate distributions, and 2) physical models that employ rain-rate density functions together with models for the spatial distribution of rain along the propagation path in the calculation of the expected attenuation distribution. The companion paper on rain attenuation statistics [2] presents the results of model vs. measurement comparisons for two models of each type. In this paper the comparison is extended to consider the predictions of the three different rain-rate distribution models used for the calculation of attenuation.

The coefficients employed in the attenuation prediction models of the regression type were obtained using all the data in the ITU-R data banks that were available at the time the model was proposed. The ACTS Propagation Experiment had, as one of its goals, the generation of attenuation statistics that are different from the data in the data banks and can be used for model verification. The role of the ACTS experiment was to provide a limited number of new observation sets that could be used to test the available models. The rain-rate distribution models are not of the regression type. The two rain climate zone models were tested earlier using the data then available in the ITU-R data bank [4]. For 46 separate locations using only one year of observation from each location, the ITU-R and Global models were statistically identical. The new rain-rate data from the ACTS Propagation Experiment can be used to extend model testing to climate regions not previously analyzed.

The current studies on the risk associated with model predictions [5, 6] are providing measures to calculate how well a model performs statistically. One of these measures, the root-mean-square deviation of the natural logarithm of the ratio of measured to modeled rain-rate values at specified exceedance probabilities (RMSD), was used in this study to judge the relative performance of each model. Because the regression models for attenuation prediction often use only the rain rate at a single exceedance probability level, 0.01% of a year, the RMSD values for that probability level are separately tabulated.

The measured rain-rate statistics presented in this paper were obtained from histogram files prepared by the preprocessing program [1] and stored in the ACTS

Propagation Experiment archives at the University of Texas [7]. The histogram files and a program to prepare empirical distributions from the data are available from the archives for use by model developers for the testing of their models for the prediction of monthly or annual distributions. Cumulative empirical distribution functions (EDFs) for rain rate were compiled for each month of observations in the December 1993 through November 1995 time period. The monthly EDFs were combined to produce annual and worst-month rain-rate EDFs. These distributions are presented in Tables 1 and 2 in the format recommended by International Telecommunications Union Radiocommunications Sector Study Group 3 (ITU-R) [8].

The annual rain accumulation estimates from the ACTS rain gauges were compared to climatologically available data to provide a quality control standard for the acceptance of the rain-rate data. Sample rain-rate measurements and statistical distributions from one of the sites are presented to introducte the rain-rate measurement problem. The distributions and statistics for five of the seven sites are then presented. The rain gauges at two of the sites did not function properly and were replaced in the second year of the measurement program. They did not provide sufficient data for the full year of observations needed to generate a valid annual EDF.

The results of predictions by three different rain-rate climate models, the Rice-Holmberg model based on the use of local climatological data [9], the ITU-R rain climate zone model, and the Crane Global rain climate zone model were considered. These models illustrate the differences in the expected rain-rate distributions for different locations, climate zones and rain intensities. The use of a fourth model, the assumption that the predicted rain-rate EDF will be the same as the distribution observed on a prior year (or years) is recommended by the ITU-R [10]. Such a model requires many years of observations to test. This model is not useful because only a few sites worldwide have a sufficient record of observations to prepare a stable distribution estimate. In an earlier testing of rain attenuation models, this model was tested for the case where the rain-rate observations were for a single year of data coincident with the attenuation observations [11]. This model did not perform as well as the rain climate models. This model was not tested using the ACTS observations.

2.0 Rain-Rate Measurements

The ACTS propagation terminals were provided with capacitor rain-rate measurement gauges. These gauges estimate the rain accumulation in a 10-s interval by measuring the capacitance change produced by a change in the height of a column of rain water collected in a vertical tube. The 1-minute average rain rate was estimated by calculating the average rate of change of the rain water column height or the rain water accumulated in the gauge in a minute. The capacitor gauge employed a high-impedance, high-gain amplifier that was susceptible to noise, especially if the input was an open circuit. As implemented in the field, occurrences of open circuit conditions were common, especially at several of the sites. To combat the noise problem, a least-squares regression procedure was used to estimate the average rate of change of rain accumulation within a minute with the restriction that the rain rate must be zero or positive [12]. With this gauge the minimum observable rain rate in a minute of observations was 2.1 mm/h; the measurement resolution was 0.3 mm/h.

The gauges supplied with the ACTS propagation terminals were difficult to calibrate and maintain. Data from three of the sites could not be used for generating rain-rate EDFs. Several of the sites used tipping bucket rain gauges to supplement or replace the capacitor gauge. The Norman, Oklahoma propagation terminal was sited on the top of a 15-story building. Horizontal wind velocity variations at gauge height made precise rate measurements difficult. For this site, the closest Oklahoma Climatological Survey (OCS) mesonet tipping bucket rain gauge was used to generate the rain-rate statistics. The gauge was sited in a large clear area (adjacent to an airport) at ground level at a distance of 5.6 km

from the ACTS terminal. Data were collected with both 5- and 1-minute accumulation times. The 1- and 5-minute average data produced identical distributions for rates less than 100 mm/h. For the compilation of statistics, only the 5-minute accumulation data were used.

A check on gauge performance was made by comparing the monthly rain accumulation totals obtained from each of the gauges at an ACTS propagation terminal with the accumulation values reported for the closest National Weather Service (NWS) or cooperative observer recording gauge. A further check on gauge operations was made by comparing the monthly accumulations with climatological accumulation data for gauges within 100 km of a site that had a rain climate similar to the that of the ACTS site. Table 3 and Figures 1 through 7 contain the monthly accumulation data for each site. This check was necessary to remove observations during periods with gauge malfunction. The failure mode for the capacitor gauge was an increase in the noise level that would result in nearly continuous rain-rate estimates. Excessive rain accumulation values were indicative of noise problems.

The climatological data used for the comparisons were obtained from 10 to 40 years of observations from 1 to 12 gauges within a square of 1 degree latitude by 1 degree longitude square centered on the ACTS propagation terminal site. For Alaska, a square of 1 degree latitude by two-degree longitude square was used. For the Canadian station, the rain gauge data were obtained from Blaine, Washington, a site southeast of Vancouver on the United States - Canadian border that met the longitude and latitude criteria and was at a location that was climatologically similar to the Vancouver site.

The NWS and cooperative observer gauges were configured with heaters and reported the melted snow water equivalent for precipitation. For Alaska, precipitation was recorded in every month by the NWS and cooperative observer gauges; however the ACTS gauge did not record precipitation from December through April. The other northern sites made measurements when they could, and the data were deleted if snow or ice were present.

The expected annual accumulation values obtained from the long-term NWS and cooperative observer data are given in Table 3, together with the annual accumulation values from the closest gauge and ACTS propagation terminal gauges for the 2 years of observation. Two sets of climatological observations are given, one obtained from hourly observations made over a 20- to 40-year observation period, and a second obtained from 15-minute accumulation data compiled over the last 10 to 20 years. The figures contain the information on the number of years and stations for the longer-term hourly data. The gauges used for the 15-minute accumulation measurement were a subset of the gauges used for the hourly observations, so the two sets of averages were not from independent observations.

Several of the ACTS propagation terminals were sited on the roofs of buildings. The highest building was the 15-story Sarkeys Energy Center on the University of Oklahoma campus. The amount of rain collected from a gauge located on the roof of a building is usually lower than is collected from a gauge located on the ground. The difference in the catch of the gauge is caused by the airflow across the gauge. The Norman, Oklahoma roof-top gauges received 20% less accumulation than the Norman OCS mesonet gauge which was located about 2 feet (60 cm) above ground in a flat area about 6 km from the Energy Center. Similar catch problems are to be expected at the Alaska, British Columbia, Florida and Virginia sites. No comparisons were possible for British Columbia, Florida or Virginia. The Alaskan data show the problem of comparing accumulation of rainwater with the accumulation of rain and melted snow and ice. The catch was less than one half.

A problem with the use of rain accumulation for verifying gauge performance is caused by the limited dynamic range of the capacitor gauge. The minimum rain rate reliably observable using the gauge was 2 mm/h. Observations of longer duration were possible but gauge noise and gauge calibration instabilities limited their usefulness. The data listed in

Table 3 are for observations greater than 2 mm/h. For the Alaska site, a logarithmic extrapolation of the observed rain-rate EDFs to lower rain-rate values would more than double the reported accumulation values. The accumulation error depends on the fraction of the accumulation value that is produced by the lower rain rates. In Alaska and British Columbia, long periods with light rain occur and lead to an accumulation under-estimation error. For the Colorado gauge, the rain is more convective and the dynamic range limitation should not be as important. For the New Mexico tipping bucket gauge, no dynamic range limitation occurs. For this site, the accumulation value matched the NWS gauge observation.

The Oklahoma capacitor gauge worked well but was not used as the primary rain gauge due to its rooftop location. In February 1995, the capacitor gauge was removed from the roof and sent to Florida to replace the gauge at the ACTS site in Tampa. A tipping bucket gauge was installed at that time. The Oklahoma data for the year 1994 through 1995 was a combination of data from the two gauges. The monthly accumulation data from the Florida capacitor gauge (Figure 4) often showed values significantly higher than the maximum value ever recorded by the NWS gauges. These data were marked bad and were not used for analysis. Data from the Virginia and New Mexico capacitor gauges were not used for the same reason.

3.0 Rain-Rate Statistics

The rain-rate statistics presented in Tables 1 and 2 are for all the rain events recorded when the data collection systems were operating. If the attenuation data were marked bad, the attenuation data were excluded from histogram compilations but the rain-rate data were included in the histograms. The EDFs for rain rate do not employ the same time base as the EDFs for attenuation. Because the rain-rate observations are point measurements and the attenuation observations are path measurements, the EDFs can still be used in equal probability comparisons between rain-rate and attenuation statistics. The rain-rate and attenuation EDFs are the best estimates based on the available data. If the time availability for either the rain-rate or attenuation data is less than 90%, the comparisons between EDFs can be misleading.

Figure 8 presents the EDFs for the Norman, Oklahoma site. In this figure, the median Crane Global rain zone model prediction for the site is also displayed, together with upper and lower bounds computed to enclose 90% of the predicted EDFs for that location (a 0.1 significance level hypothesis test for agreement between measurements and predictions). The bounds show the expected range of EDFs for locations within a rain climate zone. The two OCS gauge EDFs lie within the expected range, indicating that the model is consistent with the observations. The differences between the two OCS EDFs are to be anticipated for a statistic for a process with a wide range of expected year-to-year variations in the EDFs. The ACTS tipping bucket and capacitor gauge EDFs are from the roof of the Energy Center building. They are in surprisingly good agreement with the OCS measurements and the model predictions.

The values for the upper and lower bounds were computed from the model for the uncertainty in a rain-rate EDF due to the expected year-to-year and location-to-location variations within a climate zone, as calculated from all the rain-rate observations in the ITU-R data banks [5]. They can be used to estimate the expected uncertainties between model predictions and measurements. Because the model for distribution variability is lognormal, these bounds can be used for estimating the expected uncertainty in percentage of a year (the logarithmic scale) for a fixed rain rate for Figures 9 through 13.

4.0 Comparison to Rain-Rate Predictions

Figures 9 through 13 present the results from the first 2 years of the ACTS Propagation Experiment measurement campaign. The rain-rate scales for each figure are limited to rates below 40 mm/h to provide better resolution at the rates of interest for the

design of low-margin Ka-band communication systems. Both the ITU-R [10] and the Dissanayake, Allnutt and Haidara (DAH) [13] attenuation prediction models use only the rain-rate value at 0.01% of a year. These values are listed in Table 3. The RMSD prediction errors for this probability value are listed in Table 4. The EDFs for valid rain-rate observations are displayed for each year of observations, together with the predictions of the three models: the Crane Global rain-rate climate model [4], the ITU-R rain-rate climate model [3], and the Rice - Holmberg (RH) model [9].

The RH model uses the mean annual rain accumulation, the average number of thunderstorm days, and the maximum monthly accumulation in a thirty year period (the maximum value curves in Figures 1 through 7) to determine the two parameters needed to calculate the probability distribution for rain rate. The rain zone climate models use the rain zone map in Figure 1 of [2] and predefined rain-rate distributions for each zone.

The rain-rate models differ in design. The RH model uses locally available climatological data to estimate the model parameters. The original development of the model was based on 5-minute average extreme rain-rate observations and hourly rain-rate EDFs. They did not have 1-minute average rain-rate EDFs for statistical analysis, but engineered a plausible distribution shape from the data then available. The major problem with this model is the uncertainty in rain-rate distribution shape in the probability region between 0.001% of a year (for extreme value observations) and 0.1% of a year (for the hourly data). Unfortunately, the rain-rate values needed for the regression model predictions are at 0.01% of a year.

The Crane Global rain zone model was developed to identify rain climate regions where sparsely available 1-minute average rain-rate distributions could be combined to produce a single distribution estimate. The distributions in the model are the median distributions for the then- available short-term average rain-rate distributions. The ITU-R climate region model differs from the Crane Global model only in the procedure used to establish climate region boundaries. The major difference between the Rice-Holmberg model and the other two is in the use of local climatological data.

The root-mean-square deviations of the logarithm of the observed EDFs from the predicted cumulative distribution function (CDFs) at the same probability levels [4] (the RMSD values in Table 4) show that the Crane Global model is equivalent statistically to the RH model for the prediction of the annual EDFs and both are better than the ITU-R model (have lower RMSD values). The composite RMSD values represent model performance over the entire range of rain-rate values. The expected RMSD value at a single probability value for a perfect model is 0.27 [14]. The composite RMSD value can be used in a hypothesis test for agreement between a model and measurements. At a 0.1 significance level, the composite RMSD value should be less than 0.31 (90% of a collection of 9 site-years of data would have a smaller RMSD value for the model to be consistent with the observations). At this significance level, all the models can be rejected. In the earlier test of the climate zone models [4], the composite RMSD values were 0.31 for the Crane Global model and 0.36 for the ITU-R model. For that test, a perfect model would have an RMSD value of less than 0.29. For the larger data sample, both models were statistically equivalent and both could be rejected at a 0.1 significance level. For predictions at a single probability level, the RMSD statistics for the ACTS data should be less than 0.34. At 0.1% of a year, only the Crane Global model cannot be rejected while at 0.01% of a year, all the models can be rejected.

Empirical distribution functions were available from five sites. The predicted CDFs for each model are displayed in Figures 9 through 13. For the Alaskan site, both the Crane Global model and the ITU-R model would do well if the site were placed in another rain zone (zone A – the same identifier for each model). Then, the model predictions would match closely (lie between) the observations for '93 and '94. For the assigned climate zones, neither model did well. The RH model predictions were even higher than the two climate zone models. The annual accumulation predictions of each model were also much higher than the observed values obtained from the NWS or cooperative observer gauges.

The problems associated with limited gauge dynamic range and the use of climatological data that include snow events contribute to the modeling errors.

The EDFs for Vancouver, British Columbia matched the predictions of the ITU-R and RH models better than the Crane Global model. The annual accumulation prediction for the Global model was significantly lower than for the other two models. In this case, the Global model may need revision to properly account for the rainy conditions of the Pacific northwest. The Crane Global model C region climate zone boundaries were drawn to enclose climatologically similar regions in northwestern Europe and North America. The rain-rate distribution observations within the C region that were used to calculate the median distribution were all from Europe. These data were not sufficiently similar to the observations from Vancouver to provide a good match.

For Greeley, Colorado, the EDFs were within the expected bounds for the Global model and match the rain zone models better than the RH model. For Las Cruces, New Mexico, the EDF obtained from the tipping bucket observations matched the Global and RH models predictions at rain rates less than 40 mm/h and the ITU-R model at rates above 50 mm/h. The annual accumulation predictions of the first two models agree with the observations but the ITU-R model is in significant error. For the site in Oklahoma, the EDFs lie within the expected bounds of the Global model and match the RH model predictions quite closely. In this case, the ITU-R climate zone identifier is in error.

5.0 Conclusion

The three different rain-rate prediction models did not perform well in predicting the attenuation distributions collected by the ACTS Propagation Experiment. The performance of the rain climate zone models could be improved by changing the positions of some of the climate zone boundaries. The Crane Global climate zone model attempted to represent all possible rain climates with 12 climate zones. The ITU-R climate zone map has only 15 climate regions. These models should be considered to be the first steps in generating a rain-rate prediction model. They were necessary when only a limited number of rain-rate distributions were available. Now the ITU-R rain rate data base contains more than 200 site-years of observations. The Rice - Holmberg model may now provide the basis for an improvement where local climatological data are available. This model should be reconsidered because the data needed to precisely determine the shape of a rain-rate distribution are now available. For precise distribution estimates, more climatological data may be needed. The Rice - Holmberg model uses only two parameters. More will be necessary to estimate the shape of the distribution at probability values near 0.01% of the year. An improved model that can provide rain-rate distribution estimates at 0.1% and 0.01% of the year would provide better input to the regression analysis procedures used in the rain attenuation models that summarize the data in the data banks and ultimately improve our ability to successfully predict the attenuation statistics needed for communication system design.

References

[1] R. K, Crane, X. Wang, D. Westenhaver, and W. Vogel, ACTS Propagation Experiment: Experiment Design, Calibration, Data Preparation and Archival, Proc IEEE, this issue.

[2] R. K. Crane and A. W. Dissanayake, ACTS Propagation Experiment: Attenuation Distribution Observations and Prediction Model Comparisons, Proc IEEE, this issue.

[3] ITU-R, Characteristics of precipitation for propagation modeling, Recommendation ITU-R PN.837-1, 1994 PN Series Volume, Propagation in Non-Ionized Media, International Telecommunications Union, Geneva, 1994.

[4] R. K. Crane, Evaluation of global model and CCIR models for estimation of rain rate statistics, Radio Sci., 20(3), 865-879, 1985.

Table 1

Annual Empirical Distribution Functions

Rain Rate (mm/h) Exceeded for Specified Percentage of a Year

ACTS Site Name	Gauge Type	Start Date	0.001%	0.002%	0.003%	0.005%	0.01%	0.02%	0.03%	0.05%	0.1%	0.2%	0.3%	0.5%	1%	2%	3%	5%
FAIRBANKS_AK	RR_Cap	93_12	20.6	17.4	15.7	12.5	9.0	7.0	5.9	4.7	3.4	2.3						
FAIRBANKS_AK	RR_Cap	94_12	16.6	13.6	12.3	10.9	9.2	7.7	7.0	5.7	4.3	3.1	2.5					
VANCOUVER_BC	RR_Cap	93_12						126.8	32.5	16.1	10.3	7.6	6.4	5.1	3.6	2.3		
VANCOUVER_BC	RR_Cap	94_12					94.3	18.9	15.5	12.8	10.0	7.8	6.6	5.3	3.7	2.4		
GREELEY_CO	RR_Cap	93_12					99.2	30.2	20.9	11.8	5.3	3.2	2.4					
GREELEY_CO	RR_Cap	94_12	75.1	58.5	51.3	41.8	31.7	22.8	18.2	13.1	8.5	5.3	3.8	2.4				
LAS_CRUCES_NM	RR_Tip	94_12	119.7	101.5	89.7	76.3	54.2	18.9	12.7	8.7	5.2	2.6	1.6	0.8	0.2	0.1		
NORMAN_OK	RR_Nor	93_12			99.0	87.4	73.9	54.0	37.7	25.5	15.9	7.7	6.1	4.6	1.5	0.2	0.1	
NORMAN_OK	RR_Nor	94_12	99.2	88.1	82.2	75.3	64.8	53.2	45.3	34.8	22.1	12.0	7.3	4.9	1.6	0.4	0.2	0.1

Table 2

Worst Month Empirical Distribution Functions

Rain Rate (mm/h) Exceeded for Specified Percentage of a Month

ACTS Site Name	Gauge Type	Start Date	0.001%	0.002%	0.003%	0.005%	0.01%	0.02%	0.03%	0.05%	0.1%	0.2%	0.3%	0.5%	1%	2%	3%	5%
FAIRBANKS_AK	RR_Cap	93_12			27.1	22.6	18.6	16.1	14.4	9.8	7.5	5.6	4.6	3.4	2.2			
FAIRBANKS_AK	RR_Cap	94_12			26.9	22.3	17.0	13.1	11.4	9.5	6.8	5.3	4.4	3.5	2.4			
VANCOUVER_BC	RR_Cap	93_12										12.4	9.3	7.2	5.5	4.0	3.3	2.3
VANCOUVER_BC	RR_Cap	94_12									17.0	12.0	10.1	8.5	6.6	4.5	3.5	2.5
GREELEY_CO	RR_Cap	93_12								38.6	20.3	6.8	4.7	3.4	2.3			
GREELEY_CO	RR_Cap	94_12			135.2	111.9	81.9	58.0	45.2	34.9	25.5	14.4	10.0	6.5	3.8			
LAS_CRUCES_NM	RR_Tip	94_12						89.9	79.9	67.7	42.8	10.2	5.5	3.3	1.5	0.6	0.2	0.1
NORMAN_OK	RR_Nor	93_12							90.2	73.5	40.3	26.0	20.5	7.7	5.5	3.5	1.4	0.2
NORMAN_OK	RR_Nor	94_12						83.7	73.4	63.6	52.9	36.6	29.5	21.1	10.1	4.2	1.5	0.5

RR_Cap: ACTS Capacitor Gauge

RR_Tip: ACTS Tipping Bucket Gauge

RR_Nor: Norman Oklahoma Climatological Survey Mesonet 5 min integration time tipping bucket gauge

Table 1 from [2]

ACTS Propagation Experiment Site Locations

Organization	Location	N. Latitude (deg)	W. Longitude (deg)	Height (km)	Global Rain Zone	ITU-R Rain Zone	Elevation Angle (deg)	Azimuth Angle (deg)	Polarization deg from horizontal
U. of Alaska	Fairbanks	64.85	147.82	0.18	B1	C	8.1	129.3	45
U. of B.C.	Vancouver	49.25	123.22	0.01	C	D	29.3	150.5	72
U. of CO	Greeley	40.33	104.61	1.90	B2	E	43.1	172.8	84
U of S. FL	Tampa	28.06	82.42	0.05	E	N	52.0	214.0	77
COMSAT, VA	Reston	38.95	77.33	0.08	D2	K	39.2	213.3	76
NM State U.	Las Cruces	32.54	106.61	1.46	F	M	51.5	167.8	81
U. of OK	Norman	35.21	97.44	0.42	D2	E	49.1	184.4	86

Table 2 from [2]

ACTS Propagation Experiment Site Performance Parameters

		Availability (%)				Calibration Errors			
		20.2 GHz	27.5 GHz	20.2 GHz	27.5 GHz	20.2 GHz	27.5 GHz	Rice Holmberg	
Organization	Location	'93 - '94	'93 - '94	'94 - '95	'94 - '95	dB rms	dB rms	Mean (mm)	Beta
U. of Alaska	Fairbanks	98.3%	97.5%	97.3%	98.5%	0.26	0.22	274	0.06
U. of B.C.	Vancouver	97.0%	97.0%	96.8%	96.8%	0.58	0.54	1181	0.09
U. of CO	Greeley	81.9%	89.3%	95.9%	95.9%	0.09	0.24	444	0.18
U of S. FL	Tampa	94.8%	94.2%	97.2%	96.7%	0.31	0.28	1277	0.73
COMSAT, VA	Reston			81.4%	81.4%	0.25	0.21	916	0.28
NM State U.	Las Cruces	97.4%	97.4%	97.2%	97.3%	0.17	0.16	238	0.19
U. of OK	Norman	97.5%	97.5%	93.5%	93.5%	0.21	0.19	831	0.35

Table 3

Annual Accumulation Values (mm)

	Site Data		Local Data		Climatological Data		Model Data		
Rain Gauge Site	Year 1	Year 2	NWS Year 1	NWS Year 2	Hourly	15 Minute	Rice Holmberg	ITU-R Zone	Global Zone
Fairbanks, AK	73	110	225	235	271	288	274	863	363
Vancouver, BC	818	812			988	951	1181	1195	789
Greeley, CO	190	296	251	442	301	322	444	515	603
Tampa, FL			1192	1389	1267	1233	1277	1990	2473
Las Cruces, NM		246	199	227	212	282	238	1316	315
Norman, OK	703	903	603	744	801	876	831	515	1195
Reston, VA			1080		965	973	916	1319	1195

Table 4

Composite comparison statistics for different models

Model	RMSD	Average	0.1% of year	0.01% of year	Favorable
Rice - Holmberg	0.48	-0.15	0.41	0.7	6
ITU-R Rain Zone	0.71	0.07	0.79	0.88	3
Crane Global Rain Zone	0.51	0.09	0.25	0.83	3

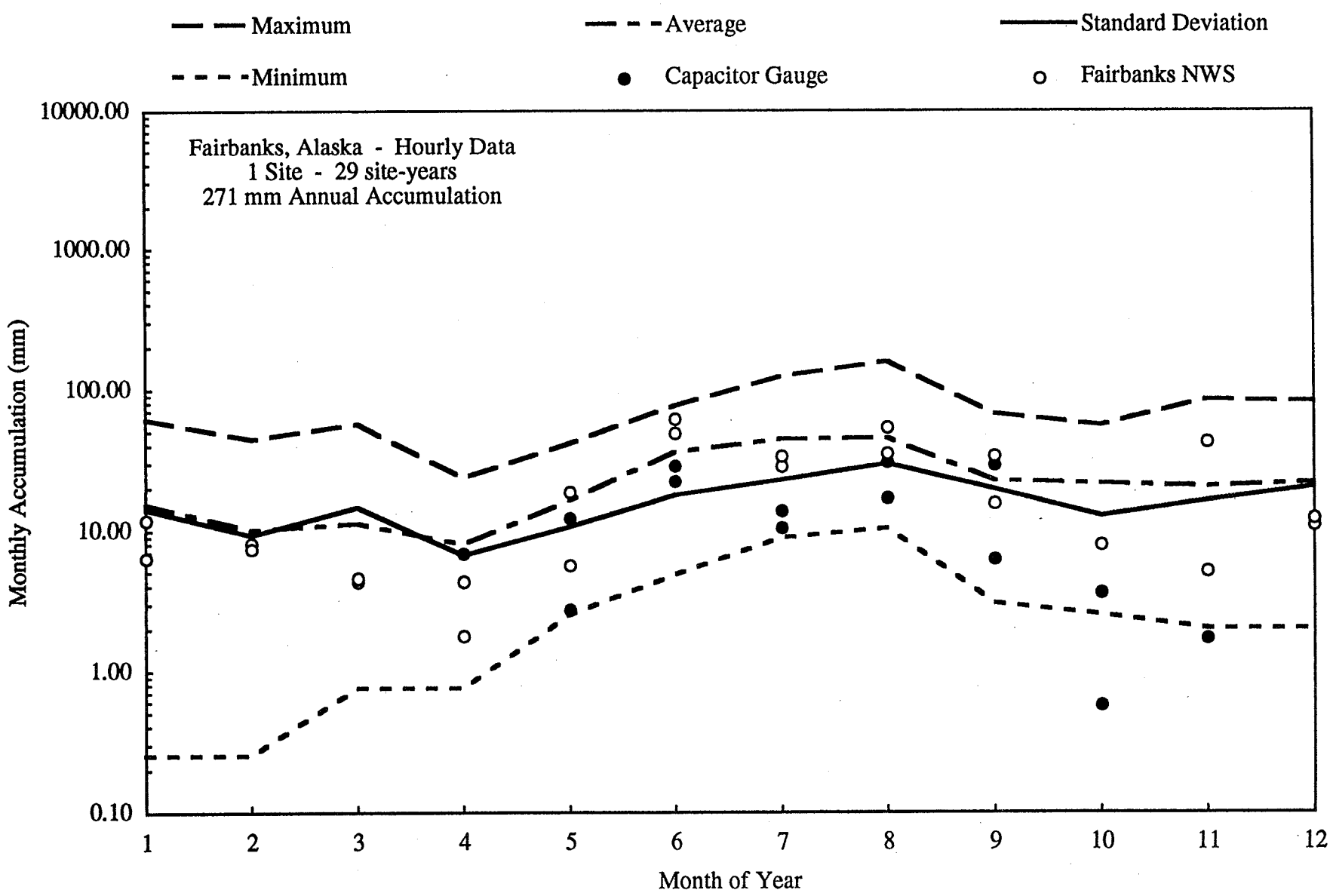

Figure 1 Monthly rain accumulations, Fairbanks, Alaska

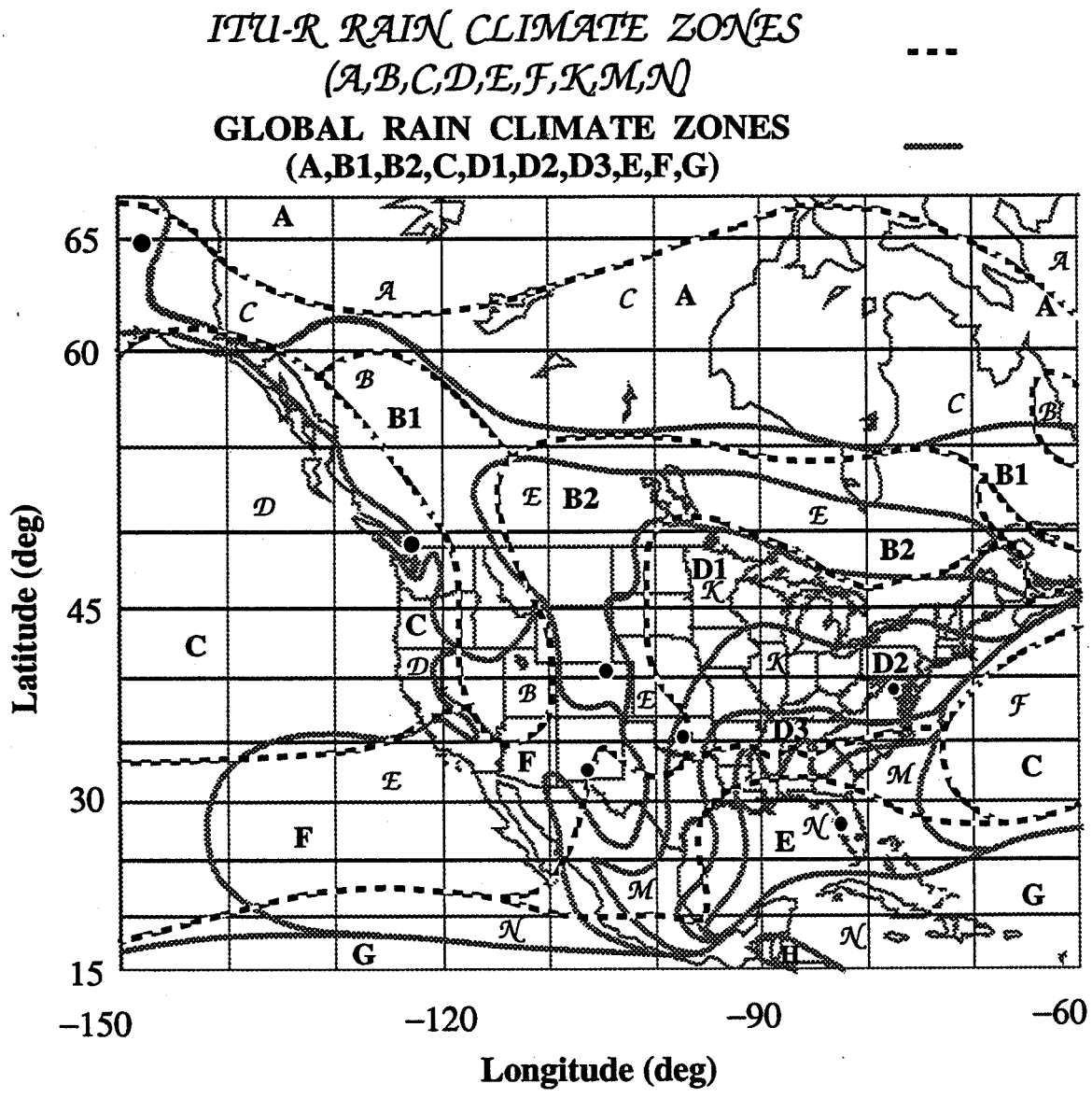

Figure 1 of [2] ACTS propagation experiment site locations and the Global and ITU-R rain zone boundaries.

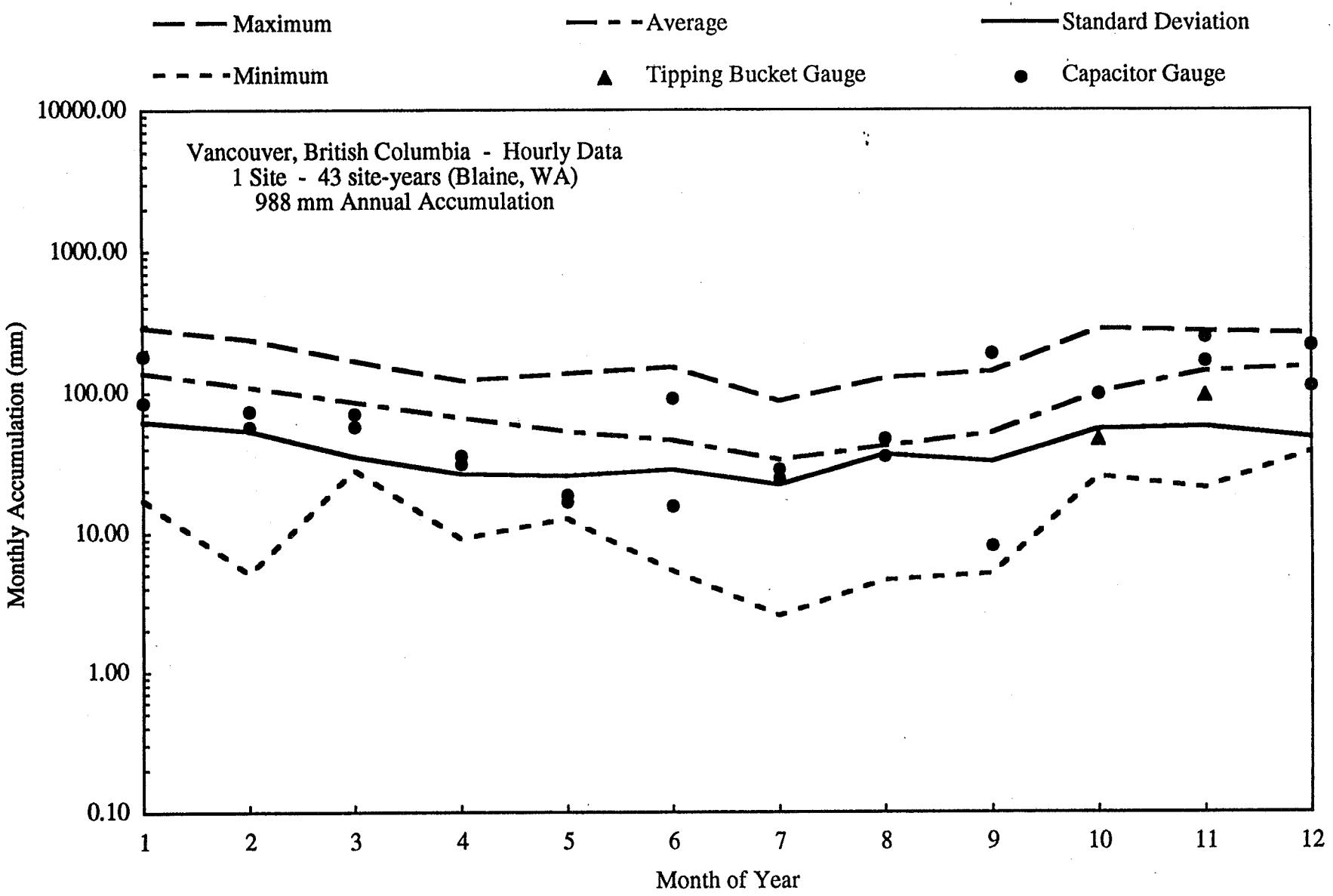

Figure 2 Monthly rain accumulation, Vancouver, British Columbia

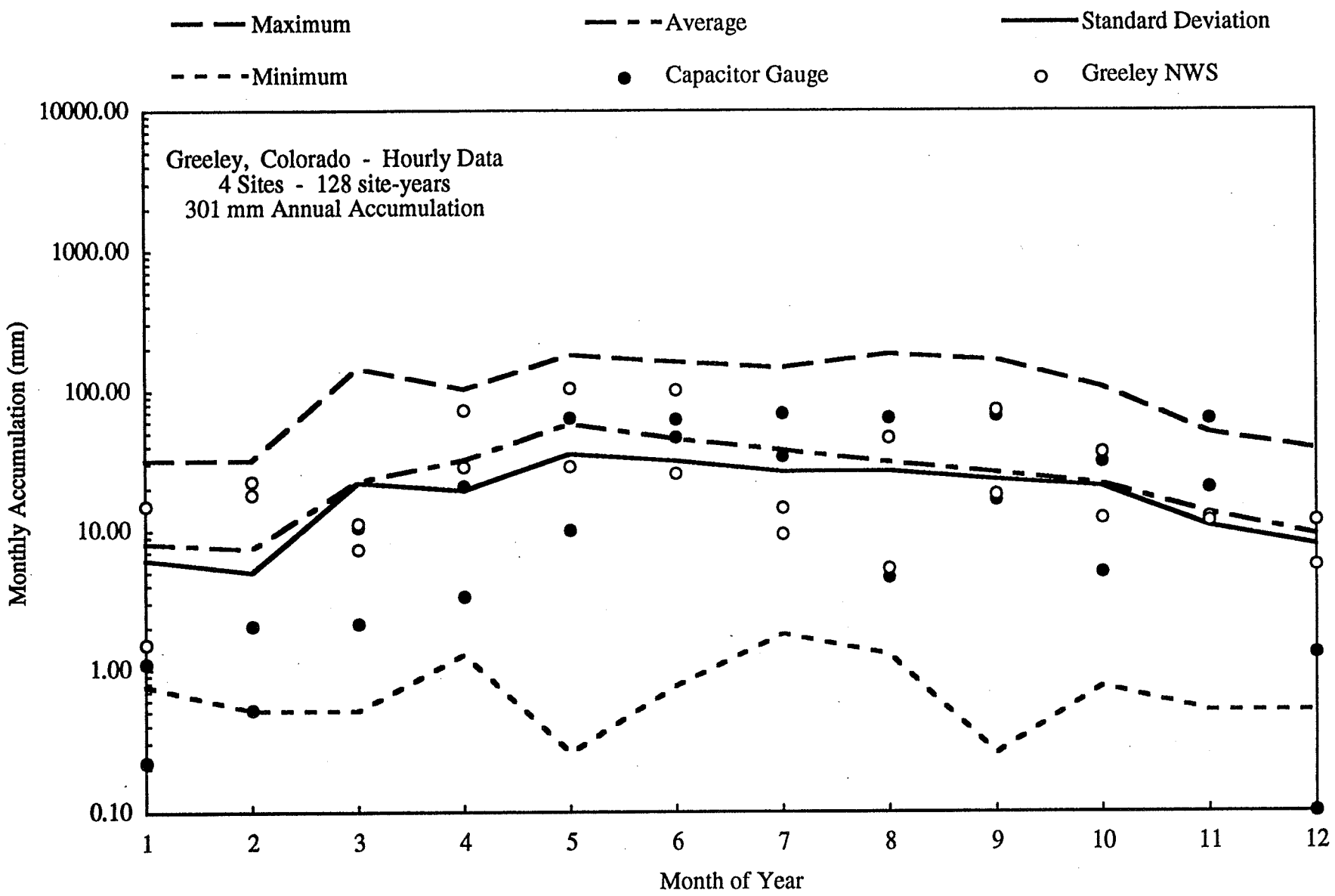

Figure 3 Monthly rain accumulations, Greeley, Colorado

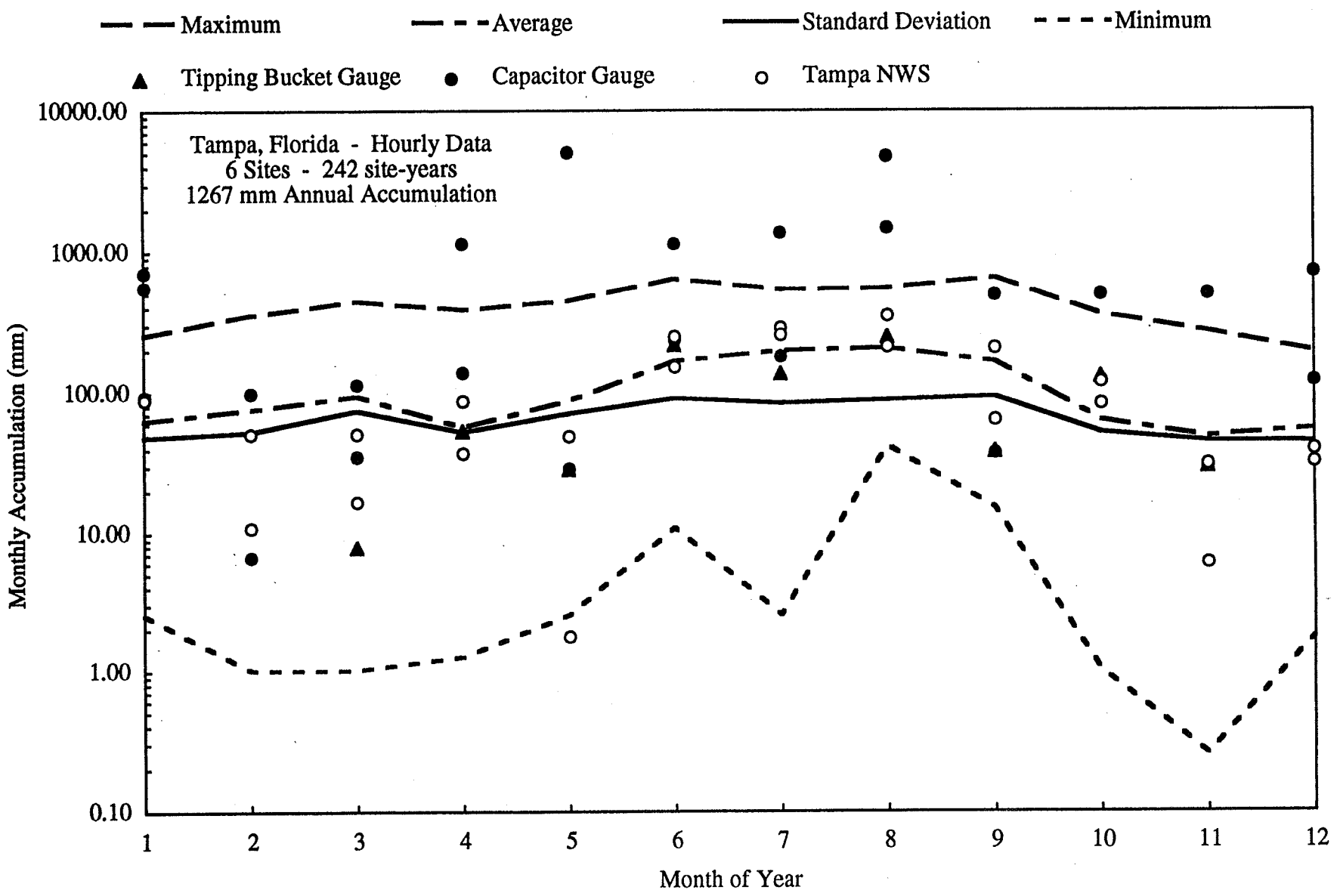

Figure 4 Monthly rain accumulations, Tampa, Florida

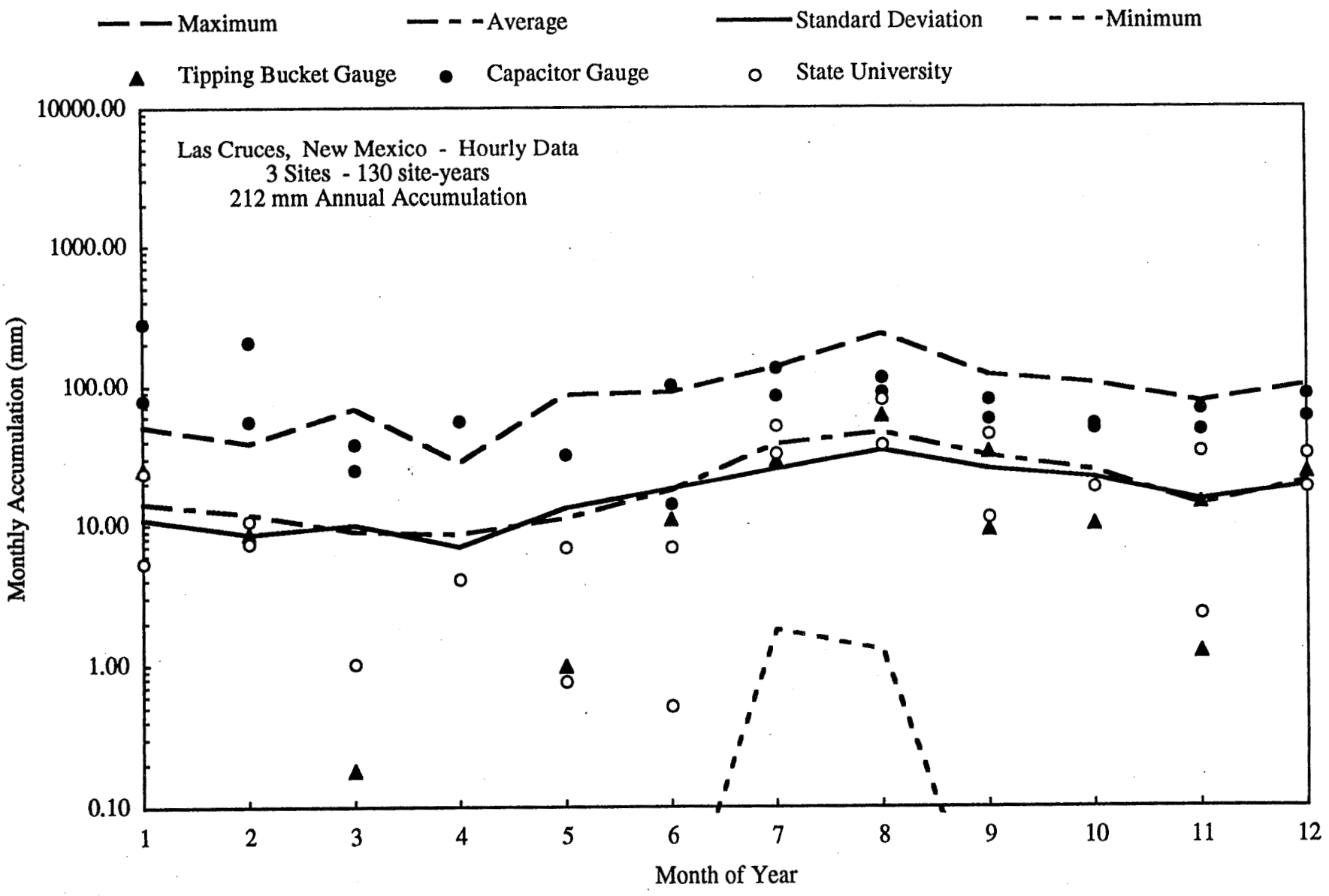

Figure 5 Monthly rain accumulations, Las Cruces, New Mexico

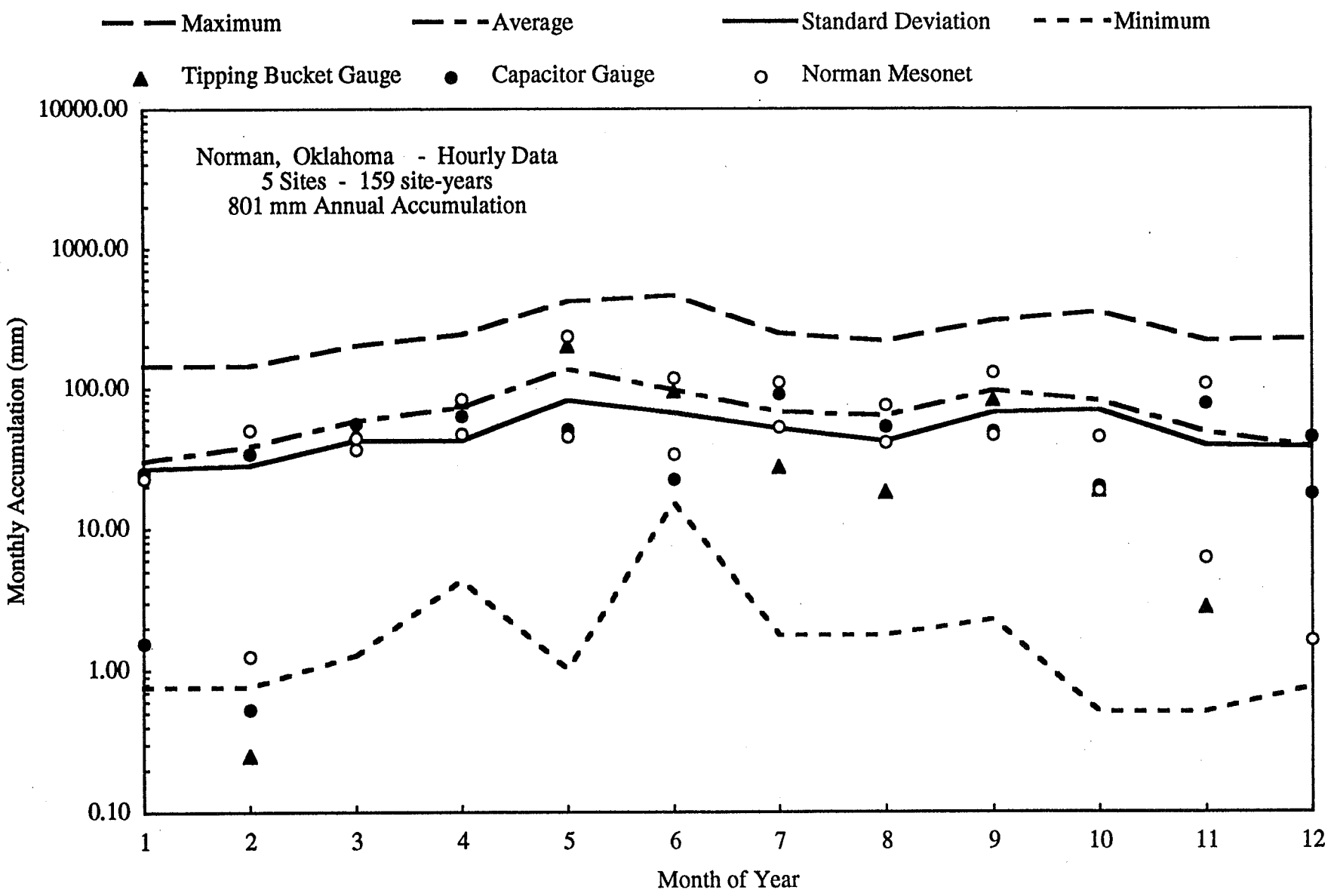

Figure 6 Monthly rain accumulation, Norman, Oklahoma

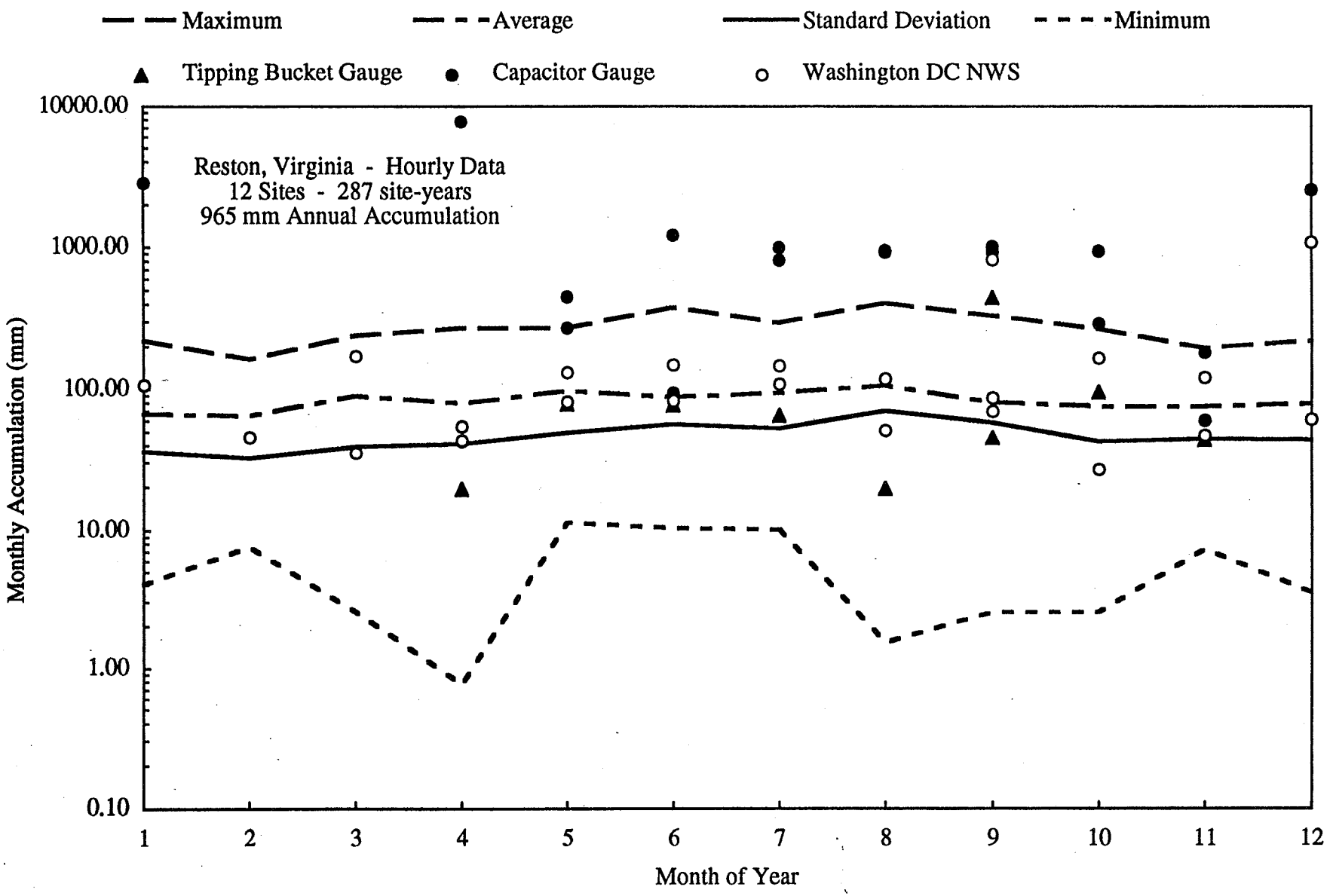

Figure 7 Monthly rain accumulation, Reston, Virginia

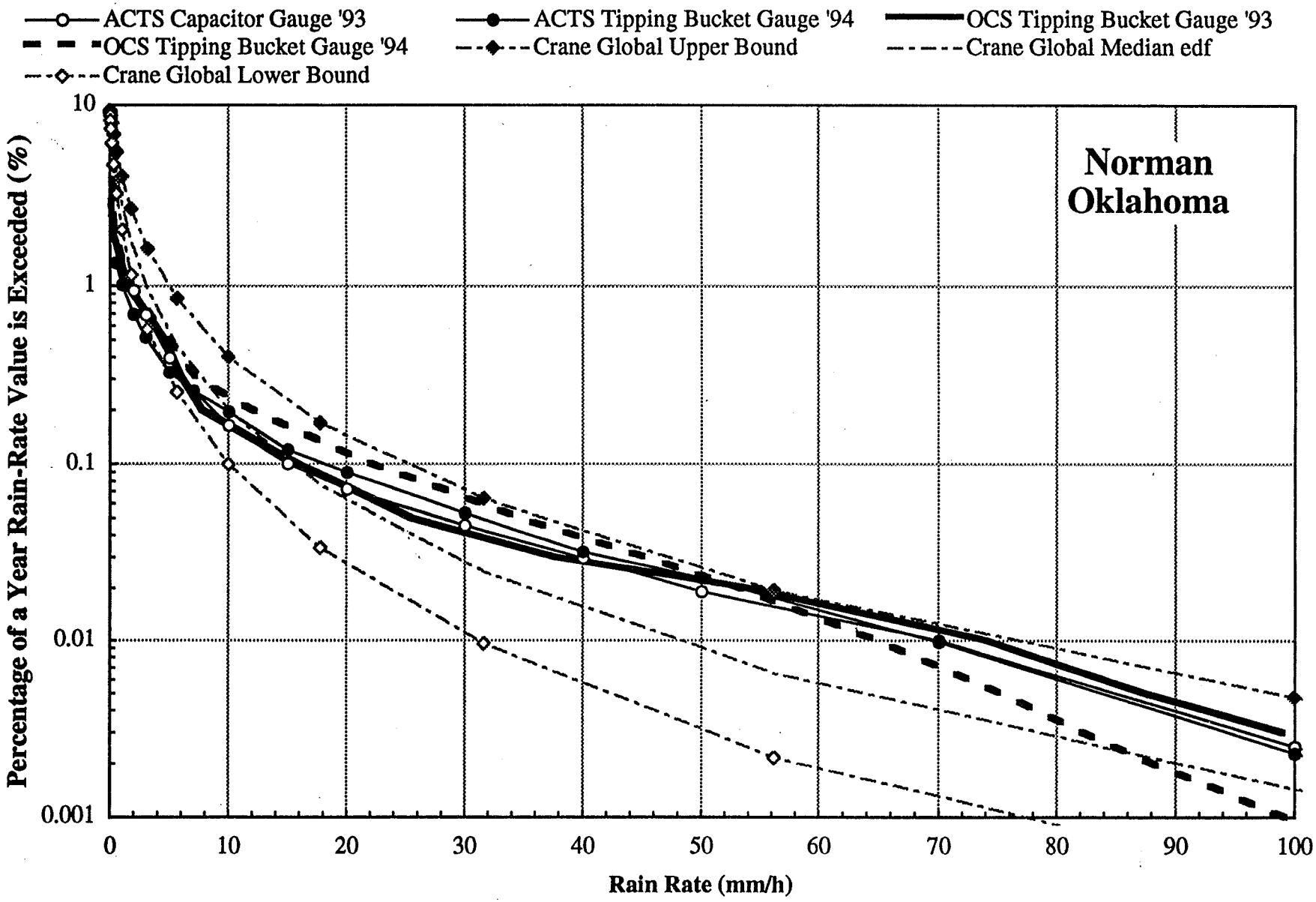

Figure 8 Single year rain-rate edf's, Norman, Oklahoma

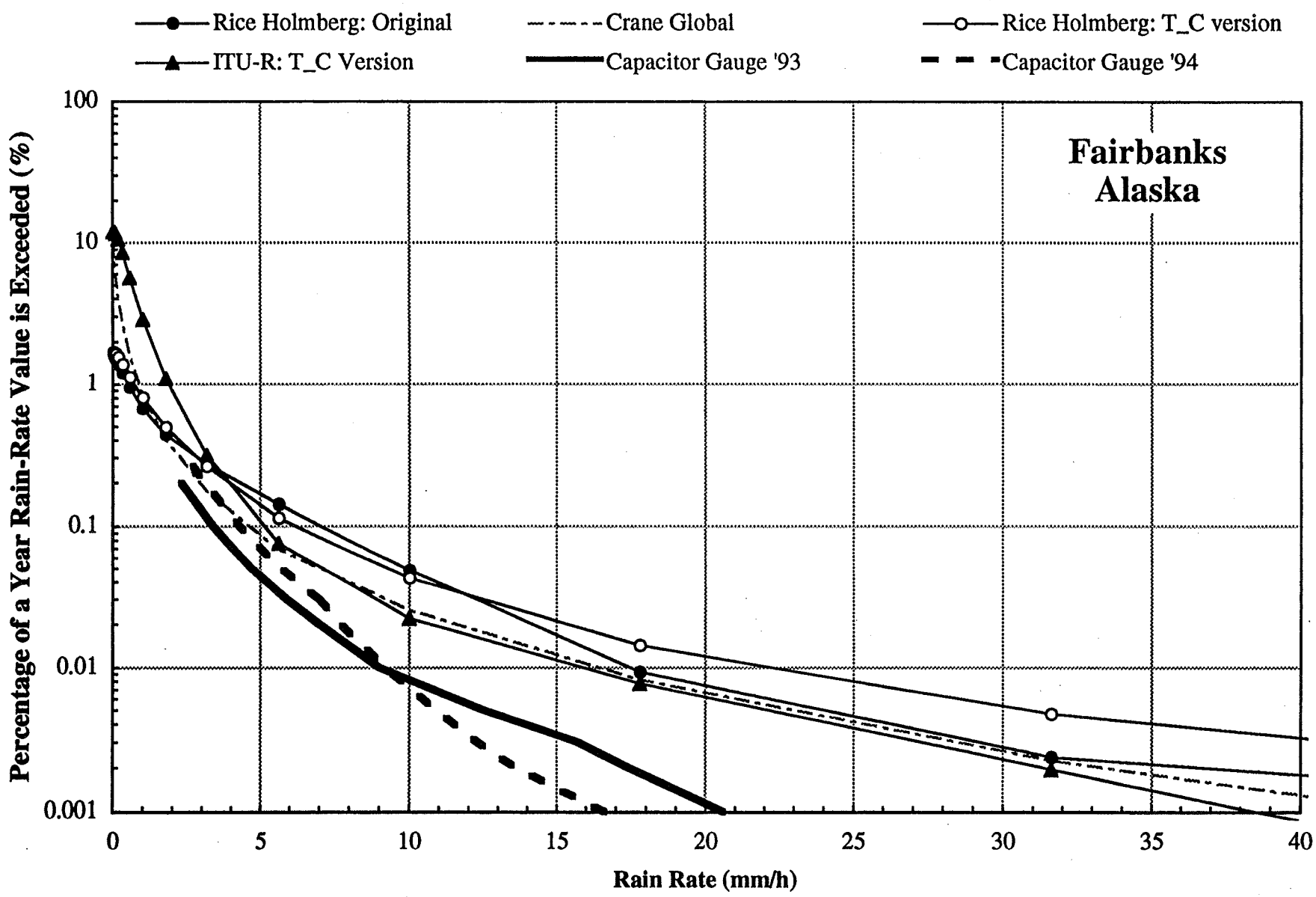

Figure 9 Single year rain-rate edf's, Fairbanks, Alaska

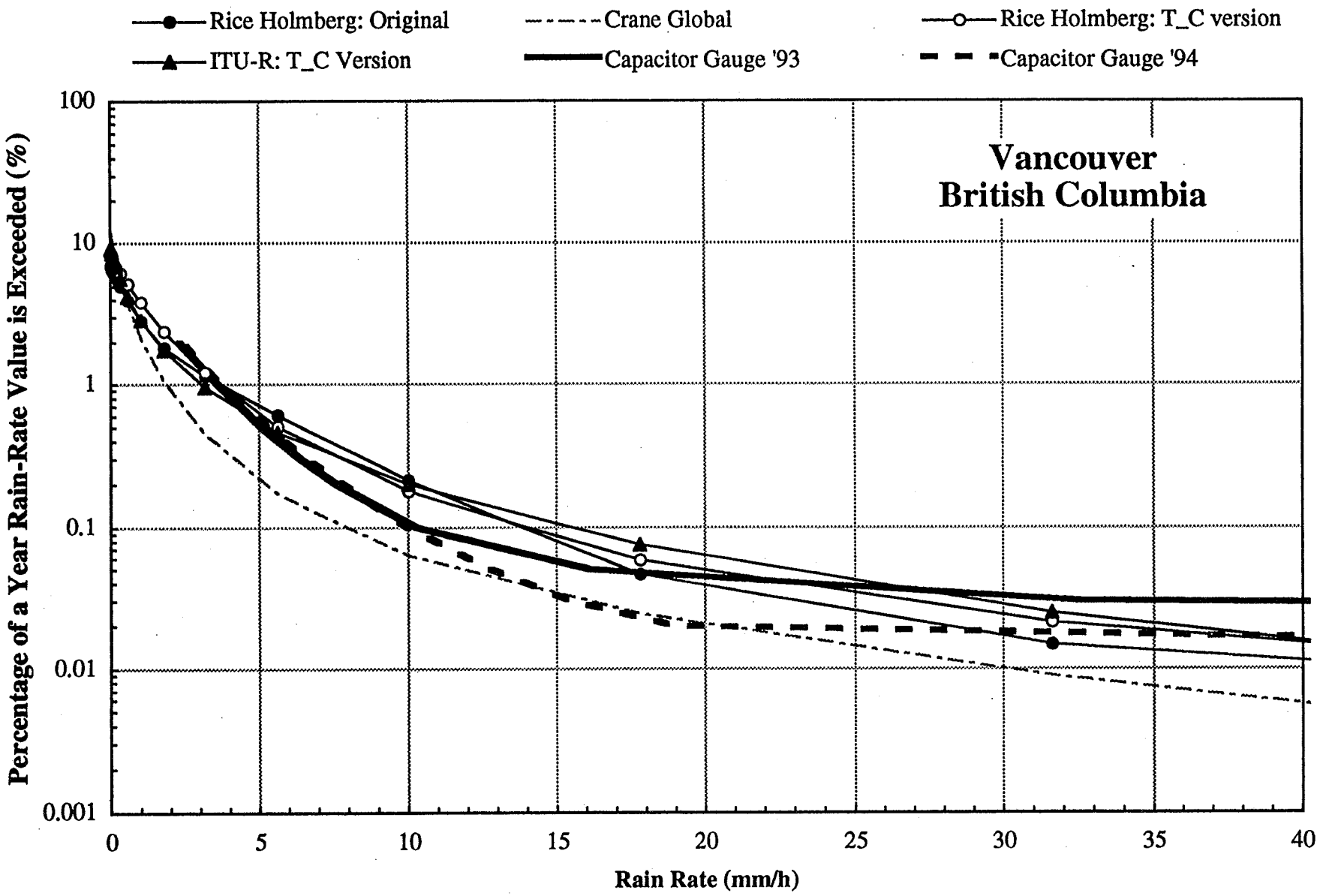

Figure 10 Single year rain-rate edf's, Vancouver, British Columbia

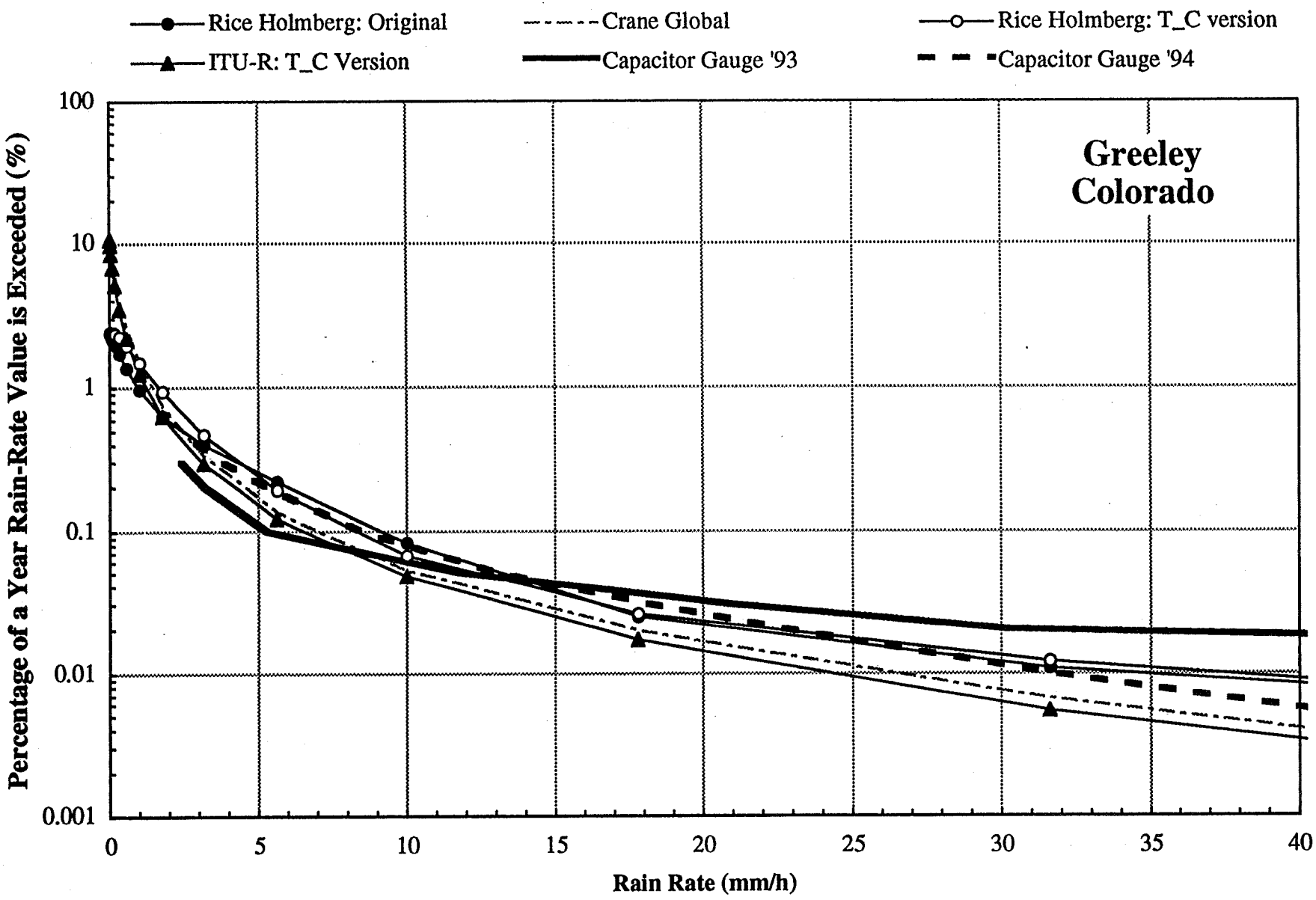

Figure 11 Single year rain-rate edf's, Greeley, Colorado

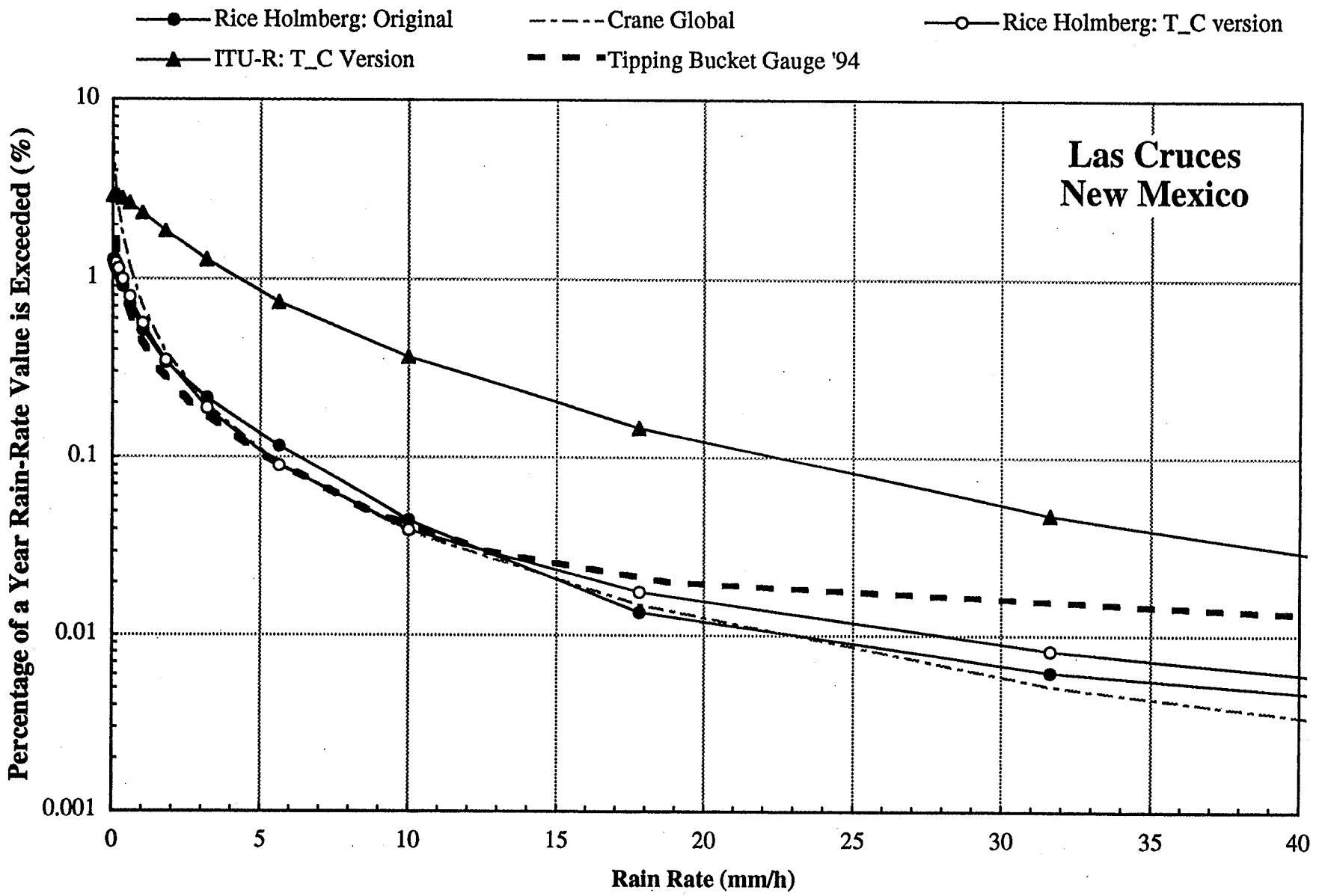

Figure 12 Single year rain-rate edf's, Las Cruces, New Mexico

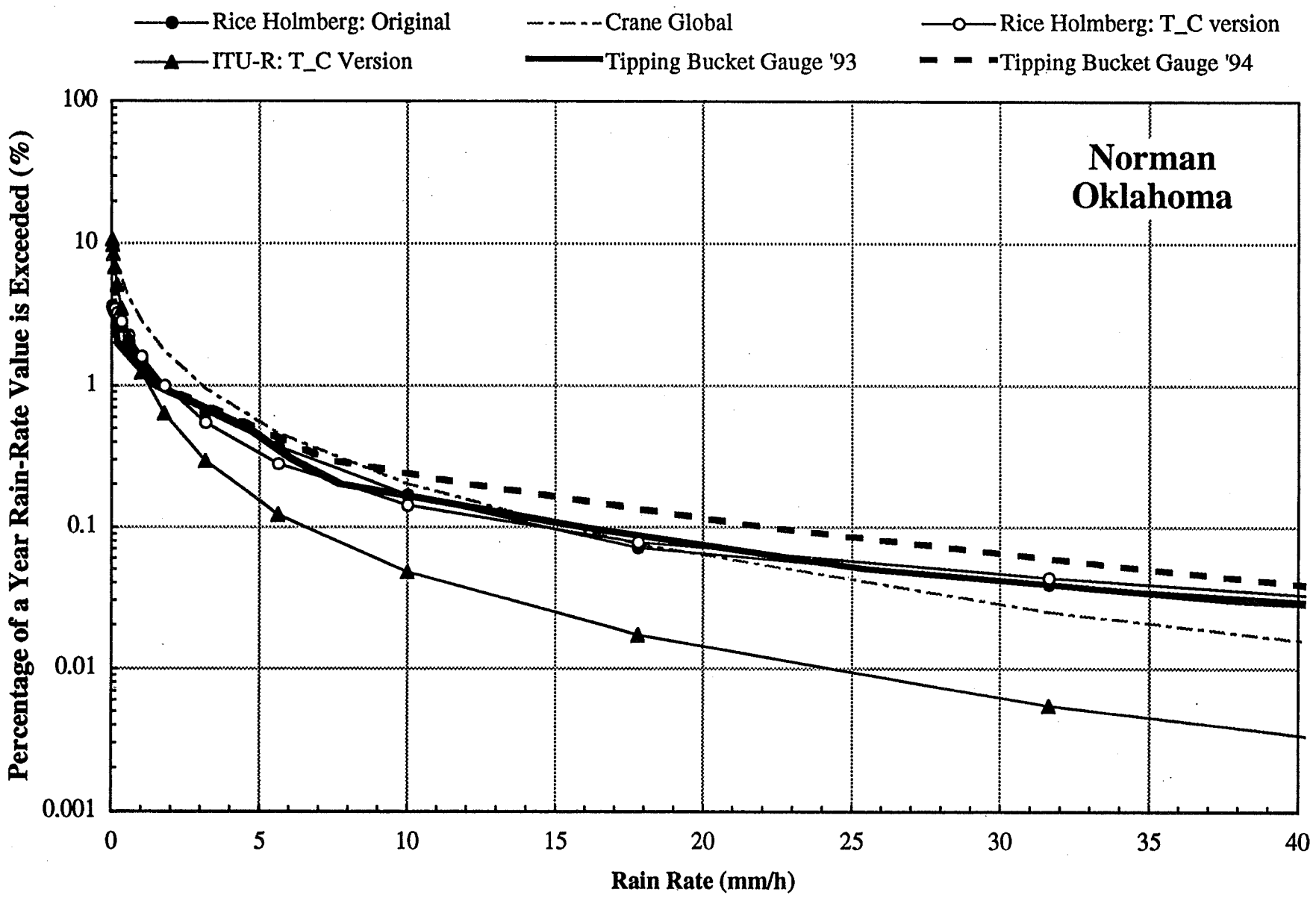

Figure 13 Single year rain-rate edf's, Norman, Oklahoma

Acts Propagation Terminals

Rain Attenuation Models Differences in Rainfall Data Base

R. Manning

NASA Lewis Research Center
Cleveland, Ohio

November 19-20, 1996

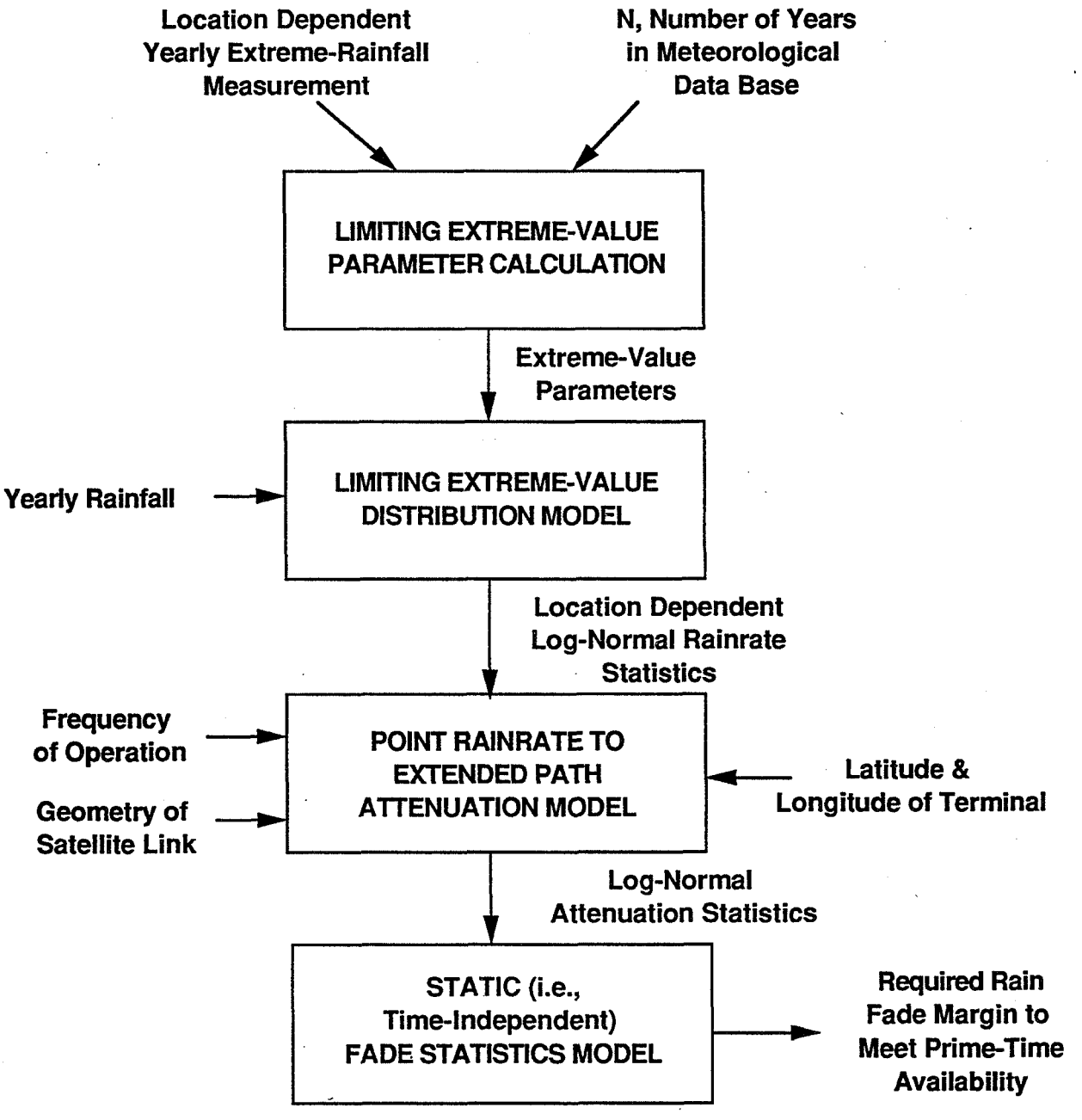

OVERALL STRUCTURE OF THE ACTS RAIN ATTENUATION PREDICTION MODEL

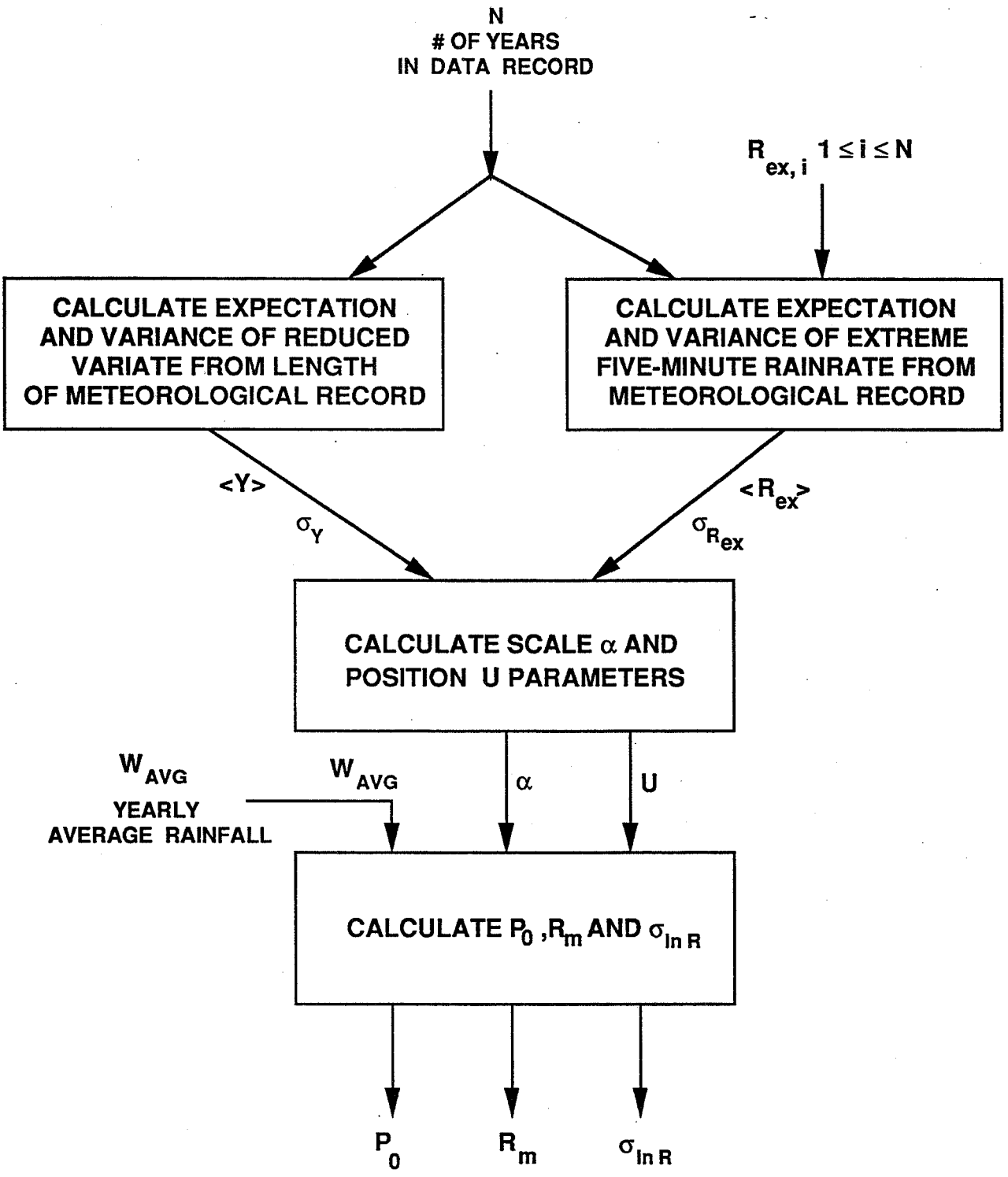

EXTREME VALUE CALCULATIONS OF FIVE-MINUTE RAINFALL LEADING TO LOG-NORMAL RAINRATE STATISTICS PARAMETERS

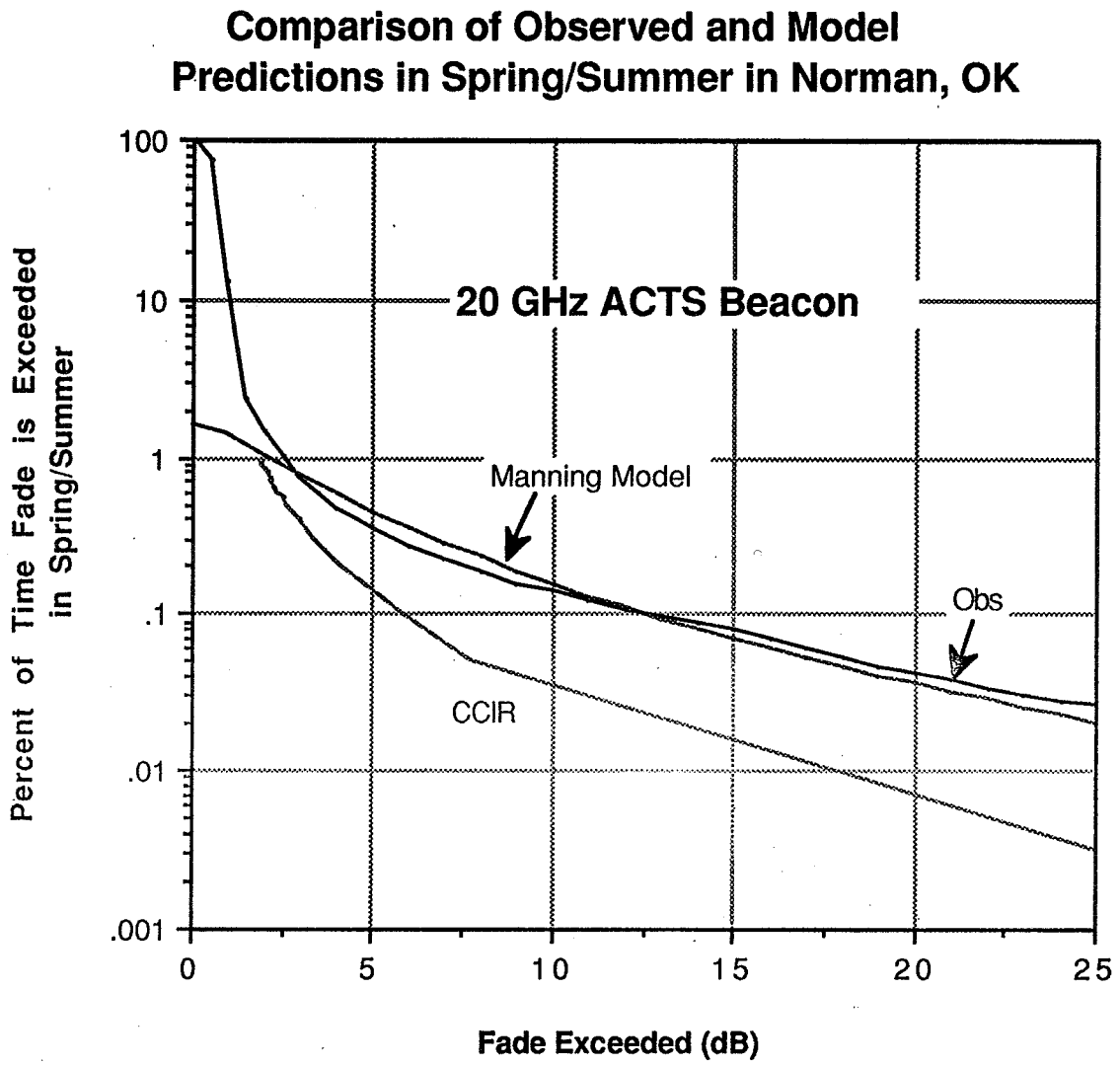
Comparison of Observed and Model Predictions in Spring/Summer in Norman, OK
20 GHz ACTS Beacon
Manning Model
Obs
CCIR
Percent of Time Fade is Exceeded in Spring/Summer
100
10
1
.1
.01
.001
0
5
10
15
20
25
Fade Exceeded (dB)

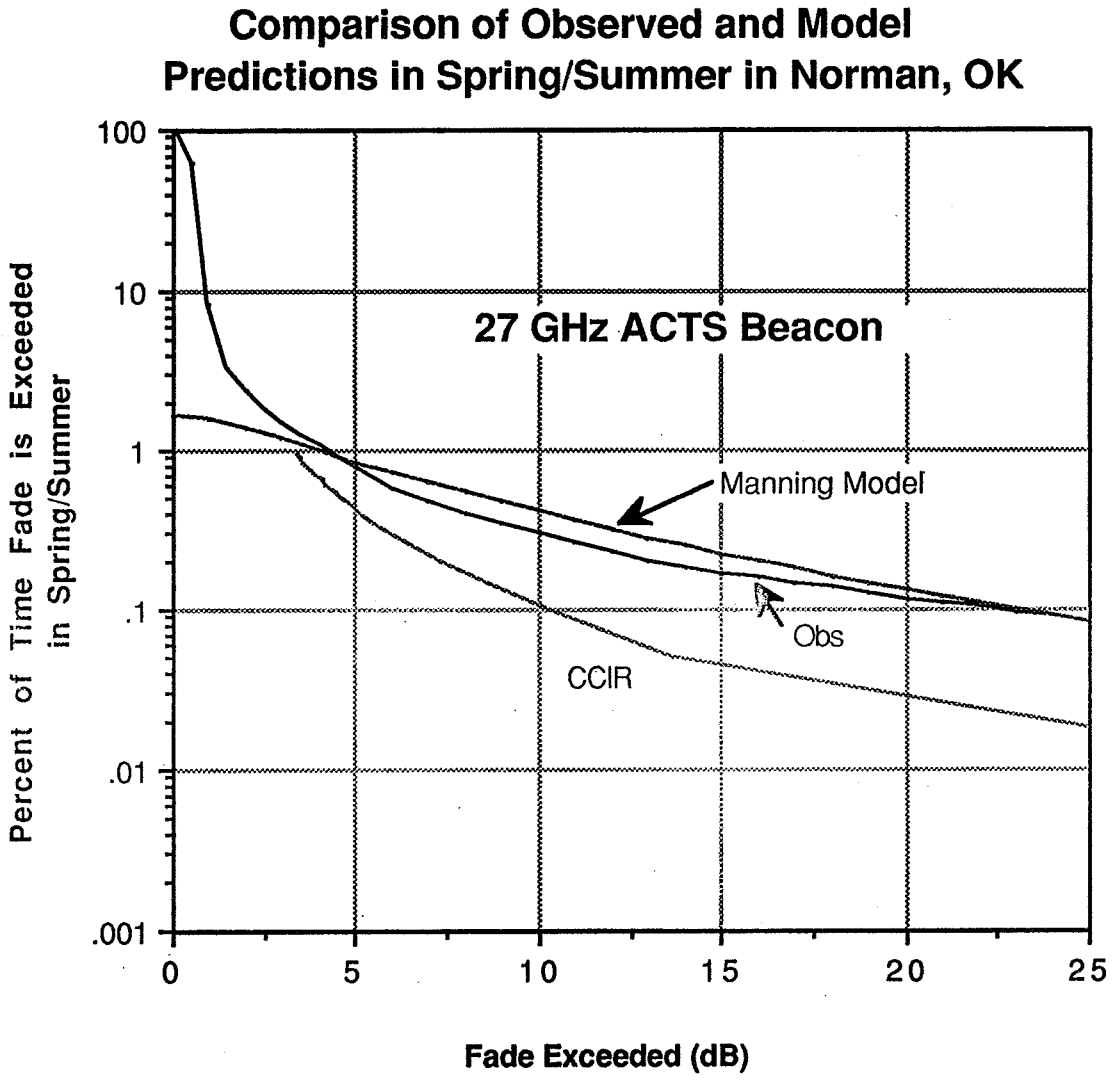
Comparison of Observed and Model Predictions in Spring/Summer in Norman, OK
27 GHz ACTS Beacon
Manning Model
Obs
CCIR
Percent of Time Fade is Exceeded in Spring/Summer
100
10
1
.1
.01
.001
0
5
10
15
20
25
Fade Exceeded (dB)

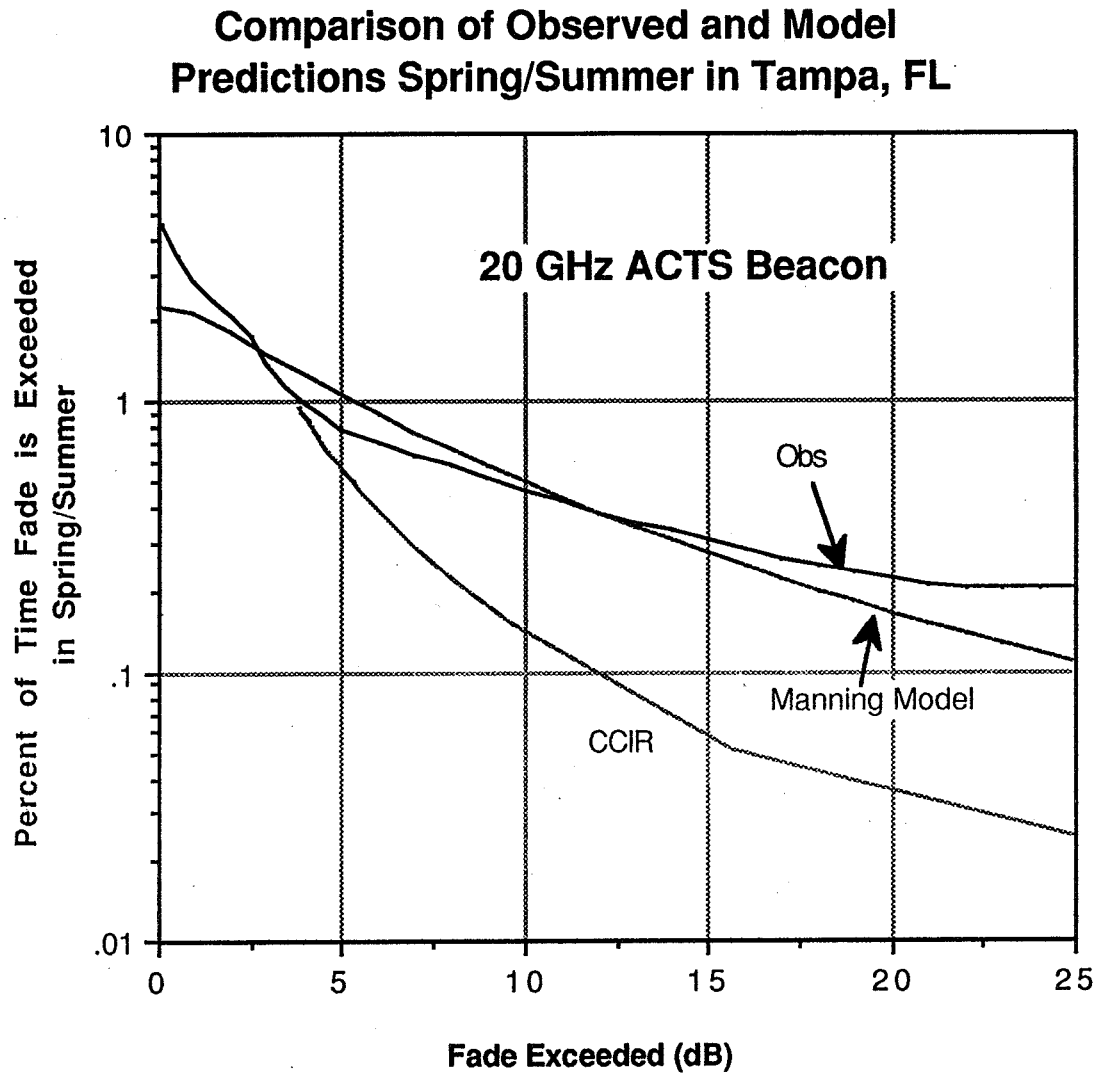
Comparison of Observed and Model Predictions Spring/Summer in Tampa, FL
20 GHz ACTS Beacon
Obs
Manning Model
CCIR
Percent of Time Fade is Exceeded in Spring/Summer
10
1
.1
.01
0
5
10
15
20
25
Fade Exceeded (dB)

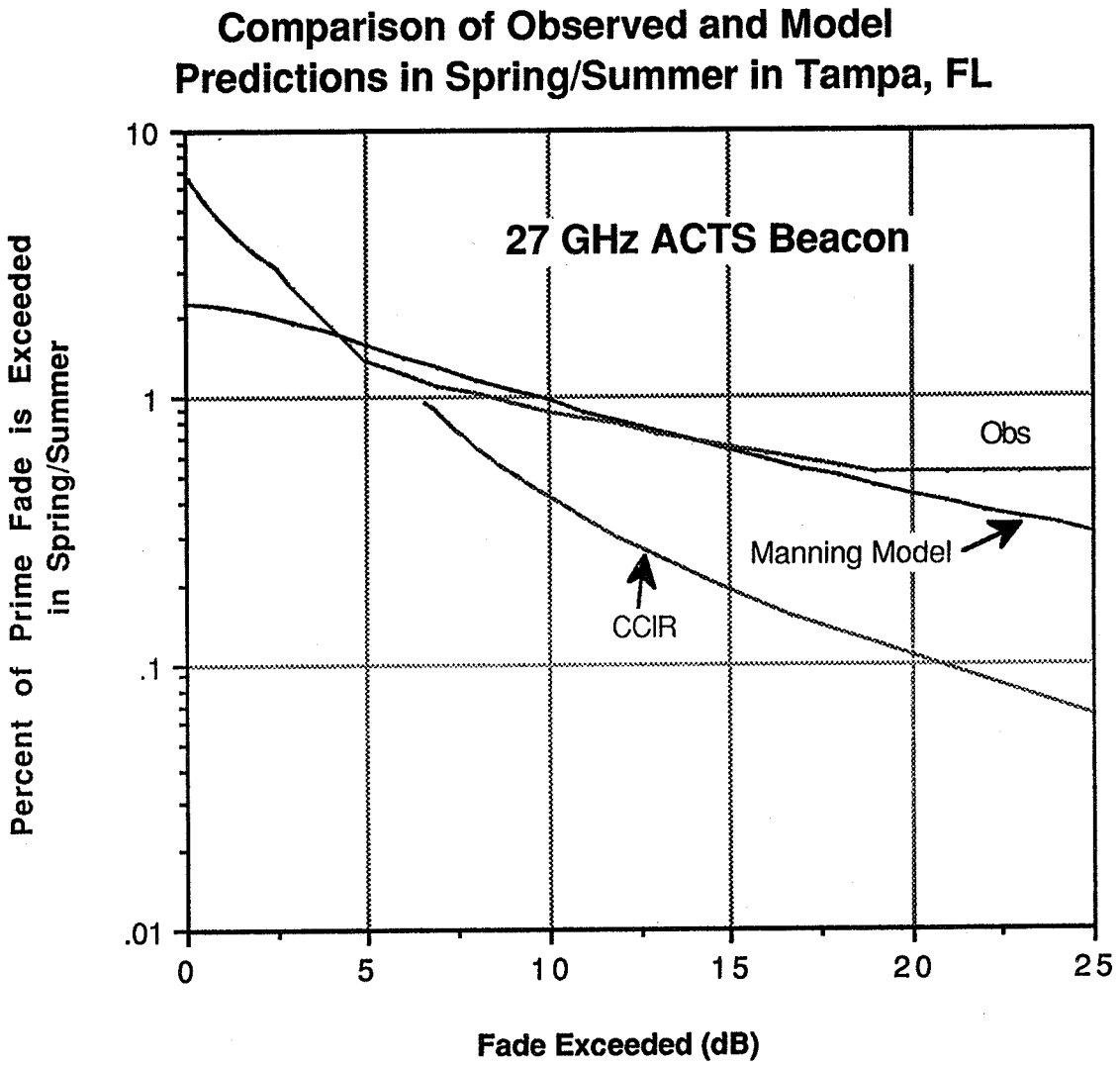
Comparison of Observed and Model Predictions in Spring/Summer in Tampa, FL
27 GHz ACTS Beacon
Obs
Manning Model
CCIR
Percent of Prime Fade is Exceeded in Spring/Summer
10
1
.1
.01
0
5
10
15
20
25
Fade Exceeded (dB)

Page intentionally left blank

A Comparison of 11 Rain Attenuation Models with 2 Years of ACTS Data from Seven Sites

Glenn Feldhake
Stanford Telecom
1761 Business Center Dr - Ste. 300
Reston, VA

News from Oslo!

- **ITU-R Working Party 3J & 3K**
  - June 1996
  - Oslo, Norway
- **Compared 10 Rain Models with ITU-R Propagation Database**
  - 22 Test Performed
    - Frequency
    - Elevation Angle
    - Latitude
    - Rain Rates
  - Error Statistics Generated
    - Mean Error
    - RMS Error
    - Error v. Exceedence

The Models...

CCIR	*1986*	From Rep 564-3
ITU-R	*1991*	Current Rec. P.618-4 - Adjusted Isotherm Height and Horizontal Reduction Factor
USA *(Dissanayake)*	*1992*	Revision to ITU-R; Adjusted Horizontal Reduction, New Vertical Reduction and Probability Extrapolation
Brazil	*1992*	Revision to ITU-R; Focus on Tropics and High Exceedance Probabilities
Japan *(Karasawa)*	*1990*	Revision to ITU-R; Extends Model over Higher Exceedance Probabilities - Uses $R_{0.01}$ & $R_{0.1}$
Two Component *(Crane)*	*1985*	Considers Rain in terms of Cell and Debris. Utilizes its Own Maps of Rain Regions.
Leitão-Watson	*1986*	Use Radar to Extract Rain Only - α/β Hold All Info
ExCell*(Capsoni)*	*1986*	Max R_P at Center of Cell v. Cell Size, Shape, etc.
Spain *(Garcia - Lopez)*	*1988*	Attempts to Reduce Error Bounds on High Attenuations. Don't Use in US when $R_P < 50$ mm/hr
Misme-Waldteufel	*1980*	Extension of Terrestrial Rain Model. Derived From Radar. Attempts to model Rain Cells.

The Results from Oslo

- **BEST PERFORMING MODEL - U.S.A. MODEL**
  - ➢ 33.2% RMS Error
  - ➢ Lowest RMS Error in 14 of 22 Tests
  - ➢ Most Consistent Model Across All Tests
- **The Rest..**

ITU-R	36.6
ExCell	36.6
Japan	37.9
Brazil	37.9
CCIR	38.5
Leitão-Watson	38.9
Misme-Waldteufel	39.1
TC	41.1
Spain	41.4

What About ACTS?

- **11 Models Applied to Seven ACTS Propagation Terminals**
  - Crane Global Model and SAM Also Included
  - Misme - Waldteufel Not Included
- **Statistics Compiled from W. Vogel's Excel Spreadsheet**
- **Error Statistics Generated**
  - RMS and Mean Error
  - First Year, Second Year, and Two Year Cumulative
  - 20.185 GHz and 27.505 GHz

Assumptions of Models

- **Reproduced Assumptions of Oslo Tests**
  - ExCell "debris intensity" was reduced to 2 mm/hr
  - Spain Model uses "world-wide" climatological values
- **% Error = $100*(A_{Predicted}-A_{Measured})/A_{Measured}$**
  - Attenuation is Calculated for E=1%, 0.5%, 0.3%, 0.2%, 0.1%, 0.05%, 0.03%, 0.02%, 0.01%, 0.005%, 0.003%, 0.002%, and 0.001%
  - Only Measured Attenuation Values < 20 dB were Considered
- **Maps of Rain Rate Regions**
  - Two Component and Global Models Used Crane Maps
  - All Other Models Used ITU-R Rec. P.837

RESULTS! - RMS Error
2 Years, All Sites

20 GHZ			27 GHZ	
USA	*39.16*		**USA**	*32.18*
ExCell	*43.11*		**ExCell**	*35.12*
ITU	*48.10*		**TC**	*39.03*
TC	*48.61*		**ITU**	*41.37*
Global	*49.09*		**CCIR**	*43.89*
CCIR	*50.56*		**Global**	*45.88*
Brazil	*50.96*		**Brazil**	*46.47*
Japan	*53.93*		**Japan**	*50.58*
Spain	*59.84*		**Spain**	*55.10*
SAM	*62.17*		**SAM**	*56.63*
Leitao	*66.91*		**Leitao**	*60.20*

% RMS Error

Ranking of Model Performance by Site
20 GHz

20 GHZ	AK	BC	CO	FL	MD	NM	OK
USA	4	**3**	**1**	**1**	4	**1**	**3**
ExCell	**1**	**2**	**2**	10	6	**2**	5
ITU	5	6	**3**	5	**3**	**3**	4
TC	**3**	11	11	6	**2**	11	**1**
Global	9	10	8	**2**	5	6	**2**
CCIR	6	8	4	9	**1**	4	6
Brazil	**2**	**1**	6	7	8	7	8
Japan	8	7	7	**3**	7	5	7
Spain	7	4	9	8	9	9	9
SAM	10	5	10	4	10	10	10
Leitao	11	9	5	11	11	8	11

Ranking of Model Performance by Site 27 GHz

27 GHZ	AK	BC	CO	FL	MD	NM	OK
USA	9	**3**	**1**	**2**	**1**	**1**	**3**
ExCell	**1**	**2**	**2**	10	6	**2**	4
TC	**2**	10	8	7	**2**	7	**1**
ITU	**3**	6	**3**	**3**	4	**3**	5
CCIR	5	8	4	6	**3**	4	6
Global	8	11	10	**1**	5	9	**2**
Brazil	4	**1**	6	8	8	6	8
Japan	7	7	7	5	7	5	7
Spain	6	4	9	9	9	11	9
SAM	10	5	11	4	10	10	10
Leitao	11	9	5	11	11	8	11

RMS Error Distribution - 20 GHz

See full size printout

RMS Error Distribution - 27 GHz

See full size printout

Conclusions...

- **U.S.A. Model is the Overall Best Performing Model in Terms of % RMS Error**
- **ExCell Model also Provides Good Results - Appears Optimal with:**
  - ➢ Low Elevation Angles
  - ➢ Lots of Low "Drizzly" Rain Rates
- **Additional Models with < 50% RMS Error**
  - ➢ 20 GHz - ITU, TC, Global
  - ➢ 27 GHz - TC, ITU, CCIR, Global, Brazil
- **RMS Errors Could Probably Be Reduced by Additional Years of Data**

Potential Future Efforts

- **Apply to Additional Ka Band Locations from Other Propagation Campaigns**
- **Analyze Trends to Determine:**
  - ≫ Where Do Different Models Have Optimal Performance?
  - ≫ What Makes a Model Work?
- **Compare Performance Between Rain Maps and Simultaneous Rain Measurements**
- **MORE DATA!**

ACS Stanford Telecom

RMS Error Distribution - 20 GHz

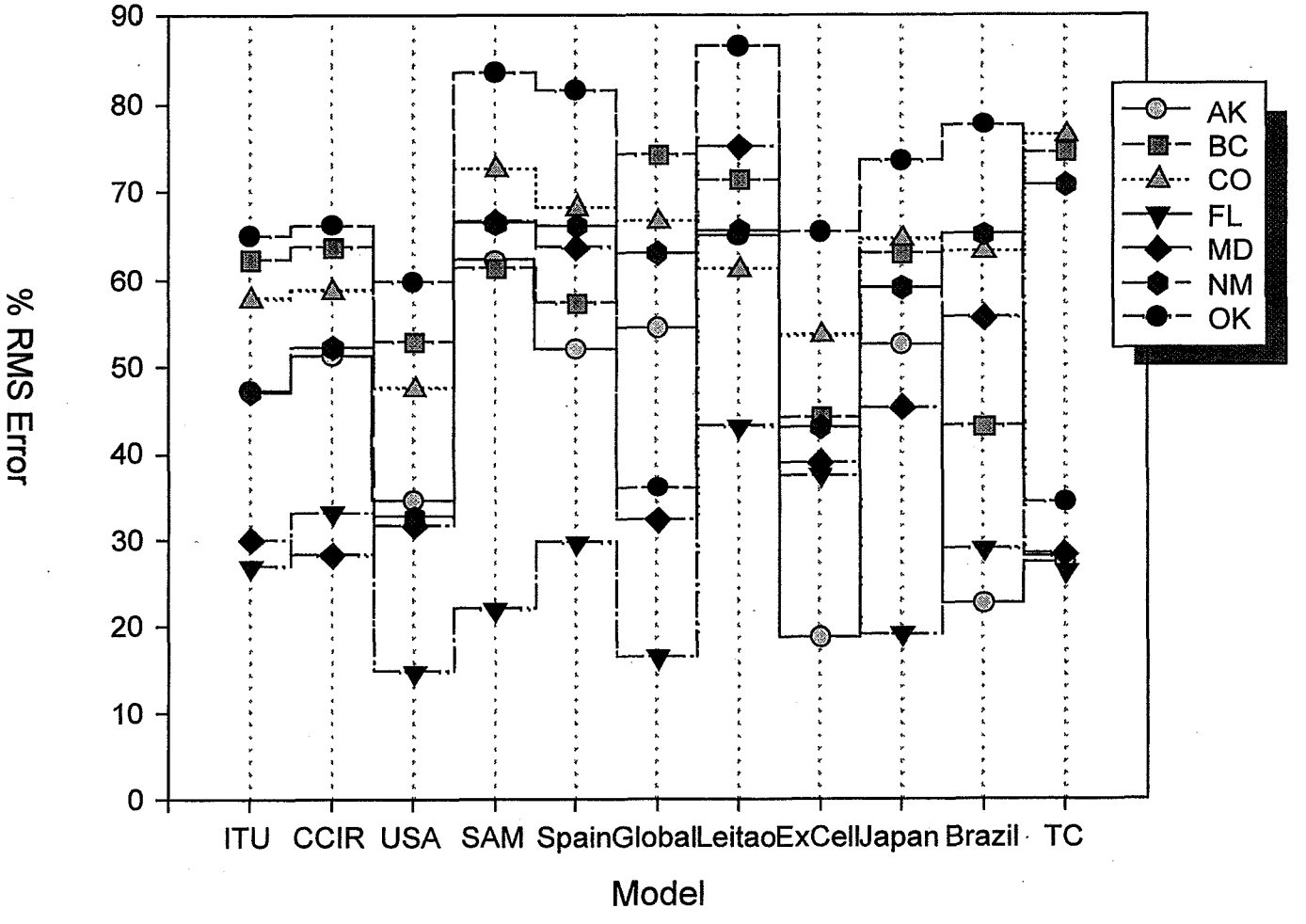

RMS Error Distribution - 27 GHz

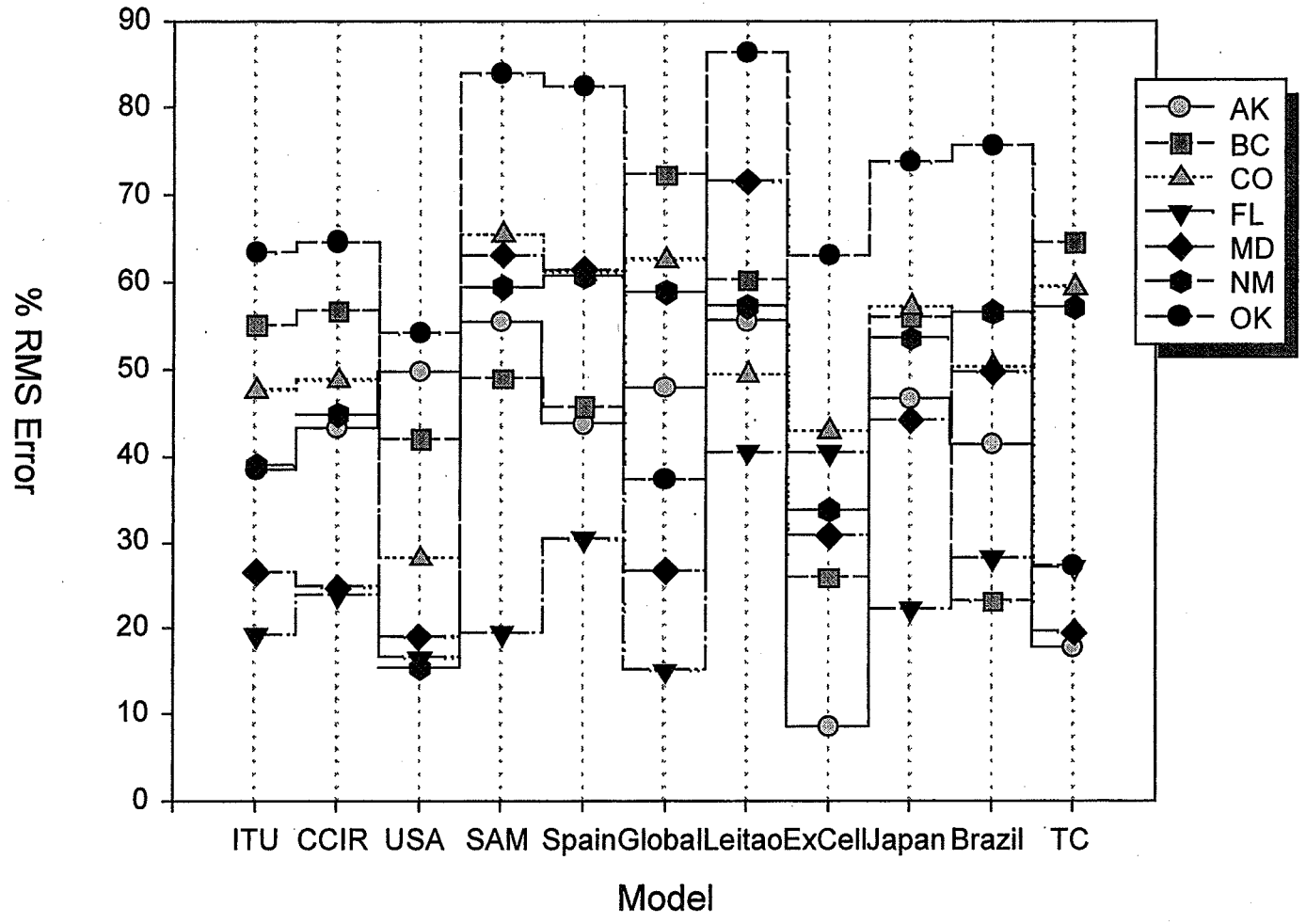

Page intentionally left blank

Propagation Effects Handbook for Satellite Systems Design

Louis J. Ippolito
Stanford Telecom

Ninth ACTS Propagation Studies Workshop
APSW IX

November 20, 1996
Herndon, Virginia

1

General Objectives of Handbook Development Program

- **Combine the Previous Two Handbooks into a Single Propagation Effects Handbook for Satellite Systems Design**
- **Provide a More Cohesive Structure for the Reader**
- **Include Tailored Propagation Analysis Procedures for Specific Types of Systems and Applications**

2

Basic Recommendations for Revised NASA Propagation Handbook

- Combine Scope of the Previous Two Handbooks into a Single Document
- Eliminate Duplication
- Provide a More Cohesive Structure for the Reader
  - Offer Several Levels of "Entrance" into Handbook
- Include Tailored Propagation Analysis Procedures For Specific Types of Satellite Applications -
  - Ka-band Systems, Ku-band Systems
  - Mobile Satellite Systems
  - Low Margin Systems
  - Direct Broadcast Systems
  - ....
- Provide Electronic Version of Handbook

3

Additional Considerations

- Revised Handbook will not duplicate information in current NASA Land Mobile Publication-
  "Propagation Effects for Land Mobile Satellite Systems: Overview of Experimental and Modeling Results," J. Goldhirsh & W. J. Vogel, *NASA Ref. Pub. 1274*, Feb. 1992
- Other Relevant Documents Will be Cross Referenced in Handbook
  - OPEX Reference Books, Five Volumes, WPP-083, November 1994.
  - ITU-R Working Party 3M, "Radiowave Propagation Information For Earth-Space Path Communications," draft April 29, 1996.

4

Handbook Revisions Schedule

Handbook Revision Study	
✓ Begin Handbook Revisions Study	29 Apr 96
✓ Preliminary Outline	20 May 96
✓ Peer Review - NAPEX XX	05 Jun 96
Base Program	
✓ Handbook Rev. Development Plan	15 Jul 96
✓ Detailed Handbook Outline	27 Aug 96
✓ Progress Review APSW IX	20 Nov 96
Section 1 Draft Completed	15 Dec 96

✓ completed

5

Handbook Revisions Schedule (cont'd)

Option Program	
Section 2 Draft Completed	5 Feb 97
Section 3 Draft Completed	26 Mar 97
Handbook Draft Completed	15 Apr 97
Complete Peer Review	15 May 97
Presentation of Peer Review and Recommendations for Final Version - NAPEX XXI	24 May 97
Delivery of Final Handbook	01 Jul 97

6

New Propagation Measurement Campaigns Included in Revised Handbook

- Olympus (ESA) - 1989
  - Propagation Beacons at 12.5, 19.77, 29.65 GHz
  - Measurements in Europe and United States
- Italsat F1 (Italy) - 1990
  - Propagation Beacons at 18.7, 40, 50 GHz
  - Measurements in Europe
- ACTS (NASA) - Launched Sept. 12, 1993
  - Propagation Beacons at 20.185 and 27.5 GHz
  - Measurements in CONUS, Alaska, Canada
- Land Mobile 1.5 GHz Measurements - 1987-88
  - MARECS-B2 , Central Maryland
  - ETS-V and INMARSAT, S.E. Australia

7

New Propagation Models and Prediction Procedures Included in Revised Handbook

- Tropospheric Scintillation (*Karasawa, Yamada, Allnutt)*
  - Based on Monthly Temperature and Humidity
  - Provides Both R.M.S. Amplitude Variance and Monthly Fade Level Statistics
- Extensive New ITU-R Recommendations
  - Rain Attenuation, Site Diversity, Tropospheric Scintillation, Gaseous Attenuation, Frequency Scaling, Worst Month, Ionospheric Effects
- Enhancements to Global Rain Model *(Crane, 1996)*

8

ITU-R Recommendations on Earth-Space Propagation

- "Propagation data and prediction methods required for the design of Earth-space telecommunications systems" *[Recommendation ITU-R P.618-4]*
- "Propagation data required for the design of broadcasting-satellite systems" *[P.679-1]*
- "Propagation data required for the design of Earth-space maritime mobile telecommunications systems" *[P.680-1]*
- "Propagation data required for the design of Earth-space land mobile telecommunications systems" *[P.681-2]*
- "Propagation data required for the design of Earth-space aeronautical mobile telecommunications systems" *[P.682-1]*
- "Ionospheric Effects Influencing Radio Systems Involving Spacecraft" *[P.531-3]*

9

New / Revised ITU-R Models and Prediction Procedures

- Rain Attenuation Modeling Procedure *[P.618-4]*
  - Precipitation Distributions and Global Maps *[P.837-1]*
  - Specific Attenuation Coefficients *[P.838]*
  - Rain Height Model *[P.839]*
- Atmospheric Gaseous Attenuation Model *[P.676.2]*
  - Reference Standard Atmosphere *[P.835-1]*
  - Surface Water Vapor Density *[P.836]*
- Attenuation due to Clouds and Fog *[P.840-1]*
- Site Diversity *[P.618-4]*
- Tropospheric Scintillation *[P.618-4]*
- Worst Month Statistics *[P.581-2]*
  - Conversion of Annual Statistics to Worst Month *[P.841]*
- Probability Distributions for Prop. Modeling *[P.1057]*

10

Basic Structure of Handbook

Three Sections

SECTION 1 BACKGROUND

Provide Overview of Propagation Effects, including Theory and Basic Concepts, Propagation Measurements, Available Data Bases.

SECTION 2 PREDICTION

Provide Descriptions of Prediction Models and Techniques, Organized By Effect. Provide Step-by-Step Procedures For Each, Where Appropriate. Include Sample Calculations.

SECTION 3 APPLICATIONS

Provide "RoadMaps" {i.e. flow charts} of Application of Prediction Models in SECTION II to Specific Satellite Systems and Applications. Include Evaluation and Impact on Systems Design and Performance. Include Sample Calculations.

11

Three Section Approach

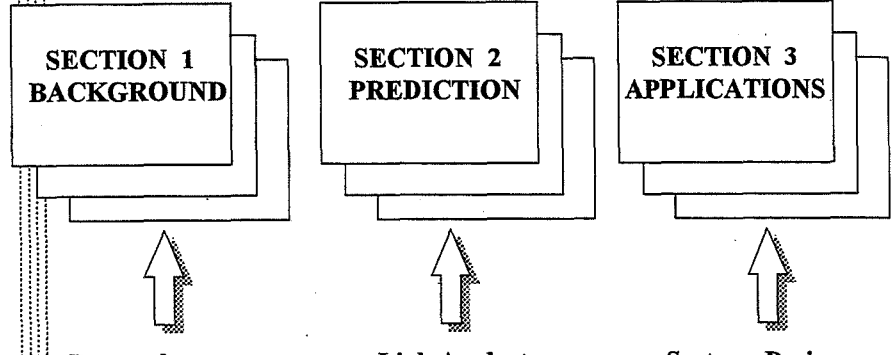

12

General Outline
SECTION 1 BACKGROUND

- ❑ Overview of Propagation Effects on Satellite Communications
- ❑ Ionospheric Effects
- ❑ Tropospheric Effects
- ❑ Radio Noise
- ❑ Propagation Data Bases
  - Meteorological Paameters
  - Slant -Path Measurements
  - ITU-R
  - Electronic Sources

13

General Outline
SECTION 2 PREDICTION

- ❑ Prediction Methods for Satellite Links Operating Below About 3 Ghz
  - Ionospheric Scintillation
  - Multipath Fading
  - Group Delay, Phase Advance, Bandwidth Coherence
  - Polarization, Faraday Rotation
  - Ducting
  - Refraction and Turbulence

  Sample Calculations

14

General Outline
SECTION 2 PREDICTION (cont'd)

- **Prediction Methods for Satellite Links Operating Above About 3 GHz**
  - **Atmospheric Gaseous Attenuation**
  - **Cloud Attenuation**
  - **Fog Attenuation**
  - **Rain Attenuation**
  - **Rain Depolarization**
  - **Ice Depolarization**
  - **Scintillation**
  - **Angle of Arrival**
  - **Fade Rate, Fade Duration**
  - **Dispersive Effects**
  - **Combined Effects Statistics**
  - **ANTENNA WETTING EFFECTS**

    Sample Calculations

15

General Outline
SECTION 2 PREDICTION (cont'd)

- **Link Restoration Models**
  - **Site Diversity**
  - **Orbit Diversity**
  - **Link Power Control**
  - **Adaptive FEC**

    Sample Calculations

16

General Outline
SECTION 3 APPLICATIONS

Flow Charts for Prediction Model Application to Specific Applications

- ❑ **Application of Prediction Models to Systems Design and Performance**
  - **General Links Analysis Procedures**
- ❑ **Mobile Satellite Systems**
  - **Land Mobile**
  - **Maritime**
  - **Aeronautical**
- ❑ **Ka-band Systems**
  - **Low Margin Fixed Service**
  - **Non-GSO Satellite Links**
  - **Mobile**
  - **Wideband Systems**

17

General Outline
SECTION 3 APPLICATIONS (cont'd)

- ❑ **Direct Broadcast Systems**
- ❑ **Low Margin VSAT Systems**
- ❑ **Frequency Reuse Systems**
- ❑ **Inter- and Intra- System Interference**
- ❑ **ITU Regulatory Considerations**
  - **PFD Limits**
  - **ITU Coordination Procedures**

  Sample Calculations

18

Section 1 Development Status

- First Draft Completed for all Chapters
- Updating of Reference Listings
- Addition of Additional References Section
- Extensive Information on Data Base Sources, Including Internet/www Addresses

19

Outline
SECTION 1 BACKGROUND

I INTRODUCTION
1.1 OVERVIEW OF PROPAGATION EFFECTS
1.2 IONOSPHERIC EFFECTS
1.3 TROPOSPHERIC EFFECTS
1.4 RADIO NOISE
1.5 PROPAGATION DATA BASES

20

Outline
INTRODUCTION

I.1 Introduction to the Handbook

I.2 Handbook Structure

I.3 How to Use the Handbook

21

1.1
OVERVIEW OF PROPAGATION EFFECTS

1.1.1 Frequency Dependence

1.1.2 Ionospheric

1.1.3 Tropospheric

22

1.2 IONOSPHERIC EFFECTS

1.2.1 Introduction
1.2.2 Effects Due to Background Ionization
1.2.3 Effects Due to Ionization Irregularities

23

1.3 TROPOSPHERIC EFFECTS

1.3.1 Atmospheric Gases
1.3.2 Clouds, Fog
1.3.3 Rain Attenuation and Depolarization
1.3.4 Ice Depolarization
1.3.5 Scintillation
1.3.6 Angle of Arrival
1.3.7 Dispersion

24

1.4 RADIO NOISE

1.4.1 Uplink Noise Sources

1.4.2 Downlink Noise Sources

25

1.5 PROPAGATION DATA BASES

1.5.1 Meteorological Parameters

1.5.2 Point Data
- 1.5.2.1 NOAA
- 1.5.2.2 ITU-R
- 1.5.2.3 Other

1.5.3 Path Data
- 1.5.3.1 Total Column Data
- 1.5.3.1.1 NASA
- 1.5.3.2 Profile Data

1.5.4 Miscellaneous Sources of Atmospheric Data
- 1.5.4.1 WMO
- 1.5.4.2 CDIAC
- 1.5.4.3 UCAR

26

1.5 PROPAGATION DATA BASES (cont'd)

1.5.5 Estimation of Rain Rate

1.5.5.1 Rain Gauges

1.5.5.2 Estimating Rain Rate From Gauge Records

1.5.6 Slant Path Measurements

1.5.6.1 UHF/VHF Mobile

1.5.6.2 1-3 GHz Mobile

1.5.6.3 C-Band, Ku-Band, Ka-band Fixed

1.5.7 ITU-R

1.5.8 Electronic Sources

27

Plans for Next Reporting Period - Through December 1996

- ❑ Complete final Draft of Section 1
- ❑ Complete Detailed Outline and Structure for Section 2 (Pending Exercise of Option)
- ❑ Initiate Drafting of New Prediction Descriptions and Sample Calculations

28

Summary

- The Process for Revision of the NASA Propagation Handbooks has Begun
- New and Updated Information Relating to Propagation Measurements, Propagation Models, Evolving Satellite Applications, and International Developments Relevant to the Handbook Have Been Identified
- A Three Section Structure, which Allows Reader Entrance At Different Levels, Has Been Devised
- Section 1 Drafting Near Completion
- A Detailed Development Plan is in Place to Provide Final Delivery of the Handbook by July 1997

Page intentionally left blank

ACTS-USAT 20 & 30 GHz
Depolarization Effects Due to Rain & Snow

Dr. Roberto J. Acosta

NASA Lewis Research Center
Cleveland Ohio, 44145

OULINE OF PRESENTATION

- **ACTS/USAT Technology Verification Program**
- **Experiment Concept & Description**
- **Background Data on Depolarization**
- **System Margin Implications - Future Work**

ACTS/USAT -Technolgy Verification Experiments

- ***Depolarization Experiment***
- **Diversity Experiment**
- **Transponder Characterization**
- **Modulation CDMA Performance**
- **SCADA - e.g., Agriculture**

RJA 11/4/96

Depolarization Experiment Concept

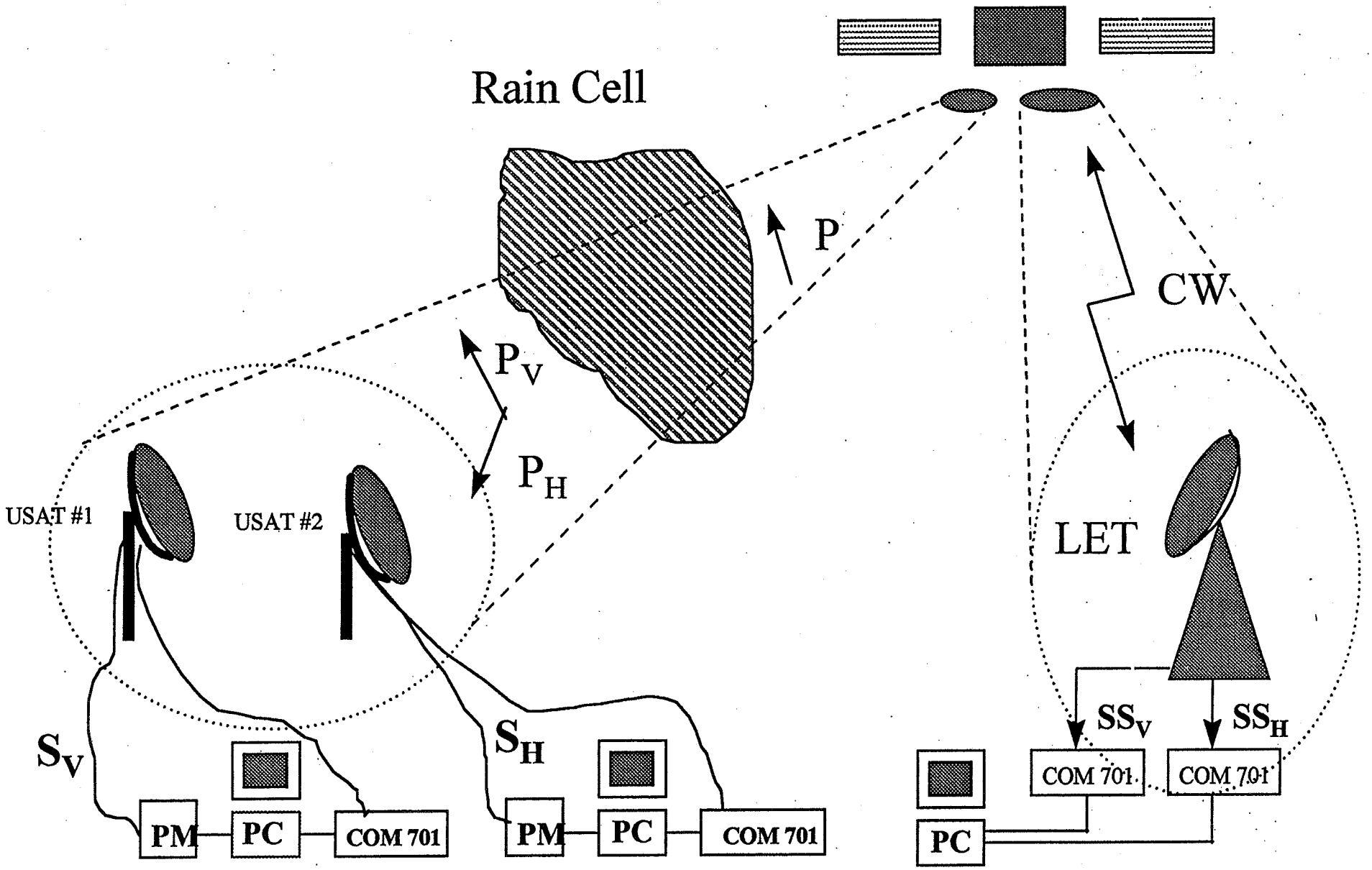

Depolarization Experiment

RJA 11/4/96

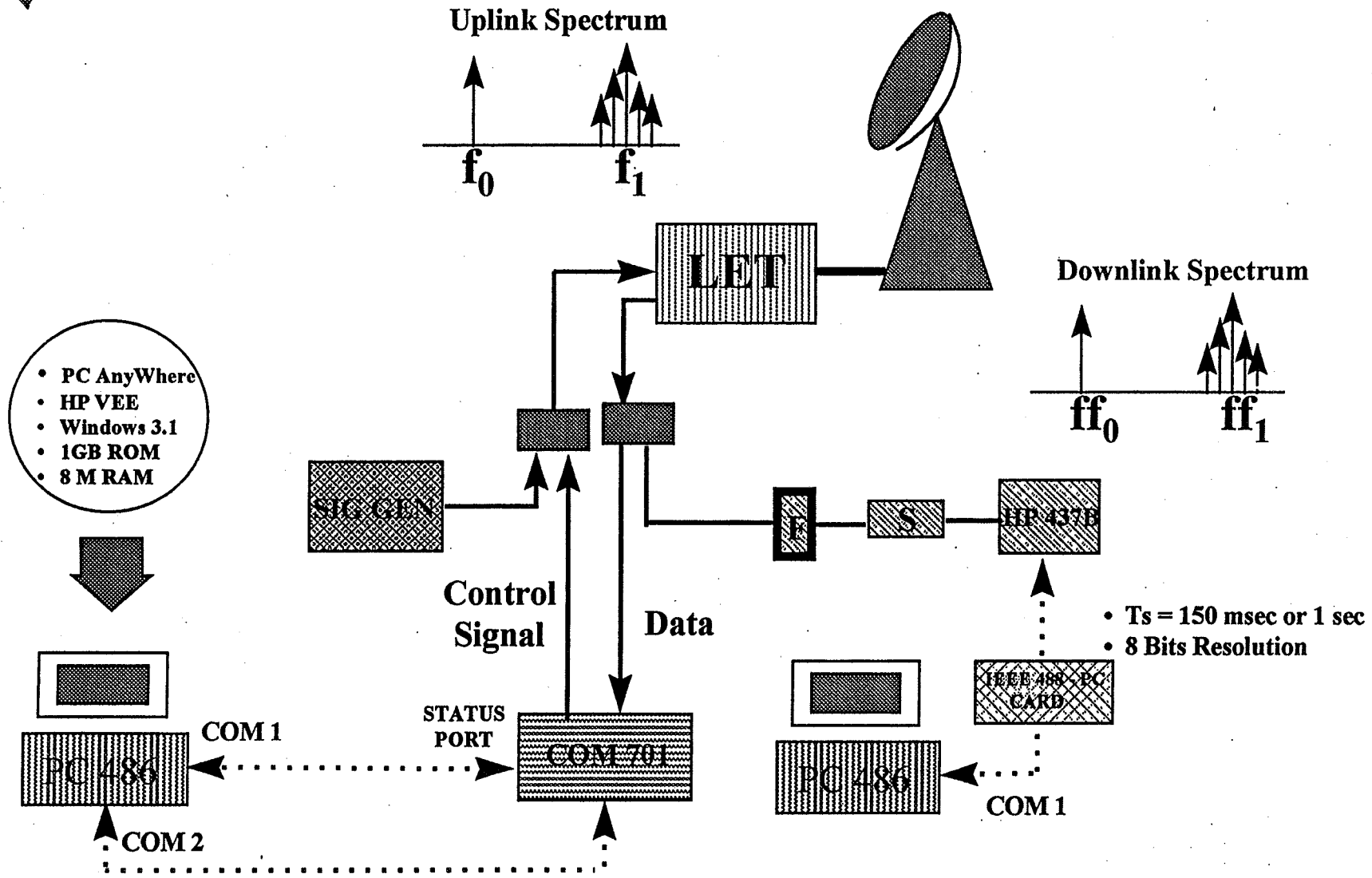

Depolarization Experiment

RJA 11/4/96

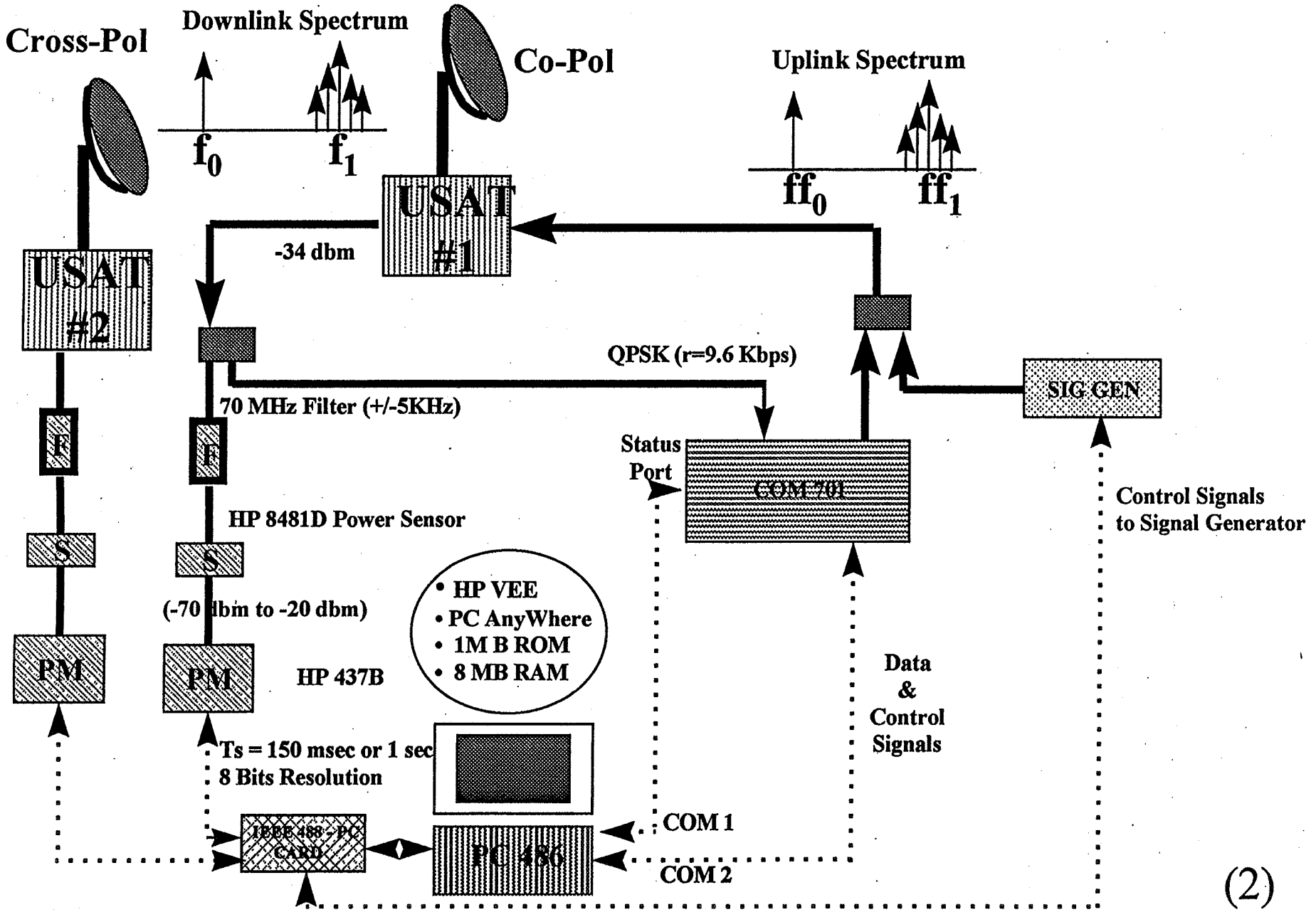

(2)

Background Data

Major Factors in the Communication Link Causing Depolarization Effects:

- ***HYDROMETEORS*** **- (Rain,Ice)**

  Differential attenuation & phase shift between two polarizations caused by non-spherical (oblate) rain drops.

- **FARADAY EFFECT (Rotation)**

- **MULTIPATH**

Background Data

Rain Depolarization @ 20GHz

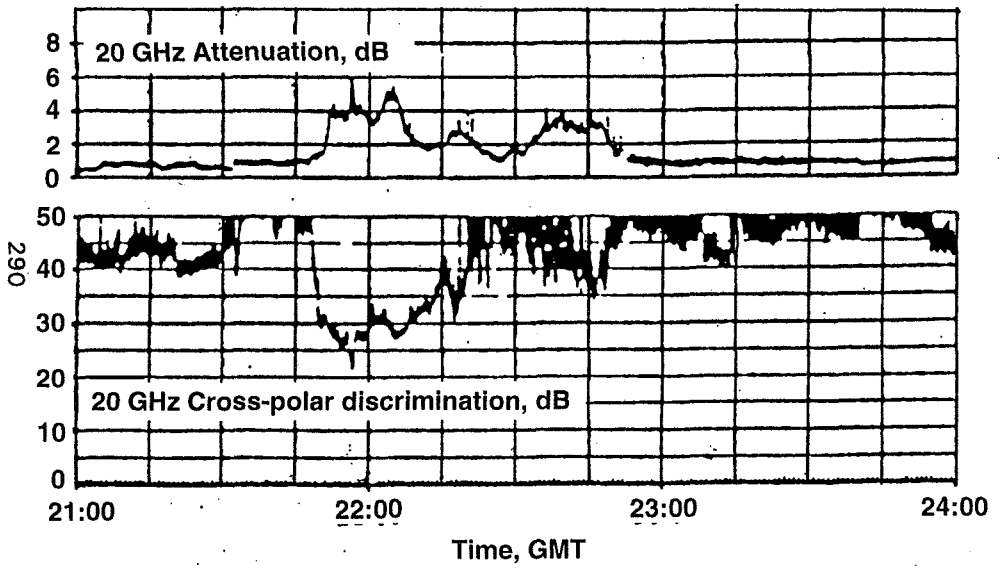

Anomalous Depolarization @ 20GHz

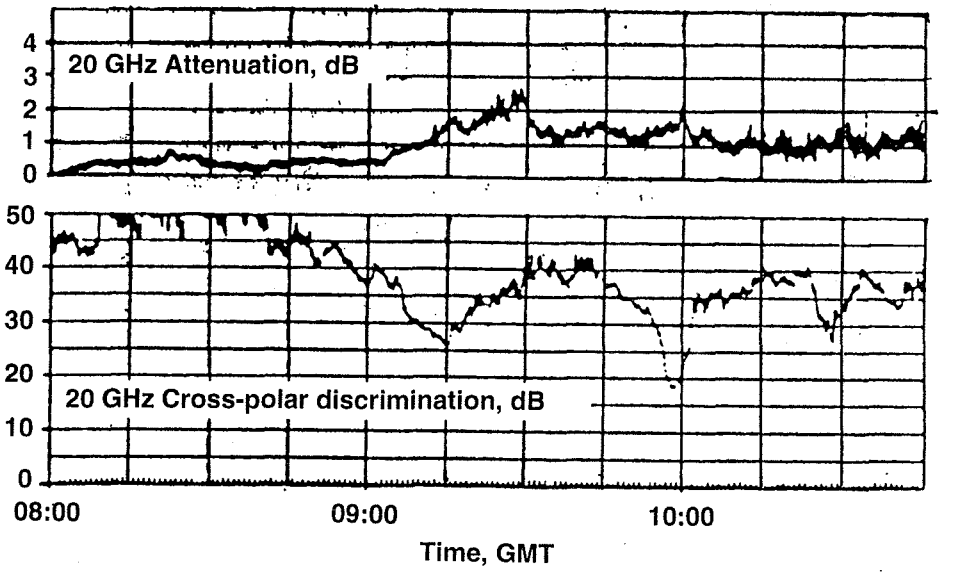

El Angle 22.7 degrees

Martlesham Heath, England (Howell & Thirlwell)

Background Data

30GHz Depolarization Data - July15 & 16, 1976

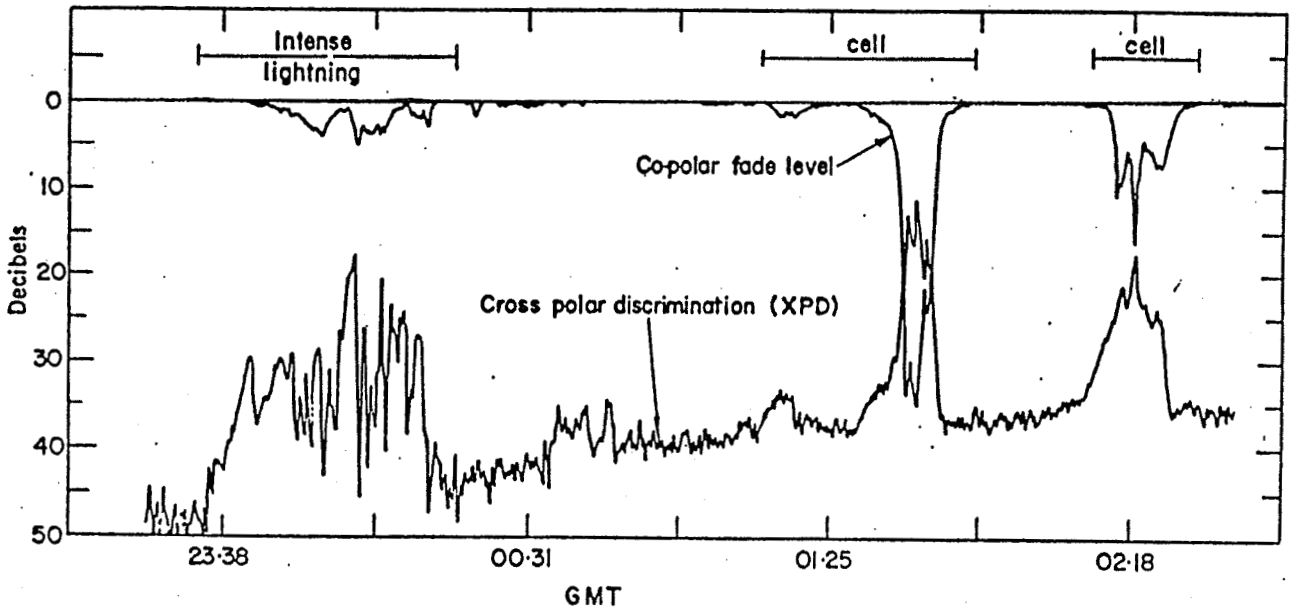

Conditions Intense Lightning
Slough, England (Shutie,Allnut & Mackenzie, 1977)
El. Angle 22.4 degrees (Beacon from ATS 6)

Background Data

***Anomalous Depolarization*:** **An event or series of events characterized by a strong signal depolarization (> 20 dB) accompanied by a very low (< 1dB) copolarized signal attenuation.**

Characteristics:

- **Not predicted by classical theories (Chu,Oguchi,Nowland,Olsen,Shkarossfky, etc.)**
- **First Observed in 1975 on ATS-6 beacons 20 & 30 GHz in England.**
- **Occurs at all frequencies where beacon data have been made.**
- **Most of the time it occurs several minutes before the appearance of a severe rain attenuation event.**
- **Has been observed in the presence of intense lighthing; clouds; clear sky; and light precipitation.**

Background Data

Physics: Differential phase shift produced in the upper atmosphere by ice particles which exhibit a preferred orientation induced by wind or strong electric fields

System Margin Implications:

- Depolarization predictions from attenuation are not 100% reliable at best!!!
- Significance of anomalous (ice) depolarization on total system performance yet to be determined (Need a serious Look !!!!)

Co and Cross Pol Patterns K-Band Antenna

H-Pol @20.195 GHz

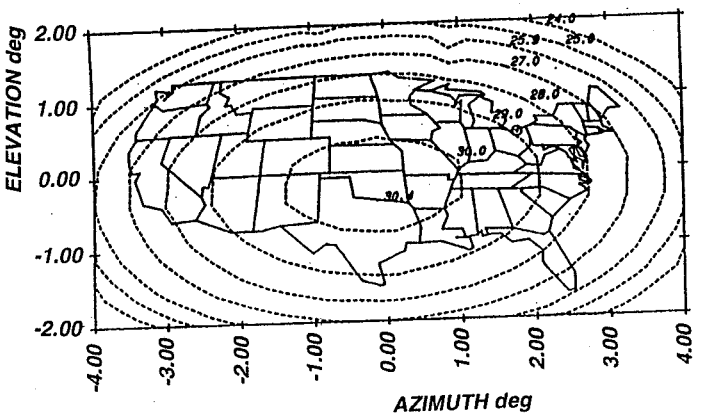

V-Pol @20.185 GHz

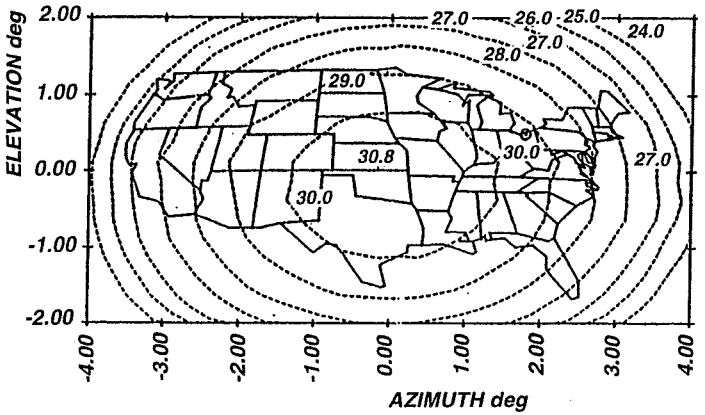

Co-pol

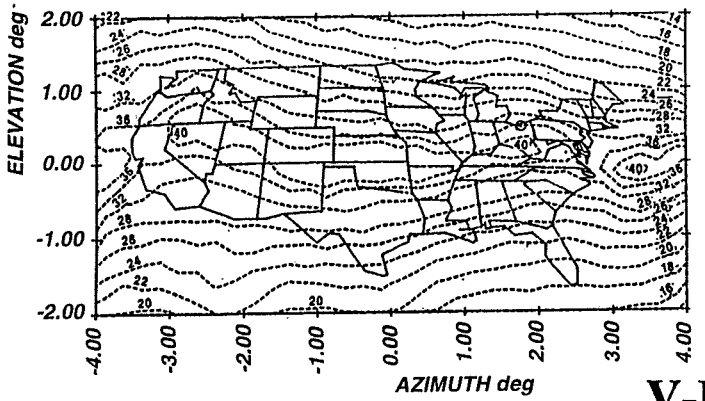

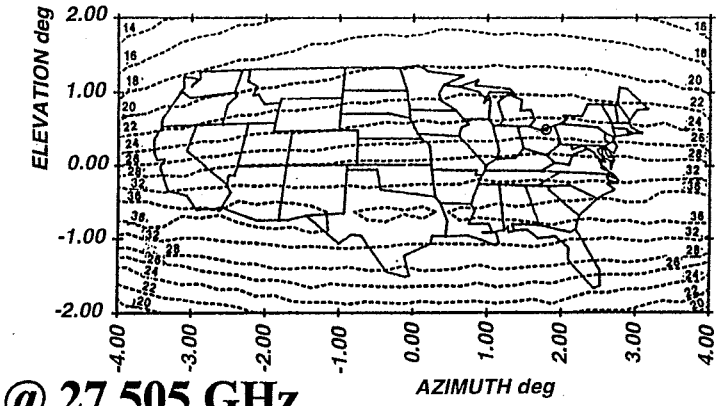

Cross-Pol

V-Pol @ 27.505 GHz

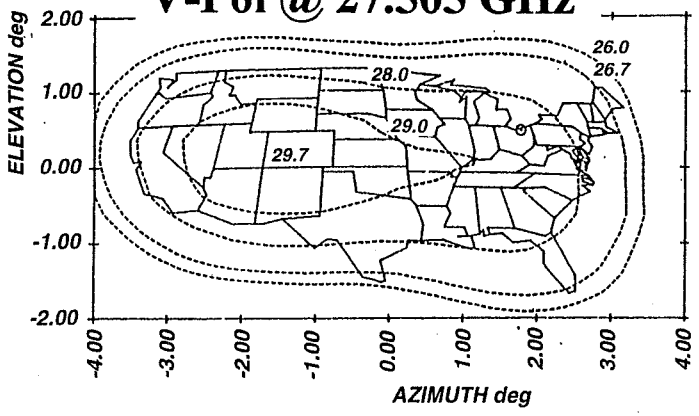

Co-Pol

APSW IX

SESSION 4

PROPAGATION PAPERS FOR IEEE SPECIAL ISSUE

F. Davarian ***(Hughes Space and Communications)***

Page intentionally left blank

Special Issue, Proceedings of the IEEE: List of Proposed Papers

No	TITLE	AUTHORS
1	System application of Ka-band earth-satellite propagation data	Rogers, Ippolito, Davarian
2	Ka-band earth-space propagation research in Japan	Y. Karasawa
3	Application of open loop uplink power control in Ka-band satellite links	A. Dissanayake
4	Analysis of the effect of wetting antenna surfaces during rain events on propagation data statistics	M. Kharadly, R. Ross, D. Rogers
5	Three-site space diversity results from ACTS 20 GHz measurements in east coast of the U.S.	J. Goldhirsh, B. Musiani, and A. Dissanayake
6	Three-frequency Ku-band and Ka-band attenuation measurements in New Mexico utilizing ACTS and TDRS	L. Ippolito, J. Feil, S. Horan
7	Channel characterization and modeling for Ka-band Very Small Aperture Terminals	M. Alouini and P. Steffes
8	The application of S-band polarimetric radar measurements to Ka-band attenuation prediction	J. Beaver and V. Bringi
9	Comparison of fade duration observations with model predictions	Helmken, Henning, Feil, Ippolito, Mayer
10	Comparison of the two processing techniques of the New Mexico ACTS propagation data	J. Feil, L. Ippolito, Horan
11	Experiment design, calibration, data preparation and archival	Crane, Westenhaver
12	Attenuation Modeling	Crane and A. Dissanayake
13	Scintillation observations and model predictions	C. Mayer, R. Crane, Jaeger
14	Rain rate modeling	R. Crane and P. Robinson
15	European research on Ka-band slant path propagation	Arbesser-Rast., Paraboni
16	Ka-band propagation measurements: An Opportunity with the Advanced Communications Technology Satellite (ACTS)	R. Bauer
17	Fade Slop Analysis	Feil et al.
18	Cumulative Fade Distribution and Frequency Scaling	Goldhirsh, Musiani, Vogel

Page intentionally left blank

SESSION 5

PLENARY

R. Crane ***(U. OK)***
D. Rogers ***(Communications Research Centre, Ottawa)***

Page intentionally left blank

REPORT OF APSW IX PLENARY MEETING

R.K. Crane and D.V. Rogers

On 20 November 1996, the ACTS Working Groups held their customary joint Plenary meeting in Herndon, Virginia, to address project issues related to experiments now being conducted with the NASA ACTS Propagation Terminals (APTs). Results of that meeting are reported here.

I. *Issues Related to Interaction with Industry*

Subsequent to the ACTS Miniworkshop Meeting in Fairbanks, Alaska, the Satellite Industry Task Force (SITF) ACTS Task Team convened in Fairbanks to develop recommendations regarding conduct of the ACTS propagation measurements. R. Bauer kindly prepared a summary sheet of the recommendations for discussion by the ACTS experimenters, as reproduced here for reference:

Item 1: ACTS propagation experiments should continue until 5 years of data have been collected.

Item 2: Increase the emphasis on data analysis and development of propagation-effect tools for Ka-band development.

a - Greater accuracy needed; resolve inconsistencies (up to 10 dB reported at NAPEX XX)

b - Must have international acceptance and be part of the ITU-R recommendations

c - Must be user-friendly

d - Must be reliable with uncertainty quantified and validated

e - Should provide total attenuation with ability to separate components of the total

f - Minimum ranges for the following:

Attenuations from 0 to 25 dB; link availability from 98.0% to 99.9%; elevation angles from 5 to 90 degrees; uncertainty less than 30% (ΔdB/dB).

g - Should be designed as add-in modules to commonly used spreadsheets.

Item 3: NASA should be custodian of the internationally accepted model(s) and perform liaison duties among other institutions and agencies.

Item 4: Expeditiously update the NASA Propagation Handbooks as suggested by NAPEX.

Item 5: NASA Propagation Studies should expand to include all climate zones and solicit international cooperation.

Item 6: A long-term plan and statement of deliverables should be developed.

Item 7: A long-term commitment should be made to the program to maintain the group of propagation experts.

Item 8: All materials should be published on electronic media such as the World Wide Web (include data, models, results, tools, handbooks).

Item 1, which recommends that the ACTS Ka-band experiments be continued for 5 years, is consistent with views expressed by the experimenters themselves in Fairbanks.

N. Golshan stated that issues related to Item 2 (increased emphasis on data analysis and development of propagation-impairments tools) will be addressed by NASA, although firm commitments have not yet been decided by NASA regarding level of effort, which necessarily also affects the schedule. He also noted that user advocacy will play a role in determining NASA's assessment of the importance of this activity.

Dr. Golshan further announced NASA's commitment to address Item 5 by expanding the studies to include all climate zones and to solicit international cooperation. He stated that he would represent NASA at the upcoming European COST-255 meeting to promote Items 3 and 5. H. Berger asked if NASA intended to report on the results of this meeting, and Dr. Golshan indicated that the group would be informed of the outcome by email.

H. Berger recognized the commitment to address longer-term issues, but asked how shorter-term issues would be handled. Dr. Golshan responded that a contract was now in place to revise the NASA Handbook on general propagation effects by July 1997 (with interim means to promote and accommodate user feedback); that improved rain impairment models (accounting for related effects such as antenna wetting, and possibly incorporating elements of the lognormal prediction model presented at the meeting by R. Manning) were planned by September 1997; and that progression to a model to be proposed for international applications was planned by December 1997. By the time of the next NAPEX meeting (mid-June 1997), it is hoped to complete the editing of the first three years of data, perform comparisons with existing rain attenuation models, and develop an interim model for rain attenuation prediction.

A. Abdelgany emphasized the importance of a unified rain-impairments prediction model for N. America, and asked how Canadian results and inputs were to be accommodated. D. Rogers responded that Canadian results would be made available and that Canada would collaborate in model development and assist in model evaluation.

II. *ACTS Experimenter Issues and Concerns*

A. *Data Collection/Quality*

R. Crane noted that several difficulties had arisen while trying to prepare consistent data sets for all the experimental sites as part of the effort related to attenuation modeling. Examples included apparent failures to identify snow events (snow accumulations on the antenna surfaces can cause large signal decreases for long time periods), potential errors caused by moisture within antenna feeds, and recently discovered problems with rain rate data. The data are being manually edited to "filter" the time series. H. Helmken urged that problems discovered during this process should be brought to the attention of the cognizant experimenters.

W. Vogel asked where the filtered data would reside and how they were to be accessed by the users. J. Feil expressed concern about filtering being subsequently applied to data sets submitted by experimenters. D. Rogers recommended that there be a single official data set for each site, fully approved by the responsible site experimenters. It was agreed that there should only be one reference data set for each site, although it is quite acceptable for the purposes of detailed analyses for specific categories of events to be removed from the data by simple descriptive procedures.

G. Torrence asked were schedule goals in jeopardy if so much work appeared necessary to rationalize the first two years of ACTS date. R. Crane responded that only one site seemed a special case (due to apparent snow events and errors seemingly related to moisture in the feed assembly), and that most of the ACTS data appear amenable for use in the present study.

D. Westenhaver reported that he is often asked by experimenters to assist in repairing raw data files. He stated that he is willing to do so, but that it is still the responsibility of individual experimenters to ensure that the revised data files are properly transmitted to the ACTS Data Center for inclusion in the archives.

ACTIONS:

R. Crane and D. Westenhaver will prepare a message concerning data filtering and integrity and send it to the ACTS doers. Dr. Crane also agreed to communicate his specific concern regarding the UBC data to the Principal Investigator for that site (who was unable to attend this meeting).

B. ***Data Reporting/Archiving***

The aforementioned discussions regarding data filtering, coupled with reported difficulties in easily using the previously archived ACTS data sets, prompted a discussion as to the proper format for data archiving. In particular, several participants expressed a preference for archival in a form that might be isolated from possible future modifications to the preprocessing software. W. Vogel observed that with the raw data and the log files, a user can proceed to generate the preprocessed files with supplied software. He suggested that raw data could be supplied on CDs such that these data would be independent of any subsequent changes to the preprocessing routines.

N. Golshan stated that there is a program commitment to supply a clean reference data set available on CDs for application by users, and he recommended that Dr. Vogel propose a practical solution to the problem of data archival on CDs. A. Abdelgany stated that he would be satisfied with only the statistical results derived from the data sets. Conversely, R. Crane noted that time series are also quite useful for application in simulations of system effects (adaptive impairment mitigation, etc.)

W. Vogel recognized a fundamental problem in accommodating revisions to the data sets based on updates, modified preprocessing procedures, etc. Dr. Golshan recommended that updates be prepared once a year, at that time accommodating any revisions to the data or processing methods.

C. Mayer pointed out that there are additional delays in data delivery imposed on sites (as Alaska) that use National Weather Service data in the calibration sequence because there is typically about a two-month delay in receipt of these data. As the Data Center must receive preprocessed data in a timely way to permit transfer to CDs within schedule constraints, it was agreed that data for the third year of operation should be received at the Data Center by 1 March 1997 for all sites except Alaska, which should observe a deadline of 30 March 1997.

ACTION:

W. Vogel is requested to propose a practical solution to the issue of archival of the ACTS propagation data in CD format.

C. *Site Support/Maintenance*

D. Westenhaver observed that of the seven ACTS sites, four have had Uninterruptible Power Supply (UPS) failures (two battery failures and two electronic failures), and cautioned experimenters to be alert for such problems. He also stated that there had been a recent PC failure.

J. Feil reported that the New Mexico site has an LNA glitch problem (previously observed at some other sites as well). Several experimenters have had problems with feed windows. R. Manning stated that UV radiation may be responsible for the damage to such windows (originally the cause was thought to be thermal shock accompanying cold-load calibrations with liquid nitrogen, but problems have continued even at sites that no longer perform such calibrations). Experimenters cannot replace the windows themselves, so the entire feed must be returned to D. Westenhaver, who arranges for the manufacturer to replace defective windows. Spare feeds are thus required to avoid downtime.

D. *General Operations*

As has been the case almost since the inception of the ACTS propagation measurements, the effects of moisture on antenna surfaces was a topic of prime concern among experimenters. R. Crane observed that the ACTS reflector surface is embedded in a dielectric coating, a design that is not conducive to minimizing the deleterious effects of precipitation on the surface. He wondered about the previous practice in similar measurement programs (OPEX, COMSTAR, etc.)

A. Dissanayake stated that in the OPEX program, most sites performed antenna-wetting tests prior to initiation of the measurements campaign, but that the effects had been observed to be small. J. Allnutt reported that in previous work, he had observed losses related to condensation on antenna feed surfaces at Ku-band, and similar effects at Ka-band, but that the effects had generally been small.

F. Davarian indicated that it will be a good idea to note the antenna-wetting problem in the Special Issue of the Proceedings of the IEEE, now in preparation, devoted to Ka-band propagation effects on slant paths.

R. Crane stressed that individual site experimenters must studiously keep abreast of the daily plots for their site in order to monitor APT performance and quickly identify operational problems as they develop (as might be caused by moisture in the antenna feed, for example).

E. *Next Meeting*

The group supported a proposal to hold the next APEX meeting near the time of the International Mobile Satellite Conference (planned for Pasadena, CA, during 16-18 June 1997). It was decided to hold the NAPEX XXI meeting in the Los Angeles area prior to IMSC'97, on the dates 11-13 June 1997.

APSW IX

REFERENCE

Page intentionally left blank

ACTS IX WORKSHOP ATTENDEES

Ahmed Abdelgany
AT&T Bell Labs, Dept. 7C-152
67 Whippany Rd.
Whippany, NJ 07981
201-386-7505
201-386-6081 (FAX)
E-mail: ahmeda@attmail.com

Roberto Acosta
NASA Lewis Research Center
21000 Brookpark Rd., MS 54-6
Cleveland, OH 44135
216-433-4460
216-433-6371 (FAX)
E-mail: R.Acosta@lerc.nasa.gov

Lynn Ailes Sengers
Stanford Telecom
1761 Business Center Drive, Suite 200
Reston, VA 20190
703-438-3195
E-mail: lailes@sed.stel.com

Jeremy Allnut
Virginia Tech
Dept. of EE/No. VA Campus
2990 Telestar CT.
Falls Church, VA 22042
703-698-6023
703-698-4718 (FAX)
E-mail: allnut@vt.edu

Dick Astrom
Motorola
Satellite Communications Group
2501 S. Price Road MD/OSC-N
Chandler, AZ 85248
602-732-3178
602-732-3171 (FAX)
E-mail: Dick_Astrom@sat.mot.com

Jack Bauer
Hughes Space and Comm.
SC/541/MS A372
P.O. Box 92919
Los Angeles, CA 90009
310-416-5267
310-662-6321 (FAX)
E-mail: jmbauer@ccgate.hac.com

Robert Bauer
NASA Lewis Research Center
21000 Brookpark Rd., MS 54-6
Cleveland, OH 44135
216-433-3431
216-433-6371
E-mail: acbauer@lerc.nasa.gov

John Beaver
Colorado State University
Dept. of EE
Ft. Collins, CO 80521
970-491-6758
970-491-2249 (FAX)
E-mail: jb686028@engr.colostate.edu

Harvey Berger
TRW Space and Electronics Group
One Space Park
Redondo Beach, CA 90278
310-813-7692
E-mail: berger@gandalf.sp.trw.com

Scott Borgsmiller
Georgia Technology
5023 Ceylor Drive
Austell, GA 30001
770-739-9563
E-Mail: gt3681c@prism.gatech.edu

Robert K. Crane
University of Oklahoma
100 East Boyd St., Room 1248
Norman, OK 73019-0628
405-325-4419
405-325-7689 (FAX)
E-mail: bcrane@uo.edu

Faramaz Davarian
Hughes Space & Communications
Bldg. S10, MS S352
2260 Imperial Highway
El Segundo, CA 90245
310-662-5375
310-662-7060 (FAX)
E-mail: fdavarian@ccgate.hac.com

Asoka Dissanayake
COMSAT Labs
22300 Comsat Drive
Clarksburg, MD 20871
301-428-4411
301-428-3638 (FAX)
E-mail: asoka.dissanayake@comsat.com

Barry Fairbanks
NASA Lewis Research Center
21000 Brookpark Rd., MS 54-6
Cleveland, OH 44135
216-433-3541
216-433-6371 (FAX)
E-mail: bfairbanks@lerc.nasa.gov

Julie Feil
Stanford Telecom
1761 Business Center Dr., Suite 300
Reston, VA 22040
703-438-7846
703-438-7921
E-mail: Jfeil@sed.stel.com

Glenn Feldhake
Stanford Telecom
1761 Business Circle, Suite 300
Reston, VA 22090
703-438-7924
E-mail: Jfeldhake@sed.stel.com

Diane Flynn
Stanford Telecom
1761 Business Circle, Suite 300
Reston, VA 22090
703-438-8141

Richard Gibbons
Mitre Corporation
1820 Dolly Madison Blvd.
McLean, VA 22102-3482
703-883-7680
E-mail: rgibbons@mitre.org

Julius Goldhirsh
Applied Physics Lab/JHU
Johns Hopkins Road
Laurel, MD 20723-6099
301-953-5042
301-953-5548 (FAX)
E-mail: julius_goldhirsh@aplmail.
jhu.edu

Nasser Goldshan
Jet Propulsion Laboratory
4800 Oak Grove Drive, MS 161-260
Pasadena, CA 91109
818-354-0459
818-393-4643 (FAX)
Nasser.Golshan@jpl.nasa.gov

Henry F. Helmken
Florida Atlantic University
777 W. Glades Road, MS SE-456
Boca Raton, FL 33445
407-367-3452
407-367-2336 (FAX)
helmkenh@acc.fau.edu

Rudolph Henning
University of So. Florida, ENB 118
4202 E. Fowler Ave.
Tampa, FL 33620
813-974-4782
813-974-5250 (FAX)
E-mail: henning@eng.usf.edu

Louis J. Ippolito
Stanford Telecom.
1761 Business Center Drive
Reston, VA 22090
703-438-8061
703-438-8112 (FAX)
E-mail: LIppolito@sed.stel.com

Anil Kantak
Jet Propulsion Laboratory, MS 161-260
4800 Oak Grove Drive
Pasadena, CA 91109
818-354-3836
818-393-4643 (FAX)
E-mail: anil_v_kantak@jpl.nasa.gov

Kuan-Ting Lin
Comsat Labs
22300 Comsat Drive
Clarksburg, MS 20871
E-mail: Kuan-Ting.Lin@comsat.com

Robert Luly
Western Communications
7283 S. Fillmore Circle
Littleton, CO 80122
303-694-0049
303-694-0090 (FAX)
E-mail: luly@netcom.com

Robert Manning
NASA Lewis Research Center
21000 Brookpark Road
Cleveland, OH 44135
216-433-6750
215-433-6371 (FAX)
E-mail: acmann@lims0.1.lerc.nasa.gov

Charlie Mayer
University of Alaska, EE Dept.
P.O. Box 755900
Fairbanks, AK 99775-5900
907-474-6091
907-474-6087 (FAX)
E-mail: ffcem@aurora.alaska.edu

David Morabito
Jet Propulsion Laboratory
4800 Oak Grove Drive, MS 161-260
Pasadena, CA 91109
818-354-2424
818-393-4643 (FAX)
E-mail: david.d.morabito@jpl.nasa.gov

Chris Pearson
Stanford Telecom
1761 Business Circle Drive
Reston, VA 22090
703-438-7845

Jennifer Pinder
Stanford Telecom
1761 Business Center Drive
Reston, VA 20194
703-438-3197
703-438-7921 (FAX)
E-mail jferry@sed.stel.com

David V. Rogers
Communications Research Centre
3701 Carling Avenue
Ottawa, Ontario
Canada K2H 8S2
613-998-5174
613-998-4077 (FAX)
E-mail: dave.rogers@crc.doc.ca

Jim Rucker
Jet Propulsion Laboratory
4800 Oak Grove Drive, MS 67-204
Pasadena, CA 91109
818-354-0859
818-393-0096 (FAX)
E-mail: James.D.Rucker@jpl.nasa.gov

Lt. Steve Scotty
Naval Post Graduate School
460 Ramona, #3
Monterey, CA 93940
408-657-9930
sdscotty@nps.navy.mil

Richard Sherman
Lockheed Martin WDL
3200 Zanker Road
San Jose, CA 95134
408-473-4401

Fred Shimabukuro
Aerospace Corporation
2350 E. El Segundo Blvd.
El Segundo, CA 90245-4591
310-336-6903
310-336-6225 (FAX)
E-mail: shimabukuro@10.aero.org

Geoff Torrence
University of Texas/EERL
10100 Burnet Road
Austin, TX 78758
512-471-8604
512-471-8609 (FAX)
E-mail: Geoff_Torrence@mail.
utexas.edu

Wolf Vogel
University of Texas/EERL
10100 Burnet Road
Austin, TX 78758
512-471-8608
512-471-8609 (FAX)
E-mail: Wolf_Vogel@mail.utexas.edu

David B. Westenhaver
WWW, Inc.
746 Lioness Ct. S.W.
Stone Mountain, GA 30087-2855
770-925-1091
707-931-3741 (FAX)
E-mail: wwwinc.@crl.com

Administrative Assistant JPL:

Mardy Wilkins
818-354-7421
818-393-4643 (FAX)
E-mail: Mardith.J.Wilkins@jpl.nasa.gov

ACTS Electronic Mailing List Address:
acts@java.jpl.nasa.gov

Page intentionally left blank

ACRONYMS

January 22, 1997

ACA	attenuation with respect to clean air (or clear air attenuation)
ACSP	advanced control signal processor
ACTS	Advanced Communications Technology Satellite
ACTSEDIT	ACTS preprocessing code (software from Virginia Technical Institute (Blacksburg, VA, generates PV1 files)
ACTSPP69	ACTS preprocessing code (software from University of Oklahoma, Norman, generates PV2 files)
ACTSVIEW	ACTS preprocessing code (software from University of Oklahoma, Norman, generates PV2 files)
AFS	attenuation with respect to free space
AGA	attenuation due to gaseous absorption
AMT	ACTS mobile terminal
APSW	ACTS Propagation Workshop
APT	ACTS Propagation Terminal (at Colorado State University)
ARCADA	backup program for reading data tapes
ARD	radiometrically derived attenuation
ATDNET/MAGIC	Advanced Technology Demonstration Network/Multidimensional Applications and Gigabit Internetwork Consortium
BBP	baseband processor
CCIR	(now changed to ITU-R --- International Telecommunications Union - Radio)
CDF	cumulative distribution functions
CDIAC	Carbon Dioxide Information and Analysis Center (U.S. Dept. of Energy)
CDMA	code division multiple access
CHILL	University of Chicago and Illinois Water Survey (radar)
CONUS	continental United States
CRG	capacitive rain gauge
CSU	Colorado State University
DAX	data acquisition and control
DRX	data receiving (collection)
DSS	Digital Satellite System
EERL	Electrical Engineering Research Laboratory (at University of Texas, Austin)
EMSAT	Advanced Technology for Emergency Medical Services
ETS-V	Engineering Test Satellite
ExCell	Exponential Rain Cell Model (developed in Italy by Capson and others)
FAU	Florida Atlantic University
FEC	forward error correcting

FFT	fast Fourier transform (or transformation)
GBS	Global Broadcast System
GSFC	Goddard Space Flight Center (Greenbelt, MD)
GSO	geostationary orbit (also GEO - geostationary Earth orbit)
GTE	General Telephone and Electric
GTEDS	General Telephone and Electric Telecommunications Division (near Tampa, FL)
HDR	high data rate
HPCC	high performance computing and communications
INMARSAT	International Maritime Satellite
IRAC	International Radio Advisory Committee
ITU-R	International Telecommunications - Radio
JPL	Jet Propulsion Laboratory (Pasadena, CA)
JSC	Johnson Space Center (Houston, TX)
LeRC	Lewis Research Center (Cleveland, OH)
LNB	low-noise (amplifier) board
MARECS-B2	(International Marine Satellite Consortium satellite)
M-P	Marshall-Palmer
MPEG	Motion Picture Evaluators Group (standard for video compression)
MSM	microwave switch matrix
NCAR	National Center for Atmospheric Research (Boulder, CO)
NOAA	National Oceanographic and Atmospheric Administration
NRaD	(U.S.) Naval Research and Development
OC3/OC12	(fiber optic carrier rates: 155 and 622 MB/s)
OPEX	Olympus Propagation Experiments
OU	Oklahoma University (Norman)
PFD	power flux density
RMS	root mean square
SAM	simple attenuation model (developed by Warren Stutzman, Virginia Polytechnic, Blacksburg)
SCADA	supervisory control data acquisition (system)
SGL	satellite ground link
STEL	Stanford TElecommunications, Inc., Reston, VA
TBG	tipping bucket rain gauge
TC	two-component model (developed by R. Crane, U. of Oklahoma, Norman)

TDRS	Telecommunications and Data Relay Satellite
TIP	Transportable Instrument Package (from Johnson Space Center)
TSR	transmit and stay resident
TSRC	transmitter-receiver
T1VSAT	(standard) terrestrial transmission rate for VSAT (1.54 MB/s)
UBC	University of British Columbia
UCAR	University Corporation for Atmospheric Research
UNC	University of Northern Colorado
USAT	ultrasmall aperture terminal (transportable 36-cm (14") station, five units in use)
USF	University of South Florida
UPS	uninterruptable power supply
UTC	universal time coordinates (Greenwich Mean Time)
VSAT	very small aperture terminal
WMO	World Meteorological Organization

REPORT DOCUMENTATION PAGE

Form Approved
OMB No. 0704-0188

1. AGENCY USE ONLY *(Leave blank)*	2. REPORT DATE	3. REPORT TYPE AND DATES COVERED
	January 15, 1997	Proceedings Nov. 19-20, 1996

4. TITLE AND SUBTITLE
Presentations of the Ninth Advanced Communications Technology Satellite Propagation Studies Workshop (APSW IX)

5. FUNDING NUMBERS
C - NAS7-1260

BP63250000000-RF295

6. AUTHOR(S)
Nasser Golshan, Editor

7. PERFORMING ORGANIZATION NAME(S) AND ADDRESS(ES)
Jet Propulsion Laboratory
California Institute of Technology
4800 Oak Grove Drive
Pasadena, CA 91109-8099

8. PERFORMING ORGANIZATION REPORT NUMBER
JPL Publication 97-3

9. SPONSORING / MONITORING AGENCY NAME(S) AND ADDRESS(ES)
National Aeronautics and Space Administration
Washington, DC 20546-0001

10. SPONSORING / MONITORING AGENCY REPORT NUMBER

11. SUPPLEMENTARY NOTES
Held in Herndon, Virginia

12a. DISTRIBUTION / AVAILABILITY STATEMENT

12b. DISTRIBUTION CODE

13. ABSTRACT *(Maximum 200 words)*

The Advanced Communications Technology Satellite Propagation Studie Workshop (APSW) is convened each year to present the results of the ACTS Propagation Campaign. Representatives from the satellite communications (satcom) industry, academia, and government are invited to APSW for discussions and exchange of information. The ACTS Propagation campaign is completing three years of Ka-Band data collection at seven sites in North America. Through this effort, NASA is making a major contribution to growth of satcom services by providing timely propagation data and models for predicting the performance of Ka-Band satellite communications systems.

14. SUBJECT TERMS
radio communication, satellite communication, radio propagation, ACTS

15. NUMBER OF PAGES
322

16. PRICE CODE

17. SECURITY CLASSIFICATION OF REPORT	18. SECURITY CLASSIFICATION OF THIS PAGE	19. SECURITY CLASSIFICATION OF ABSTRACT	20. LIMITATION OF ABSTRACT
Unclassified	Unclassified	Unclassified	Unlimited